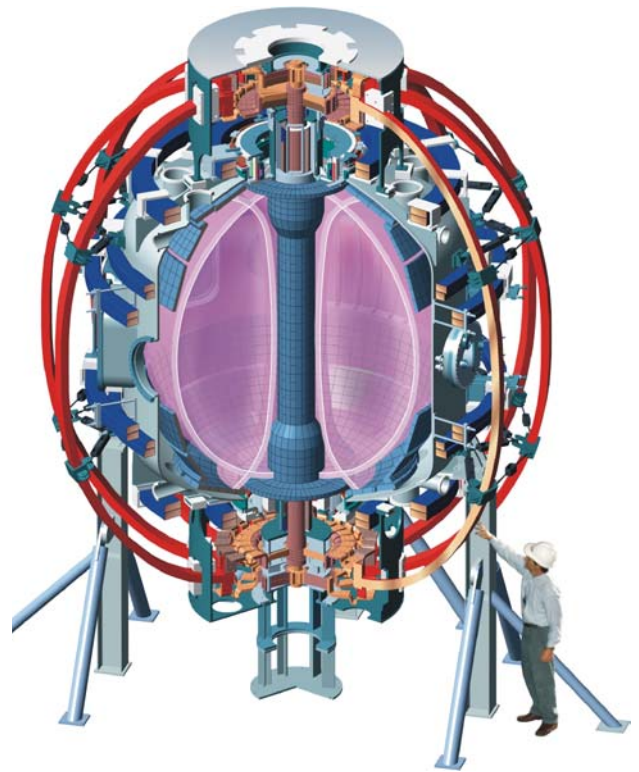


*The NSTX
Research
Program Plan
for 2004 - 2008*



*A preliminary draft report, prepared for the NSTX
PAC 14, January 21 - January 22, 2003*

Contents

1. *Introduction and overview*
2. *Facility Status*
3. *Topical Science*
 - MHD*
 - Transport and turbulence*
 - Waves, wave-particle interactions, and current drive*
 - Coaxial helicity injection*
 - Boundary physics*
 - Plasma control*
4. *Integrated scenarios*
5. *Theory and Computation Overview*
6. *NSTX and ST Next-Steps in Fusion Energy Science*

1. *The NSTX Research Plan Overview*

1.1 *NSTX and fusion energy science development*

The National Spherical Torus Experiment (NSTX) [1] research began in 1999 as a leading element in the U.S. fusion energy science program's suite of proof-of-principle experiments. It is one of many innovative concepts being used to explore the implications and possible benefits of modifying the field line structure as compared to more moderate aspect ratio devices. With respect to this, the ensemble of fusion devices with various magnetic configurations, and accordingly different ranges of plasma beta, field line geometry, stability and confinement properties, and so forth, can be viewed as presenting a powerful platform from which to strengthen the scientific basis for what ever concept eventually proves to be the preferred choice for fusion energy development.

This role for NSTX is emerging simultaneously with the emergence in the 1990's of a new era in fusion energy research, one characterized by unprecedented diagnostic, theory, and computational capabilities. Indeed, the development of the ST concept [2] represents one aspect of this emerging era, as its creation is grounded in theoretical expectations that the field line geometry that accompanies low aspect ratio operation should provide enhanced stability to global MHD modes, and thus access to beta values far in excess of those achievable on higher aspect ratio devices. Of course, along with this theory-based anticipation comes other important questions. These questions include assessing the viability of non-inductive sustained operations, the manageability of edge heat fluxes, the role of rotation in affecting MHD and equilibria, the scaling of non-ideal MHD instabilities, the viability of new heating and current drive

scenarios, and the feasibility of non-inductive current initiation strategies previously untested on devices of the scale of NSTX. The NSTX program is structured to address these and other questions, and to resolve them where possible.

The rapidly evolving sophistication of fusion science, together with a deepening appreciation by policy makers and leaders of the role that fusion can play in addressing issues of worldwide import, present the NSTX program with a unique and powerful opportunity. First, pursuit of ST research may yield a promising alternative to the standard aspect ratio tokamak when choices are made about the first deployments of systems that will generate net electricity. Second, the compact size of the ST and the promise of high ratios of plasma pressure to magnetic pressure, or beta, suggest that the ST should be given serious consideration as the centerpiece of a component test facility. Third, the prospect of advanced diagnosis with beta values comparable to those of interest in many astrophysical systems, in an era of unprecedented diagnostic, theory, and computational capability, suggests that NSTX can be a powerful laboratory by extending the range of laboratory plasma science.

1.2 Overview of the NSTX research program

1.2.1. Overarching goals - The research program of the National Spherical Torus Experiment (NSTX) is guided by two overarching goals:

1. NSTX research is directed at assessing the attractiveness of the spherical torus (ST) as a fusion energy concept, both as the centerpiece of an advanced fusion reactor and as a neutron source for a component test facility.

2. NSTX research takes maximal advantage of differences between its plasma properties and those of other magnetic configurations to extend the knowledge base on issues of broad importance to plasma science and fusion energy development in this era of advanced theory, computational, and diagnostic capability.

The NSTX research program is guided by the implementation approaches developed by FESAC in 1999 during the Integrated Program Planning Activity (IPPA). The research plan for 2004 – 2008 described here addresses the primary goals pertaining to ST research, and also addresses topical goals relevant to toroidal plasma science in areas for which NSTX plasmas are particularly well suited. As a Proof-of-Principle device in the Department of Energy portfolio of fusion energy concepts, the primary IPPA goals pertaining to the spherical torus concept are as follows:

5 year IPPA goal: Make a preliminary determination of the attractiveness of the Spherical Torus by assessing high beta stability, confinement, self consistent high bootstrap operation, and acceptable divertor heat fluxes, for pulse lengths much longer than the energy confinement time.

10 year IPPA goal: Assess the attractiveness of extrapolable, longpulse operation of the Spherical Torus for pulse lengths much longer than the current relaxation time.

This document describes the research program plan for NSTX 2004 through 2008 that is aimed at achieving the 5 year goal midway through its implementation, and at placing the program in an excellent position to strike for the 10 year goal in the near term after the end of this period.

1.2.2 Broad research themes – NSTX research is directed towards demonstration of key ST characteristics relevant to advanced ST operations, and the establishment of the required underlying physics understanding of the achievement of these regimes. While NSTX research becomes increasingly focused towards the achievement of these high performance operations with time, advanced diagnostics will be implemented where key opportunities in high beta plasma science exist, and control science will be expanded as tools are developed to enable the achievement of these goals. This platform will form a broad base from which to take the next step in ST science, one that will strengthen toroidal science in many critical areas with respect to high beta effects and field line topology. This will result in the achievement of an extrapolable, broadened base of toroidal science, to the benefit of all of toroidal confinement research.

Through 2003: Exploration of passive limits - Broadly speaking, NSTX research at present is in a period where the limits of the operating space are being established under the influence of passive limits, e.g. passive wall stabilization of MHD modes with the assistance of driven rotation. Focal points in this course of this period include the identification of control tools needs and the development of plans for their implementation. This plan focuses on a transition beyond

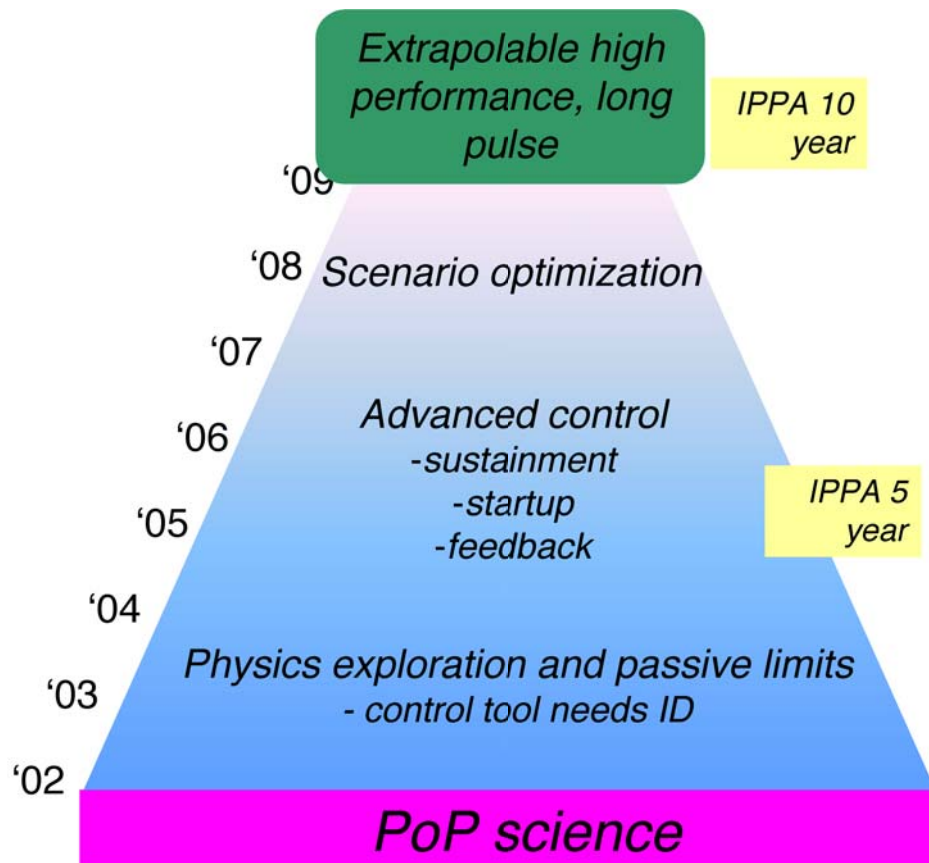


Figure 1.1. The NSTX program proceeds from a topical science foundation, with increasing focus on advanced research scenario optimization through advanced control development.

the present phase of research, and consists of the development and deployment of advanced control tools aimed at extending the stable operating space and duration of the pulse length of plasmas of very high beta and confinement, and for developing the basis for fully solenoid-free plasma startup and sustainment. The research effort at the

end of this plan focuses on the simultaneous optimization of ST plasma performance in terms of stability, confinement, and pulse length.

2004 – 2008: Develop advanced tools and optimize plasma performance – These tools include control tools, as well as advanced diagnostics. Some of these diagnostics will form elements of

the control strategy. The research described in this plan will develop and take advantage of advanced control tools that maximize device flexibility and thus enable strides in optimizing plasma performance. This flexibility also forms the basis for optimizing NSTX performance, for establishing its operating limits, and for performing controlled variations that are necessary to develop a scientific basis that has theory and experiment comparisons as its cornerstone.

The advanced diagnostics will enable taking maximal scientific advantage of unique ST properties. A flexible, well-diagnosed NSTX plasma will be well positioned to take advantage of this age of rapidly advancing capabilities in theory and advanced computation. This coupling is essential for forming an extrapolable basis from which the ST concept can be advanced, as well as for contributing to issues of broad and deep importance to advancing toroidal concepts in general.

The overall direction and sharpening of focus of the program is established by the need to integrate elements of the science that contributes to enhancing the performance of NSTX over the research period with respect to plasma stability, confinement, and pulse length.

1.3 Outline of research elements for 2004 – 2008

Major research goals have been established with respect to high levels of ST performance and demonstration of attractive spherical torus capabilities. These efforts will be supported by a program framework that promotes an emphasis on the highest quality plasma science that is enabled by advanced control, measurement, and theory and computation.

Integration and Performance Goals

With respect to integration of research elements to demonstrate high ST plasma performance and viability of approaches relevant to sustained pulse, component test facility operations, NSTX research is focuses on two major thrusts for the 2004 – 2008 time frame. During this period, the

IPPA Five Year assessment will be reached, and the NSTX program will be in a strong position to strike for the Ten Year IPPA assessment point at the completion of this research plan:

1. *High beta, high confinement, high bootstrap fraction plasmas relevant to an advanced ST reactor*— A major goal is improving the plasma quality as measured by simultaneously advancing the plasma toroidal beta, normalized beta, confinement time, and pulse length. At the end of this research period, a goal is the realization of 40% toroidal beta discharges operating near the wall stability limits, possibly using active feedback control, with bootstrap current fractions of up to 70%, and pulse durations longer than current relaxation time. These plasmas likely will benefit from strong shaping and advanced particle control tools, as well as techniques that will increase savings of inductive flux that are developed in the second major thrust (below).

2. *Solenoid-free operations at plasma parameters relevant to a component test facility* – A major goal is developing the capability to initiate and sustain plasmas without the aid of solenoid-induced flux. In the middle third of this research period, a goal is the development of plasmas with non-inductive sustained operations for pulse lengths longer than a current relaxation time at toroidal beta values comparable to those required for a component test facility. Also, in separate plasmas, NSTX aims to demonstrate fully solenoid-free startup techniques to plasmas with high poloidal beta. This will be achieved with a combination of techniques, possibly including coaxial helicity injection, poloidal field coil induction, bootstrap current, and high harmonic fast wave and neutral beam current drive.

The achievement of these goals will represent major advances in demonstrating the scientific and technical attractiveness of the spherical torus. The high level goal of establishing an extrapolable basis for moving forward demands that their achievement be grounded in the highest quality plasma science. To promote this, the program is structured largely along topical research lines for which the choices in research topic are guided by the overall demand to integrate key physics elements learned from each in order to advance the pursuit of the goals outlined above. Achieving the results outlined above and enabling these developments with the highest quality

plasma science is one aspect of fulfilling the obligations this program has as a Proof-of-Principle experiment. Highlights of topical research contributions follow.

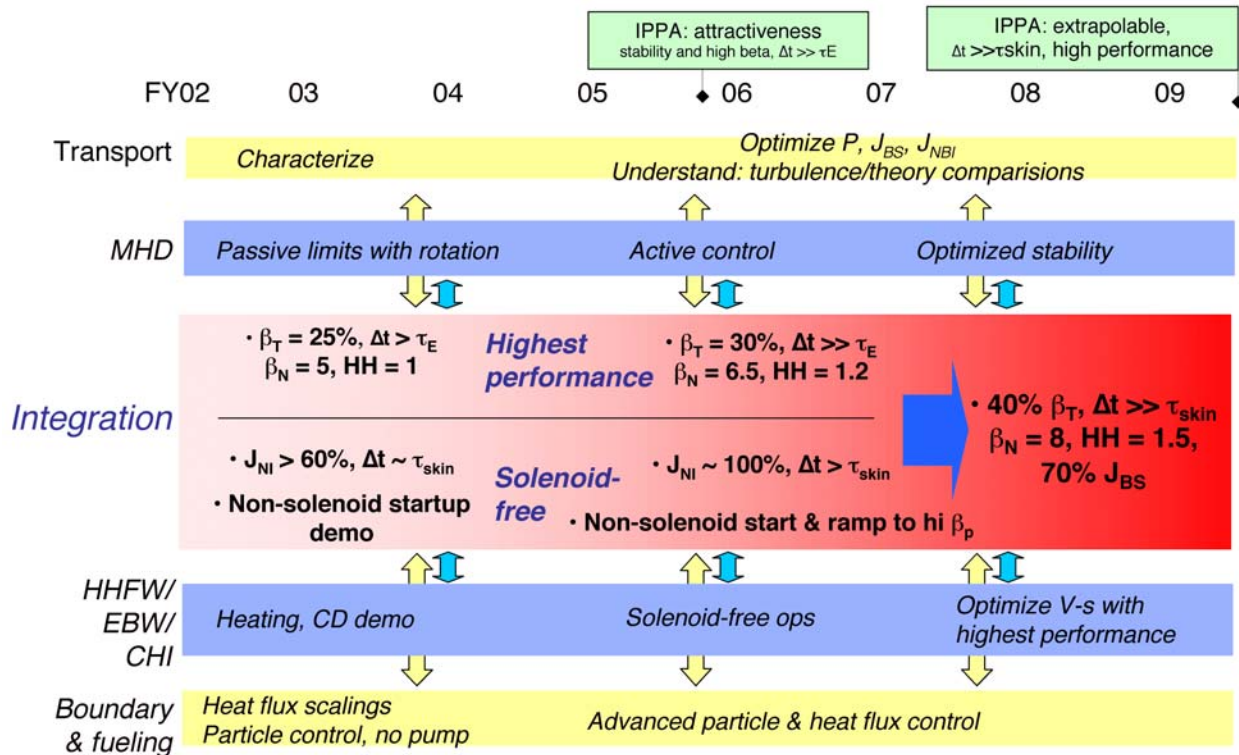


Figure 1.2 Overview of the development of the NSTX research program plan elements

NSTX Research and the IPPA Science Objectives

The performance and demonstration goals are supported by a foundation of topical science research. The research is organized along the topics of MHD, transport and turbulence, wave-particle interactions, boundary physics, and coaxial helicity injection. The first four are well aligned with the five and ten year scientific objectives outlined by FESAC in 1999. The wave-particles science effort focuses on high harmonic fast wave (HHFW) heating and current drive, Electron Bernstein Wave (EBW) emission and current drive studies, and the interactions of MHD with fast particle populations. The science underpinning coaxial helicity injection is MHD science, and an emphasis on developing an extrapolable basis for solenoid-free startup based

both on demonstrations and understanding of helicity injection MHD is central to the NSTX CHI program.

The IPPA Five Year Science Objectives, and some relevant NSTX program contributions to these objectives, follow.

Objective 1.1 - Turbulence and Transport: Advance the scientific understanding of turbulent transport forming the basis for a reliable predictive capability in externally controlled systems.

NSTX program contributions - Confinement results on NSTX up through 2002 are compelling with respect to global confinement and ion thermal transport. A major program focus is characterizing confinement scalings for the ST and to develop a turbulence-based understanding of the role of beta and aspect ratio in governing the physics of these scalings. This is within reach of the NSTX Five Year Plan. In addition to using a rapidly maturing suite of profile diagnostics, this effort involves the development of advanced systems to measure turbulence structure in sufficient detail at both low and high wave number to allow detailed comparisons with gyrokinetic codes. The regimes realized in NSTX at high beta are predicted to be characterized by emerging electromagnetic effects in plasma turbulence, and therefore represent new physics studies that will pose challenges to existing models. With these advanced diagnostics, powerful opportunities exist in testing theory predictions of the pervasive nature of turbulence suppression at low aspect ratio under the influence of high flow shear. Also, the ST geometry, with its strong field line curvature, provides opportunities for scattering measurements of turbulence that will have unprecedented spatial resolution at high wavenumber. This regime is of high relevance to understanding the physics of anomalous electron thermal transport, one of the outstanding puzzles in magnetic confinement research.

Objective 1.2 - Macroscopic Stability: Develop detailed predictive capability of macroscopic stability, including resistive and kinetic effects.

NSTX program contributions - The research program is structured to address high beta MHD properties and limits, and its active stabilization, on a broad front. For example, this research

already has been characterized by quantitative theory/experiment comparisons of global stability limits. The pursuit of active stabilization strategies to extend long pulse, high beta operations beyond the no-wall limit demands a strong coupling with experiment and theory, a coupling that already has revealed that NSTX operates routinely above the no-wall beta limit. Studying the physics of the conditions for the onset of resistive wall modes, including the coupling physics between the growing mode and external error fields, will involve detailed measurements in the presence of a controllable error field, enabling quantitative comparisons to theory. The high rotation velocities compared to the Alfvén speeds will allow tests of rotation effects on core MHD stabilization or saturation. Fast ion MHD activity is driven by beam ions that are in a new regime compared to those injected into moderate aspect ratio tokamaks, owing to the high fast particle velocities compared to the Alfvén speed. This has already yielded significant theory/experiment interactions are investigating the possibility that fast ion-induced MHD activity might play an important role in ion heating. Differences in gap structure in the Alfvén continuum between low and moderate aspect ratio devices and will be explored in joint experiments between NSTX and tokamaks.

Objective 1.3 - Wave Particle Interactions: Develop predictive capability for plasma heating, flow, and current drive, as well as energetic particle driven instabilities, in a variety of magnetic confinement configurations and especially for reactor-relevant regimes.

NSTX program contributions - NSTX has a major commitment to assessing the physics of High Harmonic Fast Wave heating and current drive. HHFW wave physics is largely unexplored experimentally. For NSTX, it offers the promise of current drive as it is expected to heat electrons directly. Experimental tests of the theory of HHFW interactions with fast ions are being and will continue to be explored. Current drive theories associated with HHFW will be tested by measuring local changes in the current density induced by HHFW with the developing MSE diagnostic. Additional tests of theory will come through the use of the HHFW antenna's ability to launch waves with variable phase. Electron Bernstein Wave (EBW) theory is being developed because of the needs of the ST for current drive tools as well as fast time-response electron temperature measurements. The NSTX research program is structured around an experimental

and theoretical assessment of EBW physics so as to ascertain the requirements for and viability of EBW current drive and heating in an ST.

Objective 1.4 - Multiphase interfaces: Advance the capability to predict detailed multi-phase plasma-wall interfaces at very high power- and particle fluxes.

NSTX program contributions - Boundary physics has a significant role in the NSTX program with respect to enabling the creation of conditions for long pulse, high beta operations. Measurements of divertor heat fluxes with spatial resolution are allowing tests of theories of the role of high flux expansion in the ST divertor region. Detailed modeling of the NSTX divertor underpins these tests. In its research plan, NSTX is considering the implementation of a liquid lithium module for the management of heat and particle fluxes. Such deployment would represent a significant investigation relevant to all toroidal confinement systems.

Objective 1.5 - General Science: Advance the forefront of non-fusion plasma science and plasma technology across a broad frontier, synergistically with the development of fusion science in both MFE and IFE.

NSTX program contributions - NSTX science will contribute broadly on many fronts. One of particular interest is contributing to the field of astrophysics. A connection has only recently been made between the fusion community and the astrophysics community of the relevance of gyrokinetic codes developed for fusion to important astrophysical problems such as the nonlinear cascade of turbulence to ion scales in plasmas with beta of order unity and above. This problem of turbulence dynamics is at the forefront of present-day thinking about the puzzle of subluminal accretion disks surrounding supermassive black holes in galactic centers. The NSTX program is already studying plasmas with beta of order unity. The implementation of advanced turbulence diagnostics on NSTX will enable detailed tests of gyrokinetic theory in this regime, providing a direct contribution to the study of these exotic astrophysical systems

High-level description of planned topical research elements

An overarching description of research activities planned for NSTX operations follows.

MHD

2002 – 2003: Beta limits will be explored and beta limiting modes will be identified, and active feedback control system needs for global mode stabilization will be identified and a system for possible implementation designed. Fast ion MHD modes will be characterized. In all cases, studies will begin comparing to standard aspect ratio. Advanced MHD theory and computation will play a critical role in the development of MHD mode control tools.

2004 – 2006: Active MHD suppression techniques and extension of NSTX operating limits through active mode control will be demonstrated.

2007 – 2008: Optimization of MHD active mode stabilization will be performed. Neoclassical tearing mode active stabilization techniques will be applied, if necessary. Electron Bernstein Waves will form the active mode stabilization tool. Both active global mode and tearing mode control will be applied to NSTX plasmas as operating regimes at 40% toroidal beta and high bootstrap fraction are developed.

Transport and turbulence

2002 – 2003: Global confinement characteristics will be identified, including parametric scalings. Edge turbulence measurements will be undertaken. Profile measurements and the first ion and electron heat fluxes will be assessed, with comparisons to microstability theory being performed. Core impurity ion transport will be studied.

2004 – 2006: Advanced turbulence diagnostics for measuring low and high k turbulence will be developed and deployed to advance the physics of ion and electron thermal heat transport. Transport modification in H mode and with core barriers, and neutral beam and high harmonic fast wave heating will be used to optimize the pressure profiles for long pulse, stable operations.

2007 – 2008: Turbulence studies will be extended. Wavenumber spectra measurements will be compared with detailed gyrokinetic theory that includes electromagnetic effects and full electron dynamics. Studies will be extended to plasmas with core betas in excess of unity. Tools that modify the transport, including heating, H mode and core barrier, and pellet injection, will be used to optimize the pressure profile and bootstrap current in very high beta, bootstrap current-dominated plasmas.

HHFW heating and current drive and EBW studies towards solenoid-free operations

2002 – 2003: High harmonic fast wave heating and current drive operations will be extended to the 6 MW level, with active phase feedback control demonstrated. Studies of Electron Bernstein Wave emission will be used to identify the system needs for an EBW antenna and launch system. Coaxial helicity injection will be coupled with ohmic induction in a demonstration of solenoid-free startup capability.

2004 – 2006: HHFW current drive will be applied to support 100% fully non-inductive operations for longer than a current penetration time at parameters relevant to a component test facility plasma in terms of beta, shape, and q. Active feedback of launched wave phase with real-time measurements of current drive effects will be deployed. HHFW will be applied as part demonstration of capability for solenoid-free startup to high poloidal beta plasmas, in conjunction with coaxial helicity injection and neutral beam injection. The first 1 MW EBW CD tests will be performed

2007 – 2008: Flux savings techniques developed with HHFW and EBW will be applied towards the demonstration of plasmas with 40% toroidal beta for times significantly longer than a current penetration time. EBW will be applied towards the active suppression of neoclassical tearing modes, if necessary.

Boundary physics

2002 – 2003: Heat flux scaling will be measured, and the plasma facing component requirements for high power operations for times longer than a skin time will be identified. Studies of the

divertor power balance will be performed. Particle control needs will be identified. Heat flux modeling will be carried out in support of these studies.

2004 – 2006: Active particle control tools will be deployed, if necessary. Active cryopumping will likely be implemented. More advanced particle control tools, including liquid lithium and CT injection, will be considered. Pellet fueling will be implemented.

2007 – 2008: Particle fueling and pumping and heat fluxes will be optimized to enable 40% toroidal beta, high bootstrap fraction operations for time scales longer than the current penetration time.

1.4 Research Highlights Through 2002

With the advent of significant levels of auxiliary heating and maturing diagnostic and operational capabilities over the last two years, the National Spherical Torus Experiment (NSTX) has begun intensive research aimed at establishing the physics basis for high performance, long pulse, solenoid-free operations of the spherical torus concept. This research is directed at developing an understanding of the physics of the ST operational space, developing tools to expand this space, and contributing broadly to toroidal science. To these ends, research in the last two years has focused on high beta MHD stability, confinement, high harmonic fast wave heating and current drive, boundary physics, solenoid-free startup, and exploration of scenarios that integrate favorable confinement, stability, and non-inductive current drive properties. Some results in these efforts include the following:

- Toroidal beta values ($\beta_t \equiv \langle p \rangle / (B_{t0}^2 / 2\mu_0)$) up to 35% with neutral beam heating have been obtained. In some plasmas at high normalized beta $\beta_N \equiv \beta_t / (I_p / aB_t)$, the no-wall stability limit is exceeded by 30%.
- Pulse lengths have been lengthened to 1 second with the benefit of bootstrap and beam-driven non-inductive currents of up to 60 % of the total.

- Normalized beta values β_N up to $6.5 \% \cdot m \cdot T/MA$ have been achieved, with operations overall bounded by ratios of β_N to the internal inductance $l_i = 10$.
- Energy confinement times in plasmas with both L and H mode edges exceed the ITER98pby(2) scaling [3] by over 50%, and the ITER89-P L-mode scaling [4] by over a factor of two for both discharge types.
- Particle transport studies of plasmas with turbulent (L mode) edge conditions reveal impurity transport rates that are consistent with and in some cases fall below neoclassical predictions in the core.
- Signatures of resistive wall modes have been observed [5,6]. With sufficiently broad pressure profiles, their onset occurs above the calculated no-wall stability limit, pointing to the presence of passive wall stabilization.
- Tearing mode activity consistent with the expected behavior of neoclassical tearing modes has been observed. These modes can saturate beta or cause beta reduction when the central q value is near unity, but for higher q values their effect on performance is modest.
- New classes of fast-ion-induced MHD have been observed [7,8,9]. These Compressional Alfvén eigenmodes (CAEs) exist near the ion cyclotron frequency. Bounce-precession fishbone bursts are seen near 100 kHz, and are associated with fast ion losses.
- Significant heating of electrons with high harmonic fast waves (HHFW) has been measured [10]. Interactions between fast beam ions and HHFW have been observed.
- The first indications of current driven by HHFW have been obtained [10].
- The application of coaxial helicity injection [11,12] (CHI) has yielded a toroidal current of up to 400 kA, with observations of $n=1$ MHD activity that may be a prerequisite for closed flux surface formation.
- Edge heat flux studies [13] divertor infrared camera measurements indicate that 70% of the available power flows to the divertor targets in quiescent H mode discharges.

-
- [1] M.Ono, Proceedings of the 18th IAEA Meeting, Sorrento, Italy, 2000.
 - [2] Y-K M. Peng, and D. J. Strickler, Nuclear Fusion 26, (1986).576
 - [3] The ITER Team, *Nucl. Fusion* **39** (1999) 2137.
 - [4] P.N. Yushmanov *et al.*, *Nucl. Fusion* **30** (1990) 1999.
 - [5] S. Sabbagh *et al.*, *Nucl. Fusion* **41** (2001)1601.
 - [6] S. Sabbagh *et al.*, Proceedings of the 19th IAEA Meeting, Lyon, France, 2002.
 - [7] N.N. Gorelenkov and C.Z. Cheng, C.Z., *Nucl. Fusion* **35** (1995) 1743.
 - [8] E.D. Fredrickson, N.N. Gorelenkov, C.Z. Cheng *et al.*, *Phys Rev. Lett.* **87** (2001) 145001.
 - [9] D. Gates, R. White, N. Gorelenkov, *Phys. Rev. Lett* **87** (2001) 205003.
 - [10] P. M. Ryan, Proceedings of the 19th IAEA Meeting, Lyon, France, 2002.
 - [11] T.R. Jarboe, *et al.*, *Phys. of Plasmas* **5** (1998) 1807-14
 - [12] T.R. Jarboe *et al.*, *Proceedings of the 17th IAEA Fusion Energy Conference*, Yokohama, IAEA-CN 69/PDP/02 (1998).
 - [13] R. Maingi *et al.*, in *Proceedings of the 11th International Conference on Plasma Physics* (Sidney, Australia, 2002), *Plasma Phys. Control. Fusion* (in press).

2. The NSTX National Fusion Facility - Status and Upgrades

The National Spherical Torus Experiment (NSTX) at the Princeton Plasma Physics Laboratory (PPPL) is a world class facility to carry out the spherical torus (ST) research. The NSTX research mission is to evaluate the physics principles of the ST plasma configuration, which is characterized by strong magnetic field curvature and high β_T , the ratio of the plasma pressure to the applied toroidal magnetic field pressure, providing a fertile ground for cutting-edge plasma research opportunities for scientists and students. The programmatic mission of NSTX is to determine, through the scientific investigation, the attractiveness of ST for developing practical fusion energy systems. The NSTX, operational since 1999, has been steadily building up the facility and diagnostic capabilities.

2.1 Facility / Diagnostic Achievements and Status

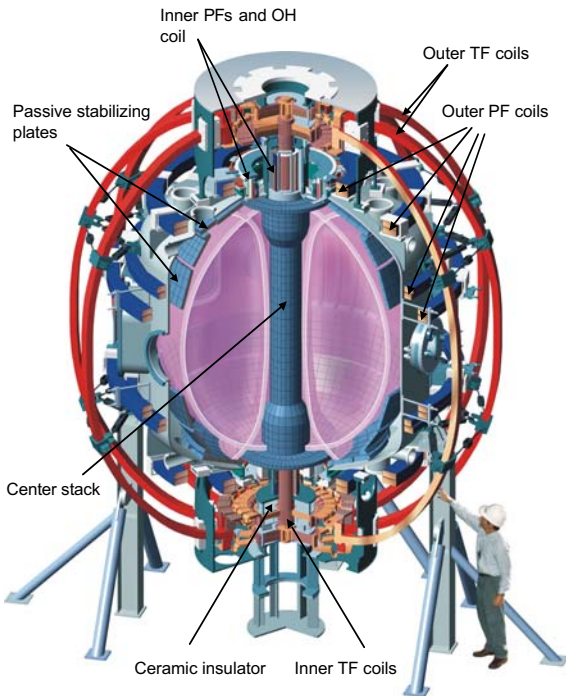


Fig. 2.1. NSTX Device Schematic

Achieved Parameters:

Bakeout	350°C
Gas fueling	LFS + HFS
Aspect ratio	1.27
Elongation	2.2
Triangularity	0.8
Plasma Current	1.5 MA
Toroidal Field	0.6T
Heating and Current Drive:	
Induction	0.7Vs
NBI	7MW
HHFW	6MW
CHI	0.4MA
Pulse Length	1.1s, (5 s with 3 kG possible)

Table 2.1. Achived Facility Parameters

NSTX is a major component of the restructured U.S. Fusion Energy Sciences Program, which emphasizes the investigation of innovative confinement concepts and the advancement of the underlying physics to strengthen the scientific basis for attractive fusion power. To accomplish this mission, the NSTX facility (Figure 2.1) is designed with the following capabilities:

- Plasma current I_p up to 1 MA, $R/a \geq 1.26$, $\delta \approx 0.6$, and $\kappa \approx 2.0$,
- Inductive solenoid and Coaxial Helicity Injection (CHI) for startup at 0.5 MA,
- High Harmonic Fast Wave (HHFW - 6 MW); Coaxial Helicity Injection (CHI), Neutral Beam Injection (NBI - 5 MW) for heating, current drive, and current profile control,
- Close-fitting conducting plates to maximize β ,
- Pulse length up to 5 sec at 3 kG \gg skin time \approx L/R time \sim 0.3 sec.

As can be seen in Table 5.1, the NSTX facility has already achieved or exceeded most of the original facility design capabilities. The plasma current, a key parameter for the plasma performance measure, reached 1.5 MA, which represents 50 % over the design value of 1 MA. In Fig. 2.2, we show the plasma current progress vs time. The figure also shows some relevant facility capabilities, which contributed to the progress.

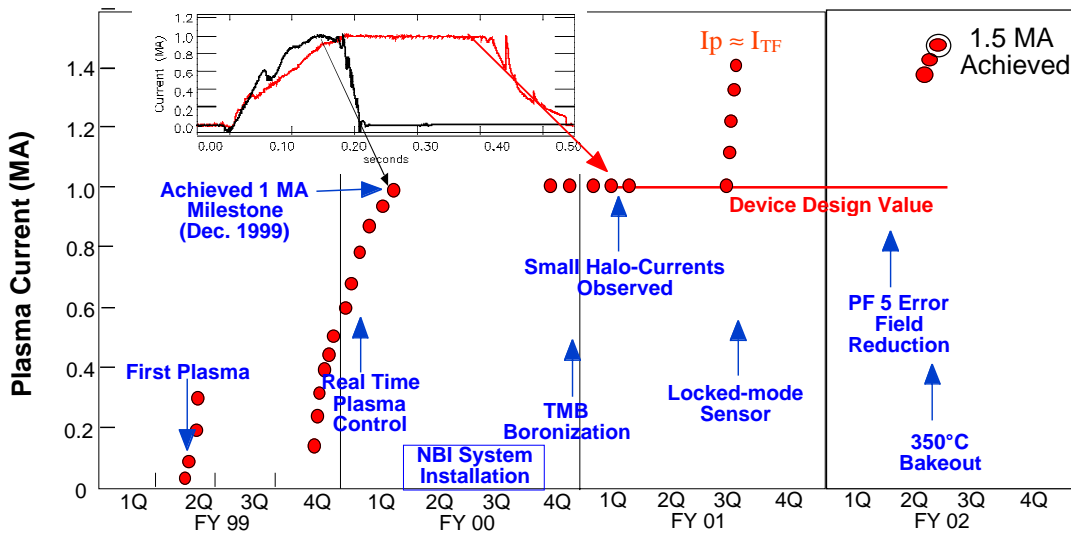


Fig. 2.2. The NSTX plasma current progress vs. time.

2.1.1. Initial Shake-Down and Ohmic Operations - As shown in the figure, the NSTX facility began operation in mid-February 1999 about three month ahead of schedule. By December 1999, NSTX reached its design plasma current of 1 MA about nine month ahead of schedule. This rapid progress to 1MA was possible due to the reliable power supplies available from TFTR and the early implementation of real time plasma control system which controls the plasma radial and vertical positions as well as the plasma current. The ORNL electron cyclotron heating preionization (ECH-P) system proved to be helpful in plasma initiation. In this period of ohmic operations, all of the plasma shapes as specified in the NSTX physics requirements were produced. In Sept. 2000, the NBI heating was introduced to increase the plasma beta. Together with the TMB (Trimethylboron) boronization, the plasma discharge improved markedly as shown in the inset figure, which compares the 1 MA discharge in Dec. 1999 and about one year later. As can be seen in the figure, the discharge improved from essentially no flat top to 200 msec of flat top during this period while the discharge duration increase by 2.5 times to 0.5 sec.

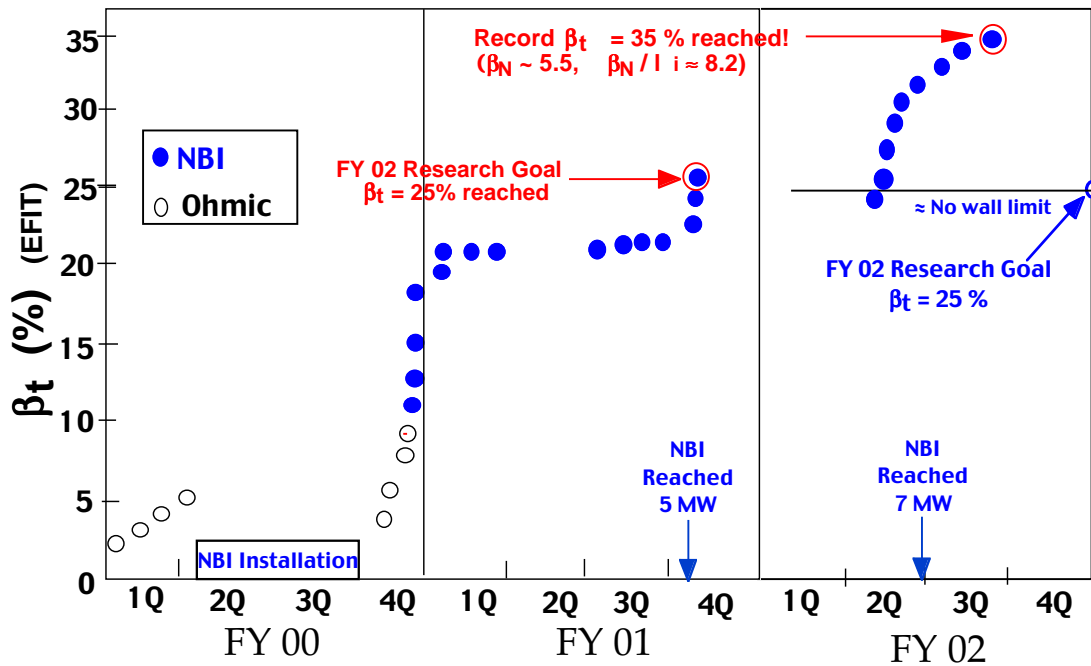


Fig. 2.3. Progress of average toroidal beta vs. time.

2.1.2. Increased Plasma Current and NBI Heating Capabilities - With the introduction of NBI, the NSTX research emphasis has moved on to investigate the strongly heated discharge regime. Figure 2.3 shows the rapid progress of achieved average toroidal beta vs time on NSTX. An important element of

this investigation is the capability of plasma current. Since the ohmic flux consumption has been gradually coming down due to the combined effect of reduced impurity by TMB and high plasma temperature (or lower resistive consumption) due to the NBI heating, a decision was made to allow the plasma current to be increased to 1.5 MA. From the device safety point of view, this decision to increase the plasma current limit from 1 MA to 1.5 MA was based on the relatively benign behavior of the wall halo-current observed in both NSTX and MAST. With the increased plasma current limit, NSTX made rapid progress and reached $I_p = 1.5$ MA goal in June 2001. In this period, the toroidal field was also increased to the design limit of 6 kG. The effort was aided by the introduction of various facility improvements including the 350°C high-pressure-helium bakeout system and the realignment of the PF 5 coils to minimize the error fields (e.g., to reduce the effects of locked modes). It should be noted that with this high plasma current, the NSTX reached another significant ST device performance milestone of the plasma current to be equal to the toroidal field coil current. Minimization of the toroidal field coil current with respect to the plasma current is an important objective for the spherical torus research to improve the attractiveness of the ST fusion power plants. The NBI system also continued to make progress and in April 2002, the NBI power was increased to 7 MW at 100 keV, significantly above the design value of 5 MW at 80 keV. Special techniques were applied to reduce gas recycling from the wall and thus permit easier formation of the edge barrier. The plasma energy was contained for about 1.5 times the duration projected from the H-mode plasma database developed from studies in many tokamak fusion experiments. Interesting to note that the plasma global confinement of over 100 msec has been achieved with NBI, which compares very favorably with only about 30 msec obtained in ohmic discharges. With the improved confinement, the plasma toroidal beta reached the FY 02 goal of 25% beta more than one year ahead of schedule. With improved facility and plasma capabilities, in March 2002, the NSTX produced H-Mode plasmas lasting essentially the full duration of the pre-programmed period of constant plasma current. The ready access to H-mode which produced favorable broad plasma pressure profiles, the plasma toroidal beta reached 35% at $I_p = 1.2$ MA in June 2002. This result represents a significant progress from the previous smaller START experimental results obtained at $I_p = 0.2$ MA.

2.1.3. Progress in Plasma Control System - The plasma control is the central element of the advanced spherical torus research. The plasma control system has been improving steadily in terms of faster processors and more control capabilities. With improved plasma control system, the very high triangularity discharge $\delta \approx 0.8$ was produced as shown in Fig. 2.4. The improved plasma shaping

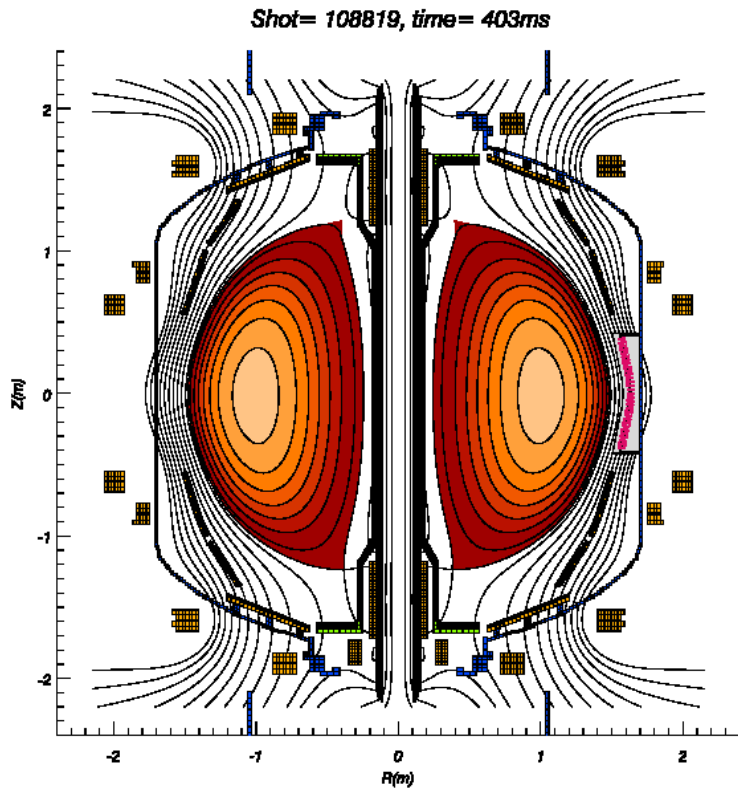


Fig. 2.4. Highly shaped ($\delta \approx 0.8$, $\kappa \approx 2.2$) high performance plasma from EFIT reconstruction.

control enabled to achieve high-triangularity high-performance plasmas of up to $\delta \approx 0.8$, well over the design value. The high triangularity produced some of the highest performing discharges to date on NSTX in terms of plasma toroidal beta and stored energy. In June 2002, the real time control system with the real time EFIT where the plasma equilibrium is calculated in real time (i.e., every 10 msec) was implemented successfully on NSTX as a joint effort with General Atomics. This was an important milestone toward developing a versatile plasma control system needed to achieve the advanced ST operational goals.

2.1.4. Progress on High Harmonic Fast Wave Heating System - High Harmonic Fast Wave (HHFW) could heat plasma electrons to high temperatures and sustain plasma current needed for steady-state fusion reactors. The high plasma beta and dielectric constant of ST plasmas make the wave accessibility particularly challenging. The modeling calculations suggest good accessibility and power absorptions of HHFW in high beta / high plasma dielectric plasmas. On NSTX, a twelve-element-antenna system was designed by PPPL and ORNL as a joint project with the Enabling Technology Program of OFES. The HHFW antenna installed on NSTX is shown in Fig. 2.5. The NSTX antenna phasing system is designed

to vary the k_{\parallel} from 14 m^{-1} to about 4 m^{-1} in real time (in other words, the wave parallel phase velocity from $1.3 \times 10^7 \text{ m/sec}$ to $4.7 \times 10^7 \text{ m/sec}$ with the transmitter frequency of 30 MHz) in order to follow the plasma discharge evolution from low temperature ($\approx 300 \text{ eV}$) start-up plasmas to high temperature (few keV) high beta plasmas in real time. Strong electron heating using HHFW was observed for the first time in NSTX experiments. Electron temperature was increased from about 5 million degrees to above 40 million degrees Kelvin using 3 MW of HHFW power. The HHFW current drive experiment has also yielded a significant drop in the loop voltage consistent with the theoretical expectations. The HHFW

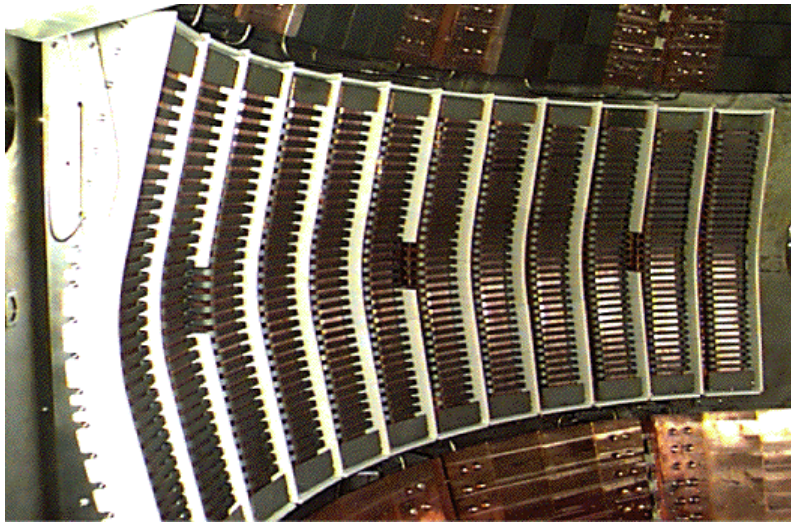


Fig. 2.5. 12-Element HHFW Antenna System in the NSTX Vacuum Vessel.

system has delivered 6 MW into the plasma, however, the system reliability at high power above 3 MW range was hampered by arc problems in the antenna feed area. The antenna feed area has been modified during the FY 02 outage to improve the HHFW reliability at high power.

2.1.5. Progress on Coaxial Helicity Injection System - For an attractive ST power plant, the OH solenoid must be eliminated in the center stack. The relatively modest magnetic flux and helicity per unit plasma current for ST tend to ease non-inductive startup requirements. The main tool being tested for NSTX is the coaxial-helicity-injection (CHI). The concept has been investigated previously in smaller experimental devices including HIT/HIT-II [4] and HIST [12]. The NSTX experiment represents a significant step in terms of plasma volume and required magnetic flux from the HIT-II experiment as shown in Table 2.2.

Machine	R (m)	a (m)	Bt0 (T)	Φ_T (mWb)	I-inj (kA)	V-inj (kV)	I-tor (kA)	I-Mult
HIT-II	0.3	0.2	0.5	50	30	0.5	200	7
NSTX	0.86	0.68	0.3	522	28	0.56	400	14

Table 2.2. Comparison of CHI systems on NSTX and HIT-II

A schematic of CHI is shown in Fig. 2.6 (a). With the ceramic insulating rings located at the top and bottom of the device, the center-stack is electrically insulated from the outer vacuum vessel, allowing bias voltage to be applied. With appropriate gas fill pressure (typically in a few m-Torr range) and with a voltage of up to 1 kV applied, a plasma discharge is initiated. Here using appropriate poloidal field coils, stronger poloidal fields are applied near the bottom gap, which reduces the connection length, so that the discharge is initiated preferentially in the lower gap region. The applied toroidal field causes the

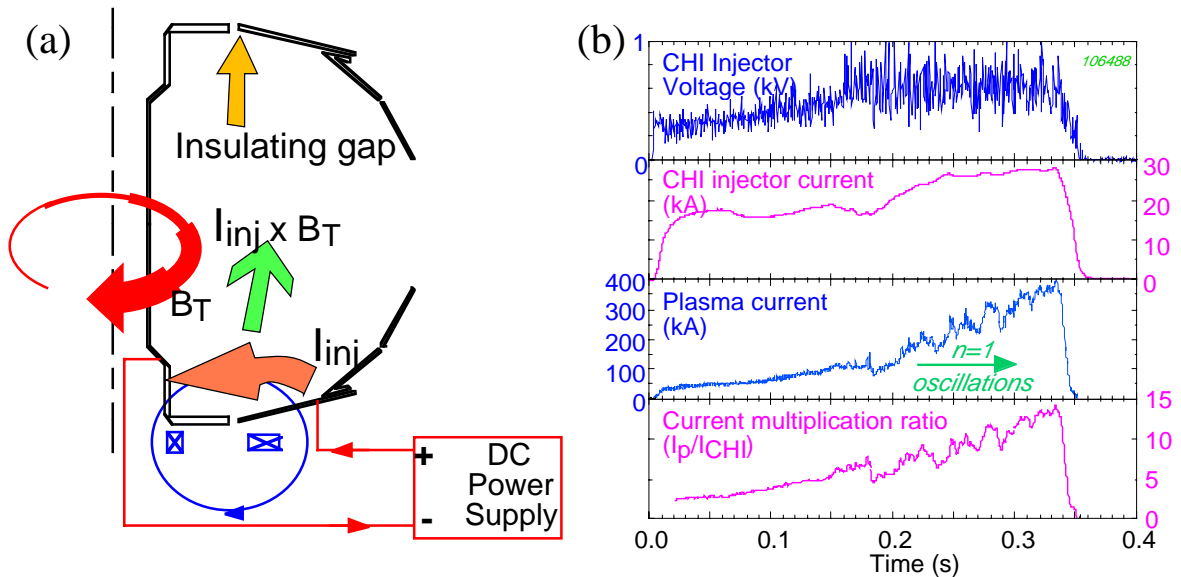


Fig.2.6 (a). Schematic of CHI Experimental setup.

(b) CHI discharge evolution.

current in the plasma to develop a strong toroidal component, the beginning of the desired toroidal plasma current. If the injector current exceeds a threshold value, the resulting ΔB_{tor}^2 or $(\mathbf{J}_{pol} \times \mathbf{B}_{tor})$ stress across the current layer exceeds the field line tension of the injector flux causing the helicity and plasma

in the lower divertor region to move into the main torus chamber. In Fig. 2.6 (b), CHI discharge waveforms are shown in which the toroidal current is driven from zero current without the ohmic solenoid. The discharge has 300 ms pulse length with a toroidal current of up to 390 kA generated with only about 28 kA of injected current, yielding current amplification factor of ≈ 14 which represents an excellent efficiency considering the much large volume of NSTX compared to HIT-II.

During the FY 02 campaign, as the plasma current is increased, the CHI discharges were frequently terminated by arcs occurring in the absorber region, which is an insulation gap at the top. When arcing occurs, the vacuum vessel forms a low impedance electrical path which terminates the helicity injection into the plasma. To solve the absorber arc problem, a new improved CHI absorber insulator was designed and fabricated in FY 02.

2.1.6. Boundary Physics Related Facility Progress and Status

It has been found that high temperature bake-out (350 °C) is needed to expedite the removal of water and CO absorbed on the plasma facing surfaces and near-surface regions of the graphite PFC's. Daily HeGDC and inter-discharge HeGDC are required for impurity and density control during high power operations. Experiments exploring the potential for real-time maintenance of boron films and the effects of cladding the plasma in a particular low-Z mantle have shown interesting promise. The wall conditioning effort to date has facilitated a broad range of encouraging advances. The future plan highlights upgrading impurity control, fueling efficiency, profile and particle control. In FY 03, after the 10th boronization, a new bake-out system was used to perform a uniform bake-out of the PFC's to 350 °C with the vacuum vessel at 150 °C. The inner PFCs on the center-stack are heated resistively by passing current through the inner inconel tube of the vacuum vessel while the outer PFCs are heated by circulating high-pressure helium through internal tubes. The nominal plasma-facing area of the vessel interior is 41 m²; about 75.6% (31 m³) consists of graphite tiles and the remaining 24.4% is vessel wall (304-SS). The mass of the graphite PFC's is 1.3x10³ kg. Of interest to note is that a 350 °C bake-out followed by boronization yielded desired lasting oxygen suppression. In addition, a similar trend occurred in the discharged-average H/D ratio for deuterium discharges, which decreased from

values exceeding 0.2 for some discharges, to below 0.05 after bake-out followed by boronization, and continued decreasing.

2.1.7. Facility Utilization - The NSTX facility utilization is shown in Table 2.3. As shown in the table, the NSTX facility operated according to the initial planned run weeks. The facility reliability has steadily improved through out the period. In FY 02, the operations actually exceeded planned 12 run weeks 2001 and achieved the 90% plasma availability. Due to the relative mature state of the NSTX facility, the number of run weeks as we move forward is mainly determined by the budget availability. The utilization of the NSTX facility by researchers, post-doctoral researchers in FY 02 as well as students is also shown in Table 2.3.

Facility Plasma Operations Availability

	<u>FY 00</u>	<u>FY 01</u>	<u>FY 02</u>	<u>FY 03</u>	<u>FY 04-08</u>
# of run weeks planned	15	15	12	12	20
# of run weeks achieved	15	15	13		
# of hours	600	600	520	480	800

Participating Research Personnel

	PPPL	non-PPPL
Researchers	45	75***
Post Doc.	3	7
Grad. Students	5	5
Undergrad. Students	3	5

*** In addition there are over 20 overseas collaborating researchers from countries including Japan, Russia, Korea, UK, Ukraine, and Canada in FY 02.

Table 2.3: Facility Utilization

2.1.6. Progress on Plasma Diagnostics - The plasma diagnostics have been steadily building up on NSTX. Due to the limited diagnostic upgrade budget, the diagnostic implementation has been mainly determined by the programmatic priorities. In this initial phase of operations, the diagnostics to measure the basic plasma properties are naturally emphasized. A list of the major diagnostics is listed in Table 2.4 below.

Existing Diagnostic Capabilities



NSTX

Core Plasma Diagnostics

- Thomson scattering (20 ch., 60Hz)
- Charge Exchange Recomb. Spect. (CHERS): T_i & v_ϕ (18 ch.)
- VB detector (single chord)
- Soft x-ray arrays (3) [JHU]
- Bolometer array (midplane tangential)
- X-ray crystal spectrometer ($T_i(0)$, $T_e(0)$)
- X-ray pulse height analyzer
- Electron Bernstein wave radiometer
- FIReTIP interf'r/polarim'r (2 ch) [UCD]
- GEM Fast 2D X-ray camera [Frascati, JHU]
- Tang. X-ray pin hole camera [U. Wisconsin]

Magnetics and MHD

- Magnetics for equilibrium reconstruction
- Diamagnetic flux measurement
- High-n and high-frequency Mirnov arrays
- Locked mode coils

Turbulence

- Edge reflectometer [UCLA]
- Edge fluctuation imaging [LANL, PSI]

Plasma Monitoring

- Fast visible camera [LANL]
- VIPS: Visible spectrometer
- SPRED: UV spectrometer
- GRITS: VUV spectrometer [JHU]
- EFIT (Columbia University)

Boundary Physics

- Divertor Bolometer
- Fast probe [UCSD]
- Infrared Camera [ORNL]
- Fast Ion Gauge [University of Wash]
- Divertor fast camera [Hiroshima Univ.]
- Divertor tile Langmuire probe array
- 1-D CCD H_α camera [ORNL]
- Visible filterscopes (H_α , OII, CII) [ORNL]
- Scrape-off layer reflectometer [ORNL]
- Fast camera (PSI)

Energetic Particles

- Fission chamber neutron measurement
- Fast neutron measurement
- Neutral particle analyzer (scanning)
- Fast ion loss probe

Table 2.4

2.2 Five Year Facility/Diagnostic Plan

The NSTX facility and diagnostic plan is driven by the overall NSTX 5 year program plan as show in Fig. 2.6. Here we shall describe the plan in three sections: Sec. 2.3 - Device Upgrades, Sec. 2.4 - Auxiliary System Upgrades, and Sec. 2.5 - Diagnostic Upgrades.

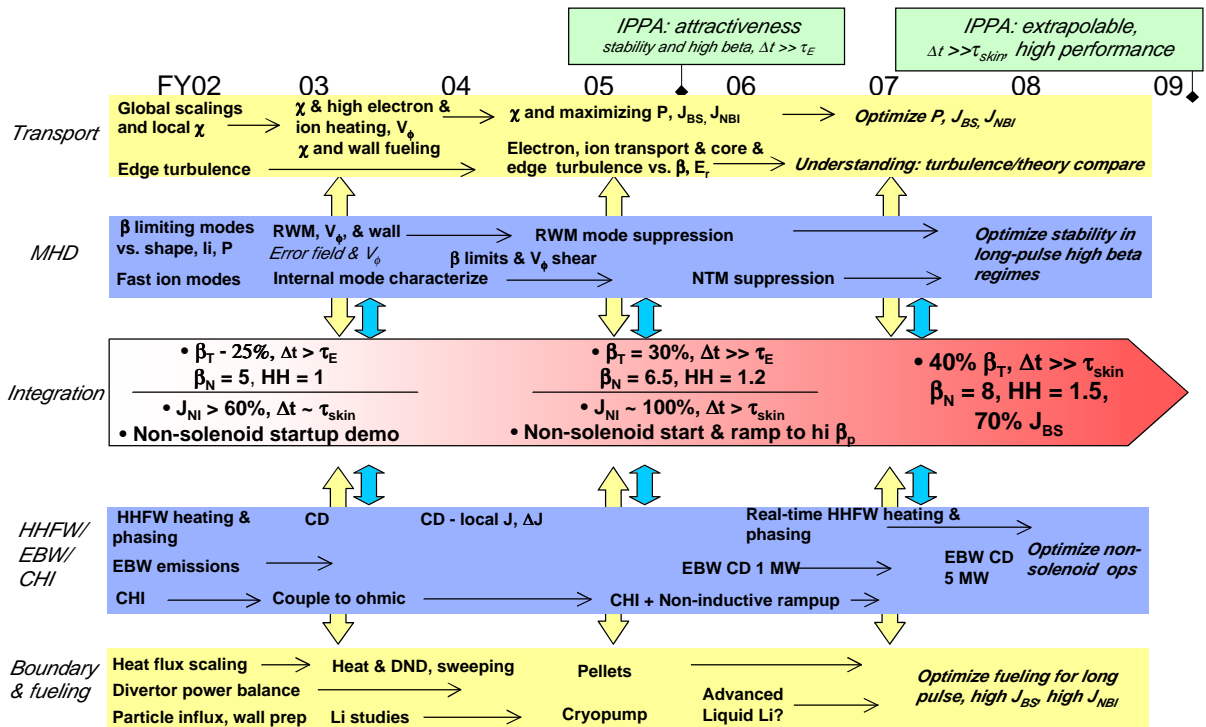


Fig. 2.7. NSTX 5 Year Plan Overview

2.3. Five Year Facility Upgrade Plan

In Table 5.5, a list of facility upgrades as described in the research plan is shown. Each of the major upgrades discussed in the subsequent sections. The gray shaded area depicts the time period of implementation.

			integration	MHD	transport	boundary	CHI	HHFW	EBW	FY03	FY04	FY05	FY06	FY07	FY08
Particle control															
	LFS DPI		x		x	x									
	HFS DPI		x		x	x									
	improved lower gas injector						x								
	CT injector		x		x	x									
	add. LFS/HFS gas injectors					x									
	Li/B pellet injector		x		x	x									
	supersonic gas injector		x			x									
	advanced Li wall conditioning		x		x	x									
	divertor cryopump					x									
	liquid lithium surface module					x									
Heating and current drive															
	HHFW antenna mods		x		x			x							
	3 MW EBW		x	x	x				x						
	NBI ground fault upgrade						x								
Passive plate upgrades															
	passive plate relocate		x	x											
	passive plate reconnect		x	x											
RWM/error field suppression															
	RWM/error field PCS interface		x	x											
	RWM/error field cor. Coils		x	x											
Plasma control mods															
	MSE/MPTS PCS interface		x	x	x										
	add. PCS processors		x	x											
	PF response improvements														
	dedicated PF4 supply & interf.		x	x											
	long pulse divertor mods		x			x									
CHI upgrades															
	Null-field Control Coils														
	PF1B at 2kV						x								
	improve response of PF2 & 3						x								
	wall current sensors, DAQ						x								
	2 kV injector capability						x								

Table 2.5. List of Facility Upgrades

2.3.1. Secondary Passive Plate Modification

A major device modification envisioned is the secondary passive plate (the passive plates which are further apart from the mid-plane) realignment. The existing NSTX passive plate configuration is designed to accommodate a wide range of plasma shaping parameters including low triangularity discharges. The NSTX experimental results suggest that higher triangularity plasmas are generally desirable for advanced ST physics investigations. As the future experiments focus toward higher triangularity discharges, there is a need to optimize the secondary passive plates. In Fig. 2.8, a schematic of a possible modified passive plates re-configuration is shown. The old plates are depicted in a gray shade.

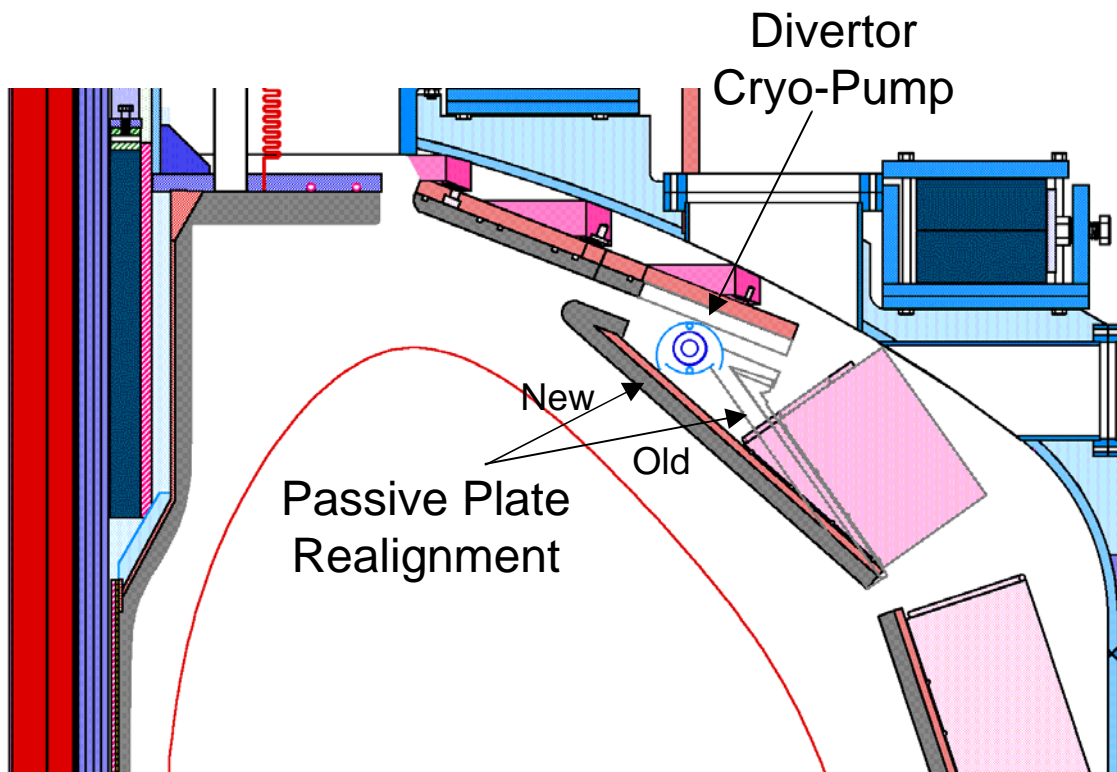


Fig. 2.8. Realigned Secondary Passive Plates and Divertor Cryo-pump Schematic.

The modification of the secondary passive plates is relatively straight forward due to much fewer diagnostic sensors in these plates compared for example to the primary plates. The secondary plates modification will allow the following improvements:

- The new configuration would permit an actively-pumped double-null high-triangularity ($\delta \sim 0.5$) divertor operations for the first time. This is an important step toward long pulse advanced ST operations.
- By tilting the secondary plates inward, the new plates are much better aligned with the high triangularity plasma boundary. This would be advantageous from the plasma MHD Stability point of view.
- The inward tilting of the secondary passive plates create an adequate space for an effective placement of the divertor cryo-pump rings as shown in Fig. 2.8. The new geometry will also facilitate the cryo-pump installation.

The basic design concept will be developed in FY 03, the engineering design and fabrication will take place in FY 04, and the installation will take place during the summer of 2004 to be ready for the FY 05 experimental campaign. In addition, the new configuration will also allow the installation of liquid lithium lower divertor tray as being envisioned by the VLT as discussed in Sec. 5.3.3. The secondary plates should also serve as a shield for the electromagnetic disturbances on liquid lithium from the plasma instabilities.

2.3.2. Toroidal Field Capability

In order to meet the NSTX five year goal of attractive ST regimes for $\Delta t \gg \tau$ -skin, it is important to make sure that the toroidal field coil system is capable of providing adequate pulse length. In Fig. 2.9, the toroidal field pulse length is plotted against the toroidal field strength. In the figure, the τ -skin of recently achieved high beta-poloidal (low-loop-voltage) is shown. The available TF-flat-top duration is much greater than the τ -skin. It should be noted that the present TF limits are somewhat conservative due to the uncertainty in the monitored temperature values. It is anticipated that the temperature monitor improvement can increase the TF limits to the higher curve in Fig. 2.9. With this improvement, the TF pulse length should be sufficiently long to achieve the NSTX 5 year research goal. It should be noted

that this goal is also consistent with the FESAC 10 year objective for the ST research. The temperature monitor improvement can be implemented relatively quickly as needed.

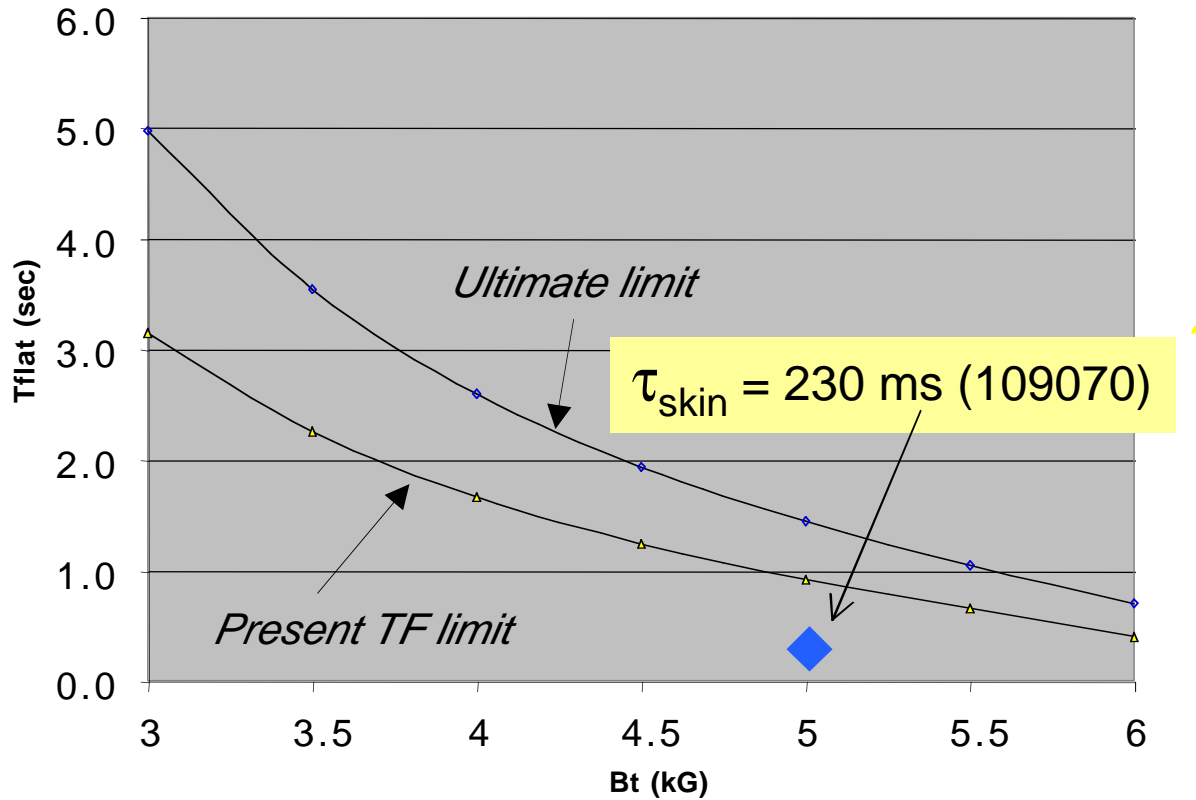


Fig. 2.9. Flattop Time vs. Toroidal field.

2.3.3. Plasma Boundary Related Facility Upgrades

The plasma boundary area will start to emphasize the power and particle handling and fueling issues to help achieve the plasma performance needed for the advanced ST research in the 5 Year Plan. The impurity reduction and control have been the main emphasis thus far as NSTX implemented a variety of surface conditioning techniques including high temperature bakeout, gas boronization, plasma boronization, and between-shot-helium GDC. These techniques enabled for the NSTX plasma operations to achieve record ST parameters. In the future, there will be incremental improvements to these techniques such as the boronization during the high

temperature bakeout and improved gas injection control. In the following, we will cover some of the key plasma boundary facility upgrades during the 5 Year period.

Lithium Pellet Injector - The capability to inject small solid and micro pellet ensembles of either Lithium, Boron, LiD, Li_2C_2 , B_4C , C, or other low-Z impurities at precise velocities from very low to high could allow a number of desirable boundary physics goals including wall conditioning, measuring edge impurity transport, measuring edge flows and rotation, enhancing charge exchange signals, controlling disruption decay, and liquid limiter simulation. It may also induce edge transport barriers (edge poloidal velocity shear and edge electric field shear) and help measure $q(r)$ profiles. A Lithium Pellet Injector will be installed with solid and powder (micro-pellet) injection capability for lithium or boron or other low-z pellet injection at controllable velocities from low velocities (20 m/s) for edge deposition to high velocities (400 m/s) for deeper deposition in FY 03.

Super-Sonic Gas Injector - The gas fueling has been a primary method of plasma fueling thus far. An in-board gas injector installed on NSTX in FY 02 improved the quality of the H-mode. An improved version of the in-board gas injector with improved control capability is being implemented in FY 03. Another system being implemented is the super-sonic gas injector. On Tore-Supra, the edge recycling was significantly reduced by the use of the super-sonic gas injector. The reported fueling efficiency of the nozzle is much greater than that of conventional gas injectors. Direct benefits to NSTX are the possibility of achieving higher densities with lower recycling which could contribute to improved plasma operations in the near-term. A supersonic Laval nozzle concept is under investigation for installation on NSTX in FY 03. The applications of the nozzle include not only the fueling, but also possible experiments on density profile control, ITB and MHD control and the utilization of the nozzle for diagnostic purposes, such as impurity injection for transport studies, GPI, and edge temperature and density measurements based on helium line ratios.

Deuterium Ice Pellet Injector - NSTX will install a multi-barrel, deuterium pellet fueling system to be used in studies of density profile control, transport barrier formation, and the modeling and development of transport barrier formation scenarios. The goal is to produce density perturbations on NSTX that generate or lower the power threshold for transport barrier formation. A candidate port for installation of the deuterium pellet the is at the end of the Bay-L

Pump Duct for midplane and possibly near-inner wall injection using guide tubes. The installation is envisioned in FY 05

CT (Compact Toroid) Injection - For a longer term research element, the ST reactor needs an attractive way of fueling the plasma core. The CT injector is an attractive fueling option for the ST configuration since one can take the advantage of the relatively low magnetic field and strong field gradient for good penetration and localized deposition. The CT injection has been explored in experiments in TdeV tokamak with some success. The implementation of the CT injector is envisioned in FY 07-08.

Divertor Cryo-pump - In the area of power and particle handling, which is likely to be required for non-inductively sustained long-pulse discharge operations, the divertor cryo-pump offers a promising solution. A schematic of the divertor cryo-pump is shown in Fig. 2.9. This system will allow the pumped divertor operations in the double-null high-triangularity discharges needed for the advanced ST operations. A conceptual study has been performed to assess technical options for feasible boundary neutral pressure control using divertor cryo-pumps. Conceptual designs for installation of upper and lower divertor cryo-pumps are in progress. The system will be fabricated in FY 04 and installed during the secondary passive plates modification in FY 05.

Liquid Surface Module - High performance (H-mode) plasmas are expected to continue as a standard operational scenario for NSTX. New density control techniques will be required to optimize H-modes. One approach that promises to provide particle removal, and also has potential power handling capability, is the liquid surface module (LSM). A major effort involving national laboratories and universities, called the Applications of Liquid-plasma Interactions Science and Technology (ALIST) Working Group supported by VLT, is developing the LSM as an enabling technology for NSTX. Its goal is to exhaust $2 - 5 \times 10^{21}$ particles/s for up to 5 s, by exposing a liquid lithium surface of about one square meter to the plasma. A concept for a divertor LSM is shown in the Fig. 2.10. The effectiveness of the particle pumping is based on measured hydrogen retention rates approaching 100%. Simulations show that new, highly stable plasma regimes, with flat electron temperature profiles and high edge temperatures, can be achieved for the first time with the extremely low edge recycling the LSM can provide. Calculations based on the measured temperature dependence of lithium evaporation rates

indicate that liquid lithium flow rates of 7 – 12 m/s are needed. Since this requirement is related to power handling, the LSM can test capabilities that can be scaled to the full requirements of fusion plasmas. As with all new technologies, there are several concerns that have to be resolved before the LSM is implemented in NSTX. These include liquid lithium MHD effects, and the consequences of ELM's, thermoelectric currents, and plasma wind. Extensive experimental and computational work is in progress to address these issues, so a decision for proceeding with the final LSM design can be made at the end of FY03. The final decision for the implementation will be made in FY 06 based on the design/modeling and the experimental results from concept exploration experiments such as CDX-U.

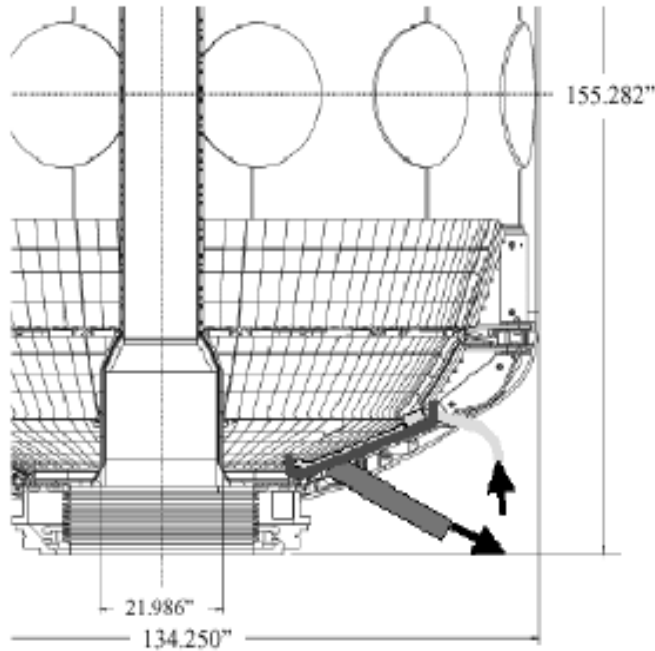


Fig.2.10. Liquid Lithium Module Schematic

2.3.4. Computer and Data Acquisition Systems

The NSTX Central I&C System have been ramping up rapidly on NSTX with the increased sophistication of the plasma diagnostic and control systems. The NSTX Central I&C System is composed of the following elements: an EPICS process control and monitoring infrastructure, a real-time plasma control system, a dual computer network, inter-system communications and data transfer for secure and open subsystems, a safety interlock and access control system, and a master timing and synchronization system. The MDSplus data acquisition system provides for sampling, acquisition, storage and display of diagnostic data, and synchronization of data sampling from master clock events. A total of 5 CAMAC highways, 2 data acquisition, 2 facilities and one NBI, provide communications to the primary control computers. There are over 90 CAMAC crates online. A 100mbps network infrastructure, which is now at full capacity, is the primary path for data analysis on the UNIX cluster and for data distribution and viewing. An NSTX diagnostic fiber infrastructure of 100 channels was completed in FY01. The new Sky II Plasma Control System was put online using the FPDP Input Multiplexing Modules (FIMM) in FY02. This new communications technique provides DMA Sky access for many additional data

channels on one fiber link. Here, we will not cover the plasma control system since a detailed description is already given in the Integration and Control Section.

In Fig. 2.11, the rapid increase in the data processing capability is shown. The pace of the ramp-up will continue as

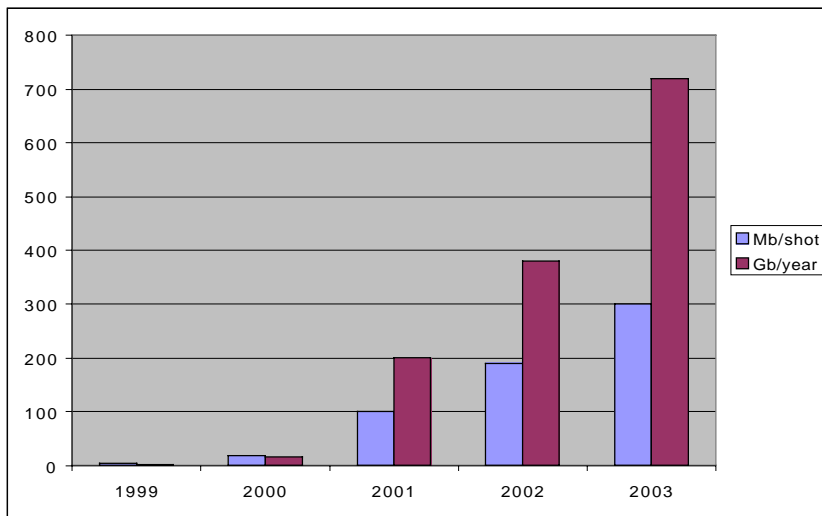


Fig. 2.11. The data acquisition capability on NSTX.

more advanced diagnostics are being implemented aided by the advance in the data processing and storage technology. The storage capability should increase by about 100 Mb/shot each year for a foreseeable future.

2.4. Auxiliary Systems

2.4.1. NBI System

The NBI system has been a workhorse of the NSTX high beta / high confinement investigation. The NBI system reliability thus far has been excellent and it has delivered 7 MW of heating power well above the 5 MW design value. The NBI system will undergo some minor upgrades to the control system, which is more than 20 years old. The system will be also improved to enable finer modulation and feed-back capability with the plasma control system.

2.4.2. HHFW System

The NSTX HHFW system is perhaps the most sophisticated high power radio-frequency antenna system to date with 12-antenna-element real time phasing control system. In Fig. 2.12, we show a schematic of the digital phase feedback control system which controls the phases among antennas 1 - 6. The relative phase is repeated for antennas 6 - 12. The decouplers compensate

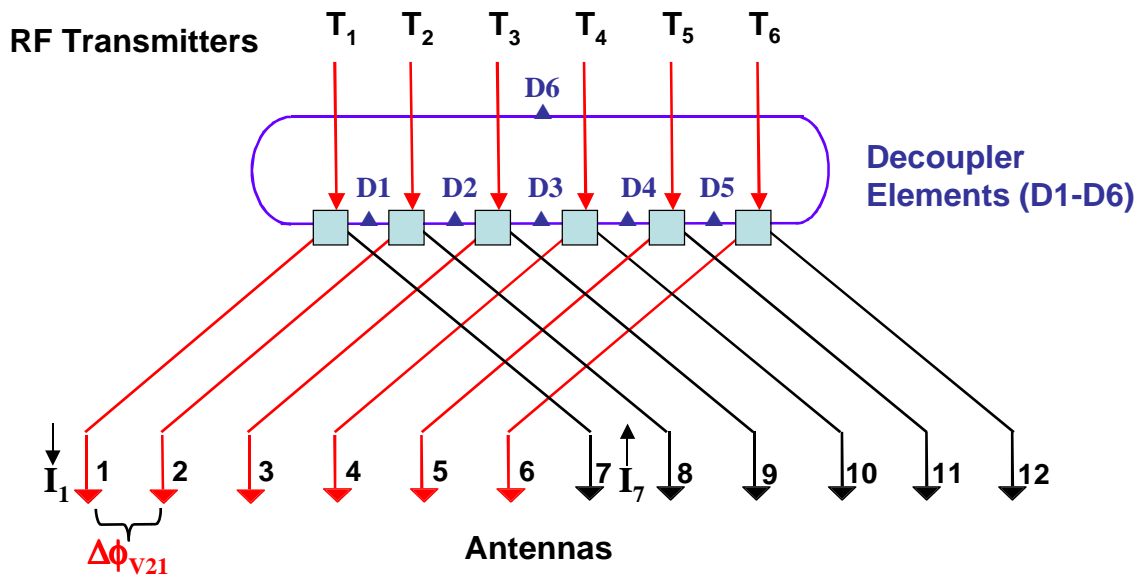


Fig. 2.12. A schematic the digital phase feedback control system.

for the large mutual coupling between antenna elements, allowing phase control.

The phasing control implementation has been successful and the system has been operated with preprogrammed phase control mode. Moving toward the feed-back mode with the plasma control system should be relatively straight forward, once the plasma response to the HHFW power is well characterized.

The operationally, the HHFW antennas had some reliability problem during the plasma operations. The antenna voltage stand-off capability significantly decreased from the vacuum conditioning value during the plasma operations. In fact, the power level of HHFW FY 02 experimental campaign was held below 3 MW due to the antenna arcing problem. During the visible examination of the antennas during the summer of 2002 outage, arc tracks in the feed-thru throat area were discovered. It should be noted that the HHFW antenna feed design was adopted from the successful TFTR ICRF antenna design. Perhaps because of low toroidal field nature of NSTX, the plasma radial diffusion in the edge scrape-off layer is much larger than TFTR. The problem may be worse during the RF pulse as evident by the pressure rise in the back of the antenna. To improve the situation, the antenna feed-thru area is modified. As shown in Fig. XX, the antenna feed-thru was thinned down by about 5 mm in radius. This increases the gap distance by 50%. If the breakdown conditioned is determined by the gap distance, then the breakdown rf power level should improve considerably. In addition, a corona ring was added in each feed-thru area to smooth the feed-area transition. In the future, if a further power handling improvement is needed, the antenna can be modified to use the end-feed, center-ground design. This will reduce the voltage on the feed-thru by roughly a factor of two or increase the power handling capability by a factor of 4.

2.4.3. EBW System

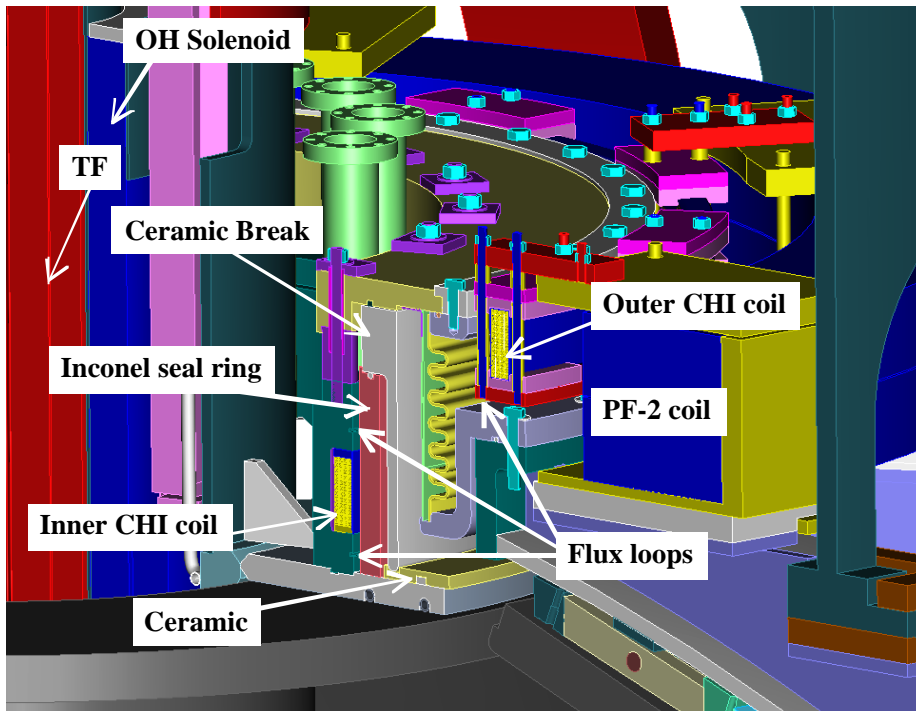
The EBW system is envisioned as a tool to control the plasma current profile for the NTM stabilization as demonstrated successfully for tokamaks by the utilization of ECCD. The EBW system can be also utilized to aid the plasma start-up. The choice of frequency will be decided by the EBW emission measurements as well as the modeling calculations in FY 03. The choice

of frequency is likely to be around 15 GHz. This is a frequency range where no existing high power tube is readily available commercially. However, the gyrotron tube technology can be applied in relatively straightforward fashion for a one MW tube. The 3 MW system is envisioned in FY 06 -07 time. The system schedule is the engineering of the system in FY 04 along with the 1 MW tube development. In FY 05, the system and related infrastructure is constructed. In FY 06, the initial 1 MW system is completed and tested. The EBW system build up to 3 MW will continue and the full capability should be available in FY 08.

2.4.4. CHI System

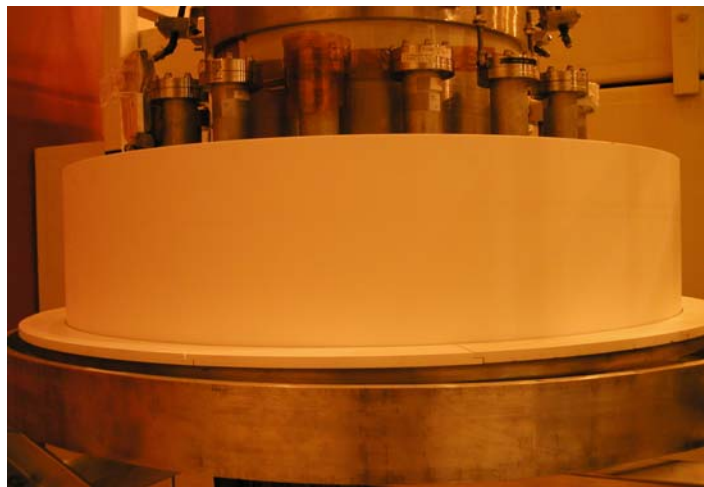
The near term goal for the CHI system is to improve its reliability at high bias voltage and high power. In the past, the absorber arcs and other external arcs have severely limited its operations. To solve the arcing problems, the following improvements are being implemented:

- A new absorber ceramic insulator assembly was designed and installed on NSTX. A picture of the insulator ring and the schematic of the absorber section is shown in Fig. 2.13 (a) and (b)The new ceramic insulator has the following number of improvements from the old design.
- Insulator on high field side - Since the unconfined plasmas in the absorber region tend to flow toward the low field direction, the original low field side ceramic likely suffered from the plasma induced arcs. The new high field side ceramic insulator should solve the absorber arc problem since plasma tends to move away from the surface. This type of absorber design was used successfully on the HIT devices.
- No simple connection path in insulator region - The potential arc path is now far longer and arduous than the previous design.
- Coils to produce local poloidal field to reduce stray field from plasma and PF coils, 1kA peak current - By reducing the local poloidal field in the absorber region, one can increase the arc path length significantly.
- Flux loops to measure field in absorber region will permit feedback - The control of the CHI driven plasma is the next major research topic on NSTX.



(a)

Fig. 2.13. (a) Absorber Ceramic Insulation Assembly Schematic. (b) Absorber Ceramic Ring Structure and ceramic floor mat.



(B)

As the applied voltage was increased, additional arcs occurred to the ex-vessel components in FY 02. In particular, the G-10 insulators, which surround the bolts in the CHI ceramic insulator assembly, developed arcs. An examination showed that the arc has started in the gap in the two-piece G-10 insulator. Those insulators are replaced with ones with a single piece design. In addition, the voltage surge protection diodes were moved close to the device. Previously it was located on the power supply side some distance away from the device. Because of the fast transient voltage spikes associated with

CHI discharges (as shown by the fast voltage monitor), it was decided that the diodes must be moved close to the machine.

The new CHI absorber insulator will be tested in FY 03. The null field coils will be implemented and tested in FY 04.

2.4.5. RWM/Error Field Correction Coil System

The Resistive Wall Mode (RWM) / Error Field Correction Coil System is being described in the dedicated MHD section in detail and therefore will not be covered here. The characterization of the RWM / Error Field will be investigated by the sensor system being implemented in FY 03. Once the characterization is completed, an active feed-back coil (Phase-I) which is likely to be an external coil system will be implemented in FY 04. After the experimental results from the Phase-I coils become available, together with the modeling, the system is expected to be upgraded to Phase-II coils, this could include some internal coil system in FY 05-06.

2.5. Plasma Diagnostic Upgrades

In Table 2.6, a list of known diagnostic upgrades are shown. The gray areas depict the upgrade system implementation period.

upgrade	comments	integration	MHD	transport	boundary	CHI	H-FW	EBW	FY03	FY04	FY05	FY06	FY07	FY08
Divertor SPRED	div. Impurities	x			x									
Additional filtered cameras	2 cameras, Da				x									
CS & divertor probe arrays	SOL profiles (20 ch)				x									
Horiz. divertor bolometer	4-16 element	x		x	x	x								
Vert. divertor bolometer	add. view for tomog.	x		x	x	x								
Additional IR camera	compact type	x			x									
Fast IR camera	30-100 kHz, periscope	x			x	x								
Additional fast gauges	Edge recycling				x	x								
Divertor visible spectrometer	flow measurements				x	x								
Helium beam spectroscopy	edge profiles	x	x	x	x			x						
Divertor Thomson scattering	1 laser, 20 ch	x		x	x									
x-point reciprocating probe	Divertor parameters				x									
DIMES probe	Surface physics				x									
MPTS (20-30 ch)	enhanced spatial res.	x	x	x	x	x	x	x						
MPTS (30-40 ch)	enhanced edge res.	x	x	x	x	x	x	x						
MPTS add. laser (60-90 Hz)	enhanced time res.	x	x	x	x	x	x	x						
Additional FIRETIP channels	n(r), B-T(r)	x	x	x	x	x	x	x						
Fast CHERS	~ 1 ms resolution	x	x	x	x									
Poloidal CHERS	vf, Er	x	x	x										
MSE (10 ch)	q(r) profile	x	x	x		x	x	x						
MSE (19 ch)	q(r) profile	x	x	x		x	x	x						
MSE LIF	E(r) profile	x	x	x		x	x	x						
Neutron collimator	neutron source profile				x									
Radial inter./polarim	j(0), DB, Dn			x	x									
Microwave backscattering	B(r), Med-k turbulence				x									
Tangential scattering	high k turbulence				x									
Impurity injector	laser blow-off				x									
Imaging reflectometer	low k turbulence				x									
Charged fusion product det	neutron source profile				x									
Additional magnetics	EFT	x	x	x	x	x	x	x						
New diagnostic access		x	x	x	x	x	x	x						

Table 2.6. A list of diagnostic upgrades

3.1 MHD

3.1.1 Macroscopic Stability Overview for 2002

Optimizing plasma stability in the spherical torus

Plasma stability at high plasma pressure is required for economically attractive operation of a thermonuclear fusion reactor based on magnetic confinement. For nearly all magnetic confinement concepts, engineering constraints limit the maximum magnetic field that can be applied to contain the plasma, so an important figure of merit for magnetic fusion devices is the plasma beta $\beta \equiv 2\mu_0 p/B^2$ where p is the plasma pressure and B is the magnetic field within the plasma. For tokamak plasmas, the plasma pressure can vary significantly across the plasma cross-section and the applied toroidal field dominates the total field and varies comparatively little within the plasma. Thus, a commonly used tokamak figure of merit is the toroidal beta $\beta_t \equiv 2\mu_0 \langle p \rangle / B_{T0}^2$ where $\langle p \rangle$ is the volume-averaged pressure and B_{T0} is the vacuum toroidal field at the plasma geometric center. Experiments to date have shown that ideal magnetohydrodynamic (MHD) stability theory provides an accurate description of the maximum stable beta for tokamak plasmas. It is expected that this should also be true for spherical torus [1] (ST) plasmas. However, the high beta and low aspect ratio geometry of the ST can lead to significant alteration of stability physics in certain important respects. Beta limit dependencies on equilibrium profiles and boundary shapes, the role of elevated safety factor, the alteration of global mode structure, the role of high rotation and rotational shear, the magnitude and physical mechanism of plasma rotation damping due to instabilities, and enhanced drive for fast-ion driven instabilities are all instances of stability physics that must be independently evaluated for the ST concept.

For the advanced tokamak (AT) and spherical torus (ST) concepts to lead to efficient steady-state reactors, high beta alone is insufficient. In particular, most reactor design studies have shown that it is important to have a large fraction of the plasma current be self-generated through the neoclassical bootstrap effect to minimize power requirements for auxiliary systems. Plasma current profiles in largely bootstrap current driven equilibria are generally broad with low plasma internal inductance, l_i . Tokamak experience has shown that another important beta parameter, the normalized beta $\beta_N \equiv \beta_t(\%) a B_0 / I_P(MA)$ may decrease with decreasing l_i [2,3,4]. Since $\beta_t \propto \beta_N^2$ when the bootstrap fraction is held fixed, it is critical to test such scalings in both the AT and ST.

The potential incompatibility between high β and efficient self-sustainment has motivated several theoretical investigations of the stabilization of highly-bootstrapped AT [5,6] and ST [7] plasmas. Significant experimental progress has already been made in removing this incompatibility in advanced tokamak plasmas by combining conducting structure (wall stabilization) with plasma rotation [8,9] and feedback systems [10] to achieve values of β_t significantly above the level possible without stabilizing systems [11]. Applying this experience and understanding to the ST is particularly important, since

design studies [12] indicate that a self-sustained ST reactor would require β_N values far above and I_i values well below those achieved in present advanced tokamaks.

A main focus of MHD studies in NSTX in the coming five years will be to determine the specific requirements for ST plasma beta optimization in discharges lasting significantly longer than a current diffusion time with beta values significantly above the non-wall stabilized limit with most of the plasma current being self-generated. The following text describes recent progress toward this goal and the associated physics understanding. Modes which are not presently, but are potentially, beta limiting are also discussed. The section ends with a summary of proposed work to be performed over the next five years.

Recent macroscopic stability improvements

NSTX has made significant progress during the past year in reaching high beta under a wide range of operating conditions. As seen in Figure 1, normalized beta values of $\beta_N > 6$ were achieved during the FY2002 run (shown in red) for normalized currents in the range of 2.5 to 5 MA/mT. By operating at high normalized current $I_p/aB_{T0} > 6$ with $I_p=1.2$ MA and $B_{T0}=0.3$ Tesla, toroidal beta values as high as $\beta_t=35\%$ with $\beta_N > 5$ were achieved. As seen in the figure, both β_T and β_N values have increased by as much as a factor of 2 relative to operation in FY2001.

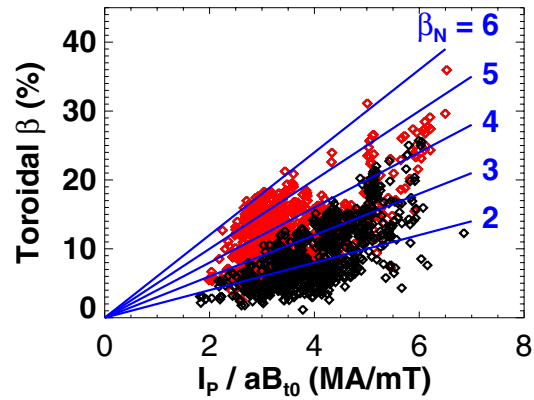


Figure 1 – Toroidal β (%) vs. I/aB [MA/mT]

Future steady-state ST devices will need to rely heavily on the neoclassical bootstrap current to generate most of the toroidal plasma current, so achieving high values of poloidal beta is essential to the ST concept. Figure 2 shows that NSTX has more than doubled its poloidal beta values in the last year and has achieved $\epsilon\beta_p \approx 0.8-1$ for cylindrical kink safety factor $q^* = 2.5$ to 3.5 where $q^* \equiv 20\epsilon\beta_p/\beta_N$. For reference, the NSTX $\beta_T=40\%$ target with bootstrap fraction $f_{BS} = 75\%$, $q^* = 2.1$ and $\beta_N = 8.5$ is shown by the green star symbol in Figure 2 and has a similar $\epsilon\beta_p$ value. As seen in the same

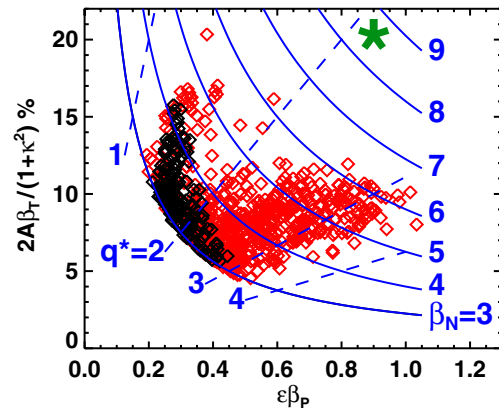


Figure 2 – Poloidal and normalized β vs. q^*

figure, a roughly 35% increase in β_N is now needed to access β_N values > 8 typical of fully self-sustaining ST based reactor and component test facility concepts.

Several operational and facility improvements aided in achieving the high stability parameters shown above. These improvements include error field reduction, more optimal plasma profiles from reliable H-mode access, improved plasma shaping, and elevated plasma safety factor. The influence of these improvements is discussed below.

Error Field Reduction

Resonant error fields resulting from loss of axi-symmetry due to coil misalignments and other construction imperfections are well known to potentially lead to tokamak performance degradation [13,14,15]. This process appears to be particularly important near and above the ideal no-wall limit [11] where error field amplification can lead to strong rotation damping and possible destabilization of the resistive wall mode (RWM) in advanced operating regimes. Early in the commissioning and calibration of the NSTX locked-mode detectors it became apparent that a large effective shift of the lower PF5 vertical field coil was generating predominantly $n=1$ error-field over much of the NSTX plasma volume. The coil was subsequently shifted and re-shaped to minimize the $n=1$ error field component. Measurements of the corrected coil shape indicate that the $n=1$ error field strength has been reduced by an order of magnitude. This reduction led immediately to improved performance - most noticeably in the locking behavior of ohmic discharges and beam-heated H-mode discharges. Figures 3 illustrates that prior to error field reduction (black curves) ohmic discharges routinely exhibited minor disruptions in plasma current and major disruptions in plasma density during the I_p flat-top phase. In contrast, the red curves in Figure 3 show that following error field reduction there is no locking behavior evident until the solenoid current limit is reached (near $t=290\text{ms}$) and strong negative loop voltage is applied which disrupts the plasma. Internal toroidal arrays of radial and vertical field sensors placed above and below the midplane are presently being commissioned on NSTX to better diagnose the helical structure of error fields, locked modes, and resistive wall modes. These sensors will be placed much closer to the plasma surface to better detect the reduced amplitude locked modes and resistive wall modes.

Measurements of the corrected coil shape indicate that the $n=1$ error field strength has been reduced by an order of magnitude. This reduction led immediately to improved performance - most noticeably in the locking behavior of ohmic discharges and beam-heated H-mode discharges. Figures 3 illustrates that prior to error field reduction (black curves) ohmic discharges routinely exhibited minor disruptions in plasma current and major disruptions in plasma density during the I_p flat-top phase. In contrast, the red curves in Figure 3 show that following error field reduction there is no locking behavior evident until the solenoid current limit is reached (near $t=290\text{ms}$) and strong negative loop voltage is applied which disrupts the plasma. Internal toroidal arrays of radial and vertical field sensors placed above and below the midplane are presently being commissioned on NSTX to better diagnose the helical structure of error fields, locked modes, and resistive wall modes. These sensors will be placed much closer to the plasma surface to better detect the reduced amplitude locked modes and resistive wall modes.

Plasma profile effects

In addition to error field reduction, NSTX now has the capability of high-temperature (350°C) bake-out of its graphite plasma facing components. This has led to comparatively easy access to the H-mode and significantly broader pressure profiles that are predicted to improve stability in various NSTX operating regimes. These

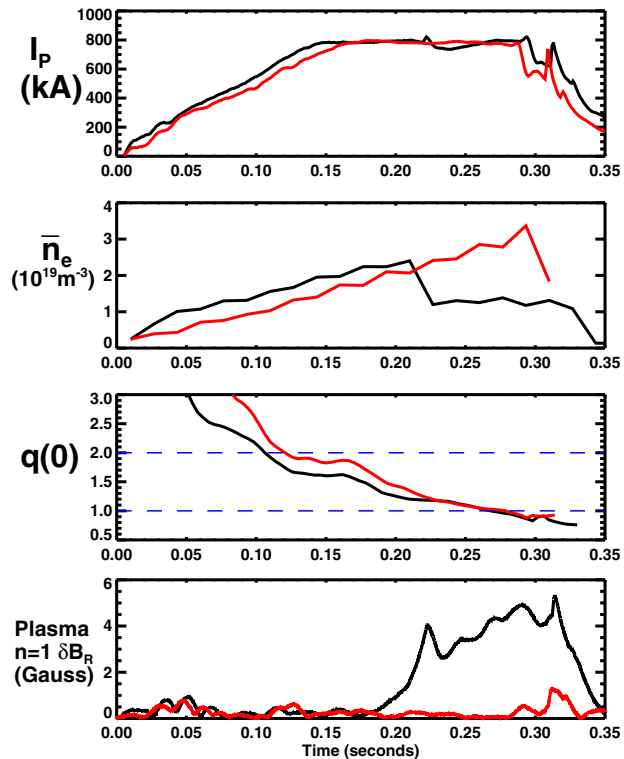


Figure 3 - Locked mode signatures before (black) and after error (red) field correction

improvements are synergistic, as H-mode operation prior to error field reduction was often degraded by the excitation of 2/1 tearing modes which routinely slowed, locked, and disrupted the plasma [16]. Consistent with theoretical expectations discussed above, Figure 4 shows a clear trend of increasing β_N with decreasing pressure peaking factor $p(0)/\langle p \rangle$ in NSTX. In this figure, the pressure peaking is determined as a best fit to external poloidal magnetics, the measured diamagnetic flux, and a scaled electron pressure profile as a loose fitting constraint. This peaking factor is typically well correlated to the peaking factor of the thermal pressure component of NSTX plasmas.

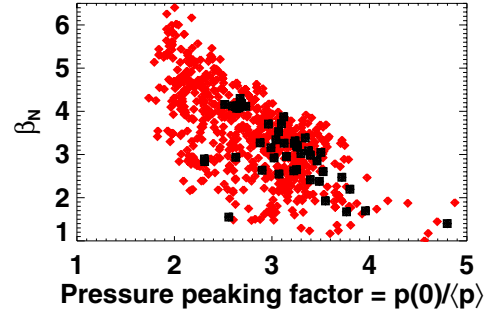


Figure 4 - β_N versus pressure peaking

Broad current profiles from the large off-axis bootstrap current density resulting from these broad pressure profiles are also predicted to improve wall stabilized beta limits by removing low order mode-rational surfaces. Given the research goal of accessing very low l_i regimes at high β_N , an important question in NSTX stability research is the beta limit scaling with internal inductance. As stated above, some higher aspect ratio experiments have shown that the no-wall normalized beta limit obeys $\beta_N \approx 4 \times l_i$ [4]. Figure 5 shows that this empirical limit has been exceeded by a factor of 2.5 at intermediate values of $l_i = 0.6$, and shows that even $\langle \beta_N \rangle \equiv \langle \beta \rangle a_{T0} / I_P$ where $\langle \beta \rangle \equiv 2\mu_0 \langle p \rangle / \langle B^2 \rangle$ exceeds $4 \times l_i$ by as much as a factor of 1.7. Perhaps more important than the high β_N / l_i ratio is the trend of increasing β_N with decreasing l_i evident in the figures. Determining if this trend is upheld at lower l_i is an important research topic, and future experiments will develop lower l_i discharges to investigate beta limits at l_i values approaching those of the NSTX design target.

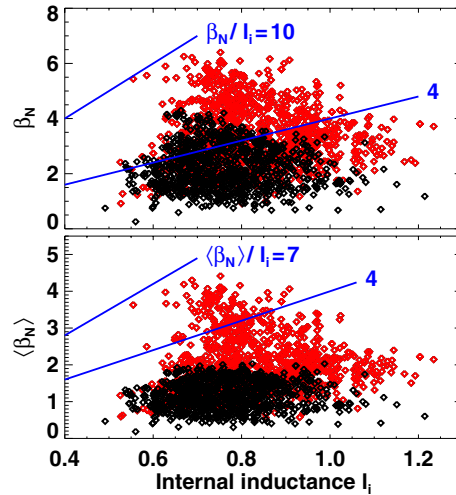


Figure 5 - β_N versus internal inductance

Influence of plasma shape

Increased plasma shaping is well known to improve tokamak ideal MHD stability, and NSTX is now able to routinely access significantly higher elongation and triangularity. As seen by the black symbols in Figure 6, there was previously little advantage to operating with elongation much above 1.8 in most discharges. Stability analysis for L-mode discharges obtained prior to machine improvements found that $n=1$ internal pressure-

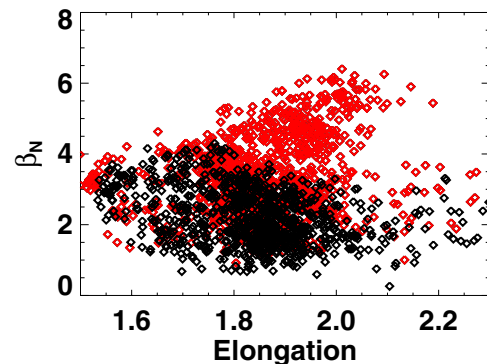


Figure 6 - β_N versus boundary elongation

driven kink mode stability is degraded for elongation values above 1.8 when the pressure profile is sufficiently peaked - consistent with the data shown in Figure 6. For the data following machine improvements shown in red, the broader pressure profile reduces the internal kink drive and excites a more global $n=1$ mode which is more sensitive to boundary shaping and the influence of wall stabilization. Importantly, NSTX data now shows a trend of increasing β_N with increasing elongation up to at least $\kappa=2.1$. The NSTX vertical control system is presently being upgraded to allow more routine access to even higher elongation to further test this trend.

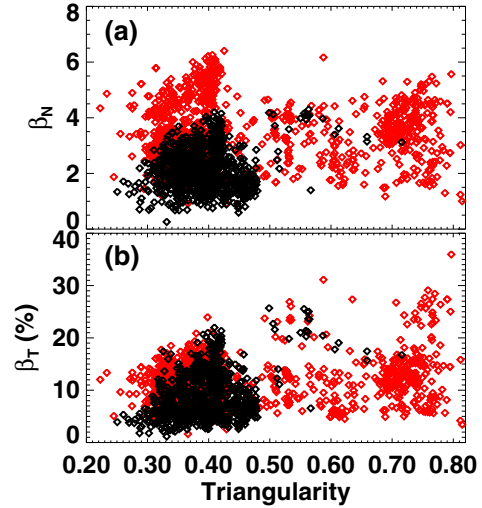


Figure 7 - β_N versus boundary triangularity

As seen in Figure 7, NSTX also now more routinely operates at higher triangularity up to $\delta = 0.8$. Figure 7a shows that there is a relatively weak dependence of β_N on triangularity for $\delta > 0.4$, but as seen in Figure 7b, the highest β_T values have been achieved at the highest triangularities. Thus, the increase in β_T is a result of the ability to operate at higher normalized current presumably due to the increased edge safety factor and shear at high δ . Figure 7a also shows that β_N values have increased for all triangularities - consistent with the finding that much of the improved stability in NSTX has come from decreased pressure profile peaking.

Beta limiting modes

Pressure-driven kink-ballooning modes and resistive wall modes have been previously shown to be beta-limiting in NBI-heated NSTX discharges [17]. Neoclassical tearing modes have also recently been shown to be a concern for any ST operating regime which relies upon high poloidal beta and bootstrap fraction [18]. The following subsections discuss the modes typically observed to limit performance at the highest β_T and β_P values achieved following recent machine improvements.

Limiting modes in highest β_T discharges

Figure 2 shows that the present operating limit of $\beta_N \approx 6$ restricts the accessible β_P and bootstrap fraction for the highest β_T discharges at low $q^* < 2$. Such discharges also often have low central

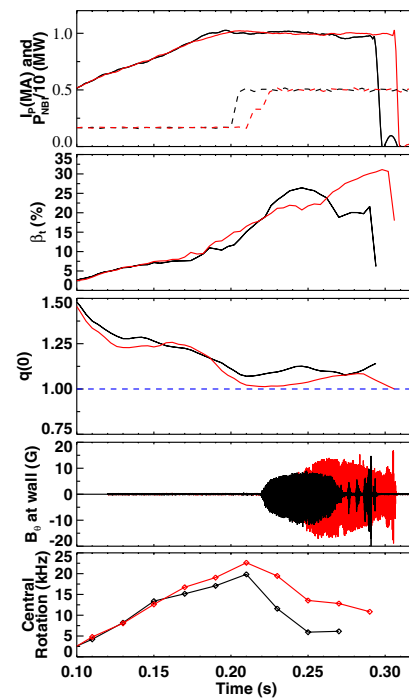


Figure 8 – Time traces of two high β_T discharges and 1/1 mode amplitudes.

safety factor near 1 at high β . In such discharges, large $n = 1$ pressure-driven internal kink modes are computed to be ideally unstable and are observed to grow on 5 to 20ms time-scales and often exhibit saturation followed by slow amplitude decay. These large internal $m/n = 1/1$ modes can also lead to saturation in β , degradation in plasma rotation, and sometimes rapid disruption. An example of such behavior for two 1MA discharges with $B_{T0} = 3\text{kG}$ which reach $\beta_T = 25\%$ and 31% is shown in Figure 8. As seen in the figure, β_T exhibits saturation from $t=225\text{ms}$ to 260ms in both discharges despite the previous increase in NBI heating power by a factor of 3. The highest β_T discharge in Figure 8 is unique in that the limiting mode amplitude decreases after $t=260\text{ms}$ allowing the stored energy to increase and ultimately reach $\beta_p = 0.7$ and $\beta_N = 6.2$ prior to undergoing an uncommonly rapid 400MA/s plasma current disruption. Insight into the structure of this limiting $1/1$ has been gained by correlating the plasma rotation profiles to fluctuation spectra from the NSTX ultra-soft X-ray (USXR) array. These studies confirm that a wide region of very weak shear and $q \approx 1$ likely contribute to the rapidity of the discharge termination.

Limiting modes in high β_p long-pulse discharges

In contrast to the lower β_p achievable at high β_T , Figure 9 shows time-traces of a typical high $\beta_p=1.2$ discharge with $I_p=800\text{kA}$, $B_{T0}=4.5\text{kG}$, and bootstrap current fraction of 35 to 40%. Figure 9a shows that during the first 400ms of this discharge, an $n=2$ mode is measured to initiate near 300ms coincident with a short burst (amplitude spike) of $n=1$ activity. At $t=430\text{ms}$, Figure 9c shows that another burst of $n=1$ activity causes a drop in β_p followed by a subsequent re-heat of the plasma. After this burst at 430ms, Figure 9d shows that a longer-lived lower-frequency $n=1$ mode initiates which may be a neoclassical tearing mode (NTM). Figure 9e shows that each continuous mode and $n=1$ burst event decreases the central rotation speed, and following the second collapse in β_p at $t=500\text{ms}$, the rotation decay is accelerated. Finally, Figure 9f shows that after the plasma rotation is everywhere below approximately 2 to 4kHz, the $n=1$ locked-mode signal increases rapidly and leads to a rapid decay in β_p prior to beam turn off at $t=600\text{ms}$. Clearly, understanding the origin of the bursting $n=1$ modes and the other continuous and long-lived modes they trigger at high β_p and β_N is an important element to further lengthening NSTX discharges and raising β_N .

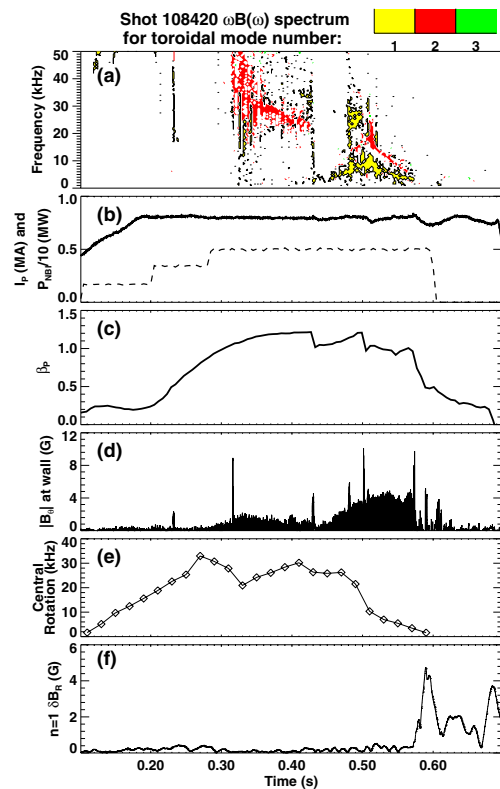


Figure 9 – Time traces of a high β_p discharge (a-c) and rotating and non-rotating ($n=1$) mode amplitudes (d,f).

To attempt to better understand the limiting modes observed in Figure 9 above, the time-evolution of the $n=1$ ideal MHD stability criteria computed with the DCON [19] code both with and without a conducting wall is shown in Figure 10 for discharge 108420. The RWM growth time as computed by the coupled DCON and VALEN [20] codes is 15 ms

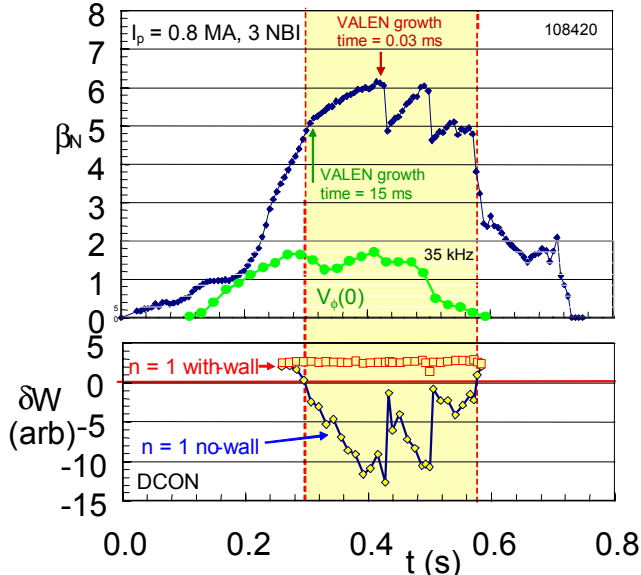


Figure 10: Evolution of β_N , V_ϕ and ideal no-wall and with-wall stability criteria for a plasma exceeding $\beta_N/\beta_{Nno-wall}=1.3$ and approaching β_{Nwall} .

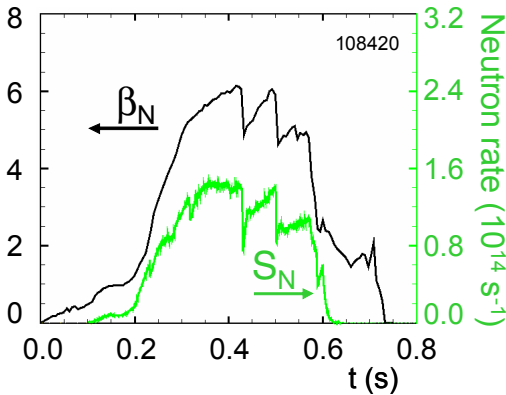


Figure 11: Correlation of neutron rate and β_N during beta collapses in high β_N plasma.

(duration of greater than $20\tau_{wall}$) at a nearly constant value of $\beta_N = 5.6$ without fast beta collapses. In the discharge shown in Figure 9, DCON shows that the plasma is also unstable to the $n=2$ mode shortly after $n=1$ instability is determined. Plasma instability to multiple n values was anticipated at high β_N , and future work will investigate the presence of $n=2$ and possibly $n=3$ signatures measured by the locked mode detector.

as β_N increases beyond the no-wall beta limit, $\beta_{Nno-wall} \approx 5$ near $t = 300$ ms. However, as β_N reaches a peak value of over 6.1, VALEN shows a greatly decreased mode growth time of 30 μs , indicating that the with-wall beta limit, β_{Nwall} , is being approached and passive wall stabilization has become less effective. At this point, a beta collapse occurs in the plasma reducing β_N to 4.8. The ideal $n=1$ no-wall stability criterion computed by DCON shows this value to be close to marginal stability. The collapse occurs over a few hundred microseconds, consistent with an ideal mode being heated through the stability limit. In addition, this initial, and subsequent beta collapses correlate exactly with collapses of the measured neutron rate as shown in Figure 11. Since neutron creation occurs almost exclusively in the plasma core, the collapses indicate that the mode is internal. Using the relatively large value of $\tau_{wall} = 15$ ms for the $n=1$ RWM perturbation computed with DCON and VALEN when β_N initially exceeds $\beta_{Nno-wall}$, a conservative estimate of the plasma duration with $\beta_N/\beta_{Nno-wall}$ greater than unity is $18\tau_{wall}$. The fast, repeated beta collapses shown in Figure 9 are correlated with the magnitude of β_N , since similar plasmas have been maintained for longer pulse lengths

Rotation damping - resistive wall modes and rapidly rotating modes

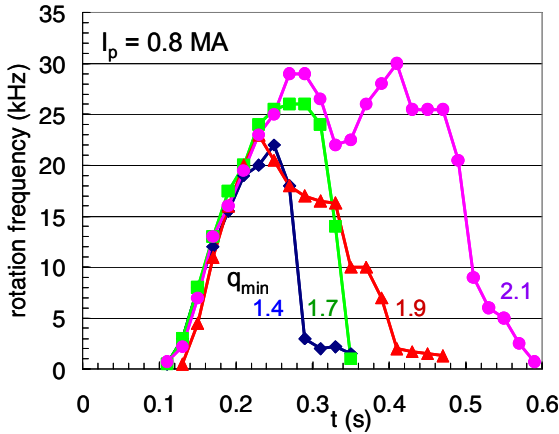


Figure 12: Alteration of rotation evolution at constant $I_p = 0.8$ MA and increasing B_t .

Figure 12 shows the evolution of the toroidal rotation frequency in the core of the plasma for several values of B_{T0} . Also shown is the EFIT computed q_{min} for each plasma at peak β_N . RWMs are observed in the discharges with $B_{T0} = 0.34$ T ($q_{min} = 1.4$) and $B_{T0} = 0.39$ T ($q_{min} = 1.7$), leading to the rapid core rotation damping. However, as B_{T0} is raised to 0.44 T ($q_{min} = 1.9$), the $n=1$ signature of the RWM is no longer apparent in the locked mode detector signal, the rotation damping rate significantly decreases, and the pulse length is extended. The fourth case shown also has $B_{T0} = 0.44$ T, but has slightly different plasma cross-section (increased elongation) and the computed q_{min} rises to slightly above 2. Empirically, systematic analysis of EFIT reconstructions (without internal magnetic field measurements from MSE) finds that only plasmas with $q_{min} > 2$ have maintained high β_N for long pulse lengths of order the current relaxation time.

Recent plasmas with reduced static error field and increased β_N exhibit significantly different behavior than RWMs at lower β_N . First, it is rare to find pure RWM activity separate from tearing mode activity. This observation might be due in part to an increased difficulty in measuring the RWM field perturbation with the present locked mode detector (LMD) at the reduced static error field. LMD signals of between 0.6 – 1.0 G are now more typical during the RWM (see Figure 13). A common feature between RWMs at high and low β_N is the strong toroidal rotation damping observed in both in spite of increased neutral beam momentum input over lower beta plasmas. The magnitude of the rotation damping, as well as the detail of the rotation profile dynamics distinguishes the RWM from tearing mode activity and suggests a very different physical mechanism for rotation damping between the two modes. In plasmas exhibiting rotating modes alone, rotation damping is relatively weak. Figure 13b illustrates the toroidal rotation profile dynamics for a plasma initially exhibiting $n=1$ and 2 rotating mode activity, with $n=2$ largely damped approximately 60 ms after the mode onset. Magnetic pickup coils show $n=1$ oscillations with a frequency slowly decreasing from 8 kHz, consistent with the observed toroidal rotation frequency, F_ϕ decrease in the region of the EFIT computed

Long pulse ST plasma operation on the order of the global resistive diffusion time with $\beta_N > \beta_{Nno-wall}$ is a goal of NSTX. Since sufficient plasma rotation is required to stabilize low- n kink/ballooning modes, the rapid rotation damping associated with RWM destabilization is potentially a major impediment in reaching this goal. However, as shown in the previous section, present results have already shown significant progress in maintaining $\beta_N > \beta_{Nno-wall}$ for many resistive wall times. A key to this success has been operation with increased applied toroidal field. Figure

$q=2$ surface. The rotation damping rate at $q=2$ is nearly constant at -29kHz/s . The profile dynamics show the damping to be diffusive, originating near the $q=2$ surface, and penetrating slowly to the plasma core. Mode locking eventually occurs 0.2s later, when rotation at $q=2$ drops to the critical value of approximately half the initial value, $\omega_0/2$. This process is in agreement with the theory of rotation damping due to a magnetic island in the presence of a conducting wall [21]. In contrast, FIG. 13a shows toroidal rotation damping occurring across most of the plasma cross-section simultaneously when the RWM is present. The process appears non-diffusive, and similar to the rotation damping process observed in error field induced locked modes when field penetration occurs [15]. The rotation damping rate near $q = 2$ in the RWM case is -174 kHz/s , six times more rapid than in the case of islands alone. It is also clear that the RWM shows only a weak signal in the locked mode detector and is accompanied by $n=1$ rotating mode activity as the RWM grows. The locked mode detector signal reaches just 0.6G before the accompanying island locks. The RWM therefore greatly reduces the time it normally

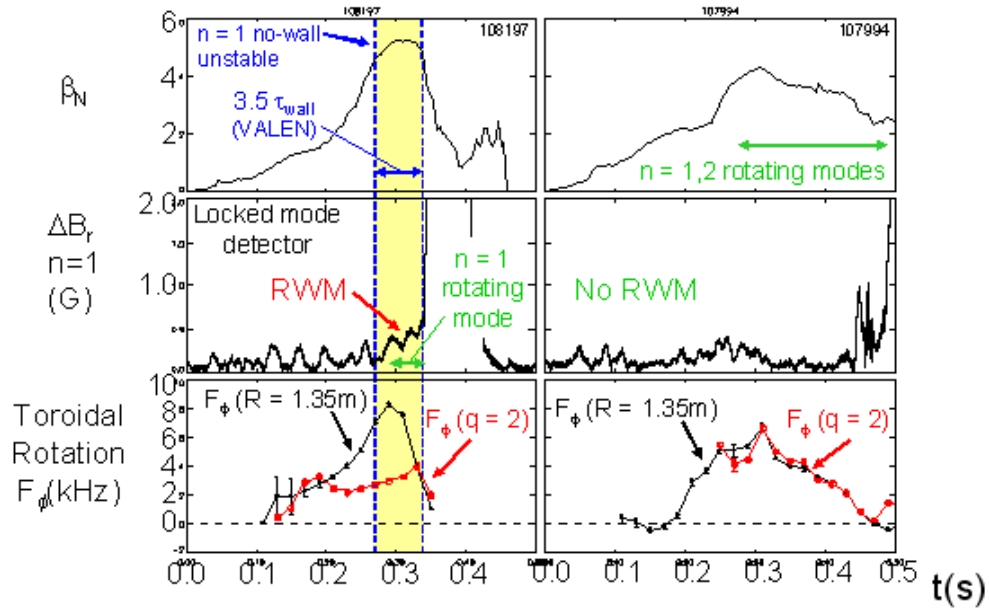


Figure 13: Evolution of β_N , locked mode signal, and toroidal rotation in recent NSTX plasmas above / below the no-wall beta limit.

takes the island to reach $\omega_0/2$. Another remarkable detail of the rotation damping process is that the edge rotation remains essentially unchanged during RWM induced rotation damping, whereas the case of slow rotation damping due to islands shows a viscous drag outside of $q = 2$. This can be qualitatively explained by invoking a model of neoclassical viscous drag in the nearly static magnetic field perturbation of the RWM [22,23]. This model has been successfully used to describe error field induced locked mode damping in JET [15]. By this physics, local rotation damping scales as $\delta B_r^2 T_i^{0.5}$, where δB_r is the local perturbed field, and T_i is the ion temperature. Therefore, it is expected that the rotation damping would be greatly reduced in the colder outer region of the plasma, consistent with the observation. The RWM growth time computed by VALEN is 20 ms , in agreement with the growth rate of the locked mode detector signal.

Neoclassical tearing modes

Prior to error field reduction and before routine H-mode operation, the effect of $q(0)$ crossing 1 varied from mild sawtoothing (if l_i was sufficiently high) to the development of large radius $n=1$ sawteeth or kink modes (for low l_i) often resulting in locked modes which disrupted the plasma. In regimes with $q(0) > 1$, $n=2$ modes were often observed to be destabilized prior to the $m/n=1/1$ becoming unstable whenever β_p exceeded 0.4 to 0.5. These $n=2$ modes had many of the characteristics of $3/2$ neoclassical tearing modes including island width evolution consistent with the modified Rutherford equation. As seen in Figure 14, the island width evolution is fit reasonably well using equation parameters similar to those of standard aspect ratio tokamaks until $t=260$ ms. At $t=270$ ms, a $1/1$ mode is measured to become unstable possibly explaining both the degraded fit just prior to $1/1$ onset and the oscillations in island width as inferred from the measured magnetic perturbation after $t=270$ ms. At present, it is not clear if the $n=2$ mode in the high β_p discharge of Figure 9 is similar to the $3/2$ NTM shown in Figure 14.

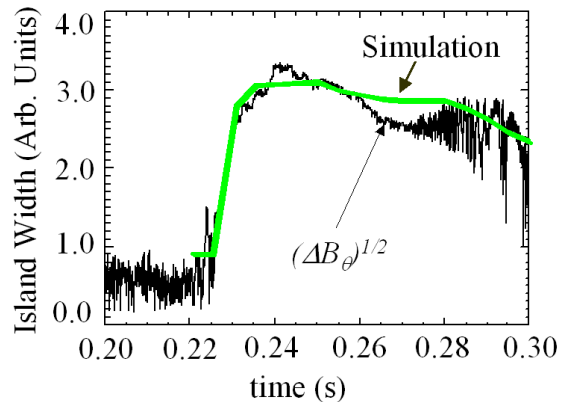


Figure 14 – Island evolution fit to a $3/2$ neoclassical tearing mode in shot 104096.

Edge localized modes

The detailed stability characteristics of edge localized modes (ELMs) have not yet been thoroughly investigated in NSTX. Empirically, separatrix configuration and shaping appear to play a large role in the type of ELMs observed. Most NSTX long-pulse discharges have favored lower single null operation both for easier H-mode access and for the longest durations free of large ELM activity. In contrast, double-null operation has thus far been more prone to larger ELMs disrupting long-pulse flat-tops. Understanding this difference is very important, as the strong shaping of highly triangular double null plasmas should enhance no-wall global stability relative to single null operation. However, ELM size also appears to be strongly related to edge fueling. Thus, edge collisionality and density effects may be complicating the interpretation of the types of ELMs observed through the edge neoclassical bootstrap current. In some modes of operation, edge MHD with some of the characteristics of an ELM can penetrate far past the pedestal region into the core plasma. This may be the result of enhanced poloidal mode coupling resulting from the enhanced toroidicity of the ST geometry. Understanding and avoiding such modes will continue to be an important element in improving long-pulse operations, since each ELM can consume a significant fraction of the available volt-seconds in the OH solenoid.

Effects of very rapid rotation

The high rotation speed of many NSTX discharges not only impacts β limits through wall stabilization, but can also modify the underlying equilibrium itself. The centrifugal force of the spinning plasma most strongly modifies force balance near the magnetic axis where the pressure gradient would otherwise be small. An outward major-radial shift in the electron density is indeed sometimes observable as shown in Figure 15 which plots profiles of electron temperature, electron density, and thermal Alfvén Mach number M_A for an MHD-quiescent L-mode discharge heated with 1.7MW of 80keV neutral beams.

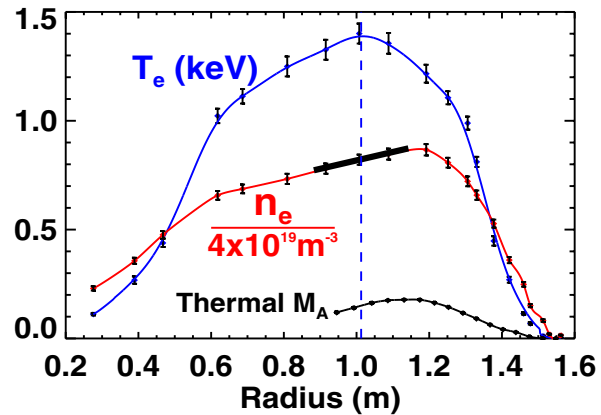


Figure 15 – Electron temperature and density profiles for a discharge showing strong in-out density asymmetry due to centrifugal effects.

For this relatively low-density discharge, approximately 2/3 of the outward centrifugal force near the axis comes from the fast ion component. The solid line overlaying the density profile in the figure represents the gradient expected from force balance arguments and is in good agreement with the measured core gradient when the fast ion centrifugal force is included.

In addition to strong flow modifying equilibria, flow shear may also impact MHD stability. Calculations using the M3D [24] code for NSTX find that for self-consistent ideal MHD equilibria with flow included, linear growth rates of $n=1$ internal pressure-driven kink modes with $q(0) < 1$ can be reduced by as much as a factor of 3 due to flow-shear. Non-linearly, if sufficient shear flow is maintained and if density and temperature within the island are anti-phase, $m/n= 1/1$ mode saturation can occur. The large saturated $1/1$ mode from M3D simulations shown in Figure 16 is consistent with the experimentally observed modes at high toroidal β as shown in Figure 8. This physics likely plays a role in the saturation of β and the gradual decay of the plasma rotation ultimately leading to mode locking and disruption.

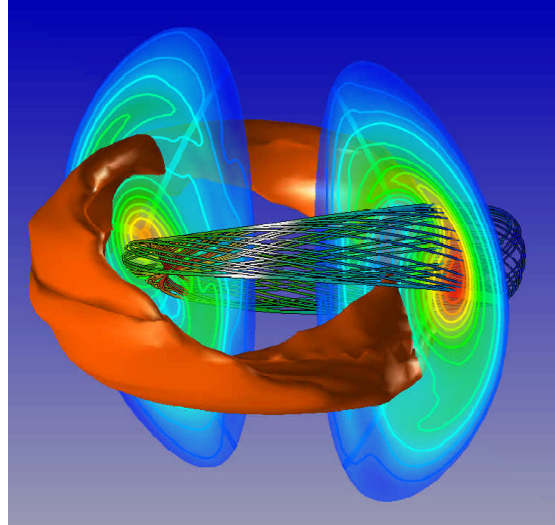


Figure 16 – Simulated contours of constant pressure (red) and island magnetic field lines (dark grey) for a saturated 1/1 mode.

Fast ion induced MHD modes

Overview

The ST in general, and NSTX in particular, is susceptible to fast ion driven instabilities due to the relatively low Alfvén speed compared to the neutral beam injection velocity which is typically 2-4 times higher. Indeed, a wide variety of beam driven instabilities has been seen in NSTX at frequencies ranging from 10's of kHz to many MHz. Three beam driven instabilities commonly seen on NSTX have been identified thus far. These include: Toroidal Alfvén Eigenmodes (TAE) or Energetic Particle Modes (EPM), fishbone-type instabilities, and Compressional Alfvén Eigenmodes (CAE). In addition, less well identified modes have also been observed. An example of a typical spectrum of MHD activity in the frequency range up to 150 kHz during NBI on NSTX is shown in Figure 17. This range includes the EPM, TAE, and fishbone, but excludes the “compressional” Alfvénic mode (CAE) activity. The first shear Alfvénic gap - the toroidal Alfvén eigenmode gap - for NSTX occurs at frequencies between about 50 and 150 kHz. These instabilities have, for the most part, an insignificant affect on fast ion confinement or performance. One exception is that bursts of TAE modes have, in some cases, been well correlated with abrupt neutron rate drops, of order 5 – 10%, and expulsion of fast ions.

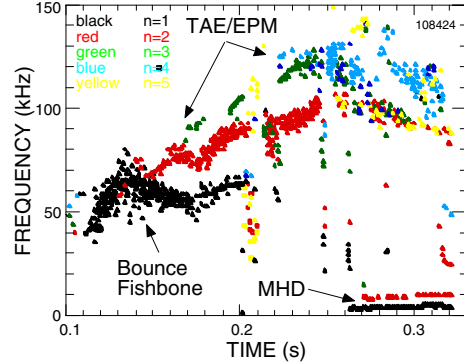


Figure 17 – Typical MHD Spectrogram for discharge with fast ion MHD

TAE modes and fast ion loss

The non-chirping modes in Figure 17, typically with toroidal mode number between 2 and 6, are assumed to be TAE modes [25]. A somewhat surprising observation is that, unlike beam driven TAE modes in conventional aspect ratio tokamaks, these modes generally seem to have a relatively small affect on the fast ion population. No obvious impact is seen on the neutron rate, nor is there an increase in the measured fast ion loss. However, in plasma conditions in which the central q is high and the beam heating is intense, the TAE evolve from continuous modes to bursting modes, with multiple modes of different n present. When the multiple n number bursting TAE modes are present, significant fast ion losses are observed. In Figure 18 are shown waveforms of the plasma current, magnetic fluctuations as measured with a Mirnov coil, neutron rate, and D_α

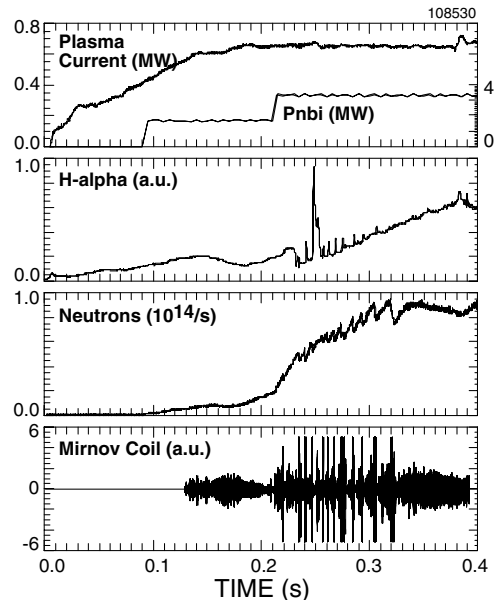


Figure 18 - Waveforms showing appearance of bursting TAE modes and fast neutron drops.

light. Coincident with the strong magnetic fluctuation bursts, sharp drops in the neutron rate, and increases in the D_α light are seen. These observations are consistent with losses of 5 – 10% of the most energetic fast ion population. In Figure 19 is shown a spectrogram of magnetic fluctuations with an overlay of symbols indicating the toroidal mode numbers. MHD bursts which are correlated with the fast ion losses are indicated by vertical dashed lines. As can be seen, the bursts appear to consist of several modes with n ranging from 2 to 4.

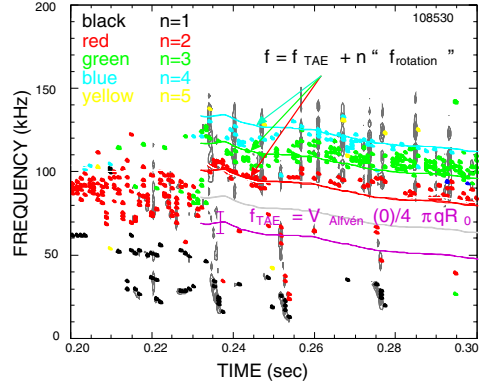


Figure 19 - Spectrogram and mode identification of TAE and other modes.

Bounce fishbone modes

The chirping modes with toroidal mode number $n = 1$ in Figure 19 are believed to be a new variant of the precession resonance fishbone [26,27] mode commonly observed in conventional aspect ratio tokamaks. The modes occur when the central q is believed to be well above unity. The fast ion resonance condition is no longer the precession drift frequency, but at the fast ion bounce frequency [28]. Subtracting the plasma central rotation rate, it is seen that the plasma-frame frequency of the mode chirps downward from about 45 kHz to 25 kHz. In Figure 20 this range of chirping is compared to the bounce frequencies (from the ORBIT code) for the fast ion distribution

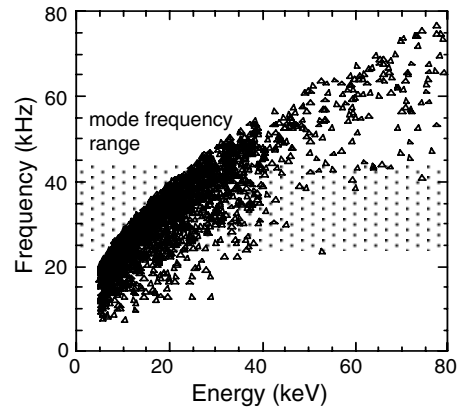


Figure 20 – Calculated distribution of fast ion bounce frequencies (ORBIT and TRANSP).

calculated with TRANSP. The modes are seen to be resonant with the large population of beam ions with energies between 10 and 30 keV. The modes appear relatively weak; they are barely detectable in the soft x-ray emission and there is not a measurable affect on the neutron rate, implying no strong loss of fast ions. This observation of bounce resonance fishbones has implications for conventional aspect ratio reactors in that the drift reversal expected to stabilize the fishbone instability may no longer be sufficient if the fast ion distribution has a fast ion population such that the average bounce angle is large, allowing resonance at the bounce frequency to drive the modes.

Compressional Alfvén Waves

The compressional Alfvén waves [29] are believed to have a relatively unique structure in low aspect ratio devices [30]. The strong gradient in toroidal field from the inboard to outboard plasma edge translates to a strong poloidal gradient in magnetic field strength. As a result, the modes can end up localized in a “well” on the outboard edge of the plasma. The experimental observations of the CAE mode are, so far, in good agreement

with the predicted mode characteristics. It was predicted that multiple CAE modes at sufficient amplitude could stochastically heat the thermal ions [31,32]. Coupled with an apparently anomalously high ion/electron temperature ratio in NSTX, this has encouraged study of the CAE modes [33]. Experiments designed to place constraints on the fraction of beam energy available to drive the CAE instability have demonstrated that it is not likely that the *observed* CAE modes can be responsible entirely for the high ion/electron temperature ratio. As seen in Figure 21, there is a clear threshold in beam energy necessary to trigger these CAE instabilities. The threshold has a strong offset linear dependence on beam voltage and toroidal field, and the threshold is more complicated than a simple $V_{\text{beam}}/V_{\text{Alfvén}}$ threshold. For typical NSTX parameters, the beam energy threshold is at least 55 kV. With only 66% of the beam power in the full-energy component, this means that less than $\approx 20\%$ of the power of 80 kV beams is available to drive the CAE. As the 60-80 kV beam population is disproportionately responsible for the neutron production, a symptom of significant CAE-ion heating would be lower than expected neutron rate and a faster decay of the neutron rate following the end of NBI, neither of which is seen.

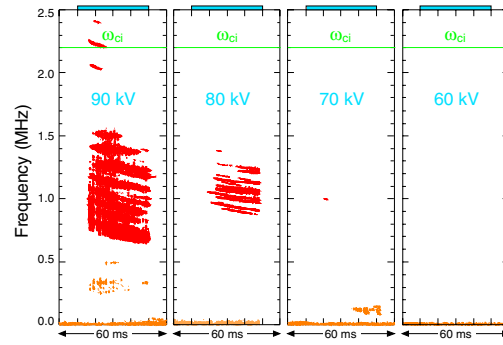


Figure 21 - Beam energy threshold for CAE.

Fast ion MHD similarity experiments

In addition to the increased ratio of fast ion velocity relative to the Alfvén speed in ST geometry, the strong toroidicity of the ST can also influence fast ion MHD characteristics. To better understand this physics, TAE similarity experiments have been performed on NSTX and DIII-D. In these experiments, the core Alfvén speed and fast ion injection energy and species were matched, as was the plasma shape. Figure 22 shows that the excitation threshold is at a similar value of beam beta in both devices. The most unstable TAE modes are expected to have poloidal wavelengths approximately 6 times the fast ion larmor radius. For NSTX parameters, this scaling implies that NSTX should observe toroidal mode numbers roughly 2-3 times lower than in DIII-D because NSTX plasmas have a higher safety factor at fixed toroidal field due to increased toroidicity (lower aspect ratio). As seen in Figure 23, lower toroidal mode numbers are observed in NSTX - consistent with expectations.

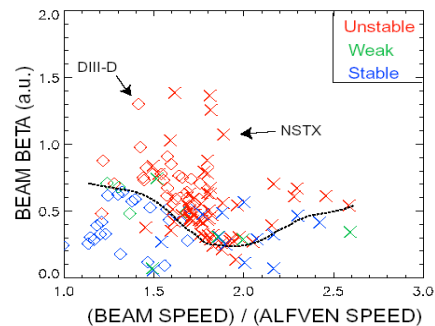


Figure 22 - comparison of TAE threshold versus beam beta in NSTX and DIII-D.

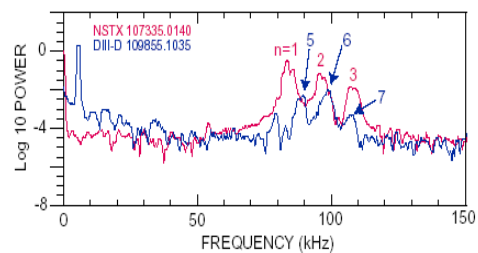


Figure 23 - Mirnov spectra for TAE modes on NSTX and DIII-D

3.1.2 Research Plans for FY2003-2008

Overview

Much of NSTX research over the next five to ten years is tightly linked to the IPPA ST 10 year goal of achieving long-pulse operation at high performance. Sub-sections of the IPPA 5 and 10 year ST operational goals and the IPPA science goal are listed below for reference. The underlined and italicized segments of the goals pertain most directly to MHD research on NSTX.

IPPA - ST 5 year goal: Make a preliminary assessment of the attractiveness of the ST regarding confinement, *stability, and high beta operations*, and non-inductive operations (to be achieved early in the 2004 - 2008 time frame)

IPPA - ST 10 year goal: Assess the attractiveness of extrapolable, *long-pulse operation* of the spherical torus for time scales much greater than the current penetration time scales (to be achieved in the 2009 timeframe)

IPPA science goal 1: Advance the *fundamental understanding of plasmas...* and enhance predictive capabilities through *comparison of experiments, theory, and simulation*

The IPPA 5 year ST goal as it relates to MHD effectively calls for a preliminary assessment of the MHD stability limits of NSTX and a further assessment as to whether these achieved limits are attractive. Ultimately, this attractiveness must be judged by whether or not the beta values obtainable in long-pulse and with high bootstrap fraction are relevant to future reactor-scale devices such as a volume neutron source, component test facility, or even a demonstration reactor.

The rapid progress of the NSTX team toward making such assessments becomes more obvious when one considers that the MHD group is already beginning to study stability physics related to the IPPA ST 10 year goal – extrapolable long-pulse operation. In particular, recent experiments within the MHD and ISD experimental task groups have obtained discharges with $\beta_N=6$,

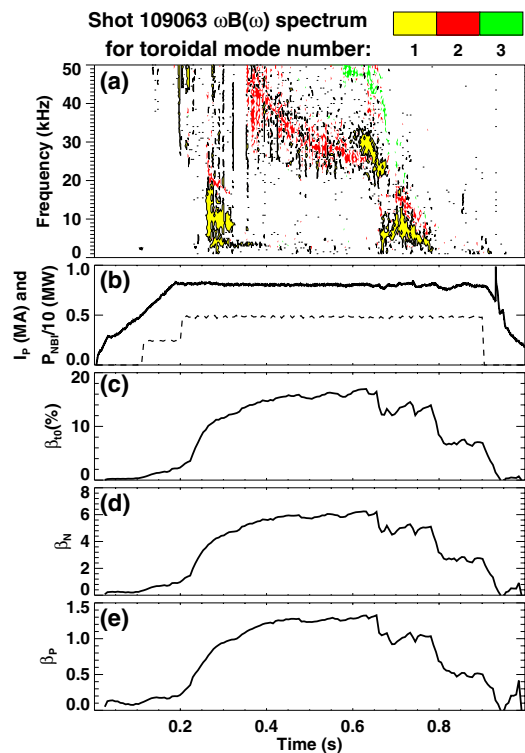


Figure 24 - Mirnov frequency and toroidal mode number spectrogram and β parameters for a long-pulse NSTX discharge with $\beta_N \approx 6$.

$\beta=16\%$, 700ms Ip flat-top, and total pulse length just over 1 second with near steady-state parameters held for a current relaxation time (200-250ms). The MHD modes present in this discharge and other β parameters of interest are shown in Figure 24. Of particular interest in these long-pulse high- β_N shots are the largely internal disruptions in stored energy whose cause is not yet fully understood. The most likely explanations given the present understanding are: 1) that the q-profile is evolving to an unstable state, possibly a reverse-shear q profile which destabilizes double tearing modes at large minor radius, or 2) as in Figures 9,10, and 11, the plasma is reaching the ideal with-wall beta limit and is undergoing a disruption with very weak external component. Without MSE, it is not yet possible to infer if double tearing modes are the cause of these disruptions. It is noteworthy that these long-pulse discharges can be run quiescently with β_N up to 5.8, while attempting to push to higher $\beta_N > 6$ often leads to internal disruptions with a prompt loss of 5-20% of the total stored energy at high $B_T > 4.5\text{kG}$. Rapidly growing ($\tau=200\text{-}500\mu\text{s}$) $n=1$ precursors are observed just prior to these collapses at frequencies (15-25kHz) well above the edge rotation frequency, so it is likely that these modes are either ideally driven or are driven by fast particles rather than by near-edge tearing modes, although strongly driven core tearing modes cannot be definitively ruled out.

Previous theoretical calculations have shown that ideal-wall beta limits with $\beta_N > 8$ are possible in NSTX with optimized profiles. In particular, a broad total pressure peaking factor < 2.5 is highly advantageous for strong coupling to the stabilizing passive plates. In addition, a q profile with $q(0) > 2$ with either monotonic or weakly reversed shear has been shown to improve low toroidal mode number stability by eliminating low-order mode rational surfaces while simultaneously aligning the total current profile with the off-axis bootstrap current resulting from the broad pressure profile. The thermal pressure peaking factor in NSTX H-modes is typically near 2. Thus, keeping the total peaking below 2.5 will require minimizing the fast ion component of pressure. This implies that operation at relatively high density and very high confinement of the thermal component is desirable. Thus, important elements in achieving very high β limits in self-sustaining operation are strongly linked to the transport properties of NSTX plasmas. Just a few examples of this transport/MHD synergy include: 1) understanding the role of plasma shape and divertor geometry in thermal confinement and impurity control, and 2) understanding the role of saturated NTMs in confinement degradation.

While β_N values near or above the no-wall beta limit have been sustained for a significant number of conducting wall times in toroidally rotating NSTX plasmas at increased toroidal field, sustaining such plasmas indefinitely may require active feedback stabilization of global MHD modes. Such a system would also allow sufficient control to study mode stabilization in ST plasmas with low toroidal rotation, as is expected in a reactor. Of particular interest is sustainment of high β_N when the toroidal rotation frequency is below the critical rotation frequency for RWM destabilization.

A physics design of an active feedback system planned to be installed in NSTX has been conducted with the DCON and VALEN codes, using equilibrium input from NSTX experiments. These calculations incorporate the NSTX conducting structure designed to provide passive stabilization of the RWM. VALEN uses a finite element representation

of thin shell conducting structures in an integral formulation to model arbitrary conducting walls, combined with a circuit representation of stable and unstable plasma modes. The VALEN code also has the capability to model arbitrary control coils, magnetic flux sensors, simple power supplies and control schemes that would be used to connect these items together to provide stabilization of plasma instabilities through active feedback.

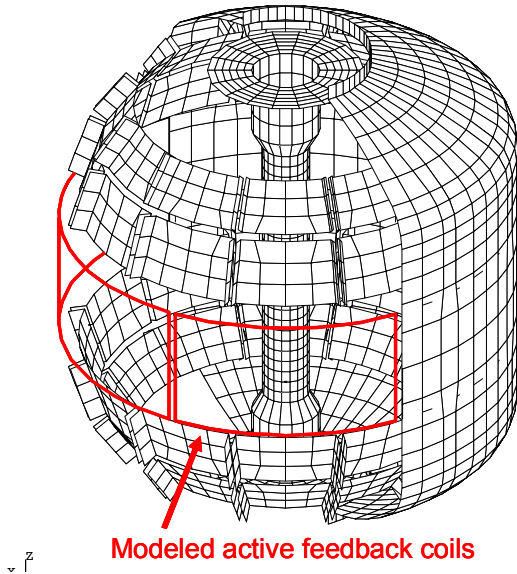


Figure 25: Conducting structure and midplane control coil modeled in VALEN.

Previous calculations using VALEN for the DIII-D device indicate that the most effective systems have control coils positioned as close as possible to the plasma and as far away as possible from major conducting structures. A mode control scheme typically uses a global array of magnetic sensors placed inside the vacuum vessel as close as possible to the plasma and oriented to sample the poloidal field of an instability while being orthogonal to the field produced by the closest control coils. The structure of the instability may then be identified and then feedback logic determines the currents or voltages applied to the control coils.

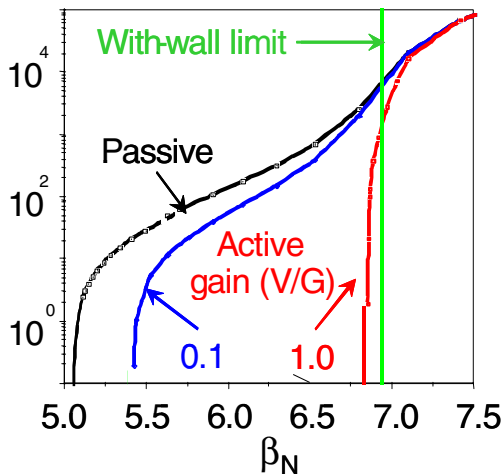


Figure 26: RWM growth rate (s^{-1}) vs. β_N as a function of gain for modeled active feedback system with internal midplane control coils.

A near optimal active feedback system designed to suppress the $n=1$ instability in NSTX has been studied computationally. In this case, the modeled sensors are positioned inside the vacuum vessel on the plasma midplane and measure the poloidal field of the instability. As shown in Figure 25, control coils were placed inside the vacuum vessel. Six equal size picture frame coils, which produce local radial fields, cover the midplane circumference of NSTX and are connected 'anti-pairwise' (control coils diametrically opposite each other are in a series circuit and their radial fields are in the same direction). The sensors have a single turn and an area of $1.e-04$ m². The flux from the sensors is multiplied by a constant gain to determine the voltage applied to the control coils.

Here, the system gain is expressed as the ratio of the control coil voltage to an input field perturbation amplitude. Figure 26 illustrates the performance of this system. At a gain of 0.1 V/G the plasma is stable for beta normal less than 5.39. Further improvement in performance may be obtained by increasing the gain up to about 1.0 V/G

where the plasma is stable for beta normal less than 6.83. The active feedback system shows no further improvement for additional increases in gain. Therefore, this system can stabilize the mode in plasmas with β_N up to 94% of the ideal wall limit. Alternatives to the 'near optimal' active feedback design were also considered. The first keeps the poloidal field sensors interior to the vacuum vessel, but moves the control coils outside. This system reaches a maximum stabilized $\beta_N = 0.72 \beta_{Nwall}$, a decrease of 22% from the near optimal design. The final configuration considered moved the control coils off the midplane and placed them in the gaps between the primary passive plates. The six coils on the midplane are replaced by six coils among the upper primary passive plates and six coils among the lower primary passive plates. This system reaches only 50% of β_{Nwall} .

Research goals by topical area

The considerations discussed above in the MHD programmatic overview highlight the need for improved diagnostics and control tools in NSTX to fairly assess attractiveness of ST concept in the near-term and in the 5-10 year time frame. The following subsections provide a list of topical areas and a suggested fiscal year timeline for achieving the required physics, diagnostic, and control tools in each area.

Influence of shape and profiles on global stability

FY2003 Utilize isoflux control algorithm of rtEFIT to improve boundary shape control during shot. Increase elongation and triangularity of lower single null discharges and/or elongation of highly triangular double null discharges to assess changes in normalized stability limits. Find optimum shape for highest global stability limit compatible with long-pulse requirement of tolerable ELMs in H-mode phase. Perform ramp-rate scans to determine fastest ramp-rate compatible with long-pulse. Assess confinement and pressure peaking as a function of discharge shape. Generate time evolving ideal stability analysis between shots to have immediate knowledge of the beta margin reached above the no-wall limit, and to generate significant statistics of such results.

FY2004 Utilizing MSE constrained reconstructions early during discharge ramp-up, use early heating and/or current drive from HHFW and/or EBW to slow current penetration. Optimize heating programming to elevate q profile above 2 with MHD-stable profile if present operating scenarios are not already doing this. Assess which MHD instabilities ameliorate the benefits of early heating and correlate with q profile dynamics. Assess normalized beta limits as a function of controllably low internal inductance. Experimentally access the second stability region to high- n ballooning modes in the ST by exploiting the synergistic stabilizing effects of low aspect ratio and high central safety factor. Determine the effect of FLR or other stabilization mechanisms of high- n modes in ST geometry by attempting to significantly violate the Mercier and high- n ballooning limits.

- FY2005 Characterize dynamic evolution of equilibrium and compare to TSC predictions to benchmark TSC internal physics models. Use physics knowledge gained to improve TSC as needed and to design controllers for heating and current drive actuators, and to predict performance in future ST devices.
- FY2006 Utilize MSE-constrained rEFITs to measure current profile in real-time. Use PCS control of HHFW and/or EBW to heat and/or drive current to achieve desired current profile for optimized stability.
- FY03-future Work to develop real-time predictive capability for stability. Consider neural network and other methods. Implement PCS control of NBI, HHFW, and EBW to allow real-time feedback control of plasma beta. Use in conjunction with real-time stability calculations to operate just below relevant MHD stability limits.

Resistive wall mode physics - rotation damping and passive stabilization

- FY2003 Propose similarity experiment with DIII-D and MAST to explore (i) aspect ratio effects of these physics topics (DIII-D), and (ii) comparison of plasmas approaching and surpassing the no-wall beta limit with and without conducting structure (MAST). Perform experiments designed to investigate the nature of RWM stabilization mechanism in the presence of rotation and investigate role of the RWM itself in modifying rotation. Using MARS code, perform theoretical assessment of expected critical rotation frequency for RWM stabilization and associated scalings with safety factor, magnetic field, shape, and aspect ratio.
- FY2004 Theoretically and experimentally determine the feasibility of operation in the “second stability region” of the resistive wall mode. Explore the existence of toroidally localized, intermediate- n kink/ballooning modes and associated RWMs created through error fields or tearing modes. Establish with MSE data if low n RWMs can be stabilized and/or rotation damping minimized through elevated q_{\min} and finite rotation for high β_N operational regimes. In regimes where RWM is passively unstable above the no-wall limit, benchmark codes such as DCON+VALEN and/or MARS+VACUUM used in predicting RWM structure, growth-rate, and frequency, against measurements from the internal RWM/EF magnetic sensor set.

FY05-future Examine the role of RWMs of multiple simultaneous unstable n values. Determine the impact of active feedback system on RWM mode structure and stabilization / destabilization of given n values. Using experimental results and comparison to theory, assess rotation required for stabilization of RWM in long-pulse high- β operating regimes. Use knowledge gained to test active feedback stabilization physics in regimes with low rotation speed and to project to future ST devices.

Neoclassical tearing modes

FY2003 Prepare neoclassical tearing mode codes to more routinely assess mode stability once $q(\psi)$ profile information is becomes available. Implement more accurate wall shape model for wall-stabilized TM stability studies, and begin implementation of simulated Mirnov sensor responses.

FY2004 Assess seeding mechanisms for NTMs in NSTX standard and advanced operating regimes. Determine if modes are excited “spontaneously” via proximity to an ideal limit or if seeded directly from other observable MHD modes. Investigate non-linear coupling of NTMs of different helicities.

FY2005 Measure poloidal mode numbers magnetically utilizing improved poloidal Mirnov array. Correlate magnetically inferred m/n data to island position measurements from SXR and possibly EBW radiometer. Infer island widths from measurements and improved modeling to assess CD needs for EBW CD feedback stabilization of the NTM.

FY2006 Perform preliminary assessment of changes in NTM stability due to global changes in current profile resulting from EBW current drive and electron heating. Assess EBW power requirements for NTM stabilization based on initial measurements of CD efficiency and required CD for mode stabilization.

FY2007 Demonstrate direct NTM suppression with pre-programmed control of launcher and plasma conditions. Verify CD requirements with NTM modeling of stabilization.

FY08-future Incorporate EBW launcher control into PCS and demonstrate first active feedback of the NTM.

Edge localized modes

- FY2003 Perform experiments to assess impact of divertor configuration, shaping, collisionality, and plasma-wall gaps on ELM stability properties. Characterize pedestal energy loss in various ELMing regimes and secondary destabilization of NTMs and other modes due to ELMs.
- FY2004 Commission very high-n array for measurement of ELM toroidal mode numbers. Correlate measured mode numbers with ELM type.
- FY2005 Use reflectometer or other high resolution near-edge profile diagnostic to perform preliminary measurements of ELM structure.
- FY06-08 Using kinetic EFITs with MSE and all available profile information, reconstruct discharges from controlled experiments designed to excite different types of ELMs. Compare ELM stability threshold, mode structure, and toroidal mode numbers to predictions from ELM stability codes such as ELITE, DCON, GATO, or PEST.
- FY03-future Throughout next 5 year research period, continue to develop best H-mode discharges in long-pulse discharges by balancing highest thermal confinement against tolerable ELM size and frequency.

Fast ion MHD

- FY2003 Perform similarity experiments on NSTX and DIII-D investigating the Compressional Alfvén Eigenmode (CAE) to assess role of toroidicity on characteristic frequencies, stability threshold, growth rates, etc. Assess if fast ion-driven modes at low frequency such as fishbone or rTAE ($f=20-40\text{kHz}$) play a role in high β_p disruptions possibly due to elevated q or destabilizing q profile (requires MSE).
- FY2004 Perform first measurements of CAE poloidal amplitude distribution and poloidal wavelength with new outboard poloidal Mirnov array at Bay H. Assess role of q profile in controlling gap structure for TAE modes. Correlate fast ion loss measurements from FLIP with mode amplitude, frequency, etc. and determine the energy of ions preferentially lost.
- FY2005 Utilize internal diagnostics including reflectometer, EBW spectrometer, or upgraded bandwidth SXR to measure internal structure of TAE, CAE, and GAE modes. Utilize fluctuation signatures and frequencies to distinguish between modes. Compare to theory and modeling with NOVA, HINST, and HYM. Assess if "pitch-angle anisotropy model" can explain drive for instabilities and thus how much energy is available to drive modes.

FY04-future Develop beam ion profile diagnostic to determine fast ion pressure profile. Use profile shape in ideal stability calculations and for fast ion MHD instability drive calculations. Assess influence of fast ion MHD on fast ion population properties such as neutron rate, power deposition, fast ion angular momentum, etc. Techniques to be considered include a neutron collimator, a 3 MeV profile diagnostic, an array of active neutral particle detectors, and D-alpha light from re-neutralized beam ions.

Influence of rotation on equilibrium and stability

FY2003 Assess the impact of toroidal rotation in equilibrium reconstructions. Determine change in inferred stored energy due to inclusion of centrifugal force. If effects are significant, incorporate rotation effect in control room equilibrium analysis when charge exchange recombination spectroscopy data is available. Utilize self-consistent FLOW equilibrium code including anisotropy.

FY04-06 Use core density gradient at magnetic axis as measurement of total centrifugal force. Compare fast ion centrifugal force to thermal, and possibly use changes in central gradient to infer changes in fast ion population due to MHD activity. Cross check against beam ion profile diagnostics if available, NPA, and FLIP. Develop stability code based on FLOW equilibrium.

Error fields and locked modes

FY2003 Commission internal RWM/EF sensor array electronics. Gather engineering data on primary passive plate misalignment and sensor positions and calibrate signals including effects of position. Begin assessment of sources of error field such as PF coils or passive plates. Perform experiments using low density locked modes and beam pulses to determine locking threshold as a function of density, rotation, magnetic field, and current. Use locking position to aid inference of error field sources.

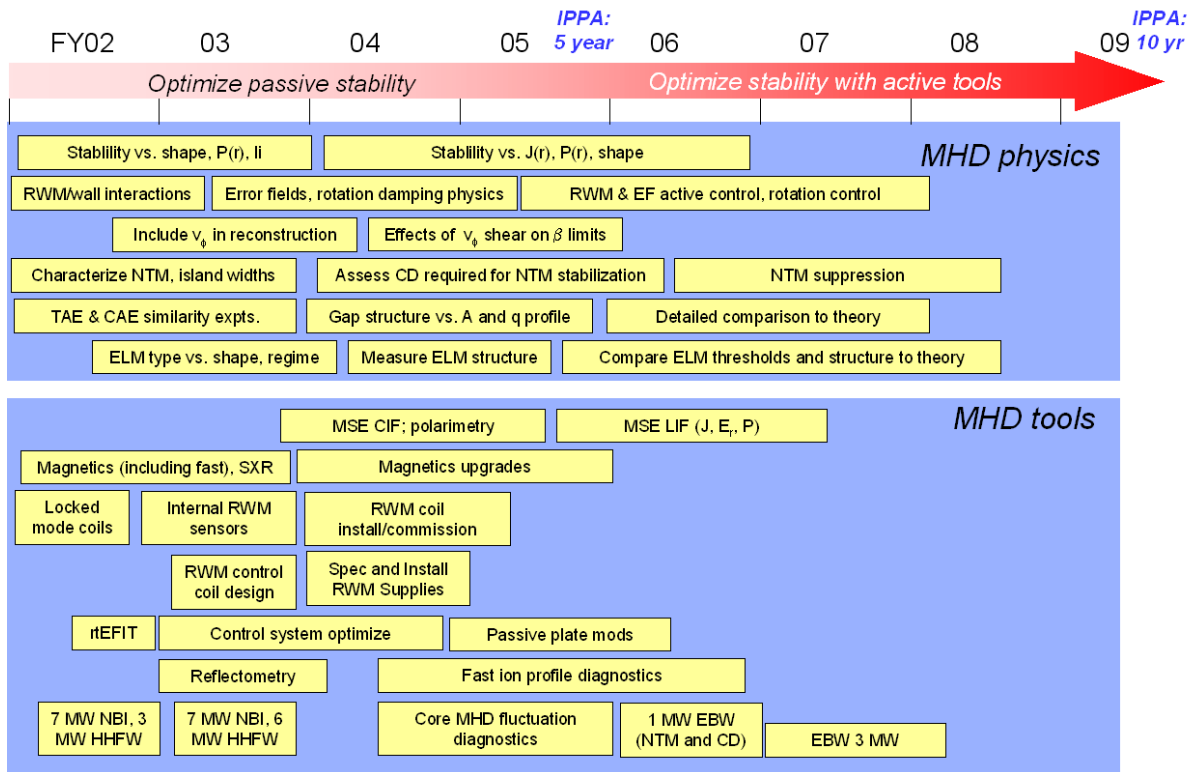
FY2004 After utilizing internal sensor measurements to infer sources of error field, correct error fields directly where possible through re-alignment.

Active RWM stabilization

FY2003 Finalize design of active coil set using DCON+VALEN analysis. System design will include control of low-n modes equal to and greater than unity. Decide on either internal or external control coil set. Initiate procurement of power supplies based on assessment of needed supply power to simultaneously correct error fields and provide fast feedback for RWM control.

- FY2004 Install active coil set and power supplies. Commission active coils and supplies. Interface supply controls to PCS. Purchase and install data acquisition for PCS to acquire needed magnetic sensor signals in real-time for feedback control.
- FY2005 Develop techniques to control rotation speed independent of beam heating power to decouple rotation from β . Flow damping from non-resonant error field excitation using active coils and/or controlled error field amplification of the RWM are possible means. In regimes where RWM is passively unstable above the no-wall limit, develop feedback algorithms to stabilize the RWM up to the ideal-wall limit. Investigate stabilization of multiple- n modes, possibly including toroidally localized ballooning modes. Utilize the implemented multi- n control coil system to create a spectrum of static m/n error fields to determine the effect on the RWM. Also, use non-resonant error fields to modify NTM island formation.
- FY06-future Apply passive and active RWM stabilization to increase safe operating distance above no-wall stability limit in high- β long-pulse discharges. Utilize RWM feedback to sustain high β_N operation close to the ideal-wall limit in optimized long-pulse discharges. Generate stochastic divertor boundary with non-axisymmetric coils. Assess impact on edge profiles and divertor heat flux in long-pulse.

Proposed NSTX MHD research program time-line:



References

- [1] Y.-K.M. Peng and D.J. Strickler, Nucl. Fusion 26, (1986) 769.
- [2] W. Howl, et al., Phys. Fluids B 4, (1992) 1724.
- [3] S.A. Sabbagh, et al., Phys. Fluids B 3, (1991) 2277.
- [4] E. Strait, Phys. Plasmas 1, (1994) 1415.
- [5] C. Kessel, et al., Phys. Rev. Lett. 72, (1994) 1212.
- [6] A.D. Turnbull, et al., Phys. Rev. Lett. 74, (1995) 718.
- [7] J.E. Menard, et al., Nucl. Fusion 37, (1997) 595.
- [8] E.J. Strait, et al., Phys. Rev. Lett. 74, (1995) 248g3.
- [9] A. Bondeson and D. J. Ward, Phys. Rev. Lett. 72, (1994) 2709.
- [10] A.M. Garofalo, et al., Nucl. Fusion 40, (2000) 1491.
- [11] A.M. Garofalo, et al., Phys. Rev. Lett. 89, (2002) 235001-1.
- [12] R.D. Stambaugh, et al., Fusion Technology 33, (1998) 1.
- [13] R.J. LaHaye, et al., Phys. Fluids B 4, (1992) 2098.
- [14] T. Hender, et al., Nucl. Fus. 32, (1992) 2091.
- [15] E. Lazzaro, et al., Phys. Plasmas 9, (2002) 3906.
- [16] R. Maingi, et al., Phys. Rev. Lett. 88, (2002) 035003.
- [17] S. A. Sabbagh, et al., Phys. Plasmas 9, (2002) 2085.
- [18] R. J. Buttery, et al., Phys. Rev. Lett. 88, (2002) 125005.
- [19] A. Glasser and M. Chance, Bull. Am. Phys. Soc. 42, (1997) 1848.
- [20] J. Bialek, et al., Phys. Plasmas 8, (2001) 2170.
- [21] R. Fitzpatrick, Nucl. Fusion, 7 (1993) 1049.
- [22] A.I. Smolyakov, et al., Phys. Plasmas 2, (1995) 1581.
- [23] K.C. Shaing, et al., Phys. Fluids 29, (1986) 521.
- [24] W. Park, et al., Phys. Plasmas 6, (1999) 1796.
- [25] N.N. Gorelenkov, et al., Phys. Plasmas 7 (2000) 1433.
- [26] PDX Group, Princeton Plasma Physics Laboratory, Phys. Rev. Lett. 50 (1983) 891.
- [27] R.B. White, et al, Phys. Fluids 26 (1983) 2958.
- [28] E. Fredrickson, R White, L Chen, (in preparation).
- [29] N.N. Gorelenkov, C.Z. Cheng, Nucl. Fusion 35, (1995) 1743.
- [30] E.D. Fredrickson, et al., Phys Rev. Lett. 87, (2001) 145001.
- [31] L. Chen, Z. Lin, and R B White, Phys. Plasmas 8, (2001) 4713.
- [32] D. Gates, R. White, N. Gorelenkov, Phys. Rev. Lett. 87 (2001) 205003.
- [33] E.D. Fredrickson, et al., Phys. Plasmas 9 (2002) 2069.

3.2 Transport and Turbulence

3.2.1 Transport Goals and Relation to IPPA Milestones

The development of the ST concept into proof-of-principle experimental devices such as NSTX and MAST has opened up new vistas in the exploration of the turbulence and transport physics that govern toroidal confinement. Both as a complement to conventional aspect ratio tokamaks and as a confinement concept in its own right, NSTX will move in a direction to identify and control the fundamental physics mechanisms that are most important in determining energy, particle and momentum transport. Among the key transport goals are:

- To establish the key scalings of both the global and local transport properties of ST plasmas with emphasis on delineating the role of electron vs ion transport and their dependences on ρ^* , β_T and rotational shear,
- To measure and relate low and high-k turbulence to the heating and transport properties of the plasma components,
- To assess fast ion confinement in an ST geometry, as well as the influence of the fast ions on neoclassical transport and turbulent heating and transport,
- To determine the influence of the radial electric field and resulting large rotational shear on turbulence dynamics and transition into high energy state (H-mode) plasmas, and, ultimately,
- To use the knowledge gained to control plasma transport as a means of producing plasma kinetic and current profiles that are optimal for high-confinement, high- β_T and non-inductive current generation.

These goals will be addressed through experimental research with advanced diagnostics, and by using theoretical and numerical tools that will allow detailed comparisons between experiment and theory.

The achievement of the overall transport goals, as outlined above, in a timely manner is essential for achieving the overarching FESAC IPPA objectives for assessing the ST as an attractive fusion concept. The two FESAC goals that are most connected to the transport goals are the five year goal (IPPA 3.1.1, end of FY2005)

- Advance the scientific understanding of turbulent transport, forming the basis for a reliable predictive capability in externally controlled systems,

and the ten year goal (FY2009)

- Develop fully integrated capability for predicting the performance of externally controlled systems including turbulent transport, macroscopic stability, wave-particle physics and multi-phase interfaces.

The achievement of the NSTX transport goals are clearly essential for being able to produce the high-performance, quasi-steady discharges required to address the nearer-term IPPA goal, and the development of a predictive capability and experimental control techniques will allow for extrapolation to a Component Test Facility and a reactor scenario.

3.2.2 Unique Opportunities of NSTX

The low toroidal field of NSTX, approximately a factor of ten lower than that in conventional aspect ratio devices, leads to plasma operations in parameter regimes that are different than those at higher aspect ratio, which in turn lead to diagnostic and theoretical challenges. Figure 1 show a set of key plasma physics parameters for various devices at conventional aspect ratio and for NSTX. The fast ion and thermal gyroradii normalized to the plasma minor radius (ρ_{fast}/a and $\rho^* = \rho_i/a$ respectively) are clearly an order of magnitude greater for NSTX than for the other devices due to the low toroidal field in NSTX, indicating the importance of including FLR effects correctly in the treatment of neoclassical and turbulent transport physics. In particular, the thermal ion

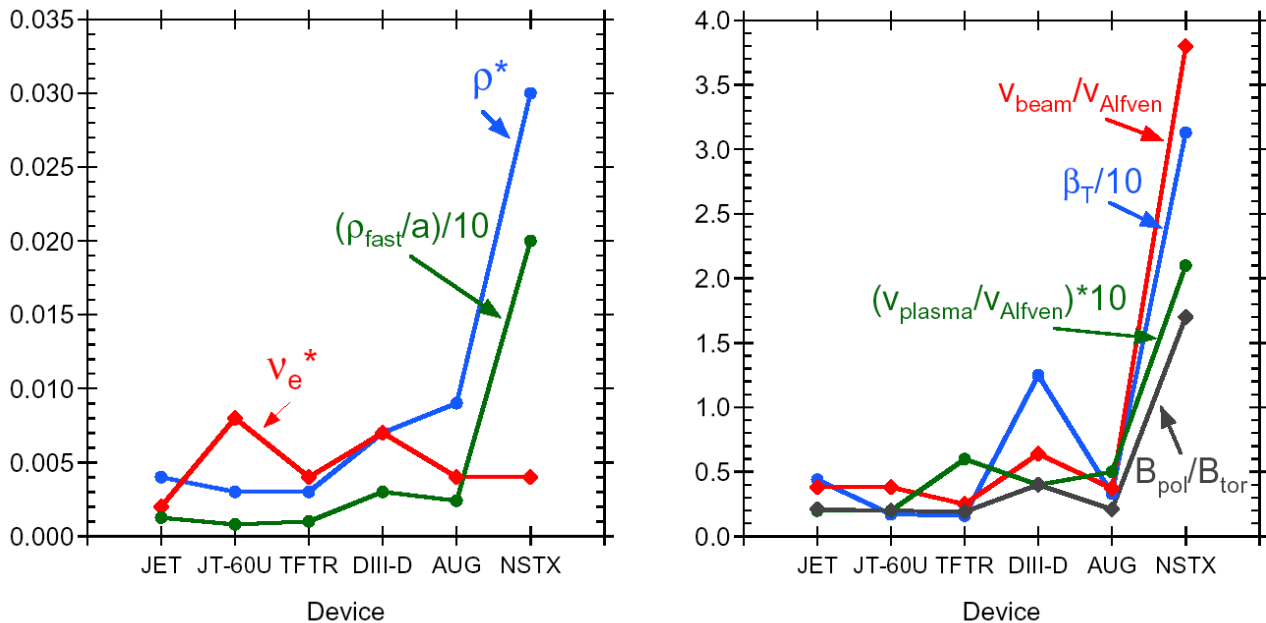


Fig. 1 Comparison of key physics parameters among various conventional aspect ratio tokamaks and NSTX. The higher values for NSTX are generally the result of lower toroidal field.

gyroradius can be between one and three cm near the outboard edge of the plasma, which implies $\rho_i/L \sim 0.2$ to 0.3 at that location, where L is a characteristic scale length (density, temperature, pressure). This brings into question the validity of the spatial scale length ordering, as applicable to NSTX, in the various transport theories. Furthermore, because of the relatively large gyroradius and trapped particle fraction, which approaches one at

this low aspect ratio, electrons can no longer be treated validly as a fluid. Low toroidal field also leads to high- β_T operation, with volume-averaged values up to 35% (right panel) and local core values near 1. Consequently, electromagnetic turbulence and magnetic stochasticity may play an important role in plasma transport. The high β_T , large gyroradius and large trapped particle fraction all indicate the necessity for further development of the gyrokinetic treatment of low aspect ratio plasmas in the neoclassical and turbulent regimes.

The plasma Alfvénic Mach number (right panel of Fig. 1) is of order 0.2, with a velocity that is a significant fraction of the sound speed, indicating potentially high flow shearing rates. High ExB flows, with flow shear rates of order 10^5 to 10^6 sec^{-1} , have been observed, and they can have a profound effect on transport by suppressing microturbulence. The ratio of fast ion velocity to Alfvén velocity is three to four, owing to the low toroidal field and high beam energy (80 to 100 keV), allowing for destabilization of fast ion driven instabilities. These Compressional Alfvén Eigenmodes (CAEs) may in turn serve to heat thermal ions anomalously [1]. Finally, the ratio of B_{pol} to B_{tor} on the outboard midplane is large enough to cause the major portion of the field line length to be in the good curvature region, thus reducing the microinstability drive [2].

3.2.3 Experimental Studies

Core Transport - Global confinement

Results

Global confinement studies in NSTX to date have been based on confinement time values determined by magnetic reconstructions of quasi-steady discharges using the EFIT code. These confinement times include the fast ion component. A sufficient range of operating space was accessed during L-mode studies to enable the development of a preliminary parametric scaling of confinement. These L-mode data indicate parametric scalings similar to those at conventional aspect ratio, but with a slightly stronger power degradation, with $\tau_E \sim I_p^{0.76} B_T^{0.27} P_{\text{heat}}^{-0.76}$, and with no significant dependence on plasma density. The L-mode and H-mode data in the NSTX confinement database, normalized by this L-mode scaling, are plotted versus heating power in Fig. 2. There is much scatter in both sets of data, but what can be seen is a general increase of the normalized H-mode confinement times, indicating a less severe power degradation than in L-mode. Indeed, $\tau_E^{\text{H}} \sim P_{\text{heat}}^{-0.50}$, which is even more favorable than in recent H-mode thermal confinement scalings [3]. Both the L-mode and H-mode data sets as a whole exhibit confinement times that are well enhanced over those from the conventional aspect ratio scalings, indicating the need for reassessing the aspect ratio dependence in the scalings.

Different parametric trends were observed in single parameter scans of more transient L-mode plasmas, where, most notably, very little dependence on plasma current ($I_p^{<0.5}$), and a very strong power degradation ($P_{\text{heat}}^{-1.0}$) were observed. A feature of these transient plasmas was that the confinement time increased throughout the course of the neutral

beam heating phase, and this increase was often associated with an increase in rotation velocity across the plasma.

Global confinement plans

FY03

Global confinement scaling studies will be pursued to determine whether the power degradation in both L- and H-modes is due to an MHD or confinement limit. In addition, more dedicated scans of H-mode plasmas, which tend to be more steady-state than L-modes, will be performed to determine the full range of parametric dependences. NSTX discharges will be analyzed to calculate the fast ion stored energy and beam losses in order to extract the thermal energy confinement time and to study the scaling of this parameter in relation to that from conventional R/a devices, with particular emphasis on the aspect ratio scaling. These data will be prepared and submitted to the ITER confinement database for this purpose. The aspect ratio dependence will be determined directly in ohmically heated plasmas in NSTX.

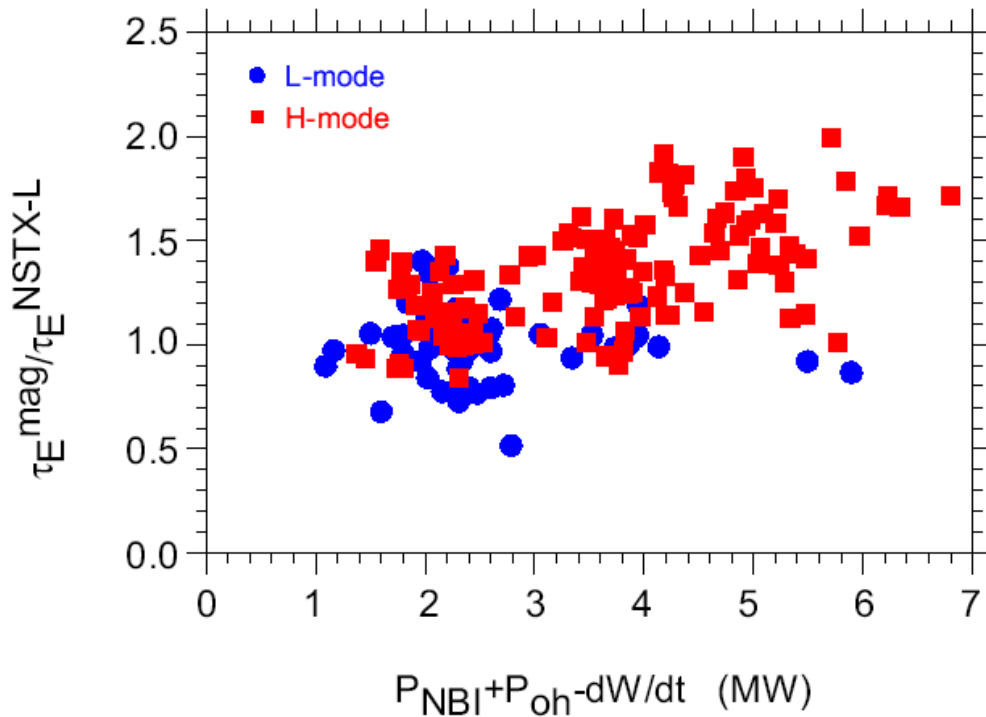


Fig. 2 L- and H-mode confinement times normalized to the parametric scaling derived only for L-modes, $\tau_E \sim I_p^{0.76} B_T^{0.27} P_{\text{heat}}^{-0.76}$.

FY04

The aspect ratio dependence will be determined in neutral beam heated plasma both within NSTX and by performing similarity experiments across platforms such as NSTX and DIII-D will be initiated. Experiments to determine how confinement scales with the dimensionless parameters ρ^* and β_T will start. The characteristics of transient versus quasi-steady discharges, and the role of rotation in confinement dynamics will be studied, the latter making use of error field correction coils to control rotation. Confinement trends will be studied in relation to variations in the q-profile, as measured by the CIF MSE system.

FY05

Rotation dynamics studies and its effect on confinement will be extended with the implementation of the poloidal CHERS system.

FY06

Studies of the dependence of global confinement on q-profile and E_r will be extended with the implementation of the LIF MSE diagnostic.

FY07-08

A causal relation between the rotation and confinement changes can be established with high time resolution (\leq msec) rotation diagnostics. The high-time resolution rotation diagnostic is presently not under development. Profile control techniques will be employed to optimize confinement for attaining high- β_T and high non-inductive current fractions.

Ion Energy Transport - Results

One of the device physics design predictions for NSTX was the possibility of suppressing ITG modes due to both geometric considerations and ExB flow shear [2, 4]. Results of NB heating experiments have indeed shown that ion transport is relatively low, inferred to be at or below neoclassical levels. An example a neutral beam heated discharge evolution is shown in Fig. 3a, where it is seen that

$T_i(0) > T_e(0)$ throughout the NBI heating phase. A snapshot of the ion and electron temperature profiles at $t=0.45$ sec is shown in Fig. 3b. Because the beam ion energy (80

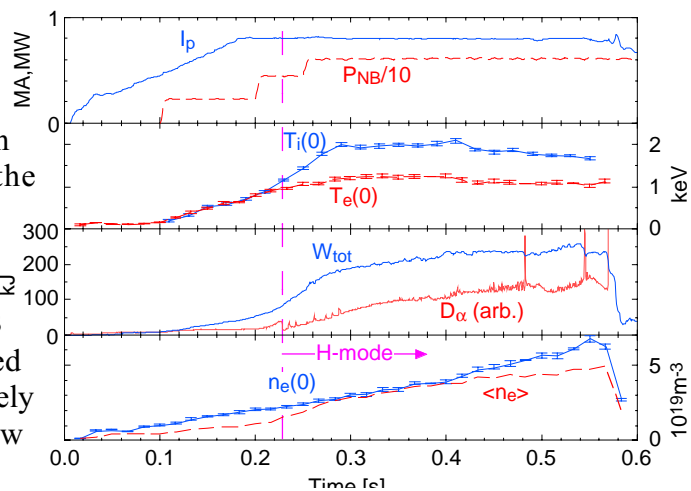


Fig. 3a Time evolution of a NB heated L-mode discharge.

to 100 keV) is high compared to the electron temperature (~ 1 keV), classical collision theory predicts that only about 1/3 of the beam heating power is deposited into the ions; this, along with the fact that T_i remains higher than T_e over most of the profile, in itself suggests good ion confinement.

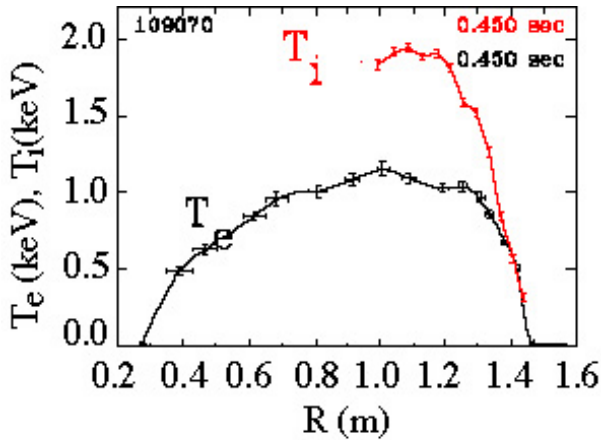


Fig. 3b Electron and ion temperatures at $t=0.45$ sec

Ion thermal diffusivities can be determined from power balance calculations and the measured profiles using the TRANSP transport analysis code in interpretive mode. The results show that $\chi_i < \chi_e$, and it is comparable to the value given by the NCLASS neoclassical theory [5]. The thermal diffusivities are seen to decrease from core to edge, a trend opposite to what is observed at conventional aspect ratio. Preliminary gyrokinetic calculations of the linear growth rate of ITG modes in NB L-mode heated NSTX discharges indicate that the ExB flow shear is large enough to suppress the residual low-k turbulence usually attributed to ITG

modes, leaving the ion thermal transport at the neoclassical level, consistent with the results of the power balance calculations.

The ion channel sometimes exhibits confinement higher than can be explained either by classical or neoclassical theory. An example of this is shown in Fig. 5. Experimentally measured T_e and T_i are plotted as a function of minor radius, as are T_i profiles predicted assuming neoclassical transport for the ions and zero transport for the ions. The neoclassically predicted T_i is well below the measured T_i profile, indicating that neoclassical is an overprediction of the thermal ion transport level. While the zero transport assumption overpredicts the measured T_i in the core region, there is a region in the outer portion of the profile in which even zero transport underpredicts the measured ion temperature within the range of the random uncertainties of the data, indicating an additional heat source or heat pinch is needed in order to reconcile the measurement. While data checks are still on going, explanations for this anomalously good ion confinement, such as anomalous heating mechanisms or inward heat pinches, must be considered.

Ion Energy Transport - Plans

FY03

Experiments on ion transport will focus on establishing the baseline for the ion thermal diffusivity through detailed comparison between experiment and theoretical expectations of neoclassical and turbulent transport. In particular, it will be determined if and the

conditions under which the ion power balance, and thus, thermal diffusivities, are anomalous. A major diagnostic need for all these studies is an independent experimental validation of the measured local ion temperatures. A diagnostic for this is presently not yet under development. The effect of ITG modes on plasma transport will be assessed starting in FY03 by varying parameters known to affect ITG growth and damping.

FY04

Experiments to assess the importance of ITG modes will continue. The ratio T_i/T_e can be varied by using RF in conjunction with NBI and/or by changing target densities, and the ExB flow shear can be modified by using RF heating instead of NBI, and by error field correction coils. It has been suggested anomalous heating of thermal ions could result from CAEs driven unstable by fast ion velocity space anisotropies [2]. Similarly, ETG modes that have cascaded to lower k_{radial} (i.e., streamers) can also heat the thermal ions [6]. Calibrated reflectometry will be used to infer these mode amplitudes at the relevant radial locations (1.35 to 1.45 m) to assess their potential for anomalous heating.

FY05

Co- versus counter-NB injection discharges will be used, in conjunction with the poloidal CHERS diagnostic to study the effect of flow shear on ion transport. Density gradients and β' will be modified using pellet injection with the implementation of a deuterium pellet injector, and will serve as a basis for perturbative studies of ITG turbulence induced transport. Initial studies relating ion transport to measured low-k fluctuations will be initiated.

The source of the apparent ion power balance anomaly will also be investigated with further development of neoclassical theory and its calculated energy and particle fluxes. Present neoclassical calculations (i.e., NCLASS) do not consider the orbits of thermal particles near the magnetic axis (i.e., potato orbits), nor is it valid where r/L is finite, a situation that can exist in the outer regions of the NSTX plasma. Exceedingly important may also be the inclusion of beam-thermal ion friction terms, which have been neglected in previous treatments but which can be important in NSTX due to the large value of $v_{\text{beam}}/v_{\text{th},i}$. The parallel force from this friction term can lead to an inward particle and heat pinch when the NB injection is in the co-direction, and an outward pinch for

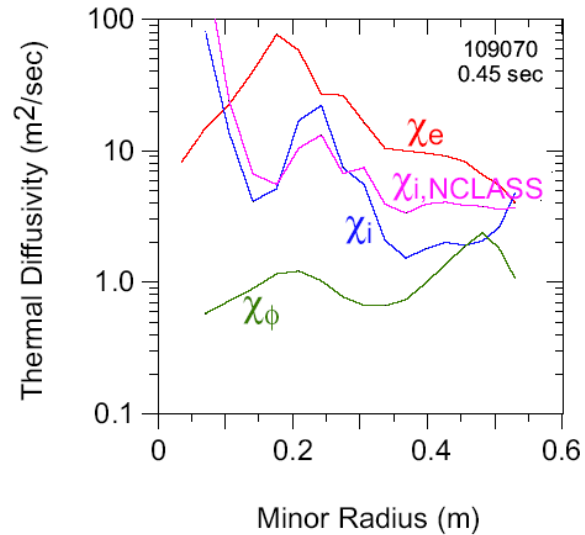


Fig. 4 Thermal and momentum diffusivities calculated from TRANSP power balance calculations. Shown for comparison is the neoclassical thermal diffusivity from the NCLASS neoclassical model.

counter-NB injection. A co/counter experimental campaign, along with theory development, would test this effect directly.

FY06

Details of the relation between ion transport and turbulent fluctuations will be studied. With the implementation of the LIF MSE diagnostic it will be possible to relate the variations in q and E_r profiles to changes in ion transport.

FY07-08

Studies of ion transport and the full k -spectrum of fluctuations will continue. Detailed comparisons between observed transport and fluctuation characteristics and predictions from comprehensive gyrokinetic calculations will be made in order to develop a high-confidence predictive capability.

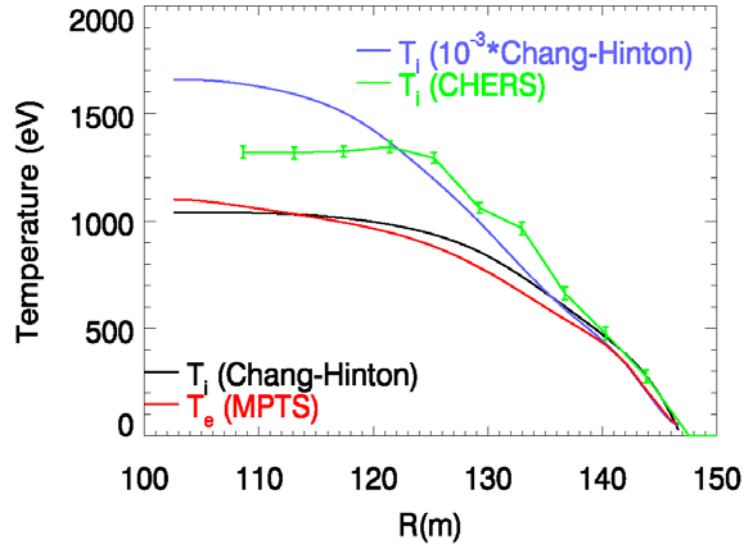


Fig. 5 Measured T_e and T_i profiles along with T_i profiles predicted assuming neoclassical transport and zero ion transport.

Electron Transport - Results

As ion transport appears to be relatively low on NSTX, the electrons are, therefore, the dominant loss channel. One of the transport goals of NSTX is to improve our understanding of electron transport and develop the means to improve it. The electrons

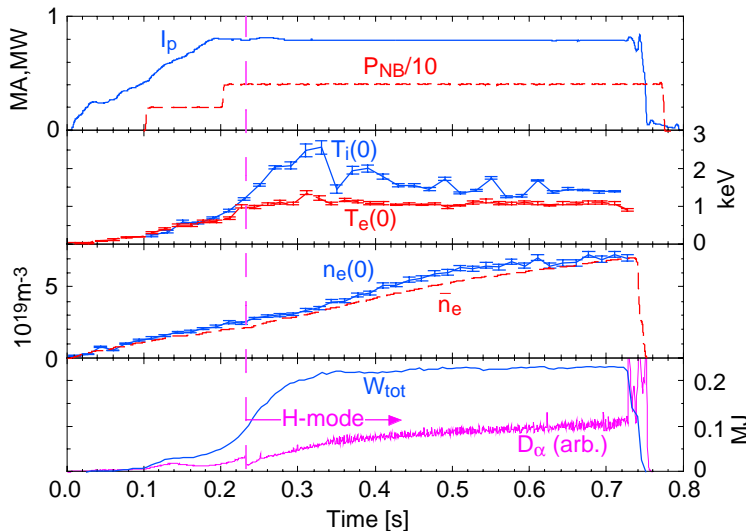


Fig. 6a Time history of H-mode discharge showing constant $T_e(0)$ despite density increase and transport events as seen in $T_i(0)$.

appear to be impervious to transport events that affect the ions, as shown in the time trace in Fig. 6a, where the $T_e(0)$ remains constant in time even as the $T_i(0)$ is seen to decrease at certain times. The electron temperature profiles exhibit remarkable resilience over a significant period of time (Fig. 6b), suggesting the possibility that the electrons are at a state of critical marginality.

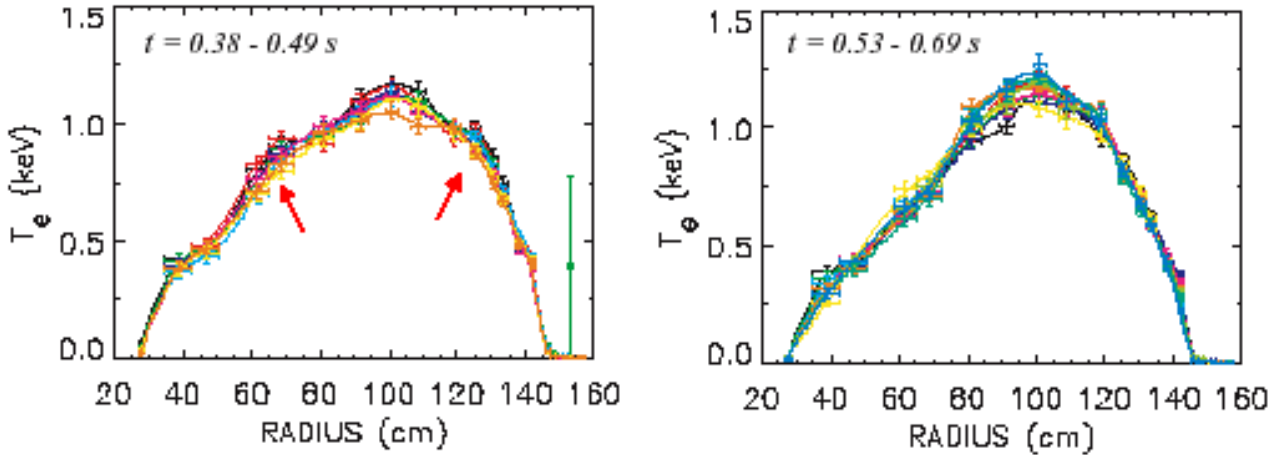


Fig. 6b Electron temperature profiles during two lengthy discharge durations exhibiting profile “stiffness”.

Internal transport barriers (ITBs), which appear to break the critical temperature gradient paradigm, have been observed in the electron temperature profiles during HHFW heating. This is seen in Fig. 7a, where the core T_e is seen to rise continuously during the HHFW heating phase. Associated with this increase is a continuous reduction in the electron thermal diffusivity, as shown in Fig. 7b. Preliminary calculations of ETG linear growth rates using GS2 indicate growth that cannot be suppressed by velocity shear alone; however, the growth rates can be reduced in a bootstrapping fashion as T_e/T_i increases [7].

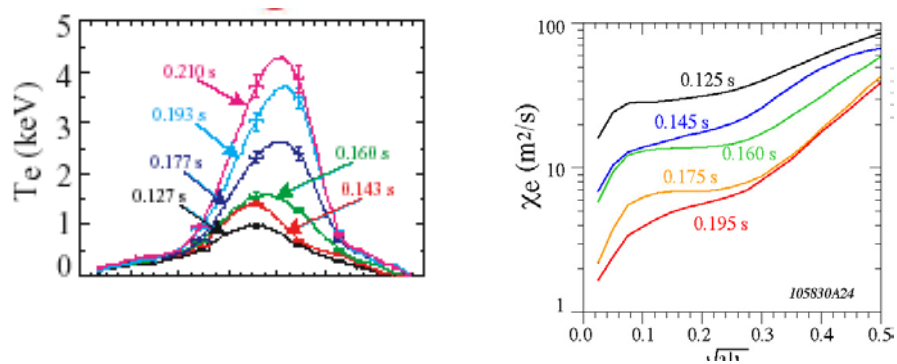


Fig. 7 (a) Electron temperature profile evolution, and (b) associated change in electron thermal diffusivity.

Electron transport - Plans

FY03

Experiments on electron transport in FY03 will focus on establishing the baseline for the electron thermal diffusivity through detailed comparison between experiment and theoretical expectations of turbulent transport.

FY04

Tests of the strength of the electron temperature profile “stiffness” will be started using modulated HHFW heating pulses and either the USXR array or mode-converted EBW emission to monitor the local response to these pulses. Tests of how target electron temperatures affect both electron and ion transport, in conjunction with gyrokinetic calculations of linear and non-linearly saturated states, will allow progress in understanding electron transport dynamics. RF current drive and heating will be used to change magnetic shear, β' and η_e , which are believed to affect ETG mode growth. These studies will be aided with actual q-measurements from CIF MSE.

FY05

Pellet injection will be used to study the effect of varying β' and η_e on electron transport and ETG mode growth. These studies will be complemented by initial fluctuation measurements in the ETG wavelength regime, which is of order several mm for NSTX and is therefore diagnostically accessible. Studies of the effect of flow shear on electron transport and ETG turbulence will be initiated, aided by measurements from the poloidal CHERS diagnostic.

FY06

Details of the relation between electron transport and turbulent fluctuations will be studied. With the implementation of the LIF MSE diagnostic it will be possible to relate the variations in q and E_r profiles to changes in electron transport.

FY07-08

Studies of electron transport and the full k-spectrum of fluctuations will continue. Detailed comparisons between observed transport and fluctuation characteristics and predictions from comprehensive gyrokinetic calculations will be made in order to develop a high-confidence predictive capability.

Momentum Confinement - Results

NSTX operates in a unique regime in which $M_A \sim M \sim 0.3$ for the main plasma species, and for which the impurity ions may in fact be supersonic. The critical role that ExB shear has on turbulence suppression underlies the importance of momentum transport studies to understand and ultimately control the turbulence. As the ion transport is low in the NBI plasmas, so too is momentum transport, with $\chi_\phi < \chi_i < \chi_{neo}$ by an order of magnitude.

Momentum Confinement - Plans

FY03

These studies will be complemented by comparisons of deduced momentum diffusivities to neoclassical expectations and by gyrokinetic calculations. A study of momentum transport starting in FY03 will involve comparisons between NBI, which provides torque through collisional processes, and HHFW, which does not.

FY04

The momentum transport studies will be extended in FY04 with comparisons between RF and NBI heated discharges. Rotation studies will make use of the error field correction coil, which will be used to vary the static island size and, thus, plasma rotation.

FY05

Co- versus counter-NBI injection comparisons which will enable assessment of the importance of non-ambipolar losses and direct torques on flow generation. The implementation of the poloidal CHERS diagnostic will be essential for this study.

FY06-08

E_r will be measured directly by LIF MSE, and it will be studied in relation to the flows as measured by the CHERS systems. The relation between flow shear generation, rational q-surfaces and ITB formation will be studied making use of these diagnostics as well. Studies to identify zonal flows and establish the causal relation between rotation and confinement dynamics will start with the implementation of a high time resolution (≤ 1 msec) CHERS diagnostic.

Particle/Impurity Transport - Results

Studying impurity transport provides another means from which to infer the transport properties of NSTX and scaling with ρ^* and β_T . Initial neon puffing experiments on NSTX have indicated that impurity ion transport from the edge to the core is low, and that the particle diffusivity is at the neoclassical level in the core region. These experiments were carried out so far only in L-mode plasmas at low- β_T . At higher β_T , the impurity transport experiments will help discriminate between electrostatic and electromagnetic transport, and the parameter regimes in which each dominate.

Particle/Impurity Transport - Plans

FY03

The impurity transport experiments will be carried out at higher β_T using standard impurity gas injection.

FY04

Perturbative particle and impurity transport experiments will continue with supersonic gas injection, which will produce a highly collimated beam and thus better control and localization of the impurity injection. New and upgraded diagnostics will aid in these

experiments. The USXR and transmission grating spectrometer will provide 1-D (radial) diagnosis of the transport, and the GEM detector, presently under development, will employ a scheme to follow both the radial and poloidal heat flux propagation.

FY05

Deuterium pellet injection will be used as a basis to study particle transport perturbatively.

FY06-08

Perturbative transport experiments will be extended.

Fast Ion Confinement - Results

The low magnetic field of NSTX means that energetic ions (neutral beam ions in NSTX and charged fusion products in a reactor-scale ST) have gyroradii which are a significant fraction of the minor radius. This can cause more rapid loss of fast ions due to orbit effects, including prompt orbit loss, MHD-induced radial transport, and other diffusive transport. Losses of fast ions may, in turn, generate radial electric fields that affect bulk plasma confinement, rotation, and flow shear. A fundamental question which must be addressed, if STs are to be run in DT or considered as reactor prototypes is whether an ST plasma can maintain good confinement of energetic ions (especially alpha particles) with a significant fast ion beta.

In the area of single particle orbit effects, initial measurements from the NPA and the decay time of the neutron signal after the beams turn off indicate classical slowing down of beam ions in the plasma. Initial loss rate measurements from fast ion probes are not, at present, in good agreement with modeling. There is also substantial variation in neutron rate from nominally identical MHD-free discharges arising from some as yet unknown effect.

Fast Ion Confinement – Plans

FY03

Studies to understand the overall fast ion confinement effects will be initiated in with detailed comparisons between measured distributions of confined and lost NB ions and theoretically predicted distributions over a wide range of plasma parameters and in L- vs H-modes.

FY04

Attempts will be made to control the beam loss fraction by varying the gap between the plasma and the outboard midplane wall.

FY05

A comparison between co-injection with counter-injection will be used as a basis for studying the effect of the non-ambipolar losses, since the loss fraction during counter-injection is expected to be much higher (40% vs 5% for 1 MA discharges with 15 cm outer gaps).

FY06-08

These studies will be continued and extended.

Edge Transport and Fluctuations - Results

Understanding and controlling L to H mode transitions are key to the ultimate success of NSTX in that H-mode operation allows for the broader pressure profiles that enable steady-state operation at high- β_T and high bootstrap fraction. It was found that entry into the H-regime required at least twice the value given by recent ITER scalings [7]. The powers required to get into the H-mode (0.5 to 1.5 MW) are not restrictive, however, and high performance H-mode operation has become fairly routine.

When the “expected” density, toroidal field and size scalings are normalized out, the threshold power exhibits a residual dependence on plasma current, as is seen in Fig. 8. A source of this current scaling may be the radial electric field resulting from fast ion loss, which is relatively much greater at low current (40% at 600 kA) than at higher current (5% at 1 MA). Supporting the contention of the importance of fast ion loss are recent observations of transitions associated with bounce-precession fishbones.

Edge turbulence diagnostics have provided an initial glimpse into the fluctuations that may be causing plasma transport in the outer region, including the scrape-off layer. Density fluctuation amplitudes generally decrease going from L-mode to H-mode. Of particular importance for both confinement states is the presence

of large scale (several cm) convective cells measured by both gas puff imaging (GPI) and fast reciprocating probe diagnostics. These cells, which break off from the main plasma

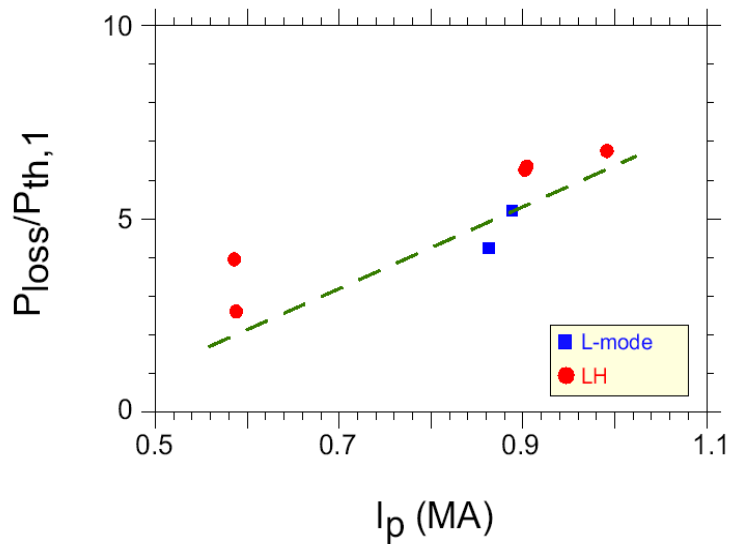


Fig. 8 Power through separatrix at the L-H transition normalized to an L-H threshold scaling versus plasma current.

near the separatrix and propagate primarily radially and poloidally, may bring into question the validity of the diffusive energy transport paradigm in this region of the plasma.

Edge Transport and Fluctuations - Plans

FY03

Discharge data near the L-H transition will be submitted to the ITER Threshold database in order to aid in the development of threshold scalings with a more accurate aspect ratio dependence. The role of E_r on L-H transitions will be studied experimentally using plasma current variations and RF heating. Edge pedestal characterization, making use of the fast reciprocating probe, will begin.

Edge fluctuations and convective cell transport will continue to be assessed in using GPI, reflectometry and the fast reciprocating probe. Radial correlation lengths, as determined from reflectometry, will be studied in conjunction with global confinement and local transport results.

FY04

Studies to determine which dimensionless parameters, other than aspect ratio, determine the L-H transition through complementary experiments in other devices and through comparisons with ST relevant theory will be initiated in FY04. Pedestal characterization will continue. Preliminary assessments of low- and high-k turbulence will be made with advanced diagnostics, to be implemented this year. Studies to assess the importance of the convective cells and intermittent transport and to determine the radial extent over which the cells exist will continue in FY04 and beyond as the edge fluctuation diagnostics become more mature. It will be important to compare fluctuation levels and structures to theory and understand how kinetic effects influence the turbulence levels. Far-infrared interferometers will be used to study low-k fluctuations in L-mode plasmas starting this year. Calibrated density fluctuation amplitudes will be made with reflectometers in different regions of the plasma will also start. Advanced fluctuation diagnostics will be implemented this year, and initial studies of both low- and high-k turbulence will begin.

FY05

Pedestal characterization will be extended with the He beam spectroscopy diagnostic to measure n_e and T_e . The role of E_r on transitions will be studied with co- vs counter-NBI injection comparisons. Studies of both low- and high-k turbulence will extend into this year as the advanced fluctuation diagnostics mature. Detailed comparisons between measured mode characteristics and non-linear results of comprehensive gyrokinetic codes will be made.

FY06-08

The fast CHERS system will be used to characterize the edge and pedestal regions. The CT injector would be used in attempts to produce edge transport barriers. Studies of the

role of E_r on transitions will be extended with actual measurements of E_r made by the LIF MSE diagnostic. Diagnosis of the full spectrum of fluctuations will continue.

Theory and Modeling - Tools

One of the mainstays of present theoretical analysis of toroidal plasma transport is the use of gyrokinetic codes which approach this problem from first principle equations incorporating as much physics as is viable computationally. Various codes using this approach are available and will be used to analyze NSTX plasmas. GS2 is an electromagnetic code that can provide both linear and non-linear simulations of ETG and ITG turbulence, and it has already been used in initial studies. Further advances in GS2 will focus on high-k ETG physics. The GTC code is a global gyrokinetic code that is presently valid for ITG modes, zonal flow and neoclassical calculations. Further development will involve incorporation of electrostatic and trapped electrons, finite- β_T effects, and 3D numerical equilibrium solutions. The neoclassical treatment in GTC will be reassessed for the large ρ/L_n and B_{pol}/B_{tor} in NSTX. The GYRO code is fully operational and can simulate the turbulent transport of energy, particles and momentum. It can, at present, handle ITG and adiabatic electrons, finite ρ^* , electromagnetic electrons and finite β , collisions and generalized geometry, but needs to be upgraded to handle non-adiabatic electrons and thus ETG modes. The BOUT, BAL and UEDGE codes will be used to study plasma transport in the edge and scrape-off layer.

The workhorse for performing interpretive transport analysis is the international standard TRANSP code, which incorporates state-of-the-art beam modeling, neoclassical (NCLASS), plasma species coupling, RF wave deposition packages and data handling modules in order to infer particle, energy and momentum transport coefficients. Up-to-date turbulent transport models (GLF23 and Multi-mode) have also been incorporated for theory/experiment comparisons when TRANSP is run in a mode that predicts temperature profiles based on these models or assumptions of ion neoclassical transport. Predictive comparisons between experiment and theory overcome many of the problems in inferring transport coefficients using kinetic profiles that are not well-resolved spatially.

Theory and Modeling - Plans

FY03

Transport coefficients from the critical gradient formalisms will be used as input to predictive TRANSP analyses, and the calculated temperature profiles will be compared to measured values to identify the theories which best reproduce the experimental results and to clarify the need for considering anomalous heating/transport processes and further theory development. This work will be starting in FY03 using analytic approximations to the diffusivities. A particular challenge for edge transport will be to assess the role of convective cells; this modeling will be done with the BAL, BOUT and UEDGE codes assuming non-diffusive transport.

A major challenge to theory in the analysis of NSTX transport results is to first ensure the validity of the various models in the low toroidal field, low aspect ratio regime. Starting in FY03, neoclassical theory will be updated to take into account the relatively large ρ/L , and beam-thermal ion friction terms, which can lead to inward or outward pinches, will be included. These updates will affect both transport fluxes as well as estimates of the bootstrap current.

Benchmarking the various gyrokinetic codes to identify the key differences among them will start in FY03 using similar treatments among codes.

Since the fast ion gyroradius can be comparable to the magnetic field gradient scale length, guiding center orbit theory begins to fail and the magnetic moment of the fast ions is not invariant. Improvements to the theoretical and computational ability to calculate how the fast ion population will redistribute and be lost due to this non-conservation will begin.

FY04

Predictive TRANSP analyses will continue in FY04 and beyond with thermal diffusivities taken directly from the gyrokinetic codes. Incorporation of large ρ^* , large trapped particle fraction, high- β_T and extreme plasma shaping effects begin. Non-linear, self-consistent calculations to determine saturated amplitudes of ITG, ETG, and CAE modes will allow a comparison between experiment and theory to assess the role of turbulence at different wavenumber and thus the potential for anomalous heating. These comparisons can be made once the advanced fluctuation diagnostics are implemented.

FY05

Inclusion of strong ExB shear and the possibility of large non-local effects due to large spatial scale lengths into the gyrokinetic calculations will start. Anomalous heating models beyond the ad-hoc stage will be developed based on results of the non-linear calculations and comparisons with turbulence measurements. Two possibilities for anomalous heating are ETG/streamers and CAEs.

FY06

Once the important physics effects are identified and incorporated into the gyrokinetic codes, these tools can be used as part of the basis for developing a high-confidence predictive transport capability.

FY07-08

Fully predictive transport simulation capabilities will continue to be developed. The transport simulations will be combined with those of MHD stability to form a fully integrated scenario development package. The results will be used as a basis for developing actual experimental scenarios to making use of pressure and current profile control techniques to achieve high-confinement, high- β_T , high-non inductive current fraction discharges.

Facility and Diagnostic Upgrades

FY03

A supersonic gas injector will be used to provide a particle source for perturbative impurity transport studies. The study of core and edge transport processes involves a suite of both profile and turbulence diagnostics. A new 51-channel, 10 msec time resolution CHERS (T_i , v_ϕ) system will be implemented. Assessing the role of flow shear and momentum transport will be aided by the implementation of a dedicated diagnostic to measure v_ϕ and v_θ at the edge by spectroscopic means. The CIF MSE diagnostic will provide initial measurements of the q-profile. Multi-sightline NPA will provide indirect measurements of beam deposition profiles through fast ion charge-exchange neutrals. A diagnostic has been developed which will resolve the pitch angle and energy of fast ions lost to the vessel wall.

These developing diagnostics will be augmented by reflectometry already implemented, which can provide a temporal overview of density fluctuations along with the determination of radial correlation lengths (FY03).

FY04

Perturbative heat transport studies can be attempted using localized electron heating from HHFW and a high-power EBW system. A higher time resolution (90 Hz) and spatial resolution (30 channels) Thomson scattering diagnostic is planned.

Density fluctuation measurements will be used to assess turbulence levels and the potential for anomalous heating. Long-wavelength turbulence is associated with ITG modes and can be detected using the technique of microwave imaging reflectometry. The diagnostic will provide a time resolved mapping of k_r and k_θ , extending the range of fluctuations that can be measured by conventional reflectometry techniques. Prior to implementation of this system, some information on density fluctuations in the ITG regime can be obtained in the core of L-mode plasmas using the Far Infrared Interferometer diagnostic.

Diagnosis of ETG modes has been an almost insurmountable challenge in conventional aspect ratio tokamaks because of the large wavenumbers and small fluctuation levels. At low field and low aspect ratio, the expected ETG wavelengths are higher (several mm), making these modes accessible diagnostically. Microwave scattering can be used for this purpose. These advanced fluctuation diagnostics for both low- and high-k fluctuations will be implemented in the FY04 or 05 time frame.

Calibrated reflectometers will provide information on CAE/GAE mode amplitudes in the outer region of the plasma.

FY05

Deuterium pellet injection will provide localized fueling that can change the density gradient dramatically and thus is key to being able to assess the role of η_e and η_i in ITG and ETG modes. Fuelling from the pellet injection will be used to study particle transport, while cold pulse propagation will be used to study heat transport. A poloidal CHERS system for v_θ measurements will be implemented. A He beam spectroscopy diagnostic will be used to measure edge T_e and n_e . Neutron collimators will provide an almost direct measurement of the beam deposition profile and comparisons to the expected neutron rates as determined by classical collisional theory.

FY06

The LIF Motional Stark Effect will provide the ability to measure the q-profile as well as E_{radial} directly to aid in the flow shear study. The fast CHERS diagnostic will provide ≤ 1 msec time resolved T_i and v_ϕ profiles.

FY07-08

An array of solid state (diamond and silicon) detectors will be added to measure simultaneously the energetic neutral flux along multiple sightlines. An impurity injector will be installed to aid in perturbative transport experiments. Liquid lithium modules and a divertor cryopump will be installed for density control. A CT injector will be used for fueling.

Research Plan Elements

To summarize, the main topical elements of transport research over the next five years are:

- Global confinement – establish general parametric scalings on engineering and dimensionless parameters, with emphasis on the dependence on aspect ratio and β_T for both L- and H-mode. Improve global confinement
- Ion transport – Establish the basis for ion transport at high- β_T with respect to neoclassical and ITG turbulent transport, considering the effects of flow shear. Relate energy transport to particle transport. Clarify need for anomalous ion heating.
- Electron transport – Establish the basis for electron transport with respect to ETG modes at high- β_T , considering the effect of flow shear. Study dynamics of ITBs.
- Momentum transport – Assess role of rotational shear, zonal flows and relate momentum transport to energy and particle transport within neoclassical framework.
- Fast ion transport – Assess fast ion confinement over a range of conditions, as well as the effect non-ambipolar losses have on the generation of E_{radial} and resulting ExB flow shear.

- Turbulence (core and edge) – Measure ITG/ETG turbulence and relate to ion/electron transport. Establish importance of electromagnetic transport at high- β_T . Assess role of edge convective cells relative to diffusive transport paradigm. Determine potential for anomalous heating from ETG, CAE turbulence.
- Theory – Enhance validity of neoclassical and gyrokinetic theory at low R/a , large ρ^* , high- β_T , large trapped particle fraction. Develop physics-based anomalous heating models. Develop predictive transport capability.
- Combine experimental and theoretical understanding to reduce transport through pressure and current profile control.

The overall five year plan is shown in Fig. 9. The plan incorporates elements from experimental research, theory and code development, diagnostic development and facility improvements to form a logical progression of research activities in pursuit of the main transport goals.

As can be seen in the plan, the emphasis over the first year or two will be on establishing global scalings, establishing reliable methods for high-performance H-mode operation and laying the groundwork for understanding the local transport properties at low aspect ratio and high- β_T . The experimental results will be compared to linear calculations of turbulence growth rates. As profile diagnostics and theory mature, more subtle effects such as the role of toroidal and poloidal rotation shear and zonal flows will be studied with detailed comparisons between theory and experiment. For instance, tests of critical gradient models will be studied using perturbative techniques. During this time, both neoclassical and turbulent transport theories will be upgraded to take into account the unique NSTX physics regime parameters. The implementation of low and high- k turbulence diagnostics will allow for direct measurement of both ITG and ETG mode amplitudes and spectra, which will then be compared with expectations from non-linear calculations. The theory and measurements will be used to determine quantitatively the role of anomalous ion heating.

These elements are steps toward the ultimate goal of understanding the turbulence and transport properties of NSTX plasmas well enough to, on one hand, develop a theoretical/numerical predictive capability, and, on the other hand, to be able to control both the kinetic profiles and current profile to understand and optimize performance in a self-consistent manner.

References

1. Gates, D., N. Gorelenkov and R. White, Phys. Rev. Lett., 87 (2001) 205003-1
2. Rewoldt, G. et al., Phys. Plasmas, 3 (1996) 1667
3. ITER Physics Team, Nuc. Fusion, 39 (1999) 2145
4. Kaye, S.M. et al., Fusion Technology, 36 (1999) 16
5. Houlberg, W. et al., Phys. Plasmas, 4 (1997) 3230
6. Menard, J., private communication (2002)

7. Bourdelle, C. et al., submitted to Phys. Plasmas, 2002
8. Snipes, J. et al., presented at 19th IAEA Fusion Energy Conference, Lyon, France (2002)

Confinement scalings

Transport physics

Momentum & power balance, strong electron & ion heating, low and high beta

Local transport & turbulence

Understanding

Low/high k spectra theory/experiment, low/high beta

Boundary transport & turbulence

Poloidal flows

V_ϕ shear & w/error field

Feedback with heating, CD, V_ϕ , fueling

*$P(r), J_{BS}$
optimize*

Global characterize

χ & pellets

MSE CIF

MSE LIF (J, E_r, P); polarimetry

Transport tools

HERS 51 ch

Poloidal
CHERS

Fast CHERS (edge)

Diagnostic X-ray

MPTS upgrades

He beam spectroscopy

Liquid Li?
CT injection?

Edge $v_{\phi, \tau}$

Turbulence diagnostics
Initial

Advanced

Li pellets

Feedback with MSE, heating, CD, rtEFIT

Neutron collimator

Impurity injector

Error field
coils

D pellets

1 – 3 MW EBW

Cryopump Solid state neutral particle

Predictive Transp (GLF23, Multi-Mode)

Transport theory

GS2 linear, non-linear

GTC trapped e⁻ Finite β High β

Gyro non-adiabatic

Neoclassical: beam-thermal friction, potato orbit, high ρ/L , B_{pol}/B_{tor}

*Full predictive transport
simulations*

Non-linear CAE

Anomalous heating

Fig. 9 Integrated Transport Research Plan

3.3 Wave-particle Physics, Heating, and Current Drive

3.3.1 High Harmonic Fast Wave Goals

The IPPA-FESAC 5-year research objective “Preliminary Assessment of ST Performance” and the 10-year research objective “Assessment of the attractiveness of the ST concept for pulse lengths long compared to the current diffusion time” require tools to heat and drive current supplemental to the ohmic systems. One such tool is RF wave heating and current drive utilizing the fast magnetosonic wave at high harmonics of the ion cyclotron frequency. Up through the first 5-year assessment point of the plan, to be reached in 2006, a comprehensive evaluation of HHFW as a tool for enhancing ST performance, heating current drive and startup, will be performed. It will be applied to help meet the goals of fully non-inductive operations for plasma parameters relevant to a component test facility, and will also be used in discharges demonstrating solenoid-free plasma current rampup to high beta operations. Afterwards, HHFW will be utilized in conjunction with other techniques to further reduce volt-second consumption and to assist long-pulse operations for the highest beta plasmas.

3.3.2 HHFW Physics

High harmonic fast waves are expected to primarily heat electrons making it a strong candidate for driving current in ST plasmas. Wave accessibility in the naturally occurring high β plasmas of an ST preclude the use of conventional ECH or Lower-hybrid heating or current drive except for the possibility of plasma startup in low-beta plasmas. An alternate high frequency RF technique utilizing mode converted electron Bernstein waves (EBW) has been proposed and will be discussed separately. In spite of the large ratio of ω/Ω_{ci} , 9-13, on NSTX at large values of β_i some power will damp on thermal ions and in addition due to the large value of $k_{\perp}\rho_i$ for NBI ions they can absorb appreciable power as well. Current drive efficiencies with HHFW waves are expected to be comparable to other fast wave and ECH techniques since they drive the same class of electrons near the thermal velocity.

3.3.3 The HHFW System

The HHFW on NSTX utilizes much of the ICRF system from TFTR. In fact the frequency employed, 30 MHz, is identical to that used on TFTR. Due to the much reduced toroidal magnetic field of NSTX compared to TFTR this corresponds to moving from $\omega=2\Omega_T$ to $\omega=10\Omega_D$ without changing ω ! Transmitters were left in place and the transmission line from the transmitters to the tuning network was untouched the output of the tuning network was rerouted from the entrance to the TFTR test cell to the NSTX test

cell. The antenna and the external power dividing and phasing network were constructed specifically for NSTX.

The antenna consists of 12 independent antenna modules. Each module contains a radiating element grounded at the bottom to the enclosure box and fed at the other end through an rf feedthrough and spool piece. The radiating element is separated from the plasma by a 50% transparent single-layer Faraday screen composed of individual u-shaped elements. Exterior to the vacuum vessel is a system of transmission lines and tuning elements that divide the power from the six transmitters into twelve feeds, cancel the mutual coupling between adjacent antenna elements and allow for the monitoring of antenna voltage, current and phase.



Figure 3.3.1 The twelve-strap HHFW antenna array.

Operation goals of the system include 6 MW of injected power for pulse lengths much longer than a current diffusion time, and potentially as long as 5 s pulses, with real time phase control of the antenna spectrum, and programmed amplitude modulation. In the design phase it was estimated that antenna voltages of ~ 20 kV would be required to support this level of operation. Vacuum conditioning of the antennas to the 25-30 kV

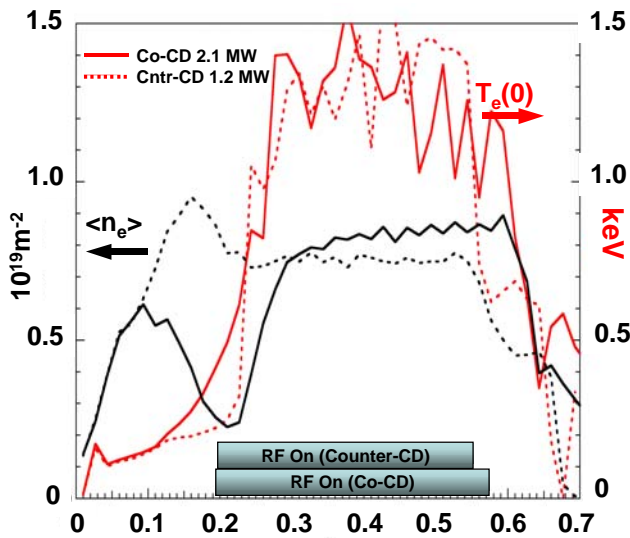


Figure 3.3.2 Evolution of $T_e(0)$ and $\langle n_e \rangle$ for co and ctr current drive discharges

level is routinely obtained. Pulse duration has been limited to < 1 s by machine limitations. 6MW of power has been achieved for short pulses but long pulse power has been limited by arcing in the vacuum region. The reliable long pulse limit has gone from 3.5 – 4 MW during the 2001 campaign to ~ 2.5 MW during the 2002 campaign. The peak antenna voltage limit for reliable operation was found to be ~ 12 kV. During the 2002 outage examination of the antennas by dismantling them uncovered a weak point in the spool-piece/feedthrough area where arcing along the magnetic field was observed. As a result modifications have been made to increase the

spacing and to reduce the electric field stress for a given rf power. These improvements will be tested in the 2003 operations period.

3.3.4 Status of HHFW Research

To date, experiments on NSTX have confirmed the strong electron damping expected by theory. In the relatively low β plasmas investigated so far, no evidence of thermal ion heating has been found. Figure 3.3.2 illustrates the basic heating results obtained on NSTX. The central electron temperature increases strongly with the application of HHFW power. The ion temperature, measured with a short NBI pulse near the end of the RF pulse using charge exchange recombination spectroscopy, is half the electron temperature. The strong absorption of HHFW waves on electrons allows heating even at the low target temperature of 300 eV. Global energy confinement is found to be in agreement with predictions from conventional scaling.

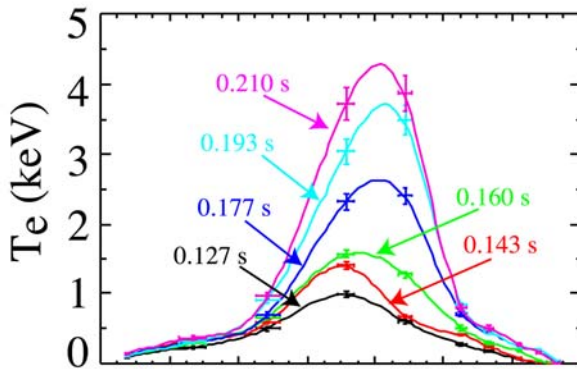


Figure 3.3.3 Temperature profile evolution of an improved confinement HHFW discharge

Improved confinement discharges have been observed with central electron temperatures reaching 4 keV, (Figure 3.3.2). The confinement improvement is observed over the central half radius with as much as an order of magnitude improvement on-axis. These discharges exhibit a continuous improvement in time, eventually terminating in a crash.

Preliminary experiments on current drive have been performed. In the absence of an internal current profile diagnostic, such as MSE, the only indicator of current drive is the response of the loop voltage. To differentiate between direct RF current drive and bootstrap current, these experiments were conducted at low values of β and in L-mode. Since NSTX operates in a mode with feedback holding the plasma current constant an internally driven current induces an immediate response in the external power supplies that shows up as a reduced loop voltage required to sustain the same total current. The absolute level of loop voltage required for a given current is a sensitive function of the plasma resistivity, which depends on the electron temperature, density and the plasma Z_{eff} . Discharges with the rf antenna phased to launch directed

current drive phasing. Discharges with the rf antenna phased to launch directed

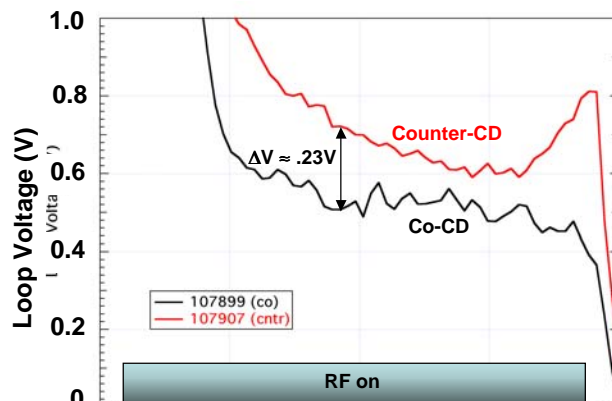


Figure 3.3.4 Loop voltage evolution for co and ctr current drive phasing

waves co- and ctr- to the plasma current were carefully matched in density, temperature and Z_{eff} by adjusting the power level and gas fueling rate, fig.3. The amount of driven current can then be estimated from the formula:

$$I_p = (V - 0.5 * I_p * dL_i/dt) / R_p + I_{BS} + I_{CD} \quad (1)$$

For the conditions of Fig. 3.3.2, the loop voltage difference of ~ 0.23 V (Fig. 3.3.3) between co- and ctr- corresponds to ~ 110 kA of driven current for the co- case. Predictions from the TORIC and CURRAY rf wave deposition and cd codes are in rough agreement with this estimate yielding 96 and 160 kA respectively. Evidence for current drive has been observed with directed wave spectra between 3 and 7 m^{-1} .

In order to demonstrate an attractive fully non-inductive scenario a large fraction of the current should be driven by the bootstrap current. This is most readily achieved in H-mode discharges with their large values of stored energy and their broad pressure profiles. In fig. 5 an H-mode discharge with $\beta_p \sim 1$ and $I_{bs}/I_p \geq 0.4$ is sustained with HHFW heating alone. The discharge has reached transport equilibrium in an elming H-mode but the current profile continues to evolve with $q(0)$ rising and I_i falling to the end of the rf pulse. The H-mode phase terminates with the removal of rf power which was programmed to go off at the time of TF ramp down. This discharge is an attractive target for long pulse sustainment by phasing the rf for current drive instead of heating.

The efficiency of RF current drive can be adversely effected by damping of the HHFW power into thermal ions or energetic NBI ions. Acceleration of NBI ions to energy's above the injection energy has been observed in the presence of HHFW heating in the

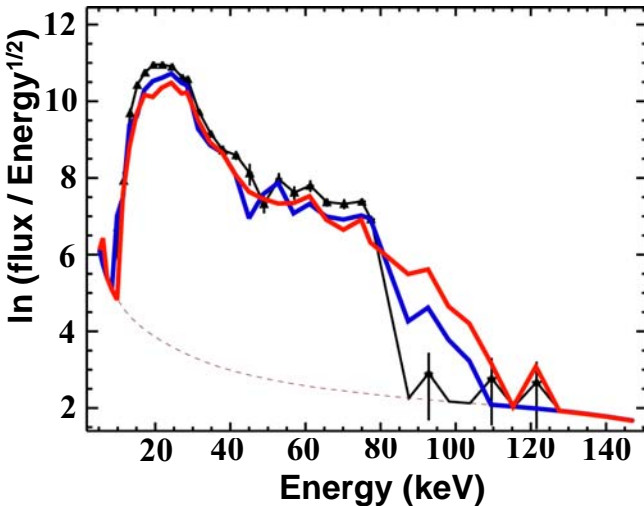


Figure 3.3.5 Escaping fast ion energy distribution as measured by a neutral particle energy analyzer. Full beam energy is 80 keV.

escaping fast neutral energy spectrum, measured with a charge exchange analyzer. A tail above the 80 keV injection energy is observed extending in some cases to 140 keV. The distribution relaxes to its no RF level after the HHFW is turned off (blue and black curves), consistent with classical slowing down upon removal of the RF power. In addition, enhanced neutron production is measured when the tail is present, confirming its existence. Behavior of the tail as parameters are varied has been investigated to ascertain the seriousness of the power loss. Increasing the electron b is seen to reduce the tail as expected from

theory, in addition no increase in the tail is observed as the wave k_{\parallel} is reduced in contradiction to theoretical predictions. Both of these results, although preliminary, are positive results for driving significant currents in the high beta long pulse target discharges.

3.3.5 HFW Theory and Modeling Status

Ono was the first to elucidate the basic theory for high harmonic fast wave (HFW) heating of high β plasmas [ref:Ono]. The fast magnetosonic wave that is used for conventional ICRF heating and current drive is also utilized in the HFW regime. Consequently, HFW heating and current drive in an ST share a common foundation, both in physics and technology, with the heating and CD scenarios that have already been extensively studied in conventional and advanced tokamak regimes. Despite this common foundation, there are features unique to the HFW regime that require significant extensions to the theory and models developed for ICRF heating and current drive in conventional and advanced tokamaks, as discussed in the section on RF Theory and Computation. In this section, some specific applications of theory and modeling to the understanding of NSTX experiment as well as future development plans are discussed.

Because the launched wave frequency is much higher than the fundamental cyclotron frequency of any ion species in an ST plasma, ion cyclotron damping occurs at high harmonics of the fundamental ion cyclotron frequencies (in NSTX experiments, typically $5 < \omega/\Omega_i < 15$). Most computational models developed for conventional tokamaks utilize a finite Larmor radius expansion of the wave fields, an approximation which is strictly valid only for fundamental and second harmonic cyclotron interactions for ions whose gyroradii are small relative to the perpendicular wavelength of the high harmonic fast wave (i.e., valid in the FLR or finite Larmor radius limit). Recently, 1D [ref; METS code] and 2D [ref: AORSA code] kinetic wave codes have been developed which include all cyclotron harmonic interactions and which are valid for ion gyroradii which can be large relative to the HFW perpendicular wavelengths but small compared to equilibrium scale lengths. Initial results from these generalized all-orders codes indicate that the wave dynamics in NSTX plasmas with moderate densities and temperatures is dominated by fast wave physics with electron absorption dominant in this parameter regime, as expected from theory. Mode conversion to short wavelength ion Bernstein waves, which in principle can occur near the various cyclotron harmonics, does not appear to be significant in these plasmas. In Figure 1, the left-hand component of the fast wave field obtained from the 1D all-orders code, METS, is shown as a function of distance along the midplane for an NSTX discharge with combined HFW and NBI heating. No excitation of short wavelength modes is evident near the cyclotron harmonics. Similar results have been obtained with the AORSA-2D all-orders code [ref:Jaeger]. Further numerical studies will be performed to determine if mode conversion is more significant at the higher toroidal fields and hence somewhat lower cyclotron harmonics anticipated in a next-step ST device..

In NSTX plasmas, because of the absence of significant mode conversion and because the ratio of the wavelength to the equilibrium gradient scale lengths is small, ray tracing

codes that are based on WKB approximations may be applicable. Power deposition profiles obtained with ray tracing codes that utilize the full hot plasma dielectric tensor to compute the ion and electron damping compare favorably with those obtained from the all-orders kinetic models for NSTX plasmas with moderate densities and temperatures. In Figure 2, excellent quantitative agreement is evident between the power deposition profiles obtained with two ray tracing codes, HPRT[ref] and CURRAY[ref], with the AORSA-2D full wave code, and with the TORIC reduced order 2D full wave code for an NSTX discharge in which the electron damping is predicted to dominate. TORIC [ref] is a full wave code that utilizes the FLR approximation and a reduced order approximation [ref; Smithe and Colestock] to solve for the fast wave fields. Both the ray tracing models and the full wave reduced order models usually require far less computational time than the full wave all orders codes, so these simpler models may offer a more practical yet accurate module for integration into a time-dependent transport analysis package, such as TRANSP. The CURRAY ray tracing code and the upgraded TORIC code are both being implemented in TRANSP. This work should be completed in FY03 in order to enable to time-dependent transport analyses of NSTX experiments.

Though thermal ion damping is usually weak for moderate temperatures in an NSTX plasma, damping on energetic ions present due to neutral beam injection (NBI) can be important, since $k_{\perp}\rho_i \gg 1$ for these ions. In recent experiments on NSTX with combined HHFW heating and neutral beam injection, direct measurement of the fast ion velocity distribution function with the NPA diagnostic indicates that substantial damping of the HHFW's by the energetic ions occurs that is accompanied by a significant distortion of the beam slowing down distribution function [ref: Rosenberg]. Though the all-orders full wave models include beam ion absorption when $k_{\perp}\rho_i \gg 1$, these codes generally assume that the ion velocity distributions are Maxwellian. Recently, as part of the SciDAC initiative, the 1D METS code has been generalized to compute wave propagation and absorption in plasmas with significant populations of a non-thermal species [ref: Dumont et al, EPS]. Initial results from the generalized 1D METS code indicate that absorption on isotropic beam distributions may be reasonably approximated by Maxwellian distributions with the same average energy. Effects of anisotropy in the beam distribution functions arising from the beam injection angles will be evaluated in FY03. However, 2D effects on wave propagation and absorption are also known to be significant in an ST plasma, as indicated by comparisons of power deposition profiles obtained with 1D and 2D models. To address the effects of non-Maxwellian species on 2D wave propagation and absorption, the 2D modeling codes will need to be generalized to include non-Maxwellian species in their dielectric tensor operators. In order to estimate the magnitude of these effects, the ray trajectories from the HPRT code will be used to specify an equivalent "1D" equilibrium for the METS code. By mapping the resulting 1D deposition profiles back into the 2D plane using the ray paths, a qualitative look at the effects of beam ion absorption in 2D will be obtained. This initial study will be completed in FY03. If significant modifications of the wave propagation and absorption are indicated, then the dielectric tensor operators in the 2D full wave codes will be generalized to include non-Maxwellian species. Since the HHFW's have been observed to modify the beam slowing down distributions, the wave codes must be coupled with a Fokker-Planck code to self-consistently compute the wave propagation and absorption. In the preliminary studies, beam velocity space distribution functions obtained from the TRANSP code will

be used to specify the non-Maxwellian species in the wave codes. Eventually, the generalized wave codes must be integrated with a Fokker-Planck code to self-consistently compute the wave propagation, absorption and velocity space modifications. The CQL3D/GENRAY code, which combines ray tracing for wave propagation with a Fokker-Planck package that includes collisions, large orbit losses and rf quasilinear diffusion in two velocity-space dimensions, will be modified and benchmarked against NSTX data. If full wave effects are found to be important, then the CQL3D package will be integrated with the generalized 2D wave codes. It is anticipated that such a combined simulation package will require a significant amount of computation time and will not likely be appropriate for use in time-dependent simulations with the TRANSP package. This code development activity is expected to last through FY05.

Because of the inherently high beta and high dielectric constant in an NSTX plasma, direct electron absorption of the waves via transit time magnetic pumping is comparable to or greater than direct ion absorption via cyclotron damping, even in plasmas with neutral beam injection. Unlike the low fast wave direct electron damping rates of <15% per pass in conventional tokamaks, it is not unusual to expect nearly 100% damping in a single pass through the NSTX plasma. In fact, since the damping is so strong at high β , the wave power can be significantly damped before it reaches the center of the plasma, resulting in off-axis power deposition profiles. When combined with appropriate control of the launched wave spectrum, noninductive control of the off-axis current profile may be possible. Loop voltage measurements in preliminary HHFW current drive experiments on NSTX without neutral beam injection are consistent with the presence of non-inductively driven currents. The experimentally inferred HHFW driven currents are comparable to those estimated with the CURRAY code and with the TORIC code. CURRAY utilizes either the Ehst-Karney parameterization[ref] of current drive efficiency or a full adjoint solution to the Fokker-Planck equation [ref] to estimate the driven current profile. At low plasma betas up to about 15%, the parameterization and the adjoint code give similar estimates for the current drive efficiency, according to studies with CURRAY package [ref:Mau]. Previous studies obtained with an earlier version of the TORIC code coupled to the adjoint code also found that the Ehst-Karney parameterization is adequate for plasma betas up to about 15% [ref: Wright] The more recent version of TORIC utilizes the Ehst-Karney parameterization, but development work is underway to couple TORIC with the CQL3D Fokker-Planck package. Further benchmarking of these codes against NSTX will continue, particularly when direct measurements of the driven currents are obtained with the MSE diagnostic. In the meantime, effects of the DC electric field arising from the ohmic current drive system, particle trapping, and electron transport will be incorporated into the full Fokker-Planck models. These theoretical and experimental studies, when combined with the generalized wave codes discussed above, will serve to elucidate the importance of various effects on HHFW heating and current drive in NSTX plasmas.

3.3.5 HHFW Research Plan for 2003 - 2008

The comprehensive evaluation of HHFW as a tool for use in ST requires experiments and modeling to confirm an understanding of HHFW heating and current drive physics

sufficient to predict its performance in future ST experiments. In the case of heating this should include an understanding of: operations in various plasma configurations, the behavior as density is controlled with gas puffing, H-mode behavior with RF, radial localization of heating as a function of plasma parameters and launched spectrum, and improved confinement regimes. For current drive this evaluation should include an understanding of efficiency as a function of plasma parameters and phase as well as configuration.

Configuration and density dependence of HHFW coupling

2003 – 2004: HHFW heating experiments have mostly been performed in limiter or lower single null configurations. Double null configurations and various values of inner and outer gap parameters should be explored. For example, preliminary data show an inverse relationship between inner gap and stored energy. Finally, as density is raised by gas puffing, heating efficiency as measured by the central electron temperature, is reduced. This may be due to a broadening of the deposition profile, a reduction in global confinement or damping of the rf power in the plasma periphery. Density control will be studied over a wider range of density owing to improved fueling capability and wall preparation techniques, as discussed in the section on boundary physics.

HHFW with heating phasing as a pressure and current profile modification tool - Heating with HHFW can modify the q profile through electron heating directly, even in the absence of current phasing. For example, higher electron temperatures can increase the plasma conductivity, increasing the current diffusion time, can increase the plasma bootstrap current, and can increase the neutral beam current drive by increasing the fast ion slowing down time.

HHFW heating, coupling with NBI, and profile modification

2003 – 2004: Internal inductance modification through heating early in the discharge - Already HHFW heating in the current ramp phase has resulted in voltage second savings, reduced the plasma internal inductance and increased $q(0)$. This work will continue and will benefit from improved plasma control and understanding of gap and configuration dependence of HHFW efficiency.

Effective coupling of HHFW with neutral beam heating – A research focus in 2003 will be the assessment of HHFW heating effectiveness in the presence of strong neutral beam heating. The efficiency of HHFW heating as a function of target plasma conditions, including plasma beta and density, will be assessed.

HHFW H-modes – H mode plasmas have been produced by HHFW heating alone and are promising targets for achieving the ultimate NSTX goals. The exact conditions under which H-modes are obtained with RF have received little attention to date. Threshold power as a function of plasma parameters needs to be determined. The conditions for achieving ELM-free or ELMy H-modes will be established, as will the configuration space for achieving the best H-mode/HHFW performance.

2004 – 2006: Initial feedback control of HHFW heating - Application of HHFW to high beta plasma targets should yield off-axis HHFW deposition, potentially enabling

broadening of the electron thermal pressure profile. Initial work in feedback of HHFW will begin towards the end of this research period.

2007 – 2008: Advanced feedback control of HHFW heating and current drive is described below.

Current drive studies and wave-particle interactions

2003 – 2004: *Improving system reliability and power levels* - The first current drive studies in 2003 will take advantage of improved high voltage standoff and higher power levels for longer pulse, enabling more definitive assessments of current drive via observations of the surface loop voltage to be obtained. These experiments will continue the investigations begun in 2002 exploring higher power, higher temperature plasma and a wider range of wave spectra. In addition, during the 2003 campaign it is expected that the MSE diagnostic will be commissioned and be in preliminary operation. Experiments with a fully operational MSE diagnostic are expected in the 2004 time frame. These experiments will explore the radial location of the driven current and the ability to control it. Wave-fast particle interactions studies, which may partly determine the efficiency of HHFW current drive and heating, will use measurements of the escaping fast ion distribution and its modifications from the launching of EBW waves.

2004 – 2006 *a. Parametric dependencies* - For current drive, it is important to establish the efficiency as a function of RF power, density, temperature, and antenna phasing. Early in this period, such dependencies will be explored. Present scenarios being examined suggest that NSTX non-inductive sustained operation in 15 – 20% toroidal beta plasmas relevant to a component test facility will require driven currents of about 100 kA with upwards of 5 MW of HHFW heating in the presence of substantial bootstrap current (see Chapter 4 on Integrated Scenario Development). Achieving higher amounts of driven current at lower input powers will add highly desirable flexibility for these scenarios. The MSE diagnostic will allow an investigation of the radial location of current drive and an exploration of the role of trapping in reducing current drive efficiency. Trapping is believed to reduce the driven current in present experiments by as much as a factor of four. It should play a larger role in off-axis current drive but its role may be reduced at high beta by the diamagnetic effect.

b. Phase feedback on current profile modifications – Phase modification within a discharge has already been demonstrated with the HHFW system. Real-time assessment of changes in the magnetic field pitch angle due to current profile changes will be possible with the MSE laser-induced fluorescence (LIF) system. It is therefore possible to modify the antenna phasing in response to modifications in the current profile in real time. Implementation of this capability will begin in the 2005 – 2006 time frame.

2007 – 2008: *Advanced HHFW heating and current drive feedback control* - HHFW will be used in both heating and current drive phasing with full feedback control of the antenna phase. The MSE LIF system will be used to measure the local current density, local plasma pressure, and radial electric field changes in real time. In conjunction with the NSTX control system and the HHFW real-time power and phasing control capability, this will allow for advanced feedback control of the pressure and current profiles.

Solenoid-free plasma startup

The use of HHFW in these studies is discussed in additional detail in Chapter 4.

2003 – 2004: Coupling with Coaxial Helicity Injection - In this time period, the transient application of coaxial helicity injection will be used to initiate a plasma discharge without the use of a solenoid. The plasma control system will be used to maintain position control of the reconnected plasma. Following on studies where the CHI is coupled to ohmic plasmas late in 2003, the next step will be the application of HHFW heating for the development of bootstrap currents, and the application of HHFW with current drive phasing for the direct drive of current.

2005 – 2006: Handoff to NBI during current ramp - When the current is driven to a level high enough to enable effective confinement of fast ions, neutral beam injection will be applied to allow bootstrap current and direct neutral beam current drive to carry the plasma current to a high poloidal beta flattop.

2007 – 2008: – Optimization of flux consumption in high performance plasmas - Techniques for flux savings developed in this research will be applied to the optimization of plasmas with toroidal beta values approaching 40% and bootstrap fractions of up to 70%, in pursuit of the demonstration of advanced, high performance ST operating scenarios.

Technical modifications to the HHFW system

2003 – 2004: – Possible additional modifications for reliability at high voltages - The antenna voltage limit must be raised to achieve routine 6 MW operation. If the recently made modifications increase this limit then further improvement should be possible by going to a double-ended configuration from the present single ended one. This would require significant modification of the antenna. Even if the present modification works to 6 MW the further change might be justified by allowing even higher power, which is available from the transmitters, or a reduction in the number of antenna elements yielding more room for diagnostics.

2005 – 2006: - Antenna reorientation with respect to field lines - An area for possible improvement is in the spectral configuration. The present antenna features elements are oriented perpendicular to the toroidal field. HHFW wave physics suggests that these elements should be perpendicular to the total magnetic field. This, of course, cannot be perfectly achieved in practice but can be approached much more closely than the present arrangement. While this was considered in the design phase from the standpoint of antenna sheath formation and predicted to be unimportant with respect to this effect, one consequence of the present configuration is an asymmetry in the antenna voltage for co- and counter- current drive phasing. As a result of this asymmetry, the voltage limit is lower for counter phasing. Tilting of the antenna straps may alleviate this condition.

3.3.6 EBW Research Program Goals

Recent experiments on CDX-U and NSTX have demonstrated that mode conversion of EBWs, emitted by thermal fluctuations in these overdense plasmas, to the X-mode can be controlled by modifying the edge density profile with a local limiter. Based on the success of these passive emission experiments, the NSTX EBW heating and current drive research program for the period 2003 to 2008 has four major goals. The first goal is to demonstrate efficient coupling of X (or O) mode waves to EBWs for high input powers (in the megawatt range). The second goal is to control the spatial location where the EBWs damp on electrons and, subsequently, heat them. These first two goals are in support of the IPPA 5-year milestone 3.2.1.3 to heat high β over-dense plasmas. The third goal is to test EBW-assisted non-inductive current startup either alone or in combination with HHFW and/or CHI. This goal supports the IPPA 5-year milestone 3.2.1.4 to make a preliminary assessment of non-inductive spherical torus (ST) startup. The fourth goal is to test neoclassical tearing mode suppression with EBW heating and/or current drive to help sustain a high β plasma for up to one second duration. This goal supports the IPPA 5-year milestone 3.2.1.2 to suppress β -limiting MHD modes. In order to accomplish these research goals within the time period covered by the 5-year plan, it is imperative that about one megawatt of EBW heating capability be installed and operational on NSTX no later than 2006. The plan also includes an upgrade to a 3 MW EBW heating and current drive system towards the end of the 5-year plan time period to provide a tool to optimize NSTX non-solenoid operation starting in 2009. This latter goal supports the IPPA ten-year milestone to assess the attractiveness of ST operation for pulse lengths much longer than the current penetration time scale.

3.3.7 Status of EBW Research and Near-Term Plans

For low- β , large aspect ratio devices, such as conventional Tokamaks, current profile control can be provided by ECCD, but for high- β plasmas, like the ST, the plasma is over-dense ($\omega_{pe}/\omega_{ce} > 1$), precluding the use of ECCD and ECH. EBWs on the other hand have the potential to heat and drive current in STs, since these waves propagate in over-dense plasma and are strongly absorbed near the electron cyclotron resonances.

The EBW emission, heating and current drive research program has so far been focused on two areas of research; optimization of the mode conversion and coupling between electromagnetic modes and EBWs and the identification and characterization of current drive and heating scenarios for NSTX equilibria through the use of ray tracing and Fokker-Planck deposition codes. Experiments to maximize EBW mode conversion to the X-mode have already demonstrated $> 95\%$ EBW to X-mode conversion on CDX-U and up to 50% EBW to X-mode conversion on NSTX. These experiments were conducted to support the development of an EBW emission diagnostic for $T_e(R,t)$ measurements as well as the proposed NSTX EBW heating and current drive program discussed here. Experiments that aim to demonstrate $\geq 80\%$ EBW to electromagnetic mode conversion via emission measurements with a local limiter are planned for the 2003 NSTX run campaign.

3.3.8 Status of EBW Coupling Theory and Modeling

EBW mode conversion can occur via two processes. The first process involves conversion of EBWs to the fast X-mode [1-3]. EBWs first convert to the slow X-mode at the upper hybrid resonance (UHR). A cutoff-resonance-cutoff triplet formed by the left hand cutoff of the slow X-mode, the UHR, and the right hand cutoff of the fast X-mode allows the slow X-mode to tunnel through the UHR to the fast X-mode (B-X conversion). This is the conversion process so far investigated on CDX-U and NSTX. The mode conversion efficiency (C) for $k_{//} = 0$ is given by [3]:

$$C = 4e^{-\pi\eta} \left(1 - e^{-\pi\eta}\right) \cos^2(\phi/2 + \theta) \quad (1)$$

where $\cos^2(\phi/2 + \theta)$ is a phase factor relating to the phasing of the waves in the mode conversion region and the term preceding this is the maximum mode conversion efficiency. Here η is a tunneling parameter, which for magnetic scale lengths much greater than the density scale length at the UHR [3], is given by:

$$\eta \approx \left[\omega_{ce} L_n / (c\alpha)\right] \left[(1 + \alpha^2)^{1/2} - 1\right]^{1/2} \quad (2)$$

where L_n , the density scalelength, and $\alpha = \omega_{pe} / \omega_{ce}$ are evaluated at the UHR layer and c is the velocity of light. From these equations it can be seen that the B-X conversion efficiency is very sensitive to changes in L_n at the UHR layer where the wave frequency, $\omega = \omega_{UHR}$. B-X mode conversion is particularly well suited for ST plasmas since the UHR layer for fundamental EBW conversion lies in the scrape off layer outside the last closed flux surface (LCFS) where L_n can be modified without affecting plasma performance. On CDX-U and NSTX the maximum mode conversion efficiency for fundamental EBWs occurs for $L_n \sim 0.3-0.6$ cm.

The second mode conversion process requires the coincidence of the X-mode and O-mode cutoffs [4-8] (B-X-O conversion), has been studied extensively on Wendelstein 7-AS both for heating [9] and as a $T_e(R)$ emission diagnostic [10]. The B-X-O emission leaves the plasma through an angular window at an oblique angle with a transmission function given by [6,8]:

$$T(N_{\perp}, N_{//}) = \exp\left\{-\pi k_o L_n \sqrt{(Y/2)} \left[2(1+Y)(N_{//,opt} - N_{//})^2 + N_{\perp}^2\right]\right\} \quad (3)$$

where: k_o is the wavenumber, $N_{//,opt}^2 = [Y/(Y+1)]$, $Y = (\omega_{ce}/\omega)$, ω_{ce} is evaluated at the cutoff and ω is the wave frequency. For NSTX this B-X-O emission window is located at about 35° from the normal to the magnetic field direction at the cutoff. The emission window has a width that increases with decreasing L_n at the O-mode cutoff. It can contribute to the measured X-mode emission if the antenna acceptance angle is large enough and if there is polarization scrambling of the O-mode emission resulting from reflections.

Because of the fundamental properties that are satisfied by the mode conversion equations: linearity, energy flow conservation, and time reversibility [11,12] the emission results from CDX-U and NSTX can be used for studying mode conversion excitation of EBWs for heating and current drive in ST plasmas.

3.3.9 Status of EBW Mode Conversion and Coupling Experiments

For fundamental and second harmonic EBWs CDX-U and NSTX are over-dense beyond the LCFS on the outboard side. Second harmonic EBWs from the plasma core convert to X-mode near the LCFS and fundamental EBWs mode-convert between the LCFS and the vacuum vessel wall. Mode-converted fundamental and second harmonic EBW emission from NSTX and CDX-U has been measured normal to the magnetic field with microwave radiometry. Radiometers have operated in the 8-18 GHz band on NSTX and 4-12 GHz band on CDX-U [13]. The radiometers are calibrated absolutely with a Dicke-switched blackbody calibration source. On NSTX, dual-ridged antennas have so far viewed the emission through a vacuum window and were oriented to accept, predominantly, X-mode polarized emission during the current flat top. On CDX-U, initial measurements were made with a similar arrangement, but later measurements used an in-vessel quad-ridged antenna that incorporates a local limiter.

The radial localization of the EBW emission source was confirmed on CDX-U by perturbing the T_e profile with a series of cold gas puffs, a technique used earlier by Laqua *et al.* [10]. The cold gas puffs locally cooled the plasma edge producing an inward propagating temperature response. The delay in the arrival time of the temperature pulse was found to be a maximum for EBWs emitted from the Shafranov-shifted magnetic axis at $R = 40$ cm [14]. This verification that the EBW emission source is localized at the ECE resonance justifies a comparison between the measured EBW T_{rad} and Thomson scattering T_e profiles.

The natural steepening of the edge density gradient that occurs at the L to H transition can enhance the conversion and tunneling efficiency of both the B-X and B-X-O conversion processes if the steepening occurs in the vicinity of the EBW mode conversion layer. This has been observed for B-X-O conversion on MAST [15] and B-X conversion on NSTX [16]. In NSTX plasmas with H-mode transitions, the mode-converted EBW emission is observed to increase by up to a factor three at L to H transitions. The emission increase is coincident with steepening of the edge density profile during the H-mode. L_n data from Thomson scattering were used to calculate C . Good agreement was found between the measured EBW T_{rad}/T_e and the calculated C

using the measured L_n [17]. However, even during the H-mode phase the B-X conversion efficiency on NSTX is only 10-15%. Similarly, on CDX-U T_{rad}/T_e has been typically $\leq 20\%$.

Recently, experiments on NSTX have used the high harmonic fast wave (HHFW) antenna structure as a local limiter to steepen L_n in the B-X conversion region and hence improve the B-X conversion efficiency. An EBW radiometer and a microwave reflectometer that measured the density profile in the scrape-off were co-located near the midplane between two of the HHFW antenna straps. When the gap between the plasma edge and the HHFW antenna was reduced from a few centimeters to close to zero, L_n shortened from ~ 2.0 cm to ~ 0.7 cm and the EBW T_{rad}/T_e increased from 10% to 50%, in good agreement with theoretical predictions using the measured L_n [3].

Rather than relying on the L_n that occurs naturally, a local adjustable limiter can control and optimize L_n for maximum C . An in-vacuum antenna/Langmuir probe assembly that can scan in major radius was installed on CDX-U [18]. In order to vary L_n for maximum mode conversion efficiency the antenna/probe assembly was surrounded by a limiter that could be positioned at different major radii relative to the antenna. Four Langmuir probes continuously measured the density profile in front of the antenna. The antenna used on CDX-U was a quad-ridged, broadband horn that could simultaneously measure O-mode and X-mode polarized emission. Data from the antenna/probe assembly showed that L_n at the fundamental B-X conversion layer could be shortened from 3-6 cm to about 0.7 cm when the limiter was inserted in front of the antenna (Fig. 3.3.6). As a result, the B-X conversion efficiency, inferred from the EBW T_{rad}/T_e ratio, was increased by an order of magnitude to $> 95\%$.

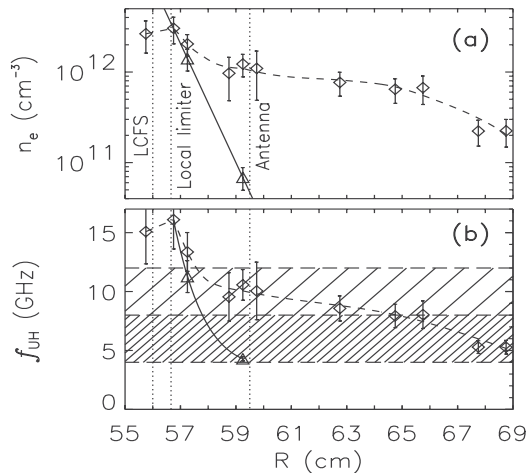


Figure 3.3.6 (a) $L_n = 3-6$ cm without a local limiter (dashed line and diamonds) was reduced to ~ 0.7 cm with the local limiter inserted close to the LCFS (solid line and triangles). (b) UHR frequencies calculated for density profiles in (a). The two shaded regions show the frequency range of fundamental and second harmonic EBW emission.

The mode-converted EBW emission on CDX-U was observed to fluctuate rapidly (~ 10 kHz) and was anti-correlated with the electron density fluctuation at the Langmuir probe closest to the B-X conversion layer. High time resolution ($\sim 1 \mu\text{s}$) electron density data,

obtained simultaneously from the Langmuir probes, has allowed measurement of L_n fluctuations and the calculation of the fluctuations in C . While there was correlation between fluctuations in C and the EBW T_{rad} , there were clearly EBW T_{rad} fluctuations that did not correlate. Refractive effects corresponding to MHD activity probably contributed about half of the EBW T_{rad} fluctuations in CDX-U but this effect should be less serious on NSTX since the plasma is considerably larger.

For the 2003 NSTX experimental campaign a pair of quad-ridged horn antennas with radially adjustable carbon limiters has been installed in NSTX in order to replicate the high B-X mode conversion results obtained on CDX-U. A frequency swept O-mode reflectometer is being integrated into the antenna assembly in order to simultaneously measure the local L_n behavior at the UHR. Also, a modification has been made to the radiometer view in the HHFW antenna used previously to measure B-X conversion so that it now views obliquely to measure B-X-O emission. The NSTX EBW emission experiments in 2003 are being performed to establish whether mode conversion efficiencies $> 80\%$ can be reliably achieved as a prerequisite for moving forward with a ~ 1 MW EBW heating and current drive system on NSTX.

3.3.10 Status of EBW Heating and Current Drive Modeling

EBW heating and current drive are attractive for ST plasmas because they may provide local heating and driven currents that can help optimize the magnetic equilibrium and suppress MHD. EBW wave steering can take advantage of the relatively strong poloidal field and large magnetic shear. $n_{//}$ shifts can result when EBWs are launched with $n_{//} = 0$ from a RF launcher poloidally displaced from the plasma mid-plane. Trapped particle effects on the low field side of the magnetic axis make deposition of EBW power on the high field side more attractive for current drive than low field side deposition. Fundamental EBW launch frequencies provide much better radial access to the high field side than second or higher harmonic frequencies. Also, since the fundamental X-B and O-X-B mode conversion layer is at densities that lie in the NSTX plasma scrape off, use of fundamental EBW launch frequencies allows a local limiter to control the density scale length at the mode conversion layer and hence maximize the tunneling and mode conversion efficiency. As a result modeling of EBW heating and current drive for NSTX has focused on fundamental EBW frequencies.

There are three β regimes that present different challenges for high field side EBW deposition on NSTX. For plasmas with $\beta < 10\%$, the low aspect ratio makes access much beyond the magnetic axis problematic. At $\beta \sim 20\%$ the mod B profile flattens around the axis which reduces the localization of the heating and current drive near the axis, but also improves access to the high field side. At $\beta > 30\%$ a magnetic well forms near the magnetic axis making the mod B profile non-monotonic and restricting high field side access.

Figure 3.3.7 shows the EBW ray trajectories calculated by the GENRAY ray tracing code [19] for 14.5 GHz EBWs launched 5° above the mid-plane into a standard $\beta = 20\%$

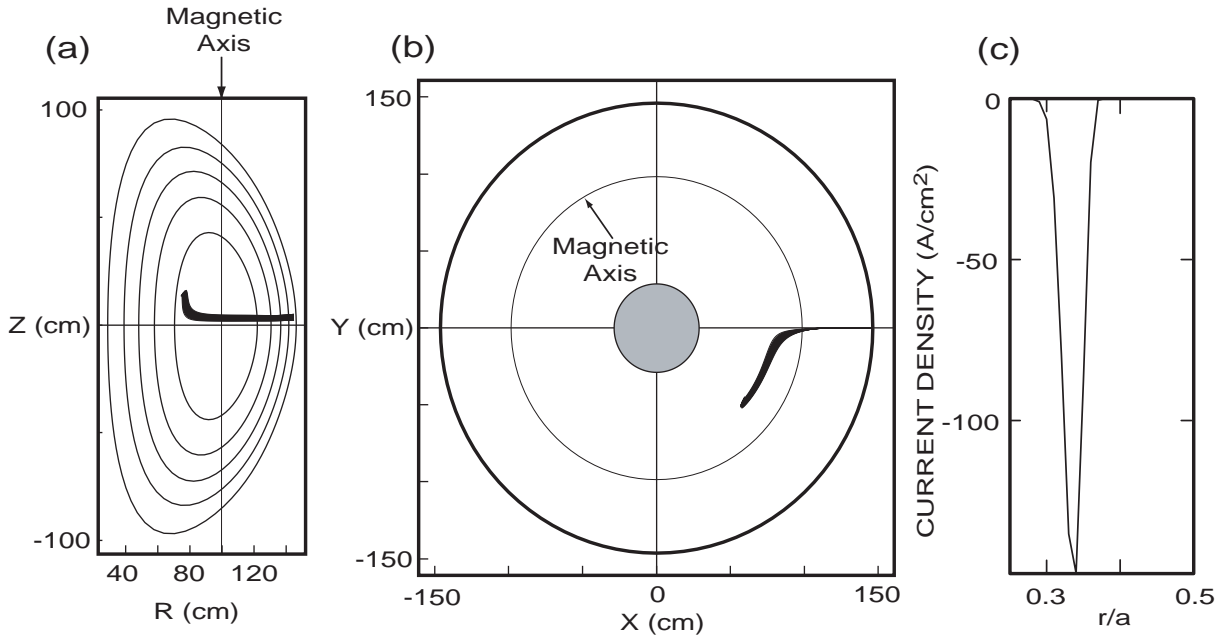


Figure 3.3.7 (a) Poloidal and (b) toroidal cross sections of an NSTX $\beta=20\%$, $n_{e0}=3\times 10^{19}\text{m}^{-3}$, $T_{e0}=1\text{keV}$ plasma showing path of 14.5 GHz EBW rays launched over a 10 cm poloidal length 5° above midplane, with $-0.1 < n_{\parallel} < 0.1$. (c) Current drive localization for this case with 1 MW of EBW power.

NSTX plasma. A bundle of rays are launched over a 10 cm poloidal length displaced 5° above the mid-plane with $-0.1 < n_{\parallel} < 0.1$. Modeling of the current drive is performed with the CQL3D bounce-averaged Fokker-Planck code [20]. The current is very localized (Fig. 2c) on the inboard side and the efficiency compares favorably to ECCD in low β plasmas (0.065 A/W at $n_e \sim 3\times 10^{19}\text{m}^{-3}$ and $T_e \sim 1\text{keV}$). A tight n_{\parallel} -spectrum is found to be necessary to avoid second harmonic damping and maintain a localized current deposition. The localization of the EBW-driven current in this case is satisfactory for EBWs to stabilize neoclassical tearing modes that limit β for this plasma [21], further work is required to determine if the driven current density ($\sim 100\text{A}\cdot\text{cm}^{-2}$ in this case) will be sufficient to suppress NTM's in this plasma.

During 2003, a scoping study to explore the sensitivity of the EBW current drive efficiency to RF launch parameters (eg. poloidal launch angle, n_{\parallel} and frequency) will be completed with the GENRAY ray tracing code and the CQL3D Fokker-Planck code. This scoping study will include developing scenarios for EBW-assisted non-inductive plasma startup. The GENRAY EBW ray tracing code presently requires rays to be launched as EBWs inside the plasma, in future the EBW modeling will include both a realistic antenna pattern and refraction at the mode conversion layer (eg. using GLOSI or cold-plasma admittance matrix modeling). Theoretical studies of the modification of EBW current drive efficiency by transport and bootstrap current will also be conducted. High RF power densities may drive parametric instabilities near the mode conversion layer, so this will be investigated theoretically. Other studies will model non-thermal

EBW emission and determine whether relativistic effects should be included in the propagation and damping of the EBWs.

3.3.11 Status of EBW RF Source Technology

Since the focus of the NSTX research program in 2004-8 will be directed towards developing tools for non-inductive startup and long pulse sustainment at $B_0 \sim 0.4-0.5$ T, a fundamental EBW heating and current drive system needs to operate at a RF source frequency between 12 and 15 GHz. There are presently no long pulse, high power RF sources that operate in this frequency range, but options for RF sources exist.

There are four 28 GHz, 350 kW, CW, gyrotrons at ORNL that could possibly be retuned to operate at 15.3 GHz. After retuning to operate at 15.3 GHz each gyrotron may generate about 200 kW. This would provide a total RF source power with four gyrotrons of ~ 0.8 MW, which would be sufficient for the first phase of EBW heating and current drive experiments in 2006-8, but not for the high power (~ 3 MW) facility proposed for non-solenoid current sustainment in 2009. There are also high voltage modulator/regulators and sockets available for these tubes at ORNL and a PPPL neutral beam power supply is available that could provide power to the facility. Before deciding to use these gyrotrons at least one tube will need to be retuned and tested for 15.3 GHz operation at ORNL in 2003. Another option being considered is to install an existing short pulse (~ 100 ms), 300 kW, 28 GHz ORNL tube on NSTX for preliminary EBW plasma startup studies in 2004.

Our preference is to develop a new megawatt level 15 GHz RF tube for NSTX. An 800kW, 15 GHz gyrotron has been proposed by MIT that would operate at up to 47% efficiency without a depressed collector. This MIT tube would be engineered and fabricated by CPI, a company that already sells a 0.5 MW, 8 GHz tube. Thales, a European manufacturer that sells a 1.1 MW, 8 GHz gyrotron, would probably also bid to develop their own ~ 1 MW, 15 GHz tube. A request for a cost and schedule quotation for developing a ~ 1 MW, 15 GHz tube will be sent out early in 2003. This development would be expensive, probably $\sim \$1$ M for the first tube and $\sim \$0.5$ M for each additional tube, but it needs to begin in 2004 if it is to be used for the megawatt level experiments in 2006-8.

At this time a high power EBW launcher design has not been defined. For EBW heating and current drive schemes a well-defined n_{\parallel} spectrum and good focusing are required and some beam steering is desirable. Either focusing mirrors close to the plasma (as is presently used on MAST) or a phased array (similar to an LHCD launcher) with 4-8 waveguides are possible candidates. Polarization control could be provided by an external waveguide or grooved mirrors. The antenna could be adjustable poloidally or the waveguide elements could be phased to control n_{\parallel} and EBW damping location or two separate antennas could be installed at different poloidal locations. For maximum flexibility the antenna could be designed for both X-B (normal incidence) and O-X-B (oblique incidence). If only an O-X-B launch is implemented the antenna could still incorporate a local limiter to widen the transmission window.

3.3.12 EBW Research Plan for 2004-8

The NSTX EBW heating and current drive research plan timeline, including relevant IPPA milestones, is summarized in Table 1. EBW heating and current drive experiments begin in 2006-8 with 1 MW of RF power, increasing to 3 MW of power by 2008. The

Timeline	Research Plan Goal	IPPA Milestone
2003	<ul style="list-style-type: none"> - Obtain $\geq 80\%$ B-X & B-X-O emission on NSTX - Possibly modify 28 GHz RF tube for 15.3 GHz operation - Request quote for 1 MW, 15 GHz tube - Scoping study for NSTX EBW heating and current drive - GENRAY/CQL3D modeling of EBW startup and non-thermal EBW emission - Determine importance of relativistic effects in EBW propagation & edge parametric instabilities during heating - Conceptual design for EBW antenna - MAST to test O-X-B heating 	3.2.1.3 Heating high β , over-dense plasmas
2004-5	<ul style="list-style-type: none"> - Complete design of 1 MW, 15 GHz EBW heating (phase I) & current drive system - Included radial transport effects in CQL3D EBW current drive modeling - Possible demonstration of startup with ~ 300 kW, 28 GHz - Begin installation of 1 MW, 15 GHz EBW heating (phase I) 	3.2.1.4 possible preliminary test of EBW startup
2006	<ul style="list-style-type: none"> - Complete installation of 1 MW, 15 GHz EBW heating system (phase I) [new 1 MW RF tube or 4x15.3 GHz ORNL tubes] - Demonstrate coupling to EBW's with 1 MW, 15 GHz - Study spatial control of electron heating by EBW's 	3.2.1.3
2007-8 Phase I	<ul style="list-style-type: none"> - Demonstrate plasma current generation & control by EBW's - Study plasma startup with EBW's with 1 MW, 15 GHz - Investigate NTM suppression with 1 MW, 15 GHz - Installation of 3 MW, 15 GHz EBW heating, and initial operations 	3.2.1.4 3.2.1.2 Suppress high β -limiting MHD
2009 Phase II	<ul style="list-style-type: none"> - NTM suppression with 3 MW, 15 GHz - Optimize non-solenoid operation with EBW sustained current drive 	3.2.1.2 Suppress high β -limiting MHD. IPPA 10-Year Milestone: $\tau_{\text{pulse}} \gg \tau_{\text{skin}}$

Table 1: EBW research plan timeline and relationship to IPPA milestones.

research plan assumes that approximately one megawatt of 15 GHz RF power will be available for experiments starting in late 2006. The design, fabrication and successful testing of a new megawatt level 15 GHz RF tube will need to be completed by late 2005. To allow two years for the RF tube development, the request for quote on cost and schedule for this RF tube should be issued during the first half of 2003. The plan assumes the demonstration of > 80% B-X or B-X-O conversion on NSTX (or MAST) and completion of the NSTX EBW heating and current drive scoping study in 2003. Mode-conversion experiments in 2003 will guide the conceptual design for the EBW launcher. The launcher design should be completed by the end of 2004.

If resources are available in 2003, the plan includes a technology assessment of the retuning of an existing 28 GHz ORNL CW gyrotron for 15.3 GHz. If the retuning shows that the 15.3 GHz gyrotron can operate at > 200 kW power levels this provides a backup option for an RF source suitable for the phase I experiments. In addition, a short pulse (~100ms) 28 GHz 300 kW ORNL gyrotron could be refurbished and installed on NSTX in 2004 to allow preliminary EBW plasma startup experiments in 2004-5.

Phase I experiments would begin in late 2006 or early 2007. Phase I goals in 2006-7 are to study the coupling of power to EBWs at the edge of the plasma, controlling this coupling with limiters (if needed), investigating propagation of EBWs inside NSTX plasmas, studying damping of EBWs on electrons and controlling the spatial location where EBWs interact with electrons. These physics studies will be used to benchmark theoretical and computational models against experimental observations. Phase I experiments in 2007-8 would study EBW assisted startup alone or in combination with HHFW and/or CHI, off-axis EBW heating and current drive experiments with EBW-driven currents of up to ~ 100 kA.

References

- [1] NAKAJIMA, S. and H. ABE, Phys. Rev. A **38**, 4373 (1988).
- [2] SUGAI, H., Phys. Rev. Lett. **47**, 1899 (1981).
- [3] RAM, A.K., and SCHULTZ, S. D., Phys. of Plasmas **7**, 4084 (2000).
- [4] PREINHAELTER, J. and KOPÉCKY, V., J. Plasma Phys. **10**, 1 (1973).
- [5] WEITZNER, H. and BATCHELOR, D.B., Phys. Fluids **22**, 1355 (1979).
- [6] MJØLHUS, E., J. Plasma Phys. **31**, 7 (1984).
- [7] NAKAJIMA, S. and ABE, H., Phys. Lett. A **124**, 295 (1987).
- [8] HANSEN, F.R., et al., J. Plasma Phys. **39**, 319 (1988).
- [9] LAQUA, H.P., et al., Phys. Rev. Lett. **78**, 3467 (1997).
- [10] LAQUA, H.P., et al., Phys. Rev. Lett. **81**, 2060 (1998).
- [11] RAM, A.K., et al., Phys. Plasmas **9**, 409 (2002).
- [12] BERS, A. and RAM, A.K., Phys. Lett. A **301**, 442 (2002).
- [13] TAYLOR, G., et al., Rev. Sci. Instrum. **72**, 285 (2001).
- [14] MUNSAT, T., et al., Phys. Plasmas **9**, 480 (2002).
- [15] AKERS, R.J., et al., Phys. Rev. Lett. **88**, 035002 (2002).

- [16] MAINGI, R., et al., Phys. Rev. Lett. **88**, 035003 (2002).
- [17] TAYLOR, G., et al., Phys. Plasmas **9**, 167 (2002).
- [18] JONES, B., et al. Princeton Plasma Physics Laboratory Report PPPL-3659 (January 2002).
- [19] SMIRNOV, A.P., and HARVEY, R.W., Bull. Am. Phys. Soc. **40**, 1837 (1995).
- [20] HARVEY, R.W., et al., Proc. IAEA Tech. Com. on Advances in Simulation and Modeling of Thermonuclear Plasmas, Montreal (IAEA, Vienna, 1993) p. 489.
- [21] GANTENBEIN, G., et al., Phys. Rev. Lett. **85**, 1242 (2000).

FY02 03 04 05 06 07 08 09
 IPPA: 5 year 10 yr

HHFW heating : density, configuration dependence
 6 MW HHFW, combine with NBI

HHFW CD V_{loop} HHFW CD local ΔJ (measured)
 HHFW wave/particle interactions

HHFW and P(r) modification
 HHFW CD, long pulse, phase feedback on ΔJ
 HHFW: P, J_{BS} mods thru feedback with heating, CD

EBW emissions & coupling
 CHI & HHFW
 CHI, HHFW, NBI Ramp to high β_p
 EBW CD, NTM Control, Startup
 Startup Optimization

HHFW/EBW physics

MSE CIF MSE LIF (J, E_r , P); polarimetry

CHERS 18 ch CHERS 51 ch

MPTS 20 ch, 60 Hz MPTS Upgrades
 Core reflectometry

Edge Reflectometry

7 MW NBI, 7 MW NBI, 6 Upgrade HHFW
 3 MW HHFW MW HHFW Antenna Strap Reorientation
 For Higher P_{rf}

HHFW Phase Control
 Feedback with MSE, heating, CD, rEFIT

HHFW/EBW tools

1 MW EBW → 3 MW EBW

3.4 Coaxial Helicity Injection

3.4.1 Research Program Goals for Coaxial Helicity Injection

The development of methods for non-inductive current initiation will improve the prospects of the ST as a fusion reactor. CHI is a promising candidate for this and has, in addition, has the potential to drive edge current during the sustained phase of a discharge for the purpose of controlling the edge current profile. Other possible benefits include inducing edge plasma rotation for transport barrier sustainment and controlling edge SOL flows.

The IPPA goal 3.2.1.4 for the ST is to: “Characterize the integration of noninductive plasma startup via magnetic reconnection such as using Coaxial Helicity Injection (CHI) with other noninductive and inductive current drive techniques. Investigate a number of noninductive techniques to start and to increase the plasma current in ST plasmas while at the same time minimizing magnetic flux and helicity injection.”

3.4.2 CHI background and implementation on NSTX

The NSTX noninductive plasma startup program addresses the IPPA goals through dedicated experiments, the development of theory to analyze the results and extrapolate techniques to future devices, and upgrades to facility capabilities to explore new techniques and to optimize the most promising of them.

The possibility of using CHI in a ST was first proposed in the late 1980's¹. Several small experiments have since then been conducted.^{2 3 4 5 6} The early experiments were sufficiently promising that a decision was taken in the design phase of NSTX to incorporate capabilities for CHI.

For NSTX, the stainless steel vacuum vessel is fitted with toroidal ceramic breaks at the top and bottom so that the central column and the inner divertor plates (the inner vessel components) are insulated from the outer wall and the outer divertor. CHI is implemented by driving current in the plasma along field lines that connect the inner and outer lower divertor plates which act as electrodes. A 50kA, 1kV

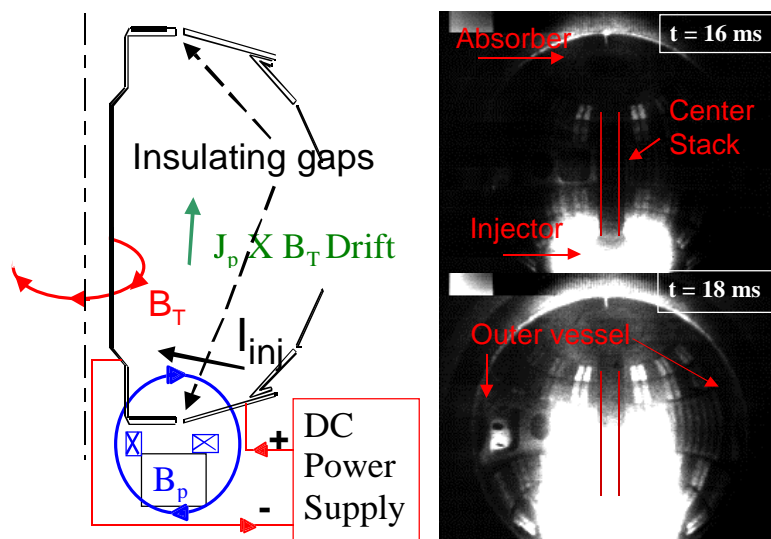


Figure 3.4.1 Schematic of aspects of an NSTX CHI experiment, showing the insulating gaps in the vacuum vessel, the biasing between the inner and outer vessels, and the $J \times B$ force that transports the plasma arc into the vessel. On the right are visible camera images of a CHI discharge on NSTX shortly after discharge initiation.

DC power supply is connected across the inner and outer vessel components, to drive the injector current. The standard operating condition for CHI in NSTX uses the inner vessel and inner divertor plates as the cathode while the outer divertor plates and vessel is the anode. A dedicated gas injection system in the lower divertor region injects gas from four ports in the lower inner divertor plates, equally separated toroidally. The CHI method drives current initially on open field lines creating a current density profile that is hollow. Taylor relaxation⁷ predicts a flattening of this current profile through a process of magnetic reconnection leading to current being driven throughout the volume, including closed field lines. Current penetration to the interior is eventually needed for usefully coupling CHI to other current drive methods and to provide CHI produced sustainment current during the long pulse non-inductive phase.

Experiments to date in NSTX have shown that CHI can be applied to a large ST for the production of substantial toroidal current.⁸ CHI in NSTX has successfully generated 390kA of toroidal current using about 28kA of injector current.⁹ Discharges lasting for 330ms have been produced using pre-programmed coil currents in the preferred "narrow" footprint condition. Results to-date show the CHI plasma to be very dynamic with indications, both on magnetic pickup coils and in the soft x-ray emission, of large scale reconnection activity. Development of an equilibrium feedback control system is needed before these high current plasmas can be made stable for the purpose of discharge characterization.

3.4.3 Theory Status

Assessment of flux closure in a driven system, which is a requirement for plasma initiation and sustainment requires several experimental and theoretical tools. Ultimately, a direct current profile measurement using MSE is needed for an unambiguous demonstration of producing closed flux during a CHI discharge. However, in transient CHI discharges, demonstrating the persistence of toroidal current after the injector current has been ramped to zero would be sufficient for a demonstration of closed flux generation. In addition, consistency between the measured electron pressure profile and the time-averaged 2-D closed flux reconstruction from an axisymmetric analysis code, such as EFIT, would provide confidence that CHI is producing closed flux.

The Thomson Scattering diagnostic needed for electron pressure characterization is fully functional. MSE is expected to be available for first experiments in 2003, and available with full profile capability in 2004. The ESC code¹⁰ has the capability for including current on open field lines and in the private flux region and has the capability for including wall currents. This code has already been used to reconstruct CHI discharges. These features have also now been implemented on the EFIT code,¹¹ by L. Lao and M. Schaffer of GA. NSTX, however, lacks good wall current measurements, which means that both ESC and EFIT have to be used without the benefit of the constraints on the fitted solution, which wall current measurements would provide. On NSTX, because of the presence of thick conducting copper passive plates inside the vessel structure, it is difficult to obtain accurate measurements of current in the passive plates and vessel walls

during CHI. In the past the MFIT code,¹² which is a magnetic fitting code, has been used for control room use to obtain approximate estimates of the location of the CHI plasmas.

The TSC code,¹³ has been used to model the evolution of CHI discharges. The installation of the new absorber is expected to allow the routine production of absorber arc free discharges. This would allow for the capability to modify and improve the CHI boundary shape. We expect to use TSC simulations to help us with designing these new discharge scenarios. The 3D MHD code, CHIP, developed by X. Tang of LANL, is being used to understand CHI reconnection physics. The code has been used to model CHI processes in a simple geometry. Implementation of the actual NSTX geometry will allow for a closer comparison of the simulation results with the experimental results, and help guide and understand the experiments.

3.4.4 Experimental Approaches to CHI: Transient and Long Pulse

Experiments on NSTX have until now focused on long pulse CHI discharges. These discharges have the potential to meet both the plasma startup requirement and the current sustainment requirement. However, recent experiments on HIT-II have successfully demonstrated a new method (referred to as transient plasma startup) for plasma startup and handoff to inductive operation.⁹ The transient plasma startup method has resulted in volt-seconds savings. It has increased the reproducibility of inductive discharges and has considerably improved the performance of the HIT-II experiment by producing record plasma currents. These new results have motivated us to decouple on NSTX the plasma startup and current sustainment goals.

There are two objectives for CHI research on NSTX. The primary objective is to start-up the NSTX plasma using CHI and to hand it off initially for inductive operation and then later to a non-inductive current drive system. The second objective is to provide edge current drive during sustained non-inductive operation, for the purpose of controlling the edge current profile.

The plan is to meet the start-up objective by using transient CHI plasmas. However, the long pulse high current discharge development experiments will be continued, as these may have the potential to provide much higher plasma startup currents and because these types of discharges are needed for developing edge current drive during sustained noninductive operation. The edge current demonstrations would require steady-state CHI discharges.

Plasma start-up using a transient CHI plasma has three steps. These involve (1) establishing a sufficiently high quality CHI discharge, (2) forcing detachment of the CHI flux footprints from the CHI electrodes and (3) applying induction from the central solenoid. During August 2002, these three steps were successfully tested on the HIT-II spherical torus at the University of Washington. CHI produced discharges that were handed-off to inductive operation resulted in significant volt-seconds savings. The current plan, therefore, is to implement the same procedure on NSTX for a demonstration

of plasma start-up and hand-off to inductive operation during Fy 03. Small NSTX hardware modifications (gas injection, speeding up CHI coils, absorber PF coil activation for absorber field control) will be implemented if needed. The 5 yr CHI program plan on NSTX is now described in greater detail.

3.4.5 New engineering tools and improvements for the CHI program

A number of engineering improvements will be implemented or are being considered for the CHI program.

1. *Investigate new methods for pre-ionization*): The ability to generate a CHI plasma discharge at low densities should produce a warmer CHI plasma with a longer current decay time. It may also produce higher initial CHI startup currents. Another benefit is the ability to operate at lower CHI injector voltages. Improvements to the pre-ionization system could range from modifications to the existing ECH system that would allow the waves to be directed into the injector region to investigating the possibility of a higher power system that can also be used to further heat a CHI plasma once it has been produced.

2. *Equilibrium control and improvements to PF coil response times* - Conduct an engineering study to determine the response time capability of various poloidal field coil systems and how they can be made as fast as reasonably possible. This is needed for equilibrium feedback control.

3. *Optimize the passive plates to improve radial and vertical position control* – Reconfiguring the passive plates for a cryopump and for global mode stabilization may provide the opportunity for optimization for CHI as well.

4. *Eliminate ground faults when NBI is used with CHI* – This is essential if CHI is to be used in conjunction with neutral beam injection. Compare in detail the NSTX and DIII-D ground fault systems to assist with a possible solution, as DIII-D has conducted CHI type experiments at the 1kV level using NBI.

5. *Wall current measurements for ESC and EFIT*: - Install halo current probes to obtain information on the current path on the vessel structure and the poloidal current density into the wall. This is needed as an input for EFIT and ESC equilibrium reconstructions.

6. *Consider higher CHI voltage capability of 2 kV*. - The goal is to reduce the injector current while increasing the CHI produced toroidal current. Conduct a study to see how the injector voltage affects this. This is an important control knob but the increased probability of absorber and external arcs at the higher voltage cannot be ignored. On the other hand, if voltage excursions during reconnection considerably exceed 2kV and the system is protected from these voltage excursions, the increased 2kV voltage requirement may not pose significant additional challenges. Fy 03 experimental operations are expected to provide experimental data that will allow for a reexamination of the need for increased injector voltage capability.

7. *Consider change of the plasma facing components* - A tungsten divertor offers the possibility of producing a higher temperature CHI discharge. Tungsten is also considered for reactor divertors. If warranted for other considerations in the NSTX program, such as pulse length extension, a tungsten divertor plate campaign will be of interest to CHI research as well.

3.4.6 Plans for 2003 - 2008

The NSTX absorber region has been rebuilt to reduce the probability of absorber arcs. This in addition to absorber poloidal field control is expected to considerably reduce the incidence of absorber arcs.

Our overall goal for this 5-yr research is to learn how to design CHI engineering systems for an ST reactor. Development of this knowledge requires the demonstration of two goals. These are: (1) transferring a CHI produced plasma to the inductive system and (2) transferring a CHI produced plasma to a non-inductive current drive system. In addition, developing the needed technology will maximize current generation using the CHI process. Other developments such as a demonstration of edge current drive and or inducing edge plasma rotation or controlling SOL flows will enhance CHI.

Solenoid-free startup and rampup of plasma current using transient CHI

Additional items related to the use of CHI and other current drive techniques in these studies is discussed in Chapter 4.

2003: Transfer a CHI produced plasma to other current drive mechanisms – Following on the success of the transient technique developed recently on HIT-II, a transient CHI scenario will be developed. The first step will be to couple to ohmic induction. This will involve the simultaneous ramp-down of poloidal field (PF) control coils with CHI current to detach the footpoints of CHI discharge, forcing reconnection and creating persistent toroidal current.

After techniques for handing a persistent CHI plasma to ohmic induction is developed, coupling studies will begin with the aim of coupling to high harmonic fast wave heating. HHFW heating will be to generate bootstrap current, and the possibility of driving current directly with CHI will be explored as well.

2004 – 2005: Refine handoff and control of CHI to HHFW– Techniques for coupling CHI-initiated discharges to HHFW will be optimized. Grounding issues pertaining to neutral beam injection in concert with the application of CHI will be addressed in this period. MSE measurements of the current distribution will be performed in this time period.

2006: Extend CHI-to-HHFW coupled discharges to discharges with neutral beam injection, with the goal of solenoid-free ramp-up to a high poloidal beta target – CHI and HHFW, along with possibly 1 MW of EBW or poloidal field induction, will be applied to raise the current to a value high enough to assure adequate fast ion

confinement with the application of neutral beams. Neutral beam current drive and bootstrap current overdrive will be applied subsequent to or in parallel with HHFW to maximize the current developed. The preferred method for startup, transient or steady-state CHI (see below), will be determined.

2007 – 2008: Apply techniques for volt-second savings to high confinement, high bootstrap fraction, high beta plasma targets. The techniques developed through 2006 may yield benefits regarding flux consumption that can be used in generating plasmas with the highest toroidal betas and high fractions of bootstrap current for periods of time longer than a current diffusion time.

Steady-state CHI operations

Even if transient CHI is successful in enabling solenoid-free startup, steady-state CHI techniques will be developed because of the possible rapid development of high levels of current within NSTX, and because of the possible benefits of edge biasing.

2003: Assess benefits of improvements in PF flexibility to increase insulation in absorber region for high current CHI operations – CHI startup to 300 kA of toroidal current will be reestablished. Absorber magnetic insulation through absorber field nulling will be assessed in scans of applied bias voltage, gas pressure, and toroidal field.

Flux closure will be assessed in the most favorable conditions using detailed magnetics measurements and a measurement of the pressure profile using Thomson scattering. Magnetics measurements will be used to constrain 3-D MHD theoretical calculations. Measurements of magnetic helicity transport will be performed using an edge probe.

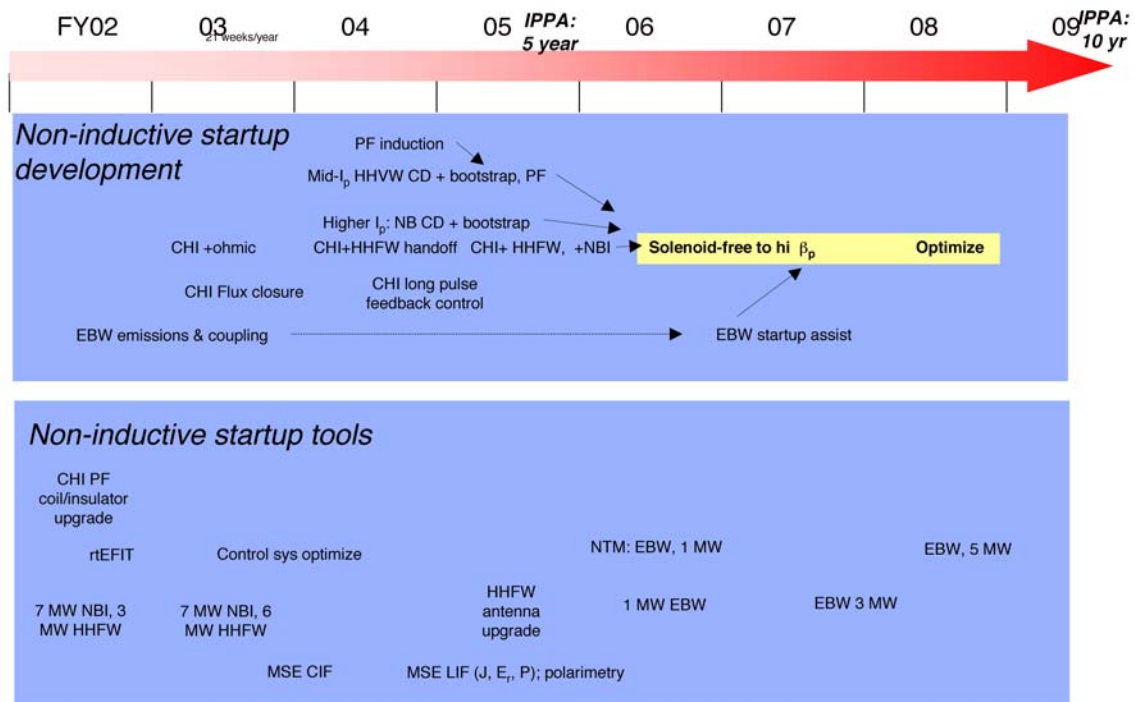
This development will take advantage of the rapidly evolving control system on NSTX. This control system will enable both programmed and feedback control of poloidal fluxes.

Develop edge current drive in ohmic plasmas – This will mark the beginning of investigations the effects of edge biasing on edge rotation, the L-H transition, impurity influxes, and edge turbulence.

2004 – 2005: Establish the preferred technique for plasma startup (transient or steady-state CHI) – This is described above in the section on transient CHI.

Establish edge current drive in an established CHI discharge – The effects on plasma performance will be assessed. Studies of edge effects, begun in 2003, will be expanded in this research period.

2006 – 2008 Extend operations to allow solenoid free rampup to high beta poloidal plasmas by 2006. Use CHI where possible to enable volt-second savings in highest performance, high beta plasmas – The goals regarding CHI rampup and volt-second optimization remain the same as for the transient CHI approach, discussed previously.



References

- ¹ Jarboe, T.R., Fusion Tech. **15**, (1989) 7
- ² Ono, M., et al., Phys. Rev. Lett. **44**, (1980) 393
- ³ Nelson, B.A., et al., Phys. Plasmas **2** (1995) 2337
- ⁴ Nagata, M., et al., 17th IAEA Fusion Energy Conference, Yokohama, IAEA-CN 69/EXP4/10 (1998)
- ⁵ Browning, P.K., et al., Phys. Rev. Lett. **68** (1992) 1722
- ⁶ Jarboe, T.R., Raman, R., Nelson, B.A., et al, 17th IAEA Fusion Energy Conference, Yokohama, IAEA-CN 69/PDP/02 (1998)
- ⁷ Taylor, J.B., Rev. Mod. Phys. **28**, (1986) 243
- ⁸ Raman, R., Jarboe, T.R., Mueller, D., et al., Nucl. Fusion **41**, (2001) 1081
- ⁹ Jarboe, T.R., Raman, R., Nelson, B.A., et al, 19th IAEA Fusion Energy Conference, Lyon, IAEA-IC/P 10 (2002)
- ¹⁰ Zakharov, L and Pletzer, A, Physics of Plasmas **6**, 4693 (1999)
- ¹¹ Lao, L.L., St. John, H., Stambaugh, R.D., Nucl. Fusion **25**, 1611 (1985)
- ¹² Lao, L.L., St. John, H., Stambaugh, R.D., Nucl. Fusion **25**, 1421 (1985)
- ¹³ Jardin, S.C., Pomphrey, N., DeLucia, J., Journal of Computational Physics **66**, 481 (1986)

3.5 Boundary Physics

3.5.1 Boundary Physics Goals

Boundary physics has both an enabling role and a science role in the NSTX program. The aim of the enabling role is to facilitate access to favorable operational regimes needed for the other elements of the research program. Activities in the enabling role to date have focused on development of conventional wall conditioning techniques, namely helium glow discharge cleaning, boronization, and high temperature bake-out of plasma facing components [1]. These conditioning techniques have enabled routine access to H-mode operation [2,3,4,5], with high stability limits due to low pressure peaking factors [6] and longer pulse length due to high bootstrap current fractions [7,8].

The aim of the science role is to understand the relevant processes governing the boundary plasma and the effect of the boundary plasma on the core. In particular, the boundary plasma research program will have a basic characterization element to test if models developed from conventional aspect ratio tokamaks fit NSTX observations. In addition, the research will address issues specific to low aspect ratio devices, such as high mirror ratio in the scrape-off layer, high magnetic field line pitch, and short connection lengths compared with conventional aspect ratio. In comparison, the research regarding the effect of the boundary plasma on the core is broader, because control of the boundary can facilitate optimization of the core and development of new scenarios.

The boundary physics program goals are closely tied to the IPPA goals. The IPPA goal 3.2.1 states the five year objective (end of FY 2005): “Make a preliminary assessment of the attractiveness of the ST by assessing high- β_T stability, confinement, self-consistent high bootstrap operation and acceptable heat fluxes for pulse lengths much greater than energy confinement times”. In addition, the implementing approach 3.2.1.5 gives more detailed guidance on the need for power and particle handling studies, and certain unique features of the ST boundary: “Study the dispersion of edge heat flux over a range of externally controllable parameters and estimate the plasma facing component requirements under high heating power in the spherical torus magnetic geometry. Determine the ability for managing intense energy and particle fluxes in the edge geometry and for increasing pulse durations significantly beyond the energy confinement time. Most elements of the physics on the edge open field lines are shared between the ST and the tokamak, while the ST introduces stronger variations of the magnetic field strength along the field lines, that are closer to the magnetic mirror. The ‘toroidal mirror’ configuration also tends to have large flux expansion in the divertor region, likely extending the physics research to new parameter regimes.” In the NSTX program, power and particle handling are the largest elements, followed by studies of the boundary features which differ in ST compared with conventional aspect ratio tokamaks.

Elements of the boundary physics program can be divided into several topics, each of which is discussed below:

1. particle (fuel and impurity) control
2. power handling and mitigation

3. H-mode and pedestal physics
4. Edge, SOL divertor and wall conditioning physics

3.5.2 Particle Control and Fueling

a. Background

The advent of gas fueling from the center stack (high-field side, HFS) in NSTX, the reduction of the intrinsic error field, and the achievement of a 350 deg. C bake-out of all graphite plasma facing components have contributed to enable reproducible access to H-mode transitions and extend the duration. As a result of these improvements, the H-mode access operational space (i.e. just before the L-H transition) has been increased [5] Typically, the density rises continuously during these long pulse discharges, owing to a combination of good particle confinement and

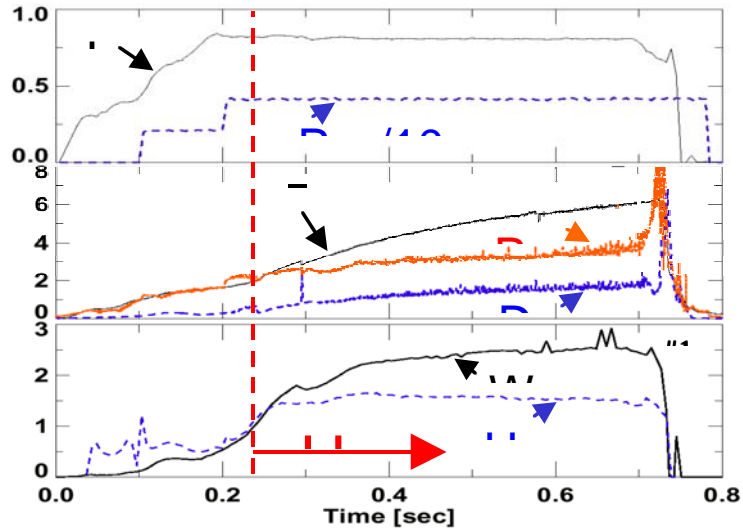


Figure 3.5.1 Long pulse H-mode with density rise

continual fueling with the high-field side gas injector and neutral beams (Figure 3.5.1). The final density approaches $0.8 \cdot \text{Greenwald scaling } (n_{\text{GW}} = I_p / (\pi a^2))$, albeit with no apparent degradation in confinement. During the H-mode phase, the dN_e/dt ($N_e \sim \bar{n}_e \cdot V_{\text{EFT}}$) decays in time similar to the decay of the center stack gas puff rate, suggesting that improved control of the center stack puffing may reduce the dN_e/dt . Also, the edge density continues to increase with time, but that the core-density fills in faster, leading to a flat density profile at the end of the discharge [4]. This also suggests that the edge source dominates the edge density, and that the core density fills in partly due to inward diffusion from the edge.

The HFS gas puffing enables a longer H-mode phase than a low-field side (LFS) injector, even when the LFS injector is programmed with identical waveforms [4]. Also, the outboard side gas-fueled discharge exhibited an L-H transition only after the NBI power was increased to 3 MW, suggesting that the L-H power threshold was higher as well. These observations corroborate the premise that fueling plays a strong role in H-mode access in NSTX.

b. Research Plan, Diagnostics, and Facility Modifications

Improved control of the fueling sources is a key element of the research plan. Several staged enhancements will be employed:

1. Additional HFS and LFS gas injectors at different poloidal locations, to determine the optimum trade-off between controllability and H-mode access. The larger the major radius at the injector, the better the control in general. (FY03-FY04)
2. Development of a supersonic gas nozzle, to increase the fueling efficiency and the neutral penetration depth. This follows development on several tokamaks. (FY03-FY04)
3. Deuterium pellet injection for deeper and more efficient fueling. We will build on experience from the outboard lithium pellet injector, and add deuterium capability first from the low-field side and possibly the high-field side, if required. (FY05, HFS in FY06)
4. Compact toroid injection. In its present embodiment, CT injection has demonstrated the ability to induce edge transport barriers. This element also addresses a needed technology development for reactor fueling and profile control. A decision will be made at the end of FY06. (FY08)

Simultaneously with the fueling source control improvements, we will increase the pumping capability through stages, first through advanced wall conditioning techniques for passive pumping and then active pumping options:

1. Improved boronization – this includes testing the effectiveness of morning boronization, between shot boronization, boronization with an elevated wall temperature. (FY03-FY04)
2. Lithium conditioning – this begins with pellet injection in the near term, followed by higher yield ablation techniques between or during discharges. (FY03-FY04)
3. In-vessel cryogenic condensation pumps – similar to DIII-D and ASDEX-Upgrade, the goal would be active density control during discharges. The plan is for active pumping of both the outer strike points in the upper and lower divertors. This requires modification of the secondary passive stabilizing plates to create baffles and plenums. (FY06)
4. Divertor lithium module – this would address both the active pumping and possibly assist with power handling. It is less sensitive to strike point location than a cryopump and thus allows more shape. A possible location is the bottom divertor. A decision will be made at the end of FY06. (FY08)

Core fueling experiments and analysis will focus on quantifying the components leading to the observed density rise, i.e. we will identify the fraction of the density rise due to the

recycling and NBI sources, and we will also identify the fuel and impurity contributions. This task involves adding visible cameras with D_α filters, and a divertor SPRED XUV system to monitor impurities. The goal is to tomographically reconstruct the poloidal D_α profile, and then map the Thomson n_e and T_e on flux surfaces to allow a direct calculation of the neutral density and the ionization profile. The edge part of this profile will be simulated with the combination of edge plasma transport codes, such as UEDGE and b2.5, and neutral transport codes, such as DEGAS-2 and EIRENE, to determine the location of the main recycling surfaces, whether in the divertor or main chamber. In addition, upgrades to the divertor and center stack Langmuir probe array are planned to provide baseline plasma profiles for these modeling codes.

Analysis of the particle balance with active pumping will require fast time response pressure gauges near the cryopump, and new diagnostics to measure the stability and uniformity of lithium in the divertor module. Also a mechanism to quantify the particle exhaust with the lithium module will be developed.

3.5.3 Power Handling and Mitigation

a. Background

Edge plasma transport calculations made during the design phase and initial operation of NSTX predicted a peak heat flux in excess of 10 MW/m^2 to the outboard divertor target in the sheath-limited heat transport regime with little impurity radiation and a range of cross-field transport coefficients. Thermal design calculations indicated that a peak heat flux above $6\text{-}8 \text{ MW/m}^2$ would cause the graphite ATJ tile temperature to rise above the 1200 deg. C administrative limit for a 5 second pulse length. Thus, infrared cameras were installed and heat flux scaling studies were begun recently.

Figure 3.5.2 shows the characteristics of an H-

mode lower-single null discharge with 2 MW input power used for power balance analysis.

Panel (c) shows that the outer divertor power

($P_{\text{div}}^{\text{out}}$, $R > 0.6 \text{ m}$) was about 3 times the inner divertor power ($P_{\text{div}}^{\text{in}}$, $R < 0.6 \text{ m}$), and that the power flow came to equilibrium by $\sim 300\text{ms}$, a little more than 100ms past the I_p flat-top time. The maximum SOL loss power is given by $P_{\text{SOL}} = P_{\text{oh}} + P_{\text{NBI}} - dW_{\text{EFIT}}/dt$, where P_{oh} is the ohmic power, P_{NBI} is the NBI power, and W_{EFIT} is the stored energy computed by EFITD. Note that no charge exchange loss (normally 10%) or core radiation is included (normally 10-20%); hence, the quantity represents an overestimate of the power flow into the SOL. Panel (d) shows that up to 70% of P_{SOL} is observed in the divertor, i.e. the power balance is remarkably good [4].

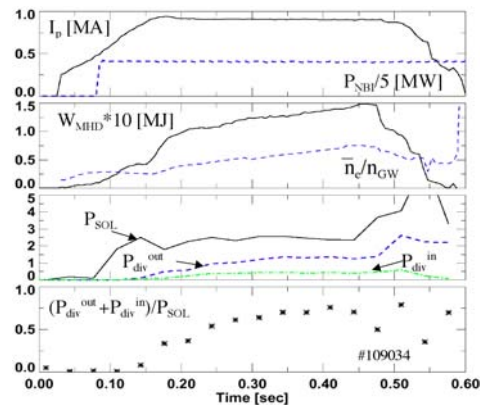


Figure 3.5.2 - Time dependence of power balance. The L-H transition time

Calibrated infrared camera measurements (Fig. 3.5.3) of the divertor reveal that the peak flux was 3 times higher on the outboard side at $P_{\text{NBI}}=2$ MW, but increased to 7 times higher at $P_{\text{NBI}}=5$ MW, i.e. the in/out ratio of peak heat flux decreased with increasing

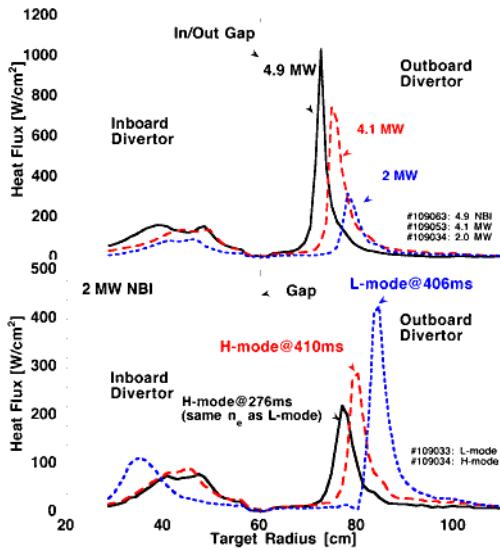


Figure 3.5.3 -Power scaling of heat flux in H-mode and L-mode/H-mode comparison

P_{NBI} . Also the outer divertor heat flux profiles were much narrower (full width, half max ~ 2 -3 cm) than the inboard ones (full width, half max ~ 10 cm). Finally the outer peak heat flux increased non-linearly with NBI power; the highest measured value in NSTX was ~ 10 MW/m², i.e. exceeding the design limit which would allow a 5 second pulse length. Extrapolation of the temperature rise of the tiles assuming a constant heat flux and time^{1/2} rise indicates a pulse length limitation ~ 3 seconds [2].

Figure 3.5.3 (b) compares the heat flux profiles during a comparable L-mode discharge and the above H-mode discharge at a comparable time (red and blue curves) and also a comparable line density (black and blue curves). The L-mode peak heat flux was higher than the H-mode at comparable P_{NBI} , because P_{OH} was higher and dW/dt was lower, i.e. P_{SOL} was effectively higher

in the L-mode case. The L-mode profile was marginally broader (2.5 cm vs. 2.2 cm), but it should be noted that the H-mode width was at the limit of spatial resolution of that camera.

Double-null discharges have lower peak heat fluxes than lower-single null, with a preliminary maximum ~ 3 MW/m² measured in the lower divertor. While this level appears acceptable for long pulse operation, the heat flux in the upper divertor has not yet been measured.

b. Research Plan, Diagnostics, and Facility Modifications

Going forward, heat flux and power balance research will have several elements:

1. quantifying the balance between divertor heat flux and core/divertor radiation
 2. quantitative comparison of single-nulls and double-nulls
 3. heat flux reduction techniques
 4. impact of off-normal events. e.g. giant ELMs, and reconnection events
- The first element requires a more quantitative estimate of the main plasma radiation, which is dominated by the carbon shell at the boundary.

The present AXUV diode bolometers have a 67% sensitivity drop in that wavelength range, and cross-calibration with a platinum foil bolometer in the main chamber will be done. Second, the divertor bolometer will be augmented to provide a profile of divertor

radiation. Investigating the trade-offs between radiation and heat flux as a function of control parameters will be a main focus.

Because single-nulls are used in pulse length studies and double-nulls are used in beta limit and performance studies, a quantitative comparison of the heat flux distributions in each configuration will be done. Included in this task is the assessment of the up/down power balance in double-nulls. Experiments on conventional aspect ratio tokamaks [9] and the MAST device [10] have indicated the importance of the magnetic flux balance in affecting the up/down split, and similar studies will be conducted in NSTX. Finally a set of experiments to measure the change in power flux distributions as the inner-wall gap is reduced will be conducted, to determine if the center stack can be used to reduce the divertor heat flux without excessive heating and while maintaining good performance. Additional IR cameras will be installed for this task.

The level of emphasis on heat flux reduction techniques will depend partly on if the temperature rise of the tiles restricts pulse length. If the central electron temperatures remain below ~ 2 keV, the current diffusion time will remain below 500 msec, and NSTX will be able to accomplish programmatic goals without the need for heat flux mitigation. On the other hand, if the central electron temperature is successfully raised to the 4-5 keV range, then the current diffusion time will approach several seconds, in which case the temperature rise of the tiles may restrict pulse length in lower-single nulls. In any case, heat flux reduction via deuterium gas puffing, impurity injection and outer divertor biasing will be studied in support of physics needs of an ST component test facility. In addition, heat flux reduction will be studied to confirm the physics detachment in an ST, discussed in the divertor physics section.

Finally, the heat flux studies to date and mentioned above are based on quasi-steady thermal response measured by IR cameras with conventional 30-60 Hz framing rate. An important set of experiments concerns tile response to giant ELMs and reconnection events. ELMs as large as $\Delta W/W_0 \sim 25\%$ have been measured on NSTX, and reconnection events caused by MHD activity or during plasma current ramp down need to be investigated to support future, larger ST designs and also design of the Lithium module for pumping within NSTX. The giant ELMs are triggered in low recycling conditions in lower-single null discharges and could become the norm when active density control is implemented. The heat flux associated with these off-normal events will be measured with a fast IR camera with framing rates in the 30 – 100 kHz range.

3.5.4 H-mode transition, pedestal, and ELM physics

a. Background

This area overlaps significantly with the transport section, and comprises three linked subject areas: transition, pedestal and ELM physics. The plans related to L-H transition physics, e.g. in terms of power threshold, E X B shear, fast ion event triggers, etc. are discussed in the transport section.

Pedestal physics and ELMs are clearly linked: it is generally believed that the steep gradients in the pedestal lead to relaxation phenomena which are manifest as ELMs. As reported previously [11], the density profile becomes hollow just after the L-H transition, forming ‘ears’ on both the inboard and outboard sides (Fig. 3.5.4) The density profile flattens [4] in the longer H-mode discharges after 300-500ms. From Thomson and reflectometer data, the density pedestal full width can be estimated as $\sim 3-4$ cm, i.e. in the

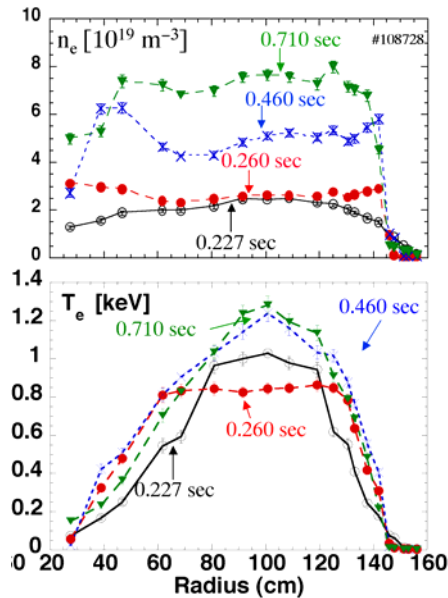


Figure 3.5.4- Density and electron temperature evolution following an L-H transition

range of the largest widths reported by the DIII-D tokamak. Mapped into normalized toroidal flux space, the pedestal extends in as far as $\Psi_{\text{NORM}} \sim 0.8$, much deeper than DIII-D’s pedestal which extends to $\Psi_{\text{NORM}} \sim 0.95$. Also of note is that the density pedestal is routinely higher on the inboard side than the outboard, as also observed on the MAST device [10]. Evolution of the temperature profile is also shown in Fig. 3.5.4 First, the temperature pedestal is rather modest, reaching a maximum of 400 eV, limited by present spatial resolution of Thomson Scattering. Second, it appears that the core temperature rides up and down on the pedestal, as opposed to experiencing a proportional increase in the core gradient.

A wide range of ELM behavior has already been observed on NSTX, with some interesting differences as compared with conventional aspect ratio tokamaks [5]. Figure 3.5.5 shows the three most prevalent D_α behavior: either ELM-free (or perhaps very rapid ELMs) in panel (a), giant ELMs dumping up to 25% of stored energy in panel (b), and ‘regular’ ELMs in panel (c). Panels (a) and (b) are both obtained in low $\delta \sim 0.4$ lower-single null discharges. The larger ELMs in panel (b) are obtained either with reduced gas fueling just above the locked mode threshold or on the first fiducial discharge in the morning of an experiment, which has lower recycling than subsequent discharges. The ‘regular’ ELMs in panel (c) are obtained in high δ ($\sim 0.6-0.8$) double-null discharges. Preliminary analysis shows that the amplitude (frequency) of these ELMs decreased(increased) with input power up to a point, i.e. a characteristic of Type I ELMs in conventional aspect ratio tokamaks.

b. Research Plan, Diagnostics, and Facility Modifications

Experiments will be carried to determine the control parameters (e.g. collisionality and neutral penetration length) of the pedestal density height and width, including the upper and lower limits and relevant density-limiting processes. Also the role of rotation and in/out magnetic field strength differences on determining the in/out pedestal heights will be investigated. Experiments to correlate the stiff electron transport observed [12] in NSTX with pedestal parameter changes will be conducted. Finally we will examine scaling of the global confinement and stored energy with pressure pedestal height. These scalings of the pedestal height, width, and maximum gradient are crucial to reactor

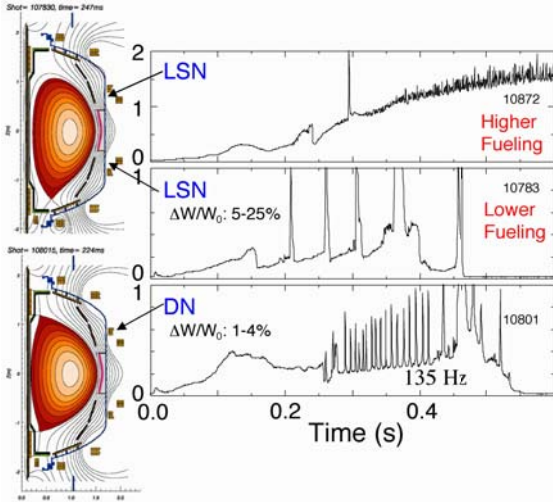


Figure 3.5.5- variety of ELM sizes and types observed in NSTX

design. With its low aspect ratio and toroidal field, NSTX (and also MAST) will provide a unique data set to the international pedestal working group, which will test predictive models of the pedestal.

On the surface, the ELM observations in NSTX are contrary to conventional aspect ratio tokamaks, where the largest ELMs are often observed in higher δ , higher performance double-null discharges. Basic ELM research will include a measurement of the ELM amplitude and frequency dependence on plasma and external parameters. In addition, ELM research will include experiments aimed at the causality

of the observed differences in double-null and single-null configurations. Experiments will also be carried out to test recent models which consider the ELM as a destabilization of peeling and/or ballooning modes. Finally, optimization of ELMs for density and impurity control will also be explored.

Quantitative comparison to pedestal, ELM, and L-H transition theories will be enabled by improved time resolution (down to 1 msec, if reasonably achievable) of the CHERS system, and increased spatial and temporal resolution of the Thomson Scattering diagnostic. A helium line ratio edge technique to obtain fast time response n_e and T_e at the outer edge is under consideration.

3.5.5 Edge, SOL divertor and wall physics

a. Background

This area covers two topics: 1) the nature of edge and divertor transport, and 2) development and evaluation of wall conditioning techniques. The classical picture [13] of divertor transport includes parallel transport on open-field lines and anomalous diffusive and/or convective transport across the field lines. In this picture, three regimes of particle and energy transport emerge: 1) a low recycling, high heat flux regime with the temperature drop occurring at the sheath; 2) a high recycling, lower heat flux regime with temperature gradients along the field lines; and 3) a detached regime in which radiation and convection dominate. In this last regime, the plasma temperature falls low enough for volumetric recombination to extinguish a portion of the plasma before striking the target; high neutral pressure is thought to play a key. From existing data, it is likely that both the sheath-limited and conduction-limited regimes have been observed in NSTX.

In addition, the paradigm of steady (but anomalous) cross-field transport may be inapplicable to NSTX. Recent experiments [14,15] on NSTX and C-MOD with the gas-

puff imaging (GPI) diagnostic have indicated the existence of localized density perturbations which propagate both poloidally and radially. Fig. 3.5.6 shows the GPI diagnostic view and two images: 1) a quiescent H-mode image, obtained by puffing Helium gas into a deuterium plasma at the outer midplane; and 2) a non-quiescent H-mode with clear structure. The smooth, curved light emission from the quiescent H-mode follows the local field line pitch near the separatrix. The bright region in the non-quiescent H-mode is indicative mainly of a local density increase. These local density perturbations can often be seen propagating radially to the RF antenna and sometimes poloidally as well. These intermittent structures are common in L-mode but also exist in H-modes. The existence of intermittent radial transport has been recently confirmed with the mid-plane reciprocating probe in NSTX.

b. Research Plan, Diagnostics, and Facility Modifications

Experiments will be conducted to document the presence or absence of the aforementioned divertor regimes, and detailed

comparisons will be made with edge plasma transport codes, such as UEDGE, and neutral transport codes, such as DEGAS-2. For example, plasma detachment has been predicted to be more difficult to obtain in NSTX due to the short connection length. Quantitative comparisons with these models will be facilitated by the installation of an improved spatial resolution divertor Langmuir probe array, and the installation of fast time response divertor neutral pressure gauges. In addition, a divertor Thomson scattering system will provide local n_e and T_e measurements, and a divertor imaging spectrometer will provide flow velocity.

Certain effects specific to low aspect ratio may alter the classical divertor picture in NSTX. For example, the total magnetic field varies by up to a factor of 4 from the outer mid-plane to the outer target in high δ plasmas. This variation in $|B|$ leads to a mirror force on scrape-off layer ions, adding the possibility of separate parallel and perpendicular temperatures. Calculation of this effect is being implemented in the UEDGE code, and diagnostics to measure the asymmetry of the temperature (e.g. energy extract analyzers) will be installed to test UEDGE predictions. In addition, the ratio of the magnetic field at the inner to outer strike points can be considerable, leading to important differences in the $E \times B$ drift pattern near the separatrix through the private flux region. A divertor reciprocating probe will be installed to measure the importance of these flows.

In the area of cross-field transport, future experiments will be conducted to fully characterize the intermittent phenomena discussed above; the results will be compared with boundary turbulence codes, such as BOUT. The effects of these bursts on mid-plane plasma decay lengths will be measured and compared with cross-field transport models. In addition, some effort will be made to compare the mid-plane turbulence with divertor turbulence, by using a fast-framing divertor camera and the new reciprocating probe, mentioned above, which will plunge into the X-point region.

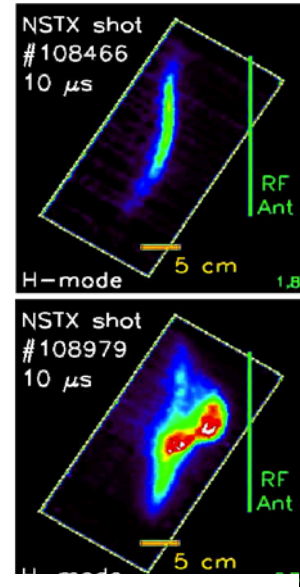
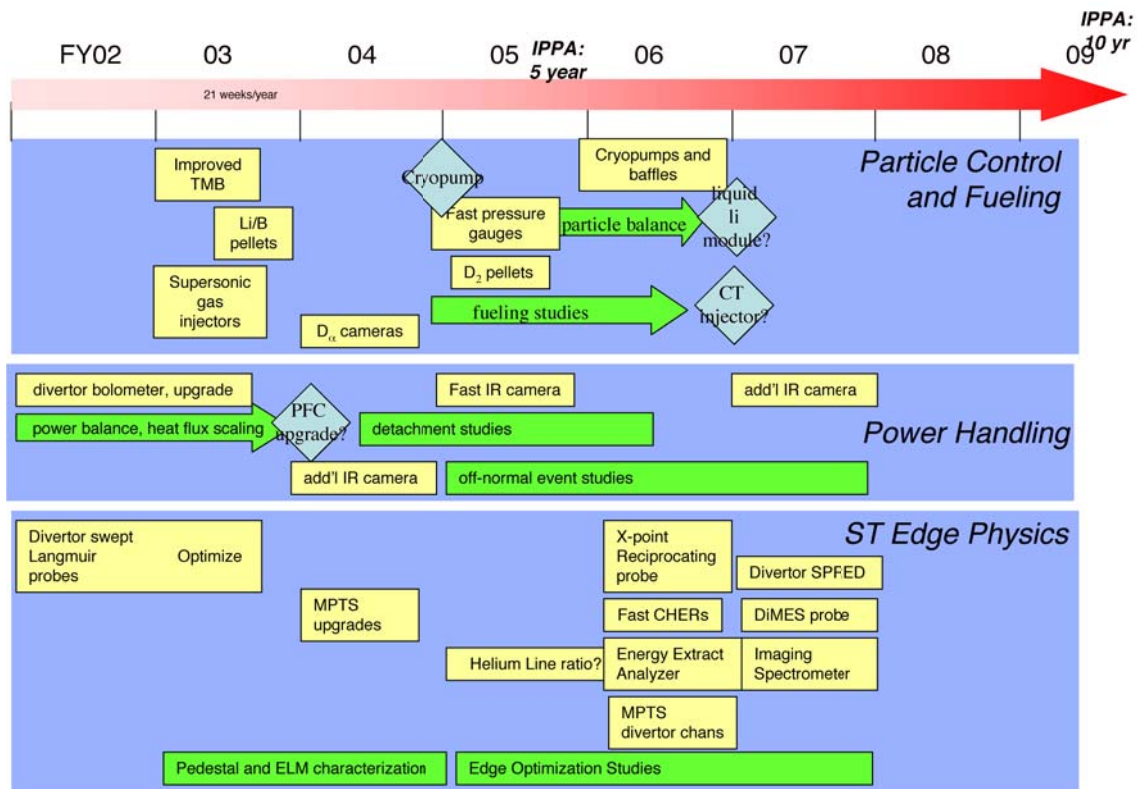


Figure 3.5.6 - gas puff images of a quiescent and non-quiescent H-modes

Evaluation and improvement of wall conditioning techniques will continue. Some of these techniques were described in the section on particle control. A Quartz crystal deposition monitor will allow correlation of wall deposition and erosion with plasma operating conditions. In addition, wall coupons will be periodically examined via standard surface analysis techniques to evaluate the film composition from various conditioning techniques and integral wall erosion due to fast charge exchange neutrals. Finally, a divertor materials probe similar to the DiMES probe on DIII-D will be installed for materials testing.



References

- [1] Kugel, H.W., et. al., *J. Nucl. Mater.* in press.
- [2] Maingi, R. et. al., *Plasma Phys. Contr. Fusion* in press.
- [3] Synakowski, E.J. et. al., submitted to *Nucl. Fusion*.
- [4] Maingi, R., et. al., submitted to *Nucl. Fusion*.
- [5] Bush, C.E., et. al., submitted to *Phys. Plasma*.
- [6] Sabbagh, S.A. et. al., submitted to *Nucl. Fusion*.
- [7] Menard, J.E. et. al., submitted to *Nucl. Fusion*.
- [8] Gates, D.A., et. al., submitted to *Phys. Plasma*.
- [9] Lasnier, C.J. et. al., *Nucl. Fusion* **38** (1998) 1225.
- [10] Carolan, P, et. al., submitted to *Nucl. Fusion*
- [11] Maingi, R, et. al., *Phys. Rev. Letts.* **88** (2002) 035003.
- [12] LeBlanc, B.P. et. al., submitted to *Nucl. Fusion*

-
- [13] Mahdavi, M.A., et. al., *Phys. Rev. Letts.* **47** (1981) 1602.
[14] Zweben, S.J. et. al., *Phys. Plasma* **9** (2002) 1981.
[15] Terry, J., et. al., submitted to *Nucl. Fusion*

3.6 Integration and Control

3.6.1 ST Research Goals and Target Plasma Conditions

The IPPA and FESAC reports have established ambitious goals for NSTX, many of which involve the integration of several plasma conditions, each one of which represents a challenge itself. For example, the IPPA goal 3.2.1.6 is to “integrate high confinement and high beta” while the FESAC 5-year Objective #2.1 involves “...assessing high-beta stability, confinement, self-consistent high-bootstrap operation, and acceptable divertor heat flux, for pulse lengths much greater than energy confinement times”.

Considerable progress has already been made in achieving high β and good energy confinement in NSTX. During the 2002 experiments, NSTX reached a normalized beta, which characterizes closeness to the MHD β -limit, $\beta_N \approx 6\% \cdot \text{m} \cdot \text{T} / \text{MA}$ in a discharge with a confinement time $\tau_E \approx 50\text{ms}$, corresponding to a confinement enhancement factor $H_{89P} \sim 2.5$ relative to the ITER-89P scaling expression, for a duration of $\sim 400\text{ms}$, *i.e.* $\sim 8\tau_E$. These parameters were obtained in a discharge with $B_T = 0.5\text{T}$, $I_p = 0.8\text{MA}$ heated by 5MW of neutral beam injection. Figure 3.6.1 compares the NSTX achievements in the figure of merit $\beta_N H_{89P}$ plotted against the pulse length normalized to the energy confinement time with the envelope of the advanced tokamak database.

Milestones for the years 2004 – 8 will extend the pulse length requirements to approach and exceed the current penetration time, which is of order 1s during auxiliary heating. Simultaneous optimizations of performance in additional areas then become necessary. With the present centerstack, longer pulses will necessitate operating with a toroidal field $B_T \leq 0.5\text{T}$ to stay within allowable limits.

Furthermore, the inductive solenoid was operated close to its full rating. Thus, unless the plasma current can also be reduced without sacrificing the confinement time, longer pulses will add the requirement for non-inductive current drive, which must be efficient, since the power applied for current drive will count against the confinement time. With longer pulses and high input power, the total energy input and the consequent heating of the divertor surfaces become issues. Control of the divertor strike-points and of means for dispersing the heat flux through the scrape-off layer will be needed in such long-pulse discharges.

The development of advanced plasma control capability in the forthcoming phase of NSTX research will provide tools for building on the foundation already established in the first three years of its operation.

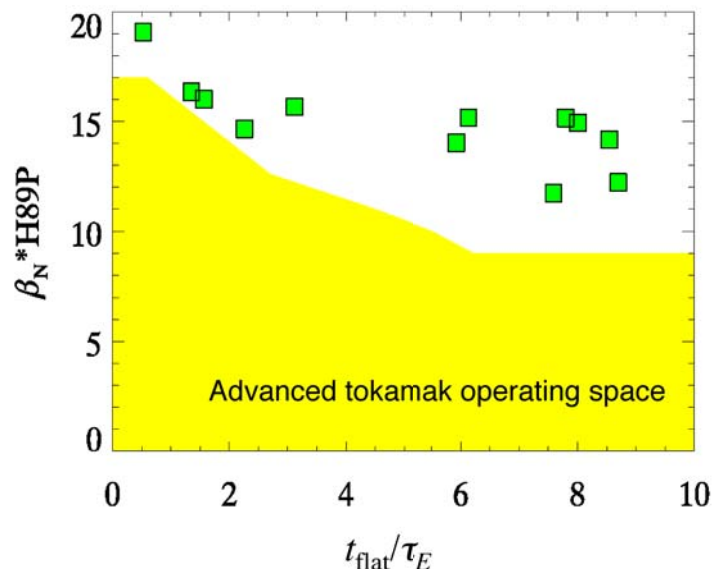


Fig. 3.6.1 Values of the product $\beta_N H_{89P}$ for NSTX (green squares) plotted against the time for which the values are maintained normalized to the confinement time. The yellow shaded area represents the advanced tokamak database.

3.6.2 Control System Status

The plasma in NSTX is presently controlled by a high-speed multi-processor computer system (SkyBolt II, currently with eight 333MHz G3 processors) which processes diagnostic measurements in real time to generate commands to the power supplies, the gas injection system and, in future, other actuators which can modify plasma behavior. The real-time algorithms are set up by a host computer running the PCS (Plasma Control Software) developed by General Atomics and adapted for NSTX under an ongoing collaboration. This software provides a convenient graphical interface for the operators to set up control parameters and reference waveforms, and also performs housekeeping functions such as archiving and retrieving control data using the MDS-Plus system. The PCS software allows different control strategies and algorithms to be applied during the various phases of a discharge, making it suitable for future experiments with non-inductive current drive and advanced plasma control.

For control of the plasma equilibrium, the control computer receives digitized diagnostic data during the pulse directly from local digitizers (currently 64 channels) and from a high-speed fiber-optical link to remote digitizers in the NSTX Test Cell (currently 96 channels) using a data transfer method known as FPDP. The FPDP streams from diagnostics in the different potential classes (these are needed for coaxial helicity injection) are combined by a multiplexing module called a FIMM, developed recently at PPPL and shown in Fig. 3.6.2. The FIMM will allow more commercial digitizer modules (32 channels each) to be added quite readily to accommodate future development. Each input signal is available to the control computer at 12-bit precision with a sampling rate of 5 kHz and a sample latency under 10 μ s. From the control computer, command signals are sent to the NSTX power supplies on the Power Conversion (PC) Link, a system developed at the beginning of TFTR. The power supplies are phase controlled rectifiers operating in either 6- or 12- pulse configuration with a line frequency of about 65Hz provided by the motor-generator sets.

Lower data rates are required for controlling the gas injection system (GIS) since the response times of both the gas valves and the plasma itself are slower. Seven channels of diagnostic data are received and four channels output to valve drivers by the real-time computer by extending its VME bus to a second crate in the NTC. To provide reproducible flow rates, pulse-width modulation of the piezo-valves is employed with the duty-cycle automatically adjusted for the gas species and its upstream pressure. At present, only the prefill pressure prior to and the gas flow rates from the different valves during the discharge are programmable.



Figure 3.6.2 The FIMM, developed at PPPL, combines FPDP high-speed data streams from different source modules for input to the SkyBolt computer.

The implementation of gas control via the VME bus has increased the I/O overhead of the real-time computer system, thereby increasing the latency in communicating with the power supplies. This is a concern, particularly for the control of highly shaped plasmas. The effective frequency response of the PC-Link and power supplies is adequate for controlling the plasma current and the radial and vertical position, provided that the elongation is not too high and the internal inductance of the plasma is low: in experiments to date, κ up to ~ 2.5 has been controlled for $i_i \approx 0.6$. However, future experiments will demand greater capability for elongation control, so methods for improving the speed of the power supply control are being investigated.

The 2002 experiments demonstrated the benefits of gas fueling from the high field side, *i.e.* injecting gas on the center stack, for obtaining H-mode transitions reliably. The real-time computer does not yet control the flow from the center-stack gas feed. The prototype injector used until now is opened fully before the start of the plasma and it empties the contents of its plenum during the discharge. For this injector, there is a time delay of about 0.2s between opening the injection valve and the appearance of gas in the vessel because the gas must flow through a long (~ 2 m), narrow (3mm diameter) pipe from the valve to the feed point at the mid-plane. The flow characteristics of this injector are essentially determined by the initial pressure of the gas in the plenum. During the 2002 outage, an additional high-field-side injector was installed using a shorter, larger-diameter pipe to convey the gas to the upper shoulder of the center stack, rather than the mid-plane. It is hoped that this injector will provide greater controllability for the gas which may permit it to be incorporated in the real-time control system in the same way as the low-field-side injectors.

Until recently, the algorithms for plasma equilibrium control on NSTX were fairly rudimentary, providing feedback control only of the plasma current, the vertical position of the current centroid, and the outboard radial gap, nominally at the midplane. Shape control was provided by programming the poloidal field (PF) coil currents in advance. The outboard gap was determined by a flux projection technique using the poloidal magnetic flux and field measured behind the passive stabilizing plates inside the vacuum vessel.

In the last week of the FY'02 run (June 2002), control of the equilibrium during the current flattop was demonstrated using an isoflux control algorithm based on a real-time solution of the Grad-Shafranov equation for toroidal equilibrium with the rt-EFIT code developed by General Atomics. This solution is a best fit to the set of about 130 measurements of coil currents and magnetic fluxes and fields currently digitized in real-time. Figure 3.6.3 compares an example of the plasma boundary computed by rt-EFIT during one of the demonstration shots with that calculated by the standard EFIT code in off-line analysis. The agreement is not perfect but some

Time = 210ms, Shot = 108965

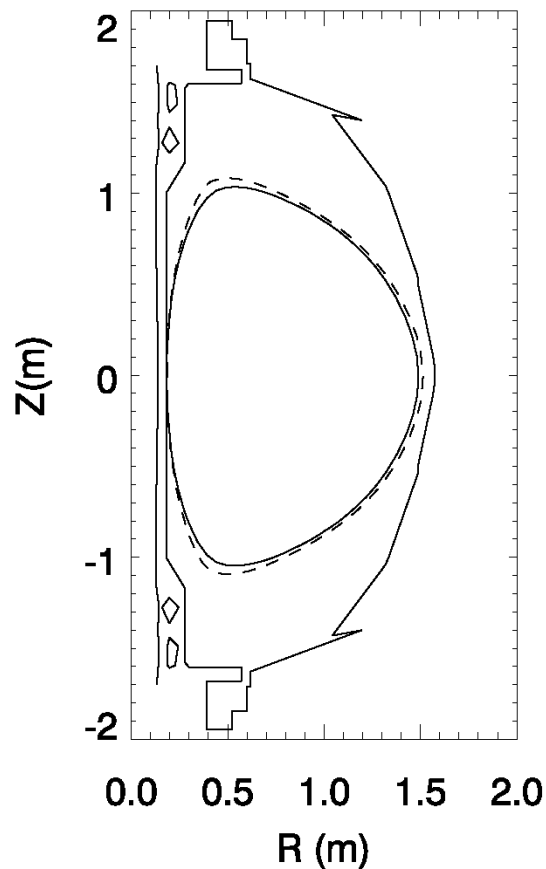


Figure 3.6.3 Plasma boundary calculated by EFIT and rt-EFIT

sources of error in the diagnostic inputs to the real-time system have since been eliminated which will reduce the discrepancies in future. During the FY'03 run, the capabilities for equilibrium control based on rt-EFIT will be expanded by implementing more control variables such as additional gaps and/or shape parameters (*e.g.* elongation, triangularity). It is anticipated that the early startup phase of each discharge will still be controlled by a flux-projection technique, but that the time window available for rt-EFIT control will be expanded.

3.6.3 Control System Upgrades and Real-time Diagnostic Data Processing

Plans and possibilities being investigated for improving plasma control by including real-time diagnostic data, including profile data, in the rt-EFIT analysis are discussed below. These will require additional input channels from sources in different locations and in different potential classes. The present SkyBolt II computer already has considerable capability for real-time processing of diagnostic data and the number of processors could be expanded further if needed.

2003 – 2005: Meeting the control requirements for resistive wall modes - An important element of the NSTX program over the next several years is identifying the control needs and implementing an active feedback system for the control of resistive wall modes (RWMs), instabilities which would be stabilized by a perfectly conducting wall close to the plasma but which can grow on a resistive timescale if the wall has finite conductivity and the rate of plasma rotation is insufficient. NSTX has already operated with normalized- β above the “no-wall” limit and the growth of the RWM in this condition has been inferred from the development of kink-link perturbations of the plasma column and the rapid slowing of the plasma rotation driven by the neutral beams.

It has been demonstrated, on DIII-D in particular, that real-time control of both extrinsic error fields arising, for example, from coil misalignments, and the fields generated by the growing instabilities themselves, can facilitate continued plasma rotation and suppress instability growth. On NSTX, a comprehensive set of detectors for non-axisymmetric poloidal field perturbations was installed during the 2002 outage. Although the requirements for real-time processing of data from these detectors to permit stabilizing RWMs is not yet known, it is likely that the required response time will be considerably shorter than that needed for axisymmetric position control. However, this should still be within the capabilities of the present data acquisition system and control computer. Most of the diagnostic signals for RWM control will be generated in the diagnostic racks close to the existing digitizers in the NTC for the real-time system. Additional digitizers will be needed, and, possibly, an additional VME crate, controller and a pair of fiber optic link modules. The actuators for RWM stabilization are discussed in Sec. 3.6.4 below.

2003 – 2005: Control system development for coaxial helicity injection (CHI) - Coaxial helicity injection (CHI) presents several challenges for real-time control. At present, the CHI discharge is established by preprogramming the coil currents and the injector voltage without feedback control over the discharge evolution. In the experiments to date, most CHI discharges have ended in an “absorber arc”, that is a localized breakdown across the insulating gap at the opposite end of the vacuum vessel from the injecting gap. These absorber arcs are believed to have been caused by an inadequate length of insulator in the absorber and the development, as the CHI discharge evolved, of an unfavorable magnetic field distribution which allowed a relatively short connection length along field lines between components at different potentials. In the 2002 opening, a new absorber insulator was installed which increases the separation of the components at different potentials. In addition, two PF coils were added to provide additional capability to null the poloidal field in the absorber region. Power supplies are now being built to energize these control coils.

The first task in implementing control for CHI is developing the appropriate control strategy for the primary CHI discharge to maximize the toroidal plasma current and to provide conditions conducive to the formation of closed magnetic flux surfaces while avoiding absorber arcs. This is needed to provide reproducible conditions for diagnosing the discharge to gain an understanding of the basic process and subsequently for coupling CHI to other methods of current sustainment. Analyzing the toroidally averaged plasma configuration during CHI will require a substantial modification of the rt-EFIT code to include current on the open field lines between the injector electrodes, so simple flux projection techniques will be employed initially. Since the reconnection to form closed flux involves non-axisymmetric perturbations, data from many magnetic pickup coils distributed toroidally may be required. The control requirements for CHI initiation will be investigated in FY'03 and feedback control will be attempted in FY'04. Also in FY'03, an assessment will be made of the need for absorber field nulling, with implementation of feedback control for this scheduled for FY'04, if it is required.

Once reliable CHI initiation has been established, a method for making the transition to inductive and/or RF-driven current sustainment must be devised. The first tests of inductive sustainment will be made in FY'03 using a simple (non-feedback) control algorithm already developed. Feedback control of the transition and subsequent discharge evolution will be introduced in FY'04. The capability for handing over to sustainment by HHFW current drive will be introduced in FY'05.

2005: Inclusion of real-time pressure measurements in the control system analysis - The raw data from the photodetectors of the multi-point Thomson scattering (MPTS) measurement will be processed in real time to provide the temperature, density and, hence, the pressure profiles of the electrons, albeit with somewhat less accuracy than the full offline analysis. The electron pressure profile shape alone has been used as an additional constraint in offline analysis with the EFIT code and shown to improve the quality and accuracy of the equilibrium. A similar technique can be employed to improve the faithfulness of the rt-EFIT analysis. With the present two lasers, the MPTS system can provide full profile data at 60Hz, which is comparable to the time-slice analysis rate for rt-EFIT on a single processor. To provide this data in real time from the MPTS instrumentation room, up to 4 32-channel digitizers (for the full 20 spatial channels), a VME crate and controller and 2 fiber optic link modules, in addition to the FIMM will be required. This upgrade will be undertaken in FY'05.

Processing the data from charge-exchange recombination spectroscopy (CHERS) to obtain the ion temperature during neutral beam injection is probably not possible. These data are recorded with a 2-D CCD array with a relatively slow readout, and the conditions in NSTX necessitate a complicated removal of background emission from the edge region of the plasma and an elaborate fitting procedure which cannot be performed in real time. However, as experience is gained with the new CHERS system, which was also installed during the summer 2002 outage, it may be possible to devise an approximate method for analysis of CHERS data adequate for use in real-time control.

If real-time analysis of the ion and electron profiles becomes available, then an approximate calculation of the contribution of fast ions to the total pressure could also be performed. This would then enable rt-EFIT analysis with full kinetic profiles for plasmas heated by NBI. Furthermore, if the capabilities of the SkyBolt computer were expanded by adding processors, it would be possible also to calculate the deposition of the High-Harmonic Fast Wave (HHFW) power during RF heating and current drive. At present, such calculations rely on separate ray-tracing of the launched waves and kinetic modeling of the wave absorption. Several advances in the speed and accuracy in the calculation of wave-plasma interactions have occurred in the last year under the auspices of the SCIDAC initiative. From numerical analysis and modeling of HHFW-heated plasmas, it should be possible to develop approximate methods

which are suitable for real-time control. These enhancements to the real-time analysis capabilities would be undertaken in FY'06 through FY'08.

2006 – 2007: Inclusion of real-time current profile and magnetic field data - Data from both the Motional Stark Effect (MSE) polarimeter and Faraday rotation measurements from the far-infrared interferometer/polarimeter (FIRETIP) will help to constrain the toroidal current profile in the rt-EFIT analysis. The first two channels of the MSE system, measuring the collisionally induced fluorescence (CIF) from the heating neutral beams, were installed during the summer 2002 outage and will be progressively commissioned starting in the FY'03 run. The remaining 8 channels of the CIF system will be added in subsequent years. When this system has been calibrated and its performance fully characterized, its data will be incorporated into the real-time analysis beginning in FY'06. The data requirements for this are modest and the calculations are relatively straightforward although a considerable amount of calibration data will be involved and provisions must be made to keep this data current. The equipment required for gathering this data from the MSE room is similar to the requirements for the MPTS data, viz. high-speed digitizers, a VME crate and controller and fiber optic link modules. Faraday rotation measurements from the FIRETIP polarimeter will also be included in the rt-EFIT analysis, although since the total Faraday rotation on a measurement sightline is the path integral of the product of the local magnetic field and the density, a double inversion of the data is required to obtain the local magnetic field.

In FY'05, a new MSE diagnostic based on laser-induced fluorescence (LIF) will be installed. This diagnostic can provide a measurement of $|B|$, the magnitude of the local magnetic field, as a function of time and space throughout the plasma. These data can be incorporated into the rt-EFIT analysis to constrain the total plasma pressure profile, including the fast ion component. This would represent a significant extension of capability for real-time control, with obvious application to future ignition devices where there will be populations of energetic alpha particles.

2006 – 2008: Real-time calculation of MHD stability limits – With the inclusion of data from both the kinetic and magnetic profile diagnostics in the rt-EFIT analysis, the calculated pressure and q-profiles could, in turn, be used to calculate the proximity of the equilibrium to stability boundaries, thereby permitting feedback on the heating power, or other means, to avoid instabilities. The first implementation of such a stability analysis might involve simple parametrizations of the MHD pressure limits in terms of normalized- β , the internal inductance l_i and the pressure profile peaking factor $p(0)/\langle p \rangle$ as has been quite successful in characterizing the limits in NSTX so far. Further development to assess the stability of specific classes of modes, such as energetic particle instabilities and edge instabilities could be added as theoretical analysis and tools are developed.

3.6.4 Provision of Tools and Actuators

2004: Improving the speed of power supplies for vertical position control - Experiments will be conducted in FY'03 to increase the plasma cross-section elongation to improve MHD stability. To control plasmas with elongation approaching $\kappa = 3$ and further away from the passive stabilizer plates than present equilibria, faster response than is available from the existing phase-controlled rectifiers and their communication link will be needed. The control requirements for these fast equilibrium control supplies, the existing PF power supplies and the RWM control supplies (discussed below) will be assessed together so that all power supplies can use common hardware and communication software. One possibility for providing greater speed is the fast-switching power supply being built in a collaboration with the University of Washington to control the current in the two new CHI control coils

installed during the 2002 outage to null the poloidal field in the vicinity of the absorber insulator. These power supplies can provide fast regulation of a DC current provided by one of the existing phase controlled rectifiers.

For controlling the vertical instability at the highest plasma elongations, a reconnection of the toroidal and top-bottom links between the passive stabilizers or even a reconfiguration of the plates to match the plasma boundary more closely may be required. Such a reconfiguration would be undertaken in FY'06 if experiments indicate a continuing favorable trend of performance with increasing elongation of the plasma cross-section.

2004: Control of the NBI heating power - It is planned to implement control of the heating power to maintain β close to but below the evolving stability limit. This depends on full implementation of rt-EFIT analysis with appropriate diagnostic inputs. With only three NBI sources available, pulse-width modulation of the sources will be required to achieve fine control. In addition to providing a suitable real-time data link from the control computer to the NBI controllers, the algorithms for choosing the modulated source(s) and the characteristics of the modulation (time on vs. off) must be developed. This control for the NBI power will be progressively enhanced as capabilities for real-time analysis of the stability limits are developed.

2005 – 2007: Feedback stabilization of MHD Instabilities - For the stabilization of MHD modes, several new tools may be required. In principle, complete control of the radial profiles of pressure and toroidal current would allow optimization of ideal MHD stability, but providing these capabilities would probably not be energetically favorable in the face of plasma transport processes, so more efficient means are required for specific classes of instability.

As expected from theoretical studies, the outboard passive plates provide significant stabilization of kink-like modes if β is sufficiently high to cause the magnetic perturbations to become large on the outboard side. The experiments in the past year indicated that the reduction in the error fields arising from the original misalignment of the PF5 coils has helped to suppress the RWM, although it has not been eliminated. To control the RWM growth at even higher β , active control of the error fields, which can be amplified by the plasma itself, will be needed. A set of coils to provide radial field corrections varying in space and time will be installed in FY'04. These coils are most easily mounted outside the vacuum vessel, but in this location they would have smaller influence at the plasma and the time response of the control would suffer. Initially, these coils will be used to null the apparent time-varying error fields responsible for the rotation damping and subsequent RWM growth. The corrections fields to be applied will be inferred from measurements in ensembles of discharges and averaged over a suitable moving time window. For this control strategy, the frequency response of the power supplies is modest. However, for eventual real-time feedback control of the RWM, the required frequency response will exceed that of the existing phase controlled rectifiers operating at standard line frequencies and additional fast power supplies will be required.

Neoclassical tearing modes (NTMs) have been identified in some NSTX plasmas when β_p exceeded a value around 0.4 and $q(0)$ ($= q_{\min}$), as determined by EFIT from the external magnetic data, was below 1.5. An example of the island structure for such a mode in an NSTX plasma is shown in Fig. 3.6.4. More recently, plasmas with $q_{\min} > 2$ have reached β_p up to 1.2 for extended periods ($>0.2s$) without the growth of NTMs. This suggests that control of the q-profile to maintain $q_{\min} > 2$ may be sufficient to avoid NTMs. However, the optimum q-profile for stability to ideal pressure-driven instabilities has not yet been determined, so it is possible that NTMs will become a problem in future high- β plasmas in NSTX. In tokamaks with normal aspect ratio, NTMs have been controlled by localized current drive.

This is applied at the location of the NTM island to replace the local bootstrap current, the absence of which is responsible for the island and which is reduced by the flattening of the pressure gradient in the island. If such active control of NTMs becomes necessary in NSTX, then suitably localized current drive will be required.

Recent experiments have demonstrated that high-harmonic fast waves (HHFW) launched with appropriate phase velocity can drive current. However, the efficiency of HHFW current drive and its localization remain issues for its application to NTM suppression. The NSTX RF system is capable of controlling in real time the wave-number spectrum of the launched waves so, in principle, it should be possible to affect where the waves are absorbed and current drive occurs. However, since the wave absorption is proportional roughly to the square of the local β , there is a tendency for the power to be deposited on axis unless the absorption can be made very high in the outer regions. Another possible complication for HHFW-CD is absorption of the waves by fast ions in NBI-heated plasmas which will reduce the efficiency of current drive.

The possibility for current drive by electron Bernstein waves (EBW-CD) is also being investigated in NSTX. Experiments in FY'03 will focus on the process of mode conversion in the plasma edge which is required to couple power from an external antenna to an EBW in the plasma. In order for EBW-CD to be successful, the mode conversion must be made efficient and reproducible. The edge conditions under which this occurs must be compatible with good plasma performance and acceptable heat loads on the launching structure. The toroidal and/or poloidal angles at which the waves are launched may need to be varied to control the coupling and power deposition. Extensive control will be needed to optimize this method of current drive if it proves feasible. A 1 MW, 15 GHz system is proposed for experiments in FY'06 with a possible expansion to higher power in the following year. The requirements for this system to be able to provide NTM control will be developed as the source and coupler designs are defined in the next three years.

2004 – 2007: Control of plasma fueling and exhaust - As in standard tokamaks, fueling and density control are major issues for the ST. Already, the limitations of gas fueling from the edge and the effects of strong recycling at the first wall are impacting NSTX operation. In L-mode plasmas the fueling efficiency is low for gas injected on the low-field side (LFS) and access to the H-mode has proved difficult with this method. Access to the H-mode has been improved by fueling with gas injected from the center column, *i.e.* on the high field side (HFS). However, this gas is introduced from an external plenum through a narrow, long pipe. Once the injector valve is opened, there is essentially no control over the flow rate which reaches a maximum determined by the fill pressure and then decays slowly, providing continuous, uncontrollable fueling. As a result, in H-mode plasmas, the density rises continuously, limiting the range of conditions available for experiments and preventing the assessment of the confinement characteristics in steady state. The H-mode density profile can also develop a significant peak near the boundary where the transport appears to be reduced but the particle source from the fueling and recycling is strong. The hollow density profiles adversely affect NBI heating and, in terms of eventual fusion performance, would reduce the fusion reactivity for a given β .

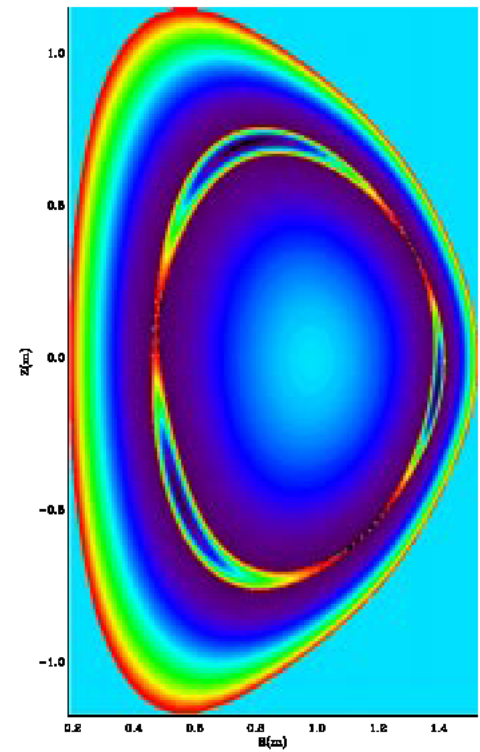


Figure 3.6.4 Simulated island structure for a $m/n = 3/2$ neoclassical tearing mode for NSTX shot 103698 at 192ms. The island width 10% of the minor radius.

For the FY'03 run, two new fueling capabilities are being introduced. First, a new HFS injector has been installed with a shorter, larger diameter pipe which will introduce the gas from the center column at the "shoulder" above the midplane, rather than at the midplane itself. It is expected that some control of the gas flow rate in time will be possible with this injector. Second, a prototype system is being developed to inject gas supersonically from a shaped nozzle near the midplane on the LFS. Supersonic gas injection through the plasma edge has been shown to be beneficial in other tokamaks. If these benefits are confirmed in NSTX, the injector will be developed into a permanent system in FY'04 and its control will be incorporated into the real-time control system.

Frozen deuterium pellets can provide central fueling although for the NSTX plasma, which has a relatively small volume for its minor radius, the size of the pellet required to penetrate to the core creates a large density perturbation, which is not ideal. In standard aspect-ratio tokamaks, pellets injected on the high field side have shown the expected improvements in penetration compared to low-field side injection. This effect, which is related to the ∇B drift, could be expected to be more significant in the ST and might permit use of smaller pellets. A deuterium pellet injector is planned for installation on NSTX in FY'05. Success was obtained in TFTR in maximizing the fueling rate from multiple pellets by triggering the injection of subsequent pellets when the electron temperature had reheated after the preceding pellet. Such control would be possible in NSTX once the electron temperature data is available in real-time in the control computer.

For controlling the density profile, modifying the wall material and providing active pumping in the divertor will be studied in NSTX. Both these techniques have proved successful in other tokamaks. For example, coating the carbon surfaces with lithium in TFTR produced dramatic changes in the recycling and improvements in confinement and fusion performance. In FY'03, an injector for low-velocity lithium or boron pellets will be installed on NSTX. If pellets of either material produce beneficial effects on recycling, density profile control or plasma performance, methods for more extensive coating of the walls, such as the TFTR DOLLOP system, could be installed on NSTX. Control of the plasma boundary relative to the actively pumping surfaces will clearly be required for optimal plasma exhaust.

A design study has been conducted for a cryo-pump to be installed in the lower divertor of NSTX. A decision on proceeding with this will be made at the end of FY'04 with availability expected in FY'06. Such a system may require a reconfiguration of the secondary passive plates and would have many implications for plasma control and integration, since the pumping rate will be highly dependent on the plasma configuration in the x-point region and through the pump throat, which in turn has consequences for plasma shaping and thus stability. Maintaining adequate flexibility for plasma shape control will be an essential component of the system design.

A possible alternative method for plasma exhaust is a liquid lithium surface module. Experiments to assess the potential of this method are being conducted on CDX-U and the PISCES facility. The major problem with this approach is making the system compatible with normal operation. In addition to control of the plasma interaction with such a module during normal operation, control strategies would have to be developed for off-normal events, to prevent disruption of the lithium containment, and possibly its flow, in its support structure. Assuming a successful outcome of the enabling research, such a module would be deployed in FY'07.

Power handling in the divertor is a critical issue for the ST. Experiments are being planned for the FY'03 run to characterize the edge plasma and the power and particle flows to the divertor. If this research indicates that power fluxes will become unacceptable in long pulse operation, one possibility for ameliorating the divertor power flux is to increase the edge radiation, either by changing the density

to enhance the radiation from intrinsic impurities or by injecting a suitable recycling (noble) gas. The issue will be localizing the radiation to the divertor while avoiding both radiation from and dilution of the core plasma. Additional gas injectors in the divertor and their integration into the overall plasma control strategy will be needed.

If high power fluxes to the divertor cannot be avoided by other means, changing the divertor tiles to a carbon-fiber composite or another advanced material and sweeping of the strike points will be needed for long pulse operation in NSTX. Feedback control on the local surface temperature on the tiles is a possibility. If the location of the X-point needs to be fixed for maintaining stability at high β , additional PF coils may be needed close to the divertor to provide the sweeping.

3.6.5 Flowchart of Planned Developments

The phased development of control capability and the integration of those elements to meet the goals of the NSTX research program are presented as a flow chart in Fig. 3.6.5.

3.6.6 Additional Possibilities for Control Enhancement

The following paragraphs describe some additional possibilities for augmenting the control of plasmas in NSTX. One or more of these items may be developed, depending on the results of experiments in both NSTX and in other devices where similar techniques are being investigated.

Additional plasma shaping possibilities – There is interest in utilizing the existing PF4 coils which are currently not connected to a power supply. This would change the shape of the plasma boundary at the outboard midplane which calculations have shown is critical for MHD stability. While it would be relatively straightforward to connect the present PF5 power supply to the PF4 coil for a dedicated experiment, both coils could not be used without providing an additional power supply, disconnect and grounding switches and cabling from the FCPC area to the NTC. The control software for the Power Conversion system would also require significant modification.

Advanced fueling – Fueling by injecting Compact Toroid (CT) plasmas is potentially well matched to the ST. The individual CTs contain fewer particles than a pellet, the injection velocities are very high and the deposition is controlled to some extent by the gradient in the magnetic field which is high in the ST. In addition to fueling, CTs can be used as a momentum source which is potentially reactor relevant. However, considerable development would be needed to provide a suitable CT injector with adequate repetition rate. The possibilities for CT injector development will be considered starting in FY'04 for a decision in FY'07 on deployment.

Additional methods of particle control – Two other possibilities for reducing edge power fluxes are ergodization of the edge by an array of small coils and segmented biasing of the divertor. The latter method has been tried with some success in the Compass tokamak and is now being investigated in MAST. Providing toroidally isolated segments of the divertor would be a major undertaking and the compatibility of such biasing with CHI operation remains to be investigated.

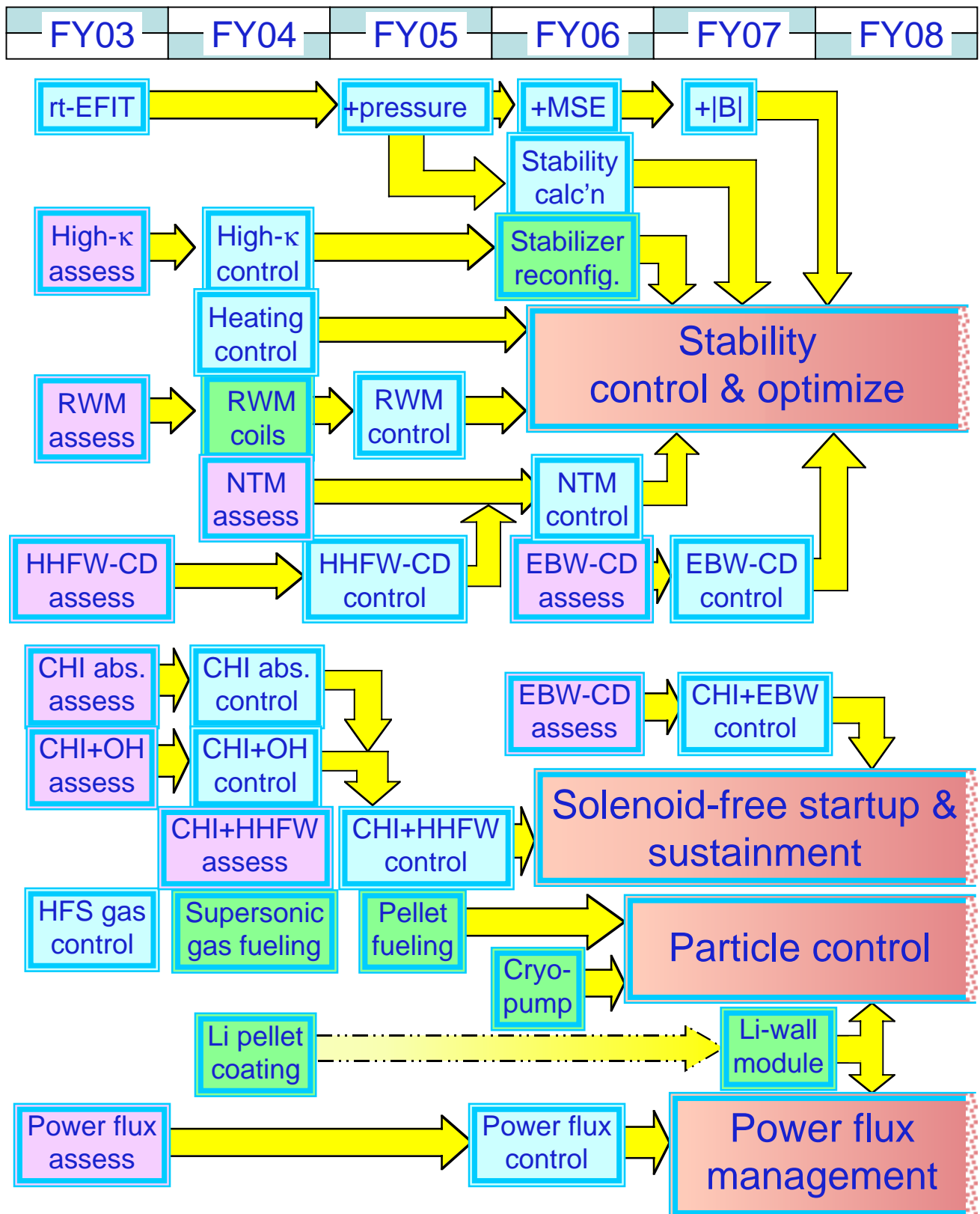


Fig. 3.6.5 Flowchart of planned developments in plasma control and their integration to achieve the research goals of NSTX. The elements with a light purple background represent experimental assessments in support of planned developments while those with a green background are major hardware developments. The elements with a blue background represent the implementation of control for each capability or tool.

4. *Integrated Scenario Modeling*

Modeling of both experimental and projected discharges is a critical component to NSTX's long term mission. Understanding the interactions of plasma transport, MHD, heating and current drive (CD), and the plasma edge, and being able to project this behavior to design future experiments is a primary theme for the next five years.

The time-dependent computer codes used for integrated modeling are TRANSP and TSC (Tokamak Simulation Code). The former provides fixed-boundary evolutions, while the latter provides free-boundary evolutions. TRANSP is typically used as interpretive, such that it uses the experimental temperature and density profiles, and plasma boundaries to guide its simulations. A predictive capability is now available. TSC is predictive, although it contains modes where it is constrained by experimental data, such as line average density, PF coil currents, etc. Although the two codes are solving the same basic transport equations for energy and current density (and particles if chosen) using equilibrium flux geometry, they have different capabilities in terms of heating and CD calculations, models for transport coefficients, impurity treatment, sawtooth treatment, plasma rotation, bootstrap current, radiation, fast particle treatment, MHD stability, neutral particles, and plasma feedback models. These capabilities are continuously being expanded and updated.

Although it is desirable to have integrated modeling with all physics models available, such a computer code does not exist, and so stand-alone analysis is important to supplement the evolution simulations with TRANSP and TSC. These stand-alone simulations typically rely on a static equilibrium at a given time slice and have no time dependent features. Since one is examining only a single time slice more sophisticated computations can be done, as opposed to integrating it into a transport code that would have to do the computations a large number of times. Examples of the most commonly used analyses are CURRAY (HHFW), HPRT(HHFW), TORIC (HHFW), TRANSP (Monte Carlo NB), EIGOL(NB), VALEN (RWM), PEST/DCON/BALMSC (ideal

MHD), CQL3D (RF), FULL (ITG/TEM), GS2 (ITG/ETG), M3D (resistive MHD), NOVA-K (fast particle instabilities) and there are several others. It should be noted, that some of these models are being incorporated into TRANSP and TSC, and will continue to be as computational capability expands. In addition, the equilibrium analysis with EFIT provides the experimental information for virtually all these stand-alone analyses, as well as guidance for both TRANSP and TSC.

Schematically shown in Fig. 4.1 is the interdependence of the stand-alone analysis, time dependent scenario modeling and experimental results. The stand-alone analysis feeds into integrated scenario modeling where it can not be included explicitly. TSC's primary strength which TRANSP can not include is its free-boundary plasma feature including interactions with the structure and PF coils, and feedback control systems. Presently TRANSP's particular strengths are the sophisticated physics models that can be included, especially the Monte Carlo

beam deposition, fast particle treatment, and full wave ICRF packages. Presently, these are not included in TSC due to their very long running times. It should be noted that analysis with TSC and TRANSP are complementary, in particular when interpretive TRANSP provides experimental thermal diffusivities and beam deposition profiles for

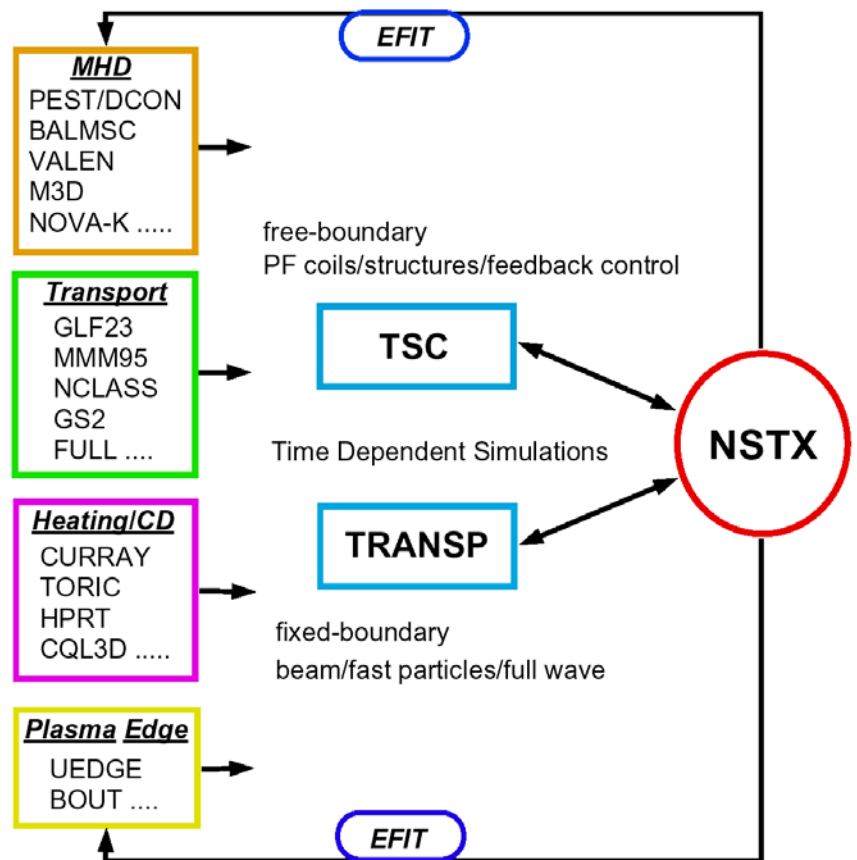


Figure 4.1 - Schematic of integrated scenario modeling for NSTX, identifying the stand-alone simulation, time-dependent simulation, and experimental contributions and interactions.

TSC simulations. The scenario modeling is intimately coupled to experimental results, and relies on continuous advancement of physics models and computational capabilities.

The spherical torus concept will provide an attractive fusion energy configuration if it can demonstrate the following major features: high plasma elongation with significant triangularity, 100% non-inductive current with a credible path to high bootstrap current fractions, non-solenoidal startup/rampup of the plasma current, stabilization of the RWM instabilities, and sufficiently high energy confinement combined with energy transport control. Demonstrating these features experimentally would certainly be achieved individually, and then simultaneously to varying degrees. Integrated scenario modeling is a key element to guide experiments toward achieving these features.

Examples of this will be described below, in which predictive simulations were done with TSC to find ways to produce a discharge out to 1.0 s with a flattop that obtained 100% non-inductive current. These discharge simulations were extensions of a particular shot 109070, where a sufficiently long pulse had been obtained. TRANSP analysis of the shot provided the beam power deposition and CD, and the thermal diffusivities. The addition of 6.0 MW of HHFW was included by prescribing a deposition profile, a total current of 100 kA, and a 50/50 power deposition in ions and electrons (based on previous stand-alone CURRAY analysis). From global theory, the bootstrap current fraction is proportional to $C_{BS}\beta_N q_{cyl}$, where C_{BS} contains profile and collisionality effects, and q_{cyl} is given by $\pi a^2 B_t (1 + \kappa^2) / \mu_0 R I_p$. Since the plasma current was already low, at 800 kA, and the toroidal field restricts the pulse length, increasing elongation (Case 1) and peaking the density profile (Case 2, which increases C_{BS}) were examined. In addition, lowering the density (Case 3) to improve the NBI CD efficiency was also simulated, based on the well known T/n dependence of non-inductive CD sources. Table 1 gives major parameters for the resulting plasmas in flattop, highlighting those parameters that have been changed from the experimental values in shot 109070. The plasma current is 800 kA, the toroidal field is 0.5 T, and Z_{eff} is 3.5 for these simulations, as it was in shot 109070. The thermal

betas and stored energies are reported, while in shot 109070 the beam contribution brings the stored energy up to 250 kJ, β_N up to 5.0, and β up to 13.7%.

Table 1. Parameters Obtained for 100% Non-Inductive Plasma Simulations

	Case 1	Case 2	Case 3	Shot 109070
I_{BS} , kA	450	440	380	240
I_{NBI} , kA	220	249	345	160
I_{HHFW} , kA	100	100	100	0
κ, δ	2.7 , 0.26	2.15, 0.27	2.1, 0.28	2.1, 0.4
q_{cyl}, q_{95}	4.0, 8.0	3.6, 9.9	3.3, 10.0	3.3, 10.0
li(1), li(3)	0.66, 0.40	0.8, 0.5	0.73, 0.5	0.67
$\beta_N^{thermal}, \beta^{thermal}$	5.0, 15.5%	5.3, 14.5%	5.8, 16.0%	3.8, 10%
$W_{thermal}$ (kJ)	250	250	235	150
τ_E (ms), H98(y,2)	25, 1.0	23, 1.1	24, 1.25	34, 1.0
$T_e(0), T_i(0)$, keV	1.7, 3.7	1.7, 3.8	1.9, 5.0	1.1, 1.8
$n(0)$, $\times 10^{20} / m^3$	0.5	0.58	0.4	0.5
$n(0)/\langle n \rangle$	1.05	1.56	1.05	1.05

Shown in Fig. 4.2 is the time history of the plasma current and peak temperatures for ion and electrons for the high elongation Case 1. The various contributions to the plasma current are shown. The bootstrap current contribution dominates and closely tracks the

plasma elongation, which is not shown, through the rise in q_{cyl} . The wide difference in temperatures between ions and electrons, observed in NSTX experiments, is preserved in

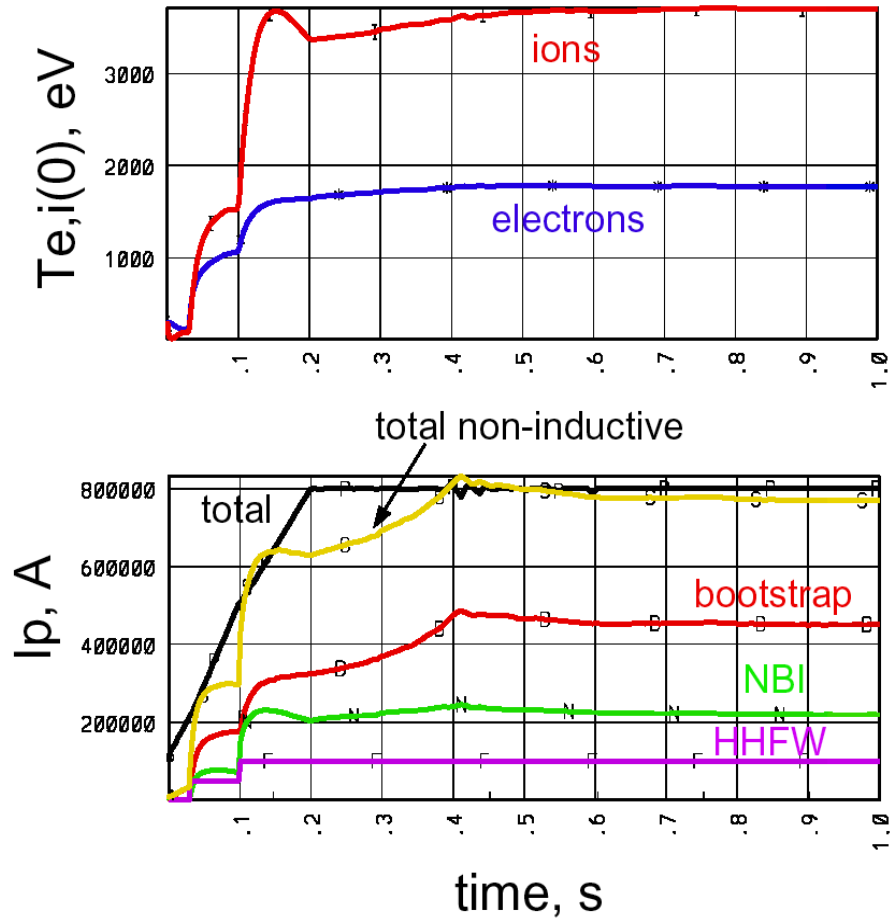


Figure 4.2. Time histories of the peak electron and ion temperatures, and various contributions to the plasma current, with the total plasma current in black and the total non-inductive current in yellow. This simulation uses higher elongation to increase the bootstrap current, and was done with TSC.

these simulations, although an additional 6.0 MW of HHFW is included, which causes both temperatures to rise over those of 109070. The yellow curve shows the total non-inductive current and it reaches the total plasma current at about 0.4 s in flattop, although it makes large contributions even in rampup due to the lower density at that time. Profiles during the flattop are shown in Fig. 4.s3. The safety factor remains above 1.5 over the full 1.0 s pulse, the density is quite broad, and the various contributions to the

current density are shown. The bootstrap current profile is broad, with a pedestal driven peak, while the NBI is centrally peaked, and HHFW has a broader central peaking.

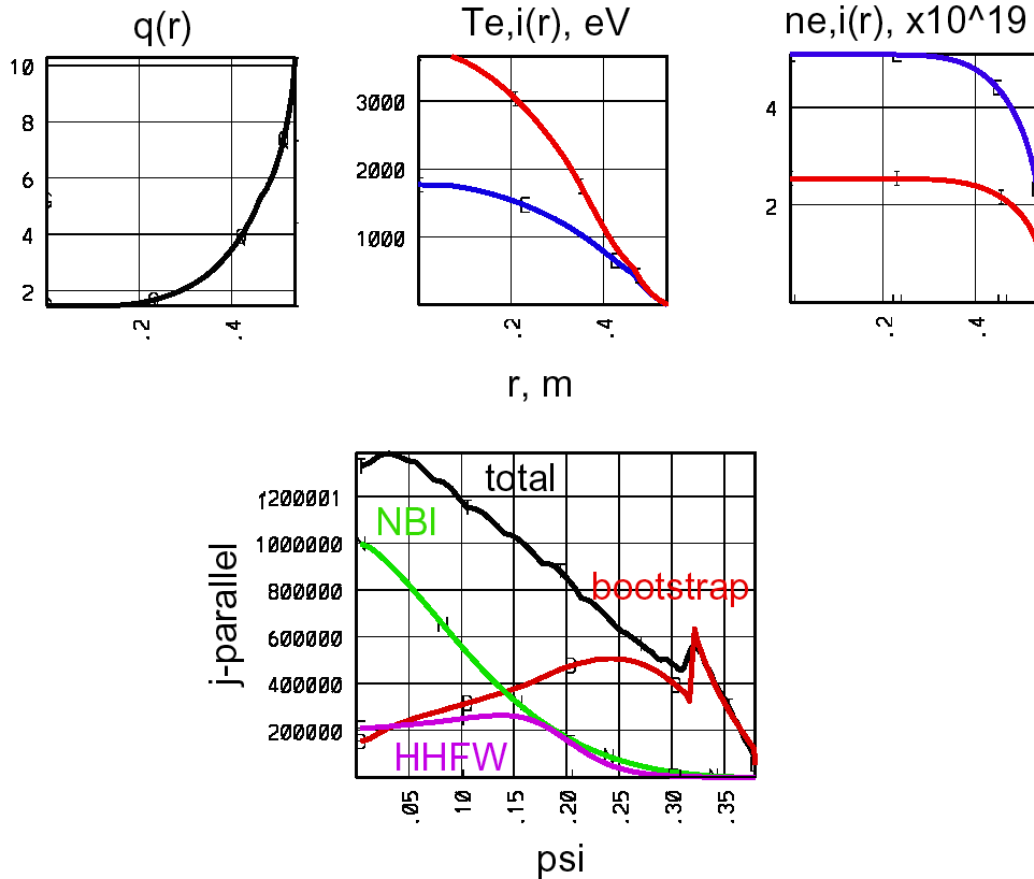


Figure 4.3. The safety factor, temperatures, and density profiles as a function of minor radius, and parallel current density profiles as a function of poloidal flux during flat-top, for the high elongation simulation shown above.

An example of stand-alone analysis done for NSTX involves using CURRAY to determine the driven current and its profile, and the split between electron and ion heating over a range of plasma densities, temperatures, T_i/T_e ratios, peak to average densities and temperatures, and impurity concentrations. This is determined using a series of k-parallel that represent launched spectra with particular antenna phasing. The analysis is used to determine discharge parameters that are optimum for HHFW current drive efficiency. Ultimately, this will provide a lookup table for use in TSC or TRANSP

dynamic evolutions where the plasma parameters vary significantly over the discharge. Efforts are also underway to integrate CURRAY into TRANSP.

Although many simulations involve constraining the transport coefficients to those of a particular experimental shot, both TRANSP and TSC have the GLF23 and MMM95, as well as L-mode and neoclassical, theory based transport models available, which are widely used in predicting tokamak behavior. Their applicability to NSTX at low aspect ratio is of particular interest and will be pursued.

The long term planning for NSTX integrated scenario modeling involves a sequence of goals aligned with the experimental milestones. These include the following, which have a number of questions to be answered by simulations and experiment as they proceed;

- 100% non-inductive discharges for $t_{\text{flattop}} > \tau_{\text{skin}}$, in vicinity of no wall β limit, utilizing NBI and HHFW CD
 - What f_{bs} is achievable
 - Can HHFW provide significant contribution
 - How will NBI contribute as Z_{eff} is lowered
 - Plasma elongation benefits
 - What are $\beta_{\text{N}}/\text{HH}$ requirements
 - Quasi-stationary current profiles
- $\beta \approx 30\%$, with $\beta_{\text{N}} \approx 6.5$ and $\text{HH} \approx 1.2$ for $t_{\text{flattop}} \gg \tau_{\text{E}}$
 - Can configuration near/above no-wall β limit be sustained
 - Can confinement improvement be sustained
 - Obtain glimpse of bootstrap current profile even though unrelaxed
 - Examine inductive current evolution to optimize future non-inductive scenarios
- $\beta \approx 40\%$, with $\beta_{\text{N}} \approx 8.0$ and $\text{HH} \approx 1.5$ for $t_{\text{flattop}} \gg \tau_{\text{skin}}$, with $f_{\text{bs}} \geq 70\%$
 - RWM stabilization by rotation and/or active feedback
 - Quasi-stationary current profile with 100% non-inductive current
 - Resulting bootstrap current profile

- What contributions from HHFW and NBI are obtained/required
- Plasma elongation benefits
- Non-solenoidal rampup tending to no-OH startup and rampup
 - Vertical field versus heating/CD required in rampup
 - Transition from early OH-blip to non-OH rampup
 - Elimination of OH-blip, CHI and/or vertical field-blip
 - Transition from no-OH breakdown to no-OH rampup
 - Time-scales and ability to integrate with high performance plasmas

Overall the integrated scenario modeling effort on NSTX will evolve with progress in physics and computations, that meet the needs of low aspect ratio exploration. The integrated scenario modeling for NSTX will greatly benefit from the SciDac supported numerical simulation of fundamental plasma processes, the continued expansion of the NTCC (National Transport Code Collaboratory) collection of portable physics modules, and the recent Advanced Computing Integrated Simulation Initiative to support integrated modeling code development in fusion sciences.

5. Theory and Modeling

5.1 Introduction

The theory and modeling plan for NSTX is based on; meeting the near-term research goals of the NSTX program; advancing the understanding of the physics of spherical torii; and addressing the longer term IPPA goal to determine the attractiveness of an ST as a reactor. Many of the theoretical challenges of spherical torii are related to their geometry: reduced aspect-ratio and increased elongation; and the relatively weaker toroidal field. In addition to these issues, NSTX also has significant NBI-induced rotation, which affects both equilibrium and stability. These challenges are reflected in all areas of plasma science: equilibrium; micro- and macro-stability, turbulence and transport; boundary physics; RF-heating and current drive; and, energetic particle effects. Some of these challenges require new theoretical models and some of them represent a greater burden on the numerical techniques, as codes have to be modified and tested.

The physics of STs are not merely extensions of the conventional aspect-ratio physics, there are some regimes where ST parameters are unique and inaccessible to conventional aspect ratio tokamaks. In particular we note that in STs the Larmor radius for both thermal and fast particles are significantly greater than in tokamaks. This has implications for theories and codes which rely on Larmor radius expansion methods. The high- β results in large Shafranov shifts and requires inclusion of electromagnetic effects in transport analysis. The high trapped-particle fraction challenges the validity of fluid treatment of electrons. The large flow and flow-shear affects micro-stability characteristics and the supra-alfvenic fast ions can drive alfven modes unstable. We discuss these issues in greater detail in the following sections.

5.2 Macroscopic theory

The MHD behavior of STs is dominated by the relatively low toroidal field and strong poloidal mode coupling due to toroidal effects. The low aspect-ratio also leads naturally to high elongation as well as high magnetic shear near the edge. There are large Shafranov shifts, even at low β and the sound speed is comparable to the Alfvén velocity. In the presence of NBI the plasma flow velocity is a finite fraction of the sound speed and has a Mach number ~ 0.5 with high velocity shear. The challenge of the large sound speeds and flow velocities and shear play is in determining the equilibrium configuration and its stability. Conventional methods of solving the single-fluid Grad-Shafranov equation break down as the equation becomes hyperbolic and two-fluid descriptions are required to describe the plasma. Analysis of stability becomes more difficult due to the additional energy from flow, which could serve as a new source for instabilities. On the other hand if the flow is non-uniform, high flow shear can be stabilizing and may also play a role in neutralizing the strong poloidal mode coupling. Assessment of NTM stability requires calculation of Δ' , the ideal Mercier criterion index. The strong poloidal mode coupling in NSTX makes this a greater challenge.

Rotation plays an important role in determining the MHD behavior of NSTX. It plays a role in the stability of the Resistive Wall Mode, RWM, which must be stabilized to achieve the high-beta regime of interest. Sheared rotation is expected to determine the coupling of tearing modes, resistive and neo-classical, with external error fields. Rotation can even affect the growth of the NTM through the polarization current term and has been shown to even reduce the growth of the ideal $m=n=1$ instability. Consequently an important thrust for theory and modeling in the macroscopic stability topical area is to include rotation at all levels of equilibrium modeling and stability analysis.

Resistive wall mode theory is routinely used for determining wall-boundary and rotation thresholds, however the dissipation mechanism responsible for slowing the rotation needs to be understood. This might also play a role in suppressing reconnection in tearing mode growth. The physics of dissipation also requires a kinetic description.

Proposed research activities in MHD

- 1) Equilibria including flows will be determined using several different physics models; MHD, two-fluids, and hybrid particle/fluid models.
 - a. Development and application of FLOW an ideal MHD equilibrium code with the capability of including sheared toroidal and poloidal flow as well as anisotropic pressure profiles including free boundary equilibrium. (2003-2004)
 - b. Development and application of M3D, a full non-linear resistive MHD code. (2003-2005)
 - c. Development and application of HYM, a full non-linear two-fluid model (2003-2006)
- 2) Linear stability studies with flow.
 - a. Extension of the VALEN code, a coupled wall-plasma model, to include flow and multi-mode coupling. (2003-2006)
 - b. Application of the MARS code (2003-2004)
 - c. Assessment of the role of rotation on the NTM, through the polarization term in the modified Rutherford equation. This will require calculation of Δ' . (2003-2004)
 - d. Computation of Δ' in realistic NSTX equilibria, including high- β regimes. (2003-2004)
 - e. Assessment of rotation on linear stability of the $m=1$ mode. This affects sawteeth as well as internal mode stability at high- β .(2003-2004)
 - f. Development and application of NOVA-F, a non-variational MHD stability code based on the NOVA series of codes. (2004-2006)
- 3) Non-linear MHD
 - a. Develop an understanding of the dissipative mechanism that governs the interaction of MHD modes with flow. (2003-2007)
 - b. Develop understanding of internal reconnection events. (2003-2008)

- c. Develop understanding of coupling of error fields to plasmas, stationary, PIES, and with flow, M3D. (2004-2008)
- 4) Performance improvements
- a. Assist in feedback stabilization of RWMs (2003-2008)
 - b. Profile optimization analysis in high-beta regimes (2003-2008)
 - c. Determine parametric stability boundaries. (2003-2008)
 - d. Examine real time stability analysis using stability database and/or fast analysis techniques. (2004-2008)

5.3 Core Confinement, Transport and Turbulence

An important feature of STs is that the toroidal magnetic field is approximately only one-tenth of that in conventional aspect ratio devices. This has several ramifications. The first is the high value of local β_t , which can approach unity in the plasma core. The second is the relatively large gyro-radius of both energetic and thermal ions, with $\rho_{\text{fast}}/a \sim 1/5 - 1/3$, and $\rho_{\text{I,th}} \sim$ a few cms near the plasma periphery. Lastly, the relatively low toroidal field leads to large ExB rotation speeds ($M \sim 0.5$) and related velocity shear. In addition to these effects, the low aspect ratio geometry leads to large trapped particle populations.

These ST features present challenges to the present treatment of both neoclassical and turbulent-induced transport. For instance, the high local values of β_t , reaching above 70% as determined from experimental measurements, implies that a full electromagnetic treatment of turbulence is necessary. Even the thermal ion gyro-radius may be comparable to typical plasma scale lengths (e.g., L_p , L_n , L_T) near the plasma edge, bringing into question the validity of the spatial scale length ordering in gyro-kinetic treatments. High rotational shears, with shear rates of up to 1 MHz, can have a profound effect on micro-instability thresholds and turbulence characteristics, and it will impact the relative roles of ion and electron transport. Linear calculations indicate suppression of ITG modes and the dominance of ETG modes, but non-linear calculations are needed in order to assess the expected levels of transport from these modes. Although, there is only

weak evidences for ETG modes in tokamaks, NSTX is one of the best places to test for the existence or absence of ETG modes.

Finally, the large trapped particle fraction, which approaches unity near the plasma edge, challenges the conventional fluid treatment of electrons.

The main tools are: gyro-kinetic linear and non-linear micro-stability and turbulence analysis codes, such as GS2, GTC and GYRO and interpretive transport analysis codes such as TRANSP.

Proposed research activities in Transport and turbulence

- 1) Analysis with experimental profiles to help interpret observed trends. Support of collisionality-scan experiments: GK calculations of transport over a wide range of collisionalities, using NSTX profiles obtained in beta scan. (FY 03-04)
- 2) NSTX transport mechanism identification preparation. Study whether turbulence-driven and collisionally dominated plasmas have different dependencies on T_e/T_i , n_e and n_i that can be distinguished in an experiment? (FY 03+)
- 3) Similar variations to determine dependence of neoclassical fluxes on background profile changes. (FY 03+)
- 4) Identify the most favorable plasma conditions for measurements of short wavelength fluctuations which could be related to ETG turbulence, predict the density fluctuation amplitude and (k, ω) -spectra from nonlinear gyrokinetic simulations. (FY 03-04)
- 5) Non-linear simulations using GS2. This will complement the linear analysis that has already been done. (FY 03+)
- 6) H-mode pedestal widths. Are observed widths consistent with any particular H-mode pedestal predictions? (FY 03+)
- 7) Development of a model for treating electromagnetic electrons. (FY 03)
- 8) Turn on and off electromagnetic effects and see if temperature dependencies of fluxes change (FY 04+)
- 9) Initiate modeling effort using GF, GK codes to develop the physics picture of plasma dynamics observed with $t \gg \tau_E$. Use or begin to develop tools appropriate for

study of transport dynamics (time-evolving kinetic profiles, in preparation of predictive capability). (FY 04-05)

- 10) Gyrokinetic calculation of fluctuation spectrum and turbulence-induced transport for NSTX, with and without “DC” electric field shear, for same 25% beta case (Mach 0 , Mach 1), when electromagnetic effects are able to be included. (FY 04+)
- 11) Identification of regions in k space most likely to be affected by flow shear, and portions of k spectra most responsible for transport. (FY 04)
- 12) Visualization of turbulence characteristics to compare with fluctuation diagnostics on NSTX. (FY 04)
- 13) Assessment of neoclassical transport in the large rho/Ln and Bpol/Btor regime. (FY 04-05)
- 14) Self-consistently predict NSTX pressure profile dynamics, using dynamic transport model, calculations of bootstrap current, local stability analysis, and comparison with experiments, in conjunction with TRANSP. (FY 06-08)
- 15) Transport control tool development: Using measured profiles, if fluctuation-induced transport dominates, estimate requirements for developing flow shear externally (e.g. with RF) to reduce or suppress turbulence. (FY 06-08)
- 16) Simulate in-out asymmetry of turbulence and associated transport which is expected to be even more pronounced in NSTX than in conventional tokamaks. Study its implications for H-mode transition. (FY 05-06)
- 17) Include kinetic effects and rotation profiles in gyro-kinetic calculations. (FY 05-08)

5.4 Solenoid-free plasma startup

Because of the limited inductive flux that can be provided by the inherently slim center stack, a major challenge for the success of STs as a fusion device is the requirement to generate and sustain toroidal current non-inductively. The NSTX program includes coaxial helicity injection as a method for achieving this goal. The method requires a pair of biased electrodes which can carry a current in the poloidal direction. The presence of the toroidal field results in current flowing along helical magnetic field lines connecting the lower divertor plates. The ratio of the applied toroidal field to the poloidal field causes

the current in the plasma to develop a strong toroidal component, the beginning of the desired toroidal plasma current. The CHI method drives current initially on open field lines creating a current density profile that is hollow. In a continuously driven system (i.e., steady state CHI), Taylor relaxation [Taylor, J.B., Rev. Mod. Phys. 28, (1986) 243] predicts a flattening of this current profile through a process of magnetic reconnection leading to current being driven throughout the volume, including closed field lines. For plasma startup and sustainment using this

scenario, current penetration to the interior is eventually needed for usefully coupling CHI to other current drive methods and to provide CHI produced sustained current during the long pulse non-inductive phase. Smaller machines have observed a non axisymmetric $n=1$ toroidal mode which is deemed necessary to provide flux closure[Nelson, B.A., et al., Phys. Plasmas 2 (1995) 2337. Nagata, M., et al., 17th IAEA Fusion Energy Conference, Yokohama, IAEA-CN 69/EXP4/10 (1998). Browning, P.K., et al., Phys. Rev. Lett. 68 (1992) 1722. Jarboe, T.R., et al, 17th IAEA Fusion Energy Conference, Yokohama, IAEA-CN 69/PDP/02 (1998).]. Assessment of flux closure in driven systems needs both experimental and theoretical tools. Theoretical tools include equilibrium reconstruction and discharge simulation codes to understand experimental data and MHD codes to understand the physics of closed flux generation. To date, good progress has been made in using the ESC (equilibrium and stability code) with capability for inclusion of current on open field lines and in the private flux region to reconstruct experimental NSTX CHI data [Zakharov, L and Pletzer, A, Physics of Plasmas 6, 4693 (1999)]. These features have also been included in the EFIT code [Lao, L.L., St. John, H., Stambaugh, R.D., Nucl. Fusion 25, 1611 (1985)]. The 3D MHD code, CHIP, developed by X. Tang of LANL, is being used to understand CHI reconnection physics. The code has been used to model CHI processes in a simple geometry. Implementation of the actual NSTX geometry will allow for a closer comparison of the simulation results with the experimental results, and help guide and understand the experiments.

Recently, a new method (known as transient CHI startup) was successfully used on the HIT-II experiment to demonstrate plasma startup using CHI. Because of this, the plasma startup and sustainment objectives on NSTX are being decoupled. Next step plasma

startup experiments on NSTX will use the transient CHI method that does not rely on non-axisymmetric modes for closed flux generation. Closed flux generation can be unambiguously demonstrated by the persistence of toroidal current after the CHI injector current has been reduced to zero. This new work considerably narrows the scope of the TSC code [Jardin, S.C., Pomphrey, N., DeLucia, J., Journal of Computational Physics 66, 481 (1986)] which will now be used specifically to develop transient startup scenarios for NSTX. Understanding steady-state CHI discharges, as described in the previous paragraph, is needed to establish the role of CHI for providing some edge current drive during full non-inductive operation and because it may have the potential for much higher initial plasma startup currents.

Proposed research activities in CHI

- 1) Modeling the experiment needs equilibrium codes with current on open field lines, (2003---)
 - a. EFIT
 - b. ESC
- 2) Modeling the evolution of the discharge and optimizing control
 - a. TSC(2003-2005)
 - b. CHIP -2D- current multiplication (2004-2008) Funding
- 3) Flux closure and reconnection (2004-2008)
 - a. CHIP – 3D – flux closure Funding
 - b. M3D
- 4) Feedback control in the presence of large asymmetric currents. TSC. (2004-2008)

5.5 Fast particle effects

In STs the low field and high density imply that the Alfvén speed is low, and fast particles due to NBI are generally super-Alfvénic with velocities of 2 to 4 times the Alfvén speed. This allows for resonance between fast ions and the various Alfvén

eigenmodes, while the pressure gradient in real and velocity space provides a source for driving various Alfvénic waves, including TAEs, toroidal Alfvén eigenmodes, EPMs, energetic particle modes and fishbones, as well as CAEs, compressional Alfvén eigenmodes.

The sub-cyclotron frequency modes observed in NSTX and identified as CAEs, have both a toroidal field dependence of their frequency, as well as a

density dependence. These modes are observed as a broad spectrum roughly equally spaced over a wide frequency range, $0.2 < \omega_{ci} < 1$, Fig 7. The multi-mode excitation observed in this figure introduces the problem of particle diffusion in real and velocity space in the presence of many mode resonances with fast ions as well as with the background ions. Both linear and nonlinear numerical modeling of such "Alfvén modes turbulence" needs to be addressed. Modeling of energetic particle interactions in STs poses new challenges to the traditional methods employed in tokamaks. Some of the additional issues that need to be addressed are: the need to keep compressional modes with ω/ω_c corrections in both MHD and kinetic codes; large Larmor radii; high-q and strong poloidal mode coupling; inadequacy of ballooning approximations requiring full geometry representation, strong anisotropy of plasma pressure and anisotropy of beam ion distribution function in velocity space. For example the CAEs are predicted to be strongly poloidally localized, while adding more poloidal harmonics into the calculations introduces an interaction with the shear Alfvén continuum in MHD codes. Resolution of such continuum damping needs kinetic effects and a fine mesh near the resonance surface in numerical codes. The ultimate challenge is to have the capability to model the non-linear consequence of these interactions self-consistently.

In addition to collective effects the confinement of fast beam ions is characterized by their large Larmor radius and large drift orbit radial width. New effects emerge from this, such as non-conservation of the adiabatic invariant μ , which has jumps in magnitude when the ion passes the equatorial plane on the low field side of the plasma. If enhanced by the bounce resonances this effect results in stochastic fast ion diffusion. This depends on the ratio of the Larmor radius to the magnetic field scale length and on the collisional scattering frequency. The large Larmor radius in NSTX make it necessary to use

numerical tools for adequate modeling of prompt ion losses. Strong electric field due to co-injection of beams needs to be properly included to interpret the measurements of particle losses at the edge

Proposed research activities in Fast Particle Effects

1) Low frequency codes

- a) Development and application of NOVA2 for assessment of non-perturbative Alfvén mode excitation. (2003-2004)
- b) Development and application of HINST for analysis of KBM and RTAE with full kinetic and non-perturbative treatment. (2004-2005)
- c) Development and application of nonlinear HYM a hybrid two-fluid plasma and gyro-kinetic fast ion δF code. (2003-2008)
- d) Development and application of nonlinear M3D as a two-fluid δF code. (2003-2005)
- e) Development and application of the Monte-Carlo ORBIT code with several fishbone dispersion relations. Bounce frequency fishbones (2003-2004)

2) High frequency codes.

- a) Need a global linear code with ω/ω_c corrections to MHD such as NOVA. (2005-2008)
- b) Need to have the capability of treating arbitrary beam-ion distributions in HYM. (2004-2005)
- c) Need to have the capability to treat fast particle resonances non-perturbatively. (2005-2008)
- d) Development and application of non-linear version of HYM to self-consistently model CAEs and GAEs. (2006-2008)

3) Particle confinement codes

- a) Change EIGOL code to model local fast ion losses into the loss ion detector. (2003-2004)
 - b) Develop model scattering frequency due to μ nonconservation basing on numerical and analytical study of such effect. (2004-2005)
- 4) Benchmarking (2003-2008) Ongoing

5.6 Radio-frequency-wave heating and current drive

The theory and modeling of radio frequency (RF) wave heating and current drive in a spherical torus is more challenging than in a conventional aspect ratio tokamak. The fundamental problem is that the ion Larmor radius, the ion banana width, the perpendicular wavelength, and the spatial separation of the ion cyclotron harmonic layers can be comparable, particularly for high energy particles. Furthermore, because of the inherently high beta and high dielectric constant in these devices, direct electron absorption of the waves via transit time magnetic pumping can be comparable to or greater than direct ion absorption via cyclotron damping. Consequently, many of the approximations and models used with conventional tokamaks may be inappropriate for RF wave dynamics in an ST plasma.

The unique features of an ST plasma affect all aspects of RF wave dynamics. In an ST plasma, the poloidal magnetic field is much larger relative to the toroidal magnetic field than in a conventional aspect ratio tokamak. The correspondingly larger tilt of the total magnetic field lines in the edge regions can modify the spectrum of waves that can be excited in the plasma by the launcher. In the core of the plasma, the larger shear in the magnetic field can modify the evolution of the local parallel wave number, thereby affecting wave penetration and absorption characteristics. In the highest beta ST discharges when an internal magnetic well is formed, the presence of a reversed magnetic field gradient at the outer edges of the plasma may affect wave accessibility and absorption profiles. Both ray tracing and full wave codes may be used for modeling

heating and current drive scenarios that utilize fast magnetosonic waves at high harmonics (HHFW) of the fundamental ion cyclotron frequency.

Though the wavelengths in this regime are sufficiently small relative to the equilibrium gradient scale lengths to justify a WKB assumption, ray tracing models can miss important 2D wave coherence effects and are not able to treat mode conversion phenomena, which may be significant at lower cyclotron harmonics. Two dimensional full wave codes exist which do not utilize a Finite Larmor Radius (FLR) assumption. However, these codes are sufficiently computationally intensive that they are impractical to use for the analysis of large number of ST discharges. Other 2D full wave models exist which use simplifying assumptions to reduce the computation time required. However, the accuracy of these simplified models has not been validated and may require the inclusion of many poloidal Fourier harmonics for proper convergence.

Finally, the HHFW systems are often used in conjunction with neutral beam injection. Experimental observations indicate that the fast ions can interact strongly with HHFW, leading to significant modifications of the fast ion velocity distributions as well as the partitioning of the wave power among the various plasma species. The wave codes need to be generalized to include effects of non-Maxwellian populations on wave propagation and absorption. Non-linear effects on the wave absorption which may arise due to overlap of the cyclotron layers for high energy particles need to be assessed. Self-consistent Fokker-Planck models need to be developed that include quasilinear diffusion at high cyclotron harmonics in an ST equilibrium. These Fokker-Planck models are also needed to assess HHFW non-inductive current drive efficiencies, including particle trapping, effects in an ST geometry.

Proposed research activities in RF heating and Current Drive

1. HHFW

- a) Develop comprehensive model of HHFW- Fast ion interaction
–time dependent, finite orbit and loss cones in CQL3D, self-consistent distribution

time-independent + loss cones in CQL3D FY2003

add finite orbit in FY2004

time-dependent by coupling to TRANSP starting in FY2004

–resonance overlap

beginning in FY2003

b) Develop comprehensive model of HHFW- Current drive

–incorporate in TRANSP – CURRAY(2003+)

–2D Fokker-Planck vs adjoint method CQL3D vs CURRAY/adjoint starting in FY 2003

–DC electric field (2004 +)

–electron transport effects (2003 +)

c) Effect of MHD on CD efficiency

2. EBW

a. Realistic antenna and refraction at mode conversion, multi-ray, non-linear effects

b. Target equilibria, kinetic profiles – antenna design (2003 +)

c. CD requirements for NTM suppression (2003-2004)

d. Parallelise GENRAY/CQL3D for scoping studies, launch angle, $n_{||}$, frequency(2003+)

e. effect of transport and bootstrap current(2004-2005)

f. edge parametric instabilities at high RF power(2004-2005)

g. Relativistic effects needed? (if needed)

5.7 Plasma-Boundary interaction

STs are often designed as high power density devices, and heating of targets can limit pulse lengths in some scenarios. For example, the peak heat flux in a diverted H-mode discharge in NSTX with 4.5 MW NBI power was measured to be $\sim 10 \text{ MW/m}^2$. At this level a 3 sec. pulse length would exceed the NSTX administrative limit. Accurate interpretation of such data and extrapolation with standard analysis codes is critical to assessment of the ST concept. Plasma boundary interactions play a critical role in H-mode transitions. Determining a model for the H-mode power threshold is a pre-requisite for assessing the ST concept. H-mode power threshold theories generally do not include

trapped-particle effects properly. Typically the equations are linearized and expanded in inverse aspect ratio, ϵ , which runs counter to the ST regime. Work to generalize those models will be needed. Another area which merits further study is the role of fueling on H-modes. Here two important areas of investigation are the toroidal viscosity, and the charge exchange loss. Interpretation of edge measurements is typically done with a 2D fluid model, such as UEDGE, and/or a neutral transport code, e.g. DEGAS-2. The unique magnetic topology in STs, however, may necessitate kinetic theory corrections to standard fluid models. First, STs can have a high mirror ratio approaching 4 in the scrape-off layer (SOL), particularly in high triangularity discharges. This mirror ratio leads to a high trapped particle fraction ($\sim 90\%$) and a change in the velocity-space loss cone. Trapped ions can experience an effective connection length much longer than the physical (rather short) connection length, allowing those ions more time to lose energy before striking and heating the target plate. A second challenge to interpretation and extrapolation of measurements is to have an accurate reconstruction of the separatrix because its radial location largely determines the power flux into the SOL. As in the MHD area, however, the high edge flow speed measured in some NSTX discharges leads to uncertainty about the equilibrium reconstruction technique, which ignores flow speed. Practically, the existing edge data will be modeled with fluid plasma and neutral transport codes, and the large number of free parameters in these codes almost assure a reasonable match between data and model. The challenge is to independently use kinetic models of the SOL to estimate the magnitude of kinetic effects, and then devise diagnostic techniques to measure those effects. If these effects are confirmed to be important, then kinetic theory ‘patches’ may be applied to the fluid models, for example with the use of free-streaming limit multipliers on parallel transport. The issue of separatrix location is complicated by the relatively large ion poloidal gyro-radius $\sim 0.5\text{cm}$ in many NSTX H-mode discharges, which could lead to an ambiguous distinction between the closed and open field lines.

Proposed research activities in Plasma-Boundary Interactions

1. Transport modeling of gas puff turbulence imaging experiments will be carried out with the DEGAS 2 code. The simulations will attempt to explain, qualitatively, the differences between the emission patterns observed in H-mode and L-mode. (2003→)

2. UEDGE - plasma boundary (2003-2005)
 - Code ready for benchmarking – diagnostics – particle fluxes
3. Experimental results will be compared to predictions from BOUT (non-linear) edge turbulence codes. (2003-)
4. Kinetic effects in edge codes
5. High fraction of trapped particles on outboard – high poloidal mirror ratio (2003-2004)
6. Experimental results will be compared to predictions from BAL (linear) (2004-manpower)
7. BOUT 3D EM turbulent transport uses UEDGE compare with exp. (2005-2008)
8. GYRO - core-edge transport. (Manpower)
9. H-mode pedestal widths. Are observed widths consistent with any particular H-mode pedestal predictions? (2005-2008 diagnostics)
10. ELITE – ELMs – intermediate-n (2005-2008 Diagnostic dependent)
11. Understanding the observed difference between the inboard and outboard density pedestal heights, possible role of local B-fields.
 - (Model needed including compression and rotation effects)
12. Kinetic effects in edge codes (Codes needed)
 - Connection length, may govern impurity transport

6. *NSTX and ST Next-Steps in Fusion Energy Science*

NSTX will advance the scientific basis for cost-effective ST Performance Extension and Fusion Energy Development (component testing) devices based on the attractive ST regime of high beta and strong toroidicity and contribute to improving the next-step tokamak burning plasma experiment, to establish the scientific and technological bases for an optimized DEMO.

6.1 *ST Contributions in an Updated Plan for the Development of Fusion Energy*

The Fusion Energy Sciences Advisory Committee (FESAC) of USDOE is currently formulating an updated plan for the development of fusion energy, and specifically for the deployment of a fusion demonstration power plant (DEMO) producing net electricity within approximately 35 years [6.1]. The Magnetic Fusion Energy (MFE) path of the plan foresees a succession of major facilities to address the scientific and technological challenges of Fusion Energy, covering the program elements of configuration optimization, burning plasma, and component testing (see figure 6-1).

An important goal for NSTX research is therefore to establish the scientific basis for a next-step Performance Extension experiment (such as the Next-Step Spherical Torus, NSST [6.2]) for configuration optimization, which in turn will provide the scientific database needed by an ST-based Component Test Facility (CTF) [6.3]. This goal is in agreement with the IPPA MFE program Goal 2, which states that configuration optimization research should “Resolve outstanding scientific issues and establish reduced-cost paths to more attractive fusion energy systems by investigating a broad range of innovative magnetic confinement configurations.” The ST is among the leading innovative concepts for configuration optimization.

The burning plasma tests are expected to be carried out in ITER [6.4] or FIRE [6.5]. The International Tokamak Physics Activity (ITPA) has been organized to coordinate the establishment of additional database for physics optimization of the burning plasma. A secondary goal for NSTX research is therefore to extend the toroidal physics basis to higher beta and stronger toroidicity (i.e., lower aspect ratio), and thereby to contribute to an improved optimization of the burning plasma experiment.

More defined ← → Less defined

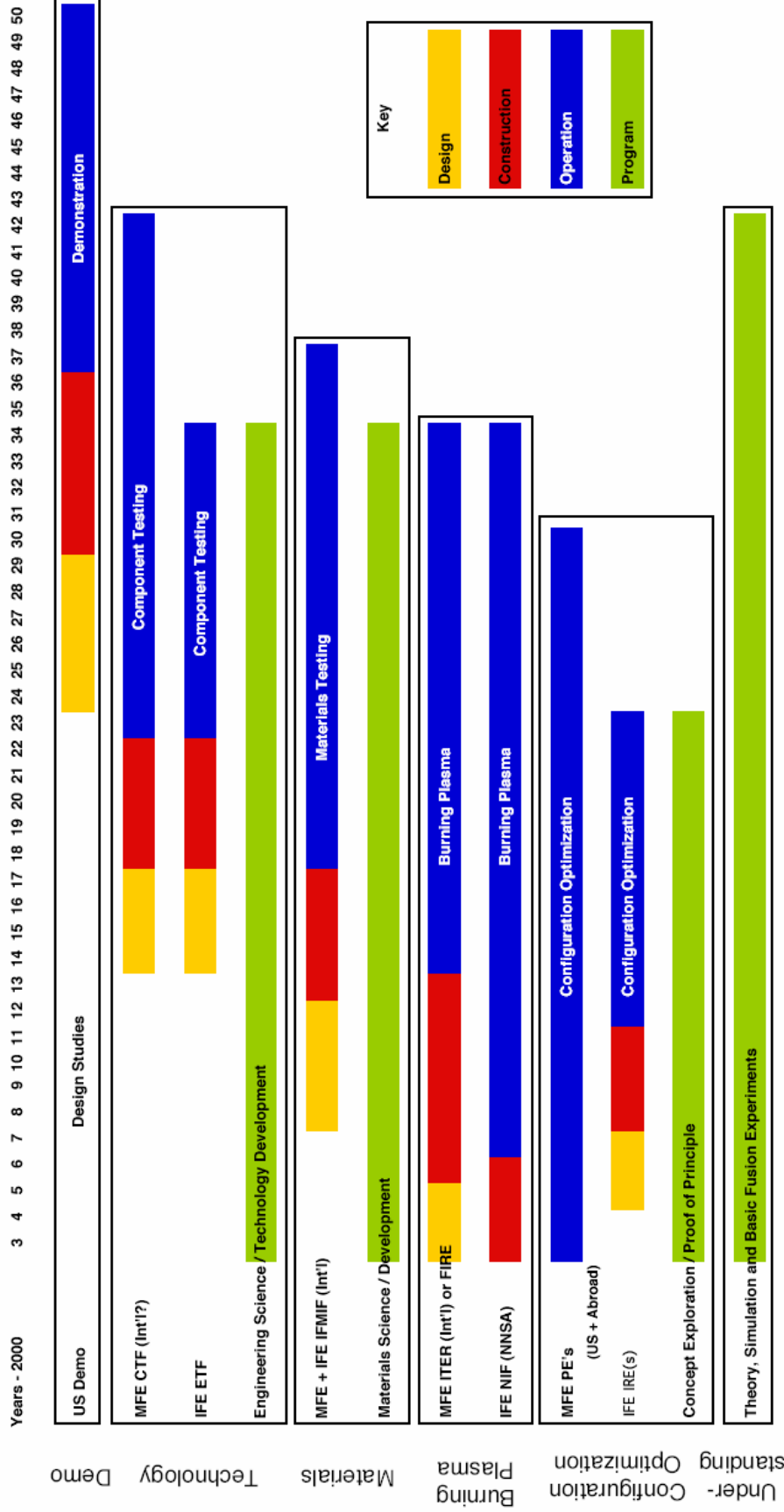


Figure 6-1: Illustrative programs and major facilities that comprise the updated fusion development plan being formulated by the FESAC Panel on Development Path (expected to be finalized in March 2003). NSTX research can make potentially critical contributions to the MFE Configuration Optimization and Component Testing.

Successful implementation of this MFE development strategy will establish the scientific and technological bases for an optimized DEMO and presage the demonstration of net electricity production in approximately 35 years (see Figure 6-2).

The design concepts for NSST and CTF are presently being explored, utilizing the latest physics results from ST research and the latest concepts for ST-based Volume Neutron Source (VNS) [6.6] and Power Plant [6.7, 6.8]. These efforts are also in preparation for the achievement of a 10-year objective of the IPPA MFE program Goal 3: “Assess potential of Spherical Torus as a basis for burning plasma studies and/or fusion-nuclear component testing.” In the case of NSST, a full solenoid may be included to provide flexibility in operating conditions for physics investigations. Multi-turn insulated TF and the solenoid coils can be used since only modest neutron fluence may be anticipated in NSST. Economy can be realized by matching the device to the existing TFTR facility. In the case of CTF, the requirements [6.9] for high fusion neutron fluence (up to 6 MW-yr/m² over >10 m² test area for the life of device) and availability (ultimately 30%) dictate that attractive ST-reactor-relevant features must be incorporated. These features include a single-turn center leg for the TF coils, elimination of the inboard solenoid coil, and straight-line remote access for all fusion core components such as power blankets, divertors, and the TF center leg in order to minimize time for component replacement. Equally important will be to maximize the Tritium breeding fraction to minimize the net consumption of Tritium while delivering the required CTF performance. These features will further require a strong emphasis on the physics basis for solenoid-free operation in NSTX research, and the subsequent extension of this emphasis to NSST research.

The initial assessments show designs for these next-step ST experiments that are compact and as a result cost-effective. Table 6-1 provides the key parameters in contrast with parameters for NSTX and future ST power plant concepts. Aside from the differences in fusion power, the NSST and CTF parameters are chosen to be similar to enable a strong emphasis in CTF on the technological mission of component testing.

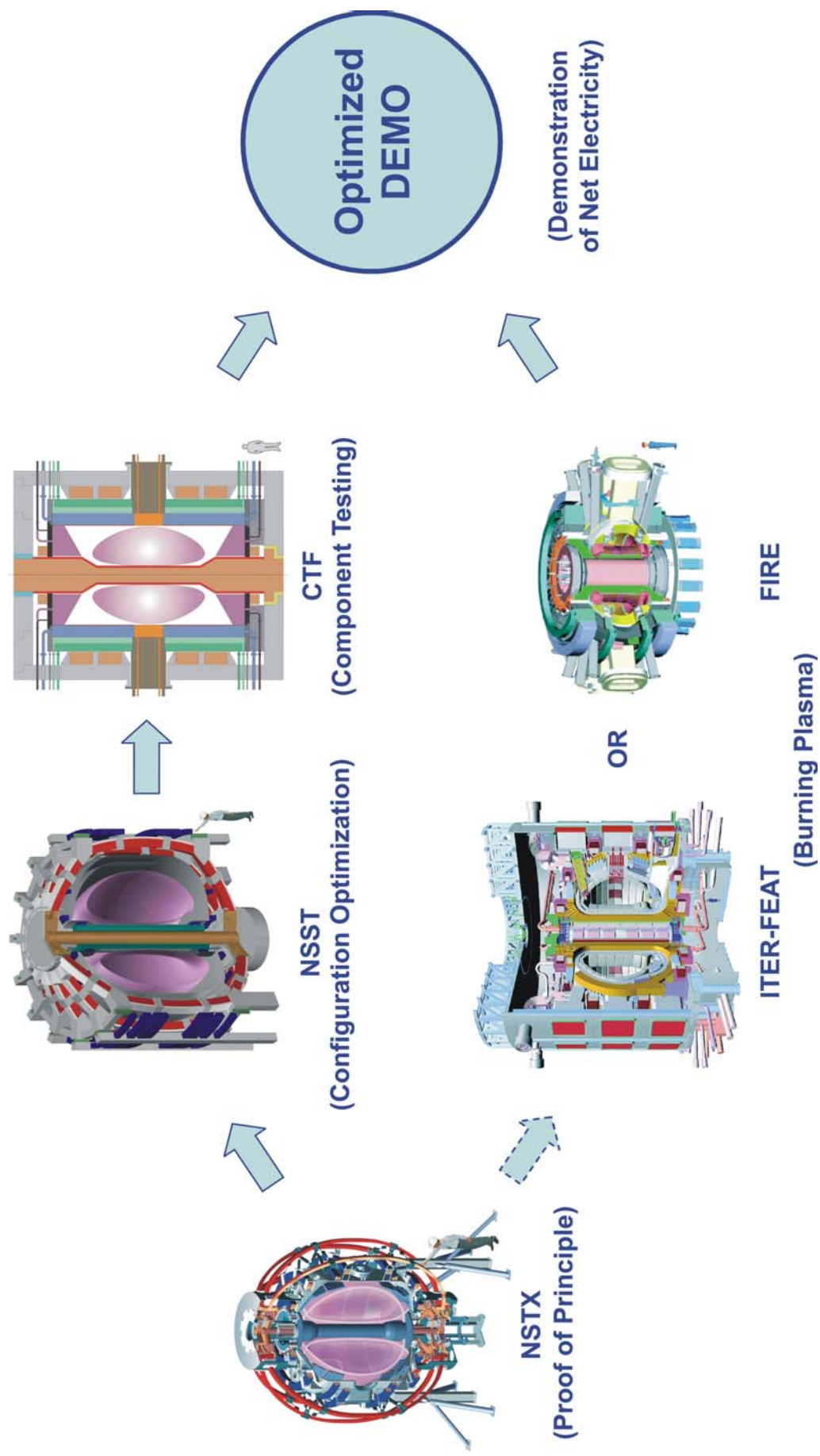


Figure 6-2: NSTX research will provide physics database crucial to the optimization of NSST and CTF, and contribute to the improvements of tokamak burning plasma experiment.

Table 6-1: Initial concepts parameters for NSST and CTF, in contrast with NSTX and possible future ST power plants

	NSTX	NSST	CTF	Power Plant
Major radius, R_0 (m)	0.85	1.5	~1.5	~3
Aspect ratio, A	≥ 1.3	1.6	~1.5	~1.4 – 1.6
Nominal elongation, κ	2	2.5	~3	≥ 3.4
Max triangularity, δ	0.8	0.6	~0.5	~0.5
Toroidal field at R_0 , B_T (T)	0.3 – 0.6	1.1 – 2.6	~2.5	~2
Plasma current, I_p (MA)	~1	5 – 10	~10 – 15	~30
Nominal fusion power (MW)	–	0 – 100	~100 – 500	~3000
Solenoid induction flux (Wb)	0 – 0.6	0 – 15	0	0
Pulse length (s)	5 – 1	50 – 5	Steady state	Steady state

6.2 *NSTX Contributions to NSST and CTF Concept Definition and Optimization*

Since the application of auxiliary heating in FY2001 on NSTX and MAST, ST research has progressed rapidly to the level where cost-effective next ST steps (NSST and CTF) have become intriguing possibilities for the next decades. The research planned for NSTX will be in a crucial position to shape the key physics features of these next-step experiments by addressing essential issues and to enable realistic extrapolation from the NSTX plasmas to these experiments. The key physics parameters of interest to this research have been identified and are provided in Table 6-2.

The relative increments in these parameters from NSTX to NSST to CTF and to Power Plant can be chosen to be most significant between NSTX and NSST. This ensures that new physics is most likely to be challenged for the first time in NSTX and NSST research. Measurements and successful physics modeling at these steps are therefore expected to bring high confidence to projections of the plasma conditions in CTF and Power Plant. The following provides a discussion of the relatively unique importance of the NSTX research in light of these parameter increments.

Table 6-2: Key physics parameters estimated for NSST and CTF that indicate substantial extrapolation from NSTX, together with those for NSTX and future ST power plant concepts

	NSTX	NSST	CTF	Power Plant
Internal poloidal flux (Wb)	0.5	3 – 10	5 – 8	~15
Internal inductance, l_i	0.4 – 0.8	0.25 – 0.5	~0.25	~0.13
Average temperature (keV)	~1	3 – 6	~10	~15
Nominal Greenwald density	~0.5	~0.5	~0.5	~0.5
Average toroidal beta, β_T	0.2 – 0.4	0.2 – 0.4	0.2 – 0.4	~0.5
$V_{\text{Plasma}}/V_{\text{Alfvén}}$	0.3	?	?	?
Collisionality, ν^*	0.2	0.04	~0.02	~0.02
Thermal ion minor radius, a/ρ_i	40	80 – 120	~110	~140
Beta gradient, β' (/m)	0.25 – 0.5	0.13 – 0.26	0.13 – 0.26	0.13
Flow shearing rate ($10^5/s$)	1 – 10	?	?	?
Beam ion minor radius, a/ρ_{Beam}	5	15 – 22	~22	~25
Fusion α minor radius, a/ρ_α	–	N/A – 6	~6	~10
$V_{\text{Beam}}/V_{\text{Alfvén}}$	4	1	~1.2	~1.2
$V_\alpha/V_{\text{Alfvén}}$	–	N/A – 4	~4	~4
$\omega_{pe}^2/\omega_{ce}^2$	50	50 – 20	~20	~20
P/R (MW/m), $f_{\text{rad}} = 0.5$	8	13 – 20	20 – 40	100
$\tau_{\text{pulse}}/\tau_{\text{skin}}$	~3	~10 – 0.5	∞	∞

- Solenoid-free initiation, ramp-up, and sustainment of plasma current – NSTX research on this topical area will aim to establish the physics principles for MA-level plasmas that contain only a fraction of Wb in internal poloidal flux content ($\sim\mu_0 R_0 l_i I_p$). NSTX data and modeling must therefore be advanced adequately to enable reliable projections of a 5 to 6-fold increase in plasma current and internal poloidal flux estimated for the NSST long pulse operation. Subsequently, the projections would only be about factors of 2 to CTF and then to Power Plant, with increased confidence. The range of internal inductance (l_i) in NSTX is expected to be a factor of 2 above that anticipated for NSST (non-inductive operation) and CTF, which in turn may be a similar factor above that anticipated for Power Plant.
- Stability limits – The plasma toroidal betas relative to the MHD limits and plasma densities normalized to the Greenwald limit are expected to remain in the same range for these ST

steps. This points to the unique relative importance of NSTX research in stability limits, the shaping-dependence of which is believed to be relative well understood. However, the large Alfvén Mach number ($V_{\text{Plasma}}/V_{\text{Alfvén}}$) in NSTX has already exhibited measurable effects on plasma equilibrium and stability. NSTX data and modeling on this topic must therefore be advanced to enable reliable projections to NSST and CTF. The physics that dictates the projections of $V_{\text{Plasma}}/V_{\text{Alfvé}}$ to larger ST devices is therefore a critical topic of NSTX research. On the other hand, the stability limit and the ELM bursts of the H-mode pedestal plasma in ST is expected to depend strongly on the plasma shaping (κ and δ) at the pedestal, as suggested by recent tokamak investigations. NSTX research will have the first opportunities to investigate the effects of strong toroidicity, as a form of global shaping of the plasma, on the pedestal stability limit, for direct applications to NSST and CTF. Further, the collisionality (ν^*) at the pedestal is expected to affect strongly the stability of the pedestal by restraining of the local bootstrap current driven by the steep pedestal gradient. The effects of strong reduction in ν^* due to substantial decreases in bounce time of outboard trapped ions resulting from strong toroidicity will also be encountered in NSTX research.

- Turbulence and energy and particle transport – The key parameters of interest to this broad topical area are expected to include ν^* , a/ρ_i , β' , and the flow shearing rate. The greatest increments in the former three of these parameters (with factors of 5, 2 – 3, 2, respectively) are estimated to occur between NSTX and NSST. In addition, an in-depth understanding of plasma viscosity and momentum transport acquires a critical importance in view of the large uncertainties in this topic at present, and its importance to the stability limits. Recent measurements and modeling of the NSTX plasma suggested the strong possibility that the Ion Temperature Gradient (ITG) driven modes are likely stabilized by a combination of large flow shearing rates and large β' obtained in NSTX under tangential neutral beam heating. The desirability to extend this highly attractive confinement condition to NSST and CTF could not be over-emphasized. Further, NSTX has shown the likely ability to investigate electron and electromagnetic turbulence and transport in the absence of the ion and electrostatic turbulence and transport (or in the presence of neoclassical ion transport). NSTX research will likely be favored with the condition where only the electrons could provide, over a large portion of the plasma core, free energies for micro-instabilities that drive turbulent transport. Manipulations of the above parameters, plus magnetic shear q' etc. will afford highly coveted opportunities on NSTX to study electron energy transport with a relatively high degree of isolation. Simultaneous achievement of strongly reduced ion and

electron turbulence loss channels, and extrapolation of such results to larger ST devices is therefore of very high leverage in NSTX research.

- Energetic ion confinement and driven MHD instabilities – The key parameters of interest in this topical area are expected to be the minor radius normalized by the gyroradius of the fast ions (a/ρ_{fast}), the ratio of fast ion speed over the plasma Alfvén velocity ($V_{\text{Beam}}/V_{\text{Alfvén}}$), and the strong in-out asymmetry of the magnetic field structure. To increase confidence in extrapolation from the NSTX results, it is desirable that these parameters for neutral beam ions in NSTX (5 and 4, respectively) are similar to those for fusion α particles in NSST (inductive pulsed) and CTF (non-inductive sustained). Data and physics modeling for the fast ion effects in NSTX are thus directly applicable to the same effects in NSST and CTF. The effect of different anisotropy in the fast ion velocity distribution between beam ions and fusion α 's is a remaining topic of importance in NSTX research, to ensure reliable extrapolations to NSST and CTF.
- RF heating and current drive in over-dense plasmas – A key parameter that determines the nature of HHFW and EBW interactions with the ST plasma is the ratio $\varepsilon^2 = \omega_{\text{pe}}^2/\omega_{\text{ce}}^2$, which are in the high range of 50 – 20 for all ST devices identified in Table 6-2. NSTX research to investigate the effects of this range of ε^2 on HHFW- and EBW-plasma interactions will provide critical data for application of RF heating and current drive in NSST and CTF. A strong source in EBW power can further be applied to investigate pure RF initiation of the plasma current, in addition to current drive to ramp up the plasma current following initiation. This is a unique opportunity for ST research at the MA level, in contrast with the rapidly growing success in current initiation in tokamaks using combinations of ECW and LHW. Strong database in this area will enable critical optimization and cost savings in the NSST and CTF design concepts, at the multiple-MA to 10-MA level.
- Power and particle handling – As indicated in Table 6-2, the magnitude for the heat flux scale factor, P/R, is estimated to increase in steps of about factor of 2 from NSTX to NSST to CTF and finally to Power Plant. The large values of P/R for future ST devices are anticipated to be a great challenge, as in the case of all compact fusion devices of high performance. NSTX investigation and physics modeling in this topical area will be extended to exploratory studies of the effects of the strongly increased magnetic mirror ratio of the SOL (due to the strong toroidicity) in the case of diverted and inboard limited plasmas with varied mirror ratios. Technology innovations in plasma facing materials, such as wall coating and liquid Lithium surfaces, will likely be required to develop satisfactory solutions in combinations with the physics solutions, such as enhancing radiation from the core and divertor plasmas. Progress

in this area will ultimately determine the practical sizes and fusion neutron wall flux achievable in future ST devices, and indeed determine the economic attractiveness of fusion power based on the ST configuration. Present ST research using large heating power and varied plasma edge configurations will provide the critical information needed to take the step to the next level of ST plasmas suggested for NSST and CTF.

- Integrated high performance operation for pulse lengths far beyond the plasma skin time – It is critically important for NSTX to test plasma properties for durations much larger than (~2 – 3 times) the plasma skin time. Such plasmas need to have simultaneously high beta, good confinement, high fractions of non-inductive currents (bootstrap current combined with non-inductively driven currents from neutral beams and rf power), progressively reduced reliance on inductive current drive, and adequate power and particle handling. Measurement and physics modeling of such plasmas in NSTX will be incorporated into simulation codes to identify viable techniques and plasma operation scenarios that extend the durations of high-performance ST plasmas. Successful operating scenarios can then be extended to even larger multiples of the skin time (to about 10 or higher in NSST) at multiple-MA level. These results will provide a solid foundation for extending the techniques of steady state operation to CTF.

The above discussion indicates that, by choosing comparable physics parameters for the next-step Performance Extension-level ST experiment (e.g., NSST) and the Component Test Facility (CTF), and by incorporating into CTF the features anticipated for an attractive ST Power Plant, the greatest degree of extrapolation in parameters will occur from NSTX to NSST. Table 6-2 provides a summary of such extrapolations in key physics parameters, which ranges from factors of 5 – 6 (such as in internal poloidal flux content and v^*), to factors of 2 – 3 (such as in I_i , average temperature, a/ρ_i , β' , $\omega_{pe}^2/\omega_{ce}^2$, P/R , τ_{pulse}/τ_{skin}), and to no extrapolation (such as in Greenwald density, β_T , a/ρ_{fast} , and $V_{fast}/V_{Alfvén}$). It is estimated that the extrapolations required from NSST to CTF are generally close to unity, and on occasions close to 2 (such as in I_i , average temperature, v^* , and P/R). From CTF to Power Plant, it is estimated that close to factor of 2 scale-up occurs only for internal poloidal flux, I_i , a/ρ_{fast} , and P/R . It is further estimated that large uncertainties exist at present in the physics basis for extrapolation of the plasma Alfvén Mach number and flow shearing rate.

NSTX research at the Proof of Principle level will therefore likely meet the largest ST physics challenges for extrapolation to future ST experimental devices, such as the NSST. Successful investigation in NSTX of the key physics issues identified here, and subsequent

verification of these issues in NSST, would establish a solid scientific basis for making relatively moderate extensions to CTF and Power Plant. These key physics issues for a cost-effective development of magnetic fusion energy using the ST configuration are identified here and incorporated into the NSTX 5-year plan.

6.3 NSTX Contributions to Improving Predictability and Performance of Tokamak Burning Plasma Experiment

The International Tokamak Physics Activity (ITPA) was established in 2001 to coordinate and enhance the development of the physics basis for tokamak burning plasmas. This activity continues the tokamak physics R&D activities that were carried out on an international level for many years to broaden the physics basis in support of the ITER design, and bring substantial benefits to general tokamak research and all fusion programs worldwide. The activity aims to provide validated experimental data, analyzed experimental results, and theoretical models and simulation results to advance the understanding of toroidal fusion plasma physics. Such understanding in turn provides a solid basis to study fusion performance of and identify and resolve diagnostics issues for the tokamak burning plasmas, such as ITER. The ITPA will carry out a comprehensive attack on the key physics issues anticipated of the tokamak burning plasma. A set of ITPA high priority issues and research topics have been identified recently to focus the ITPA efforts.

NSTX research has recently succeeded in extending the fusion plasma physics to regimes of substantially higher β and stronger toroidicity. NSTX data and analysis can therefore provide valuable information in resolving some the high priority issues identified by the ITPA, particularly those involving substantial uncertainties relating to β and aspect ratio dependence. The following provides a preliminary discussion of such contributions from NSTX. More topics of interest to the ITPA are likely to be identified as further progress is made in NSTX research.

- β -scaling of confinement in ELMy H-modes – A recent β -scan at fixed a/ρ_i and v^* on DIII-D has shown that confinement can be independent of β . This is not consistent with the ITER confinement scaling for the ELMy H-mode plasmas, which contains a strong inverse β dependence ($\tau_E \propto 1/\beta$). This uncertainty in confinement scaling is expected to have large effect on Power Plant concepts that assume higher β . A β -scan can be carried out on NSTX at $B_T = 0.6$ T and at a/ρ_i and v^* values close to those of similarly shaped DIII-D plasmas at the same field. This will in effect extend the range of β values by about a factor of 2 – 3 and

help resolve this important issue for the ITER confinement scaling expressions, and reduce the uncertainties in making confinement projections to a future tokamak Power Plant.

- β -limits with internal transport barrier (ITB) operation – The achievable β -limit has been a key issue in developing steady state operation scenarios for ITER plasmas with a strong ITB and the associated pressure profiles. It has been experimentally shown that the β -limit varies strongly with the types of ITB and the q-profile. This dependence needs to be resolved for reliable predictions of the sustained plasma operation needed in the second (technology testing) phase of ITER. NSTX has recently achieved pulse lengths beyond the skin time by a combination of H-mode and q-profile variations, achieving β_T values as high as 17%. The pressure profile can in principle be varied over a range in such plasmas by variations in the edge fueling rates and the sources and power level of the neutral beams. The dependence of the achievable β_T on the variations of pressure- and q-profiles can be measured and analyzed to help reduce this uncertainty.
- Impact of ELMs on the pedestal and SOL, and effect of aspect ratio – The scaling for the pedestal width is an urgent issue for predicting the ITER H-mode conditions. Recent studies of ELMs in tokamaks show strong dependence on plasma triangularity and overall magnetic structure. It is therefore anticipated that the ELM behavior and limits will show substantial dependence in the aspect ratio. Data from NSTX concerning the impact of ELMs on the pedestal and SOL will therefore contribute to resolving this uncertainty in pedestal width and help develop techniques to improve the ITER plasma conditions in ELMy H-mode.
- Aspect ratio comparison of Neoclassical Tearing Modes (NTM) – Recent comparison experiments for the NTM properties between MAST and DIII-D with exact plasma shape and current helped confirm important aspects of the NTM theory in the low aspect ratio regime. However, detailed analysis indicates that large increases in plasma resistivity need to be assumed in order to match the quantitative behavior between theory and measurement. Further, NTM behavior is theoretically predicted to also depend on bootstrap current, β_p , and the local ion drift velocities, which are expected to have diverse variations in aspect ratio dependence. It is suggested that β ramp-up and ramp-down operation following sawtooth-seeded NTM is observed would reveal important dependence of NTM on the seeding process as well as on the above mentioned plasma parameters. Using the same plasma shape and current, it is possible for NSTX to provide NTM measurements at a different range of values in plasma neoclassical resistivity, bootstrap current fraction, β_p , and the ion drift velocities.

Such information would help resolve the remaining uncertainties in making NTM predictions for the ITER sustained operation at high β_p .

By making detailed comparison with similar tokamak plasmas, NSTX research can not only make substantial contributions to improving the tokamak burning plasma experiment, but also receive substantial benefits in understanding of the ST plasmas.

References

- [6.1] FESAC Panel on Development Path, "A Plan for the Development of Fusion Energy, Preliminary Report to FESAC," November 25, 2002.
- [6.2] M. Ono et al, "Next-Step Spherical Torus and ST Development Path," FEC 2002.
- [6.3] M. Peng et al, "Options for a Component Test Facility," presented to the FESAC Panel on Development Path, October 28, 2002, Livermore, California; report to be issued in March 2003.
- [6.4] R. Aymar et al, Nucl. Fusion **41** (2001) 2041.
- [6.5] D. M. Meade et al, "Mission and Design of the Fusion Ignition Research Experiment (FIRE)," FEC 2002.
- [6.6] I. Sviatoslavsky et al, "Mechanical Design Considerations of a Center Post for Volume Neutron Source," Fusion Engineering & Design **45** (1999) 281.
- [6.7] F. Najmabadi et al, Proc. of Fusion Energy Conference, Yokohama (1998) FTP/08.
- [6.8] H. R. Wilson et al, "The Spherical Tokamak Power Plant," FEC 2002.
- [6.9] M. A. Abdou et al, "Results of an International Study on a High-volume Plasma-Based Neutron Source for Fusion Blanket Development," Fusion Technology **29** (1996) 1.